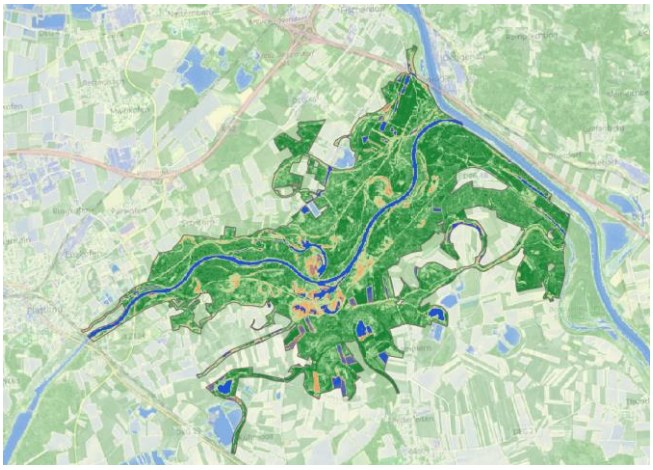

VITALITY OF RIPARIAN VEGETATION UNDER CLIMATIC STRESS CONDITIONS. PLANT VITALITY ASSESSMENT OF SELECTED SITES IN THE FLOODPLAIN AREA OF THE RIVER ISAR USING REMOTE SENSING

Supervised by
Prof. Dr. Stefan Heiland and
Dr. rer. nat. Aude Zingraff-Hamed

MASTER THESIS

Technical University Berlin
Faculty VI Planen Bauen Umwelt
Institute of Landscape Architecture and Environmental Planning
Department of Landscape Planning and Landscape Development

Katrin Koch
Thumseestrasse 4B
83435 Bad Reichenhall
Study Program M.Sc. Environmental Planning
Enrolment Number 396812
11. March 2022

Eidesstattliche Erklärung

Hiermit erkläre ich, dass ich die vorliegende Arbeit selbstständig und eigenhändig sowie ohne unerlaubte fremde Hilfe und ausschließlich unter Verwendung der aufgeführten Quellen und Hilfsmittel angefertigt habe.

Berlin, 11. März 2022

Katrin Koch

Acknowledgements

At this point I would like to thank Dr. Aude Zingraff-Hamed for her trusting and reliable supervision throughout the entire course of this thesis. Her suggestions and committed support, as well as her valuable insights were greatly appreciated. Additionally, I would like to warmly thank Prof. Dr. Stefan Heiland for supervising my thesis and offering support whenever needed.

Invaluable encouragement was offered by my family and friends, particularly my father, to whom I would like to express my gratitude.

Abstract

Floodplain areas are rated to be some of the most biodiverse and structurally rich habitats worldwide, while simultaneously being ranked among the most rapidly vanishing ecosystems. Those water-sensitive ecosystems provide essential habitats to an uncountable number of species while, due to their linear structure, additionally operate as connecting elements in transnational habitat networks. Next to anthropogenic influences, the increasing occurrences of extreme climate events, especially droughts, are threatening the vitality of floodplain areas, their productivity rates, as well as their beneficial ecosystem services to humankind. Research on the vitality of floodplain areas and their response to drought events is thus crucial to further the comprehension on their interaction with site-specific meteorological and hydrological conditions, their reactions to alterations in those conditions, and in particular, their potential resilience to drought episodes. Using such insights will help to adequately design or adjust the measures required to mitigate the impacts of, or to adapt floodplain areas to, abnormally hot and dry episodes at least to the extent possible. Floodplain areas are at the forefront of European environmental policy, but research on those water-related ecosystems in the DACH region is scarce. This work investigated the plant vitality of five floodplain areas alongside the Isar River in Bavaria, Germany, throughout the time period 2016-2020 using remotely sensed data and two vegetation indices. The main goal of this thesis was to assess potential impacts and possible legacy effects that the drought occurring in 2018 over Central Europe had on the vitality of riparian vegetation, when compared to the reference year 2016. Besides investigating entire study areas, this work paid special attention to the analysis of individual biotope types (Forested Areas, Shrubs, Hedges and Bushes, Dry Habitats of the Open Landscape, Wet Habitats of the Open Landscape). Moreover, the applicability of remote sensing technology and the use of vegetation indices in the context of plant vitality assessments, specifically for water-related ecosystems, was tested.

Although the analysis revealed significant reductions in index values for each study area and for all investigated biotope types following the drought conditions in 2018, no direct linkages to potential legacy effects could be made. In contrast with the original hypotheses, particularly the positive anomalies in air temperature could be linked to direct decreases in index values, whereas the negative anomalies in precipitation rates appeared rather secondary. However, groundwater refilling and thus water availability is conditional upon precipitation rates throughout the previous year, respectively. Reduced precipitation rates can be therefore connected to decreases in index values, or rather shortages in groundwater/ soil moisture availability, during the following vegetative period. The results of the individual biotope type assessment indicate that Forested Areas and Wet Habitats of the Open Landscape are slightly more drought resistant than Shrubs, Hedges and Bushes or Dry Habitats of the Open Landscape.

This report concludes that both indices have proven to function quite well in the context of assessing the vitality of riparian vegetation, as long as results are obtained using high-quality data from reliable sensors with adequate temporal and spatial resolution, as well as clearly defined data processing methods. The Normalized Difference Vegetation Index displayed some advantages and showed to adequately assess the vitality of riparian vegetation, both on a study area scale, as well as for individual biotope types with smaller spatial extents. The Normalized Difference Water Index, however, tested to be slightly less robust in this context. Distortions stemming from overlapping values, particularly on the larger scale, caused some uncertainties. Further research is needed to verify the results of this analysis for floodplain areas of other biogeographic regions, as well as to particularize the impacts of site-specific meteorological and hydrological conditions on the vitality of riparian vegetation.

Zusammenfassung

Flussauen werden weltweit zu den Lebensräumen mit einer der höchsten Biodiversitäts- und Strukturvielfalt gerechnet. Gleichzeitig jedoch zählen sie zu den am schnellsten verschwindenden Ökosystemen. Als vom Wasser abhängige und zugleich durch Wasser geprägte Ökosysteme bieten sie einerseits unzähligen Arten einen Lebensraum und fungieren andererseits aufgrund ihrer linearen geographischen Ausdehnung als Bindeglieder in transnationalen Habitat-Netzwerken über Ländergrenzen hinweg. Neben der Einflussnahme durch den Menschen stellen für sie insbesondere die zunehmenden extremen Klimaereignisse, allem voran Dürren, eine existenzielle Bedrohung dar. Hierbei werden neben der Vitalität der Flussauenvegetation auch deren Produktivitätsrate und die von ihnen bereitgestellten Ökosystemdienstleistungen beeinträchtigt. Die Erforschung der Vitalität von Flussauen und ihre Reaktionen auf extreme Dürreereignisse ist daher von zentraler Bedeutung. Durch sie kann es gelingen, die Zusammenhänge der wechselseitigen Abhängigkeit zwischen ortspezifischen meteorologischen und hydrologischen Bedingungen und ihre mögliche Resilienz gegenüber extremen Dürreepisoden zu verstehen. Diese Erkenntnisse werden helfen, zielgerichtete Maßnahmen gegen die Auswirkungen ungewöhnlich heißer und trockener Witterung in Flussauen zu planen oder diese so weiterzuentwickeln, dass der Einfluss von Dürren auf das Mindeste beschränkt wird.

Auengebiete stellen zwar ein zentrales Thema in der europäischen Umweltpolitik dar, ihre wissenschaftliche Erforschung im deutschsprachigen Raum (DACH) erscheint jedoch bislang noch gering. Diese Arbeit befasst sich daher mit der Vitalität der Vegetation von fünf Flussauen entlang der Isar im deutschen Bundesland Bayern in den Jahren 2016 bis 2020. Ziel der Arbeit war es hierbei mögliche Auswirkungen und Folgen der mitteleuropäischen Dürreperiode im Jahr 2018 im Hinblick auf die Vitalität der Vegetation in den Uferzonen mit den Referenzwerten des Jahres 2016 zu vergleichen. Neben der Betrachtung der gesamten Untersuchungsgebiete, lag ein Hauptaugenmerk auf der Einzelanalyse folgender Biotoptypen: Wälder, Sträucher, Hecken und Büsche sowie trockene und feuchte Habitate in Offenlandschaften. Weiterhin wurde durch diese Arbeit geprüft, inwiefern sich Fernerkundungstechnologien und die Anwendung von zwei abgeleiteten Vegetationsindizes für eine Bewertung der Vitalität von Pflanzen in wasserbezogenen Ökosystemen eignen.

Im Ergebnis zeigt sich, dass obwohl die Analyse der Daten einen Rückgang beider Indexwerte für alle untersuchten Gebiete und deren Biotope nach der Dürre im Jahr 2018 nachweist, es aber keine direkten Verbindungen zu langfristigen Beeinträchtigungen innerhalb der Folgejahre gibt. Darüber hinaus konnte festgestellt werden, dass im Gegensatz zur ursprünglichen Hypothese besonders die Temperaturanstiege zu einer direkten Abnahme der Indexwerte führt. Ein verminderter Niederschlag scheint dafür dagegen von geringer Bedeutung zu sein. Allerdings haben geringere Niederschlagsmengen Einfluss auf die Grundwasserneubildung und somit auch auf die Verfügbarkeit von Wasser im Folgejahr. Somit ergibt sich also ein Zusammenhang zwischen reduziertem Niederschlag und sinkenden Indexwerten, die auf geringere Grundwasserverfügbarkeit oder Bodenfeuchte in der folgenden Vegetationsperiode zurückzuführen sind. Da die Bodenfeuchte in dieser Arbeit allerdings nicht betrachtet wird, empfiehlt es sich in zukünftigen Analysen deren Relevanz genauer zu untersuchen. Aus der individuellen Betrachtung der jeweiligen Biotoptypen kann man folgern, dass Waldgebiete und Feuchte Habitate der Offenlandschaften resistenter gegen anhaltende Trockenheit sind als Sträucher, Hecken und Büsche oder Trockenhabitate der Offenlandschaften.

Als Fazit dieser Arbeit lässt sich festhalten, dass beide verwendeten Vegetationsindizes gut geeignet sind, um die untersuchten Zusammenhänge darzustellen, solange eine Verwendung von qualitativ hochwertigen Daten und zuverlässiger Sensoren mit einer entsprechend hoher zeitlichen und

räumlichen Auflösung möglich ist. Weitere Voraussetzung ist die konsequente Anwendung einer strikt festgelegten Methode der Datenverarbeitung. Der Normalized Difference Vegetation Index – kurz NDVI – erwies sich insgesamt als geeigneter, um die Vitalität der Ufervegetation sowohl für ein gesamtes Untersuchungsgebiet, als auch für einzelne Biotoptypen von geringerem Flächenausmaß vergleichend auf einer Skala beurteilen zu können. Die Daten des Normalized Differenz Water Index – kurz NDWI – waren dagegen hier weniger robust, da überlappende Werte, insbesondere bei größerem Maßstäben, häufig zu Verzerrungen und Auswerteunsicherheiten führen. Allgemein ist festzustellen, dass es weiterer Forschung an Flussauen in anderen biogeografischen Regionen bedarf, um die Ergebnisse dieser Arbeit dort zu verifizieren. So wird es schließlich möglich sein, die Auswirkungen standortspezifischer meteorologischer und hydrologischer Bedingungen bei der Bewertung der Vitalität von Ufervegetation genauer zu bestimmen.

Table of Contents

List of Tables

List of Figures

List of Maps

Abbreviations

BayLfU	Bavarian State Ministry of the Environment
BNatschG	Federal Nature Conservation Act (Bundesnaturschutzgesetz)
ESA	European Space Agency
ESS	Ecosystem Services
FFH Directive	Flora-Fauna-Habitat Directive
GW	Groundwater
LAI	Leaf Area Index
MGT	Mean Growing Season Air Temperature
MGP	Mean Growing Season Precipitation Rate
NDVI	Normalized Difference Vegetation Index
NDWI	Normalized Difference Water Index
NIR	Near Infrared
SWIR	Short-wave Infrared
VPD	(Atmospheric) Vapour Pressure Deficit
WFD	European Water Framework Directive (WFD)

1 Introduction

Floodplain areas are rated as some of the most biodiverse areas worldwide, providing essential habitats to an uncountable number of species, as well as offering numerous ecosystem services (ESS) to human societies (EEA 2018; BfN 2015b; D. Russi et al. 2013; Schindler et al. 2016b). Besides providing the most distinct function of flood protection to settlements, floodplain areas benefit people in manifold ways and oftentimes on different scales. These benefits include water purification, space for recreation, highly fertile agricultural lands, a supply in raw material and food or carbon sequestration, to only name a few (EEA 2018; BfN 2015b; Capon et al. 2013; BMU 2021). Due to their linear structure, riparian ecosystems additionally operate as connecting elements in transnational habitat networks, facilitating continuous lateral, longitudinal, and vertical exchange of energy, material and biota (EEA 2018; BfN 2015b; Ballinger and Lake 2006; Jongman, Külvik, and Kristiansen 2004).

Species richness and functionality of riparian ecosystems is intimately linked to the hydrosphere of respective rivers. The composition of riparian vegetation is orchestrated by the rhythm of seasonal flooding events, which alternate with episodes of seasonal droughts. Following the concept by (Junk, Bayley, and Sparks 1989), flood pulses provide contingencies of sediment exchange, fauna migration and habitat (re-)structuring. This directly and indirectly influences both the habitat complexity and heterogeneity, and in consequence, the quality of riverine ecosystems (Junk, Bayley, and Sparks 1989; Jongman, Külvik, and Kristiansen 2004). Productivity of riparian vegetation is suggested to follow a (natural) four-phase adaptive cycle, comprising of a wetting, wet, drying and dry phase, to which productivity rates are subject to (Thapa et al. 2016; Sims and Thoms 2002). Within this cycle, moderate seasonal flooding/wetting with intermediate return frequencies is named key driver for high productivity rates, hence high vitality of associated plant communities (Thapa et al. 2016; Sims and Thoms 2002).

As described, specific and reoccurring environmental conditions initially determine the particular composition, species richness, structural complexity and productivity of floodplain biotopes, as well as their critical role in both the nutrient and the carbon cycle (BfN 2015; Feld et al. 2011; Capon et al. 2013; Russi et al. 2013). Although floodplain areas have been commonly chosen by humans for settlement, the interconnectivity and interdependency between the different components of riverine landscapes and their values have, historically seen, rarely been sufficiently acknowledged or incorporated into decision making processes (Russi et al. 2013). Highly fertile soils, good transport possibilities or the constant availability of water (Schober, Hauer, and Habersack 2015; Böck, Polt, and Schülting 2018) are part of the wide array of advantages floodplain areas offer, but the expansion of settlement areas and river engineering for flood protection or facilitated shipping resulted worldwide in a continuous loss of floodplain areas. Hydro-morphological changes and structural means heavily impacted floodplain areas and the associated riparian vegetation, causing floodplain areas to be some of the most altered and degraded ecosystems in the world, as well as earning them a rank among the most rapidly vanishing ecosystems (Schindler et al. 2016b; BfN 2015a; D. Russi et al. 2013; Tockner and Stanford 2002). In hindsight, human-induced interventions to floodplain areas, their structures and functions oftentimes ironically amplified the risk of natural disasters (Schindler et al. 2016a) and enhanced the loss of beneficial services and habitat connectivity.

Taking up the aforementioned aspects, the perception of riverine landscapes, their functions and values significantly changed throughout the past decades (Brander, Brouwer, and Wagtendonk 2013). Recently, riverine landscapes have been at the forefront of European environmental policy. The

protection of those sensitive ecosystems has been legally consolidated in multiple frameworks, including the European Water Framework Directive (WFD), the Floods Directive or the FFH Directive. Human-induced interventions have (mostly) been regulated and various projects and programs for the protection of floodplains initiated (e.g. the German Auenschutzprogramm). Aim of those projects and programs is the enhancement of floodplain statuses or the restoration to their original state. Thereby the vitality of floodplain areas is supposed to be (re-)established and safeguarded, as only integrally functioning floodplain ecosystems can reliably provide the desired ESS and functions (BfN 2015b).

Despite the efforts of enacted statutory provisions, certain environmental factors are beyond regional/ local control. Extreme climate conditions and their concomitants, such as altered precipitation patterns, differences in fluvial dynamics and changes in temperature regimes were observed to adversely affect floodplain areas of multiple biogeographic regions and several contexts in a progressive manner (Kowalska et al. 2020; Gangashe, Andani 2018; Mikac et al. 2018; Horner et al. 2009). Although floodplain areas have, as all other ecosystems, experienced changes in environmental conditions and have even adapted to the previously described specific rhythm of altering conditions, it is precisely this dependency on the natural wetting and drying cycle that makes them even more vulnerable to changes in site-specific meteorological and hydrological conditions. Understanding the adverse effects of extreme climate conditions on the vitality of riparian vegetation is a key research challenge which, in the likelihood of increased frequency, duration and intensity of such events, urgently needs to be addressed.

Extreme weather events are understood as anomalies in the values of weather variables above or below certain thresholds and close to the (upper or lower) ends of respective ranges (DWD 2008; Seneviratne et al. 2012). Occasional heat waves, intense precipitation events or gale-force winds, as examples of such events, are not regarded as particularly exceptional when considered within specific, geographically bound, climatological normal periods (IPCC 2014; BR 2021). Such events have at all times influenced the Central European environment and have been recorded since instrumental climate documentation exists (Hanel et al. 2018a; Della-Marta et al. 2007; Barriopedro et al. 2011). Several consecutive heat waves have been recorded throughout the last half century and have been more closely specified by (Spinoni et al. 2015), for instance. Studies revealed that recurring episodes with abnormally warm and dry weather conditions commonly resulted in water and heat stress for vegetated areas, adversely impacting plant vitality. Nevertheless, when in seasonal moderation, aforesaid episodes oftentimes promoted subsequent plant vitality regeneration rather than resulting in long-term impacts on plant vigour and are sooner seen as key driver in the cyclical regeneration of some ecosystems (Mikac et al. 2018).

Global climate change, majorly attributable to anthropogenic impacts through the non-sustainable (ab)use of resources, is recognised as main driver of extreme weather events or changes in weather patterns (Vogel et al. 2019; Leach et al. 2020; Coumou and Rahmstorf 2012; Seneviratne et al. 2012; IPCC 2014). An unequivocal upward trend in the occurrence of extreme weather events throughout the last century, has been revealed by an uncountable number of analyses and can be led back to the warming of the climatic system (IPCC 2014; Barriopedro et al. 2011; Della-Marta et al. 2007; Trenberth et al. 2007). The year 2015 has for instance experienced a doubling in climatological extreme events and a fourfold increase hydrological events on the global scale (easac 2018; EEA 2021).

Especially when long-lasting or as compound effects, those extreme weather events can cause extreme climate events (IPCC 2014). Examples for extreme climate events are droughts for instance, which

affect all natural and human systems more substantially and more lastingly, when compared to single extreme weather events (IPCC 2014; Stephenson 2008; Seneviratne et al. 2012). A growing body of literature investigates the impacts of recent drought events on, and their consequential changes in natural and human systems revealing unidirectional results. Changes in natural systems became more evident throughout the last decades and include, but are not limited to alterations in the hydrological cycle (Van Lanen et al. 2016), temporal deferrals in the vegetative period, as well as shifts in composition, function and vitality of native flora and fauna (Beillouin et al. 2020; Bastos, Fu, et al. 2020; Bastos, Ciais, et al. 2020; Ciais et al. 2005; Hanel et al. 2018a; UNEP 2004; Allen and Breshears 2007; Buras, Rammig, and S. Zang 2020; Backlund et al. 2013).

Particularly the latter, the effects of drought episodes on plant vitality, are still associated with uncertainties. Species adaptation capacities and their vitality responses to increased and intensified occurrences of drought episodes, are broadly discussed amidst the current discourse on adaptation and mitigation measurements for vegetated areas. Contrasting results were obtained by several studies, where some reported (immediate) degradation of plant vitality (Schuldt et al. 2020; Rohner et al. 2021; Beillouin et al. 2020; Bastos, Fu, et al. 2020) following a drought episode, whereas others reported little to no responses (Lindroth et al. 2020; El-Madany et al. 2020) or even unexpected increases in plant vitality (Kowalska et al. 2020). Multiple studies addressed the disparate results obtained between different ecotones (Barros, Thuiller, and Münkemüller 2018a) or regional asymmetries (Gharun et al. 2020; Bastos, Ciais, et al. 2020), emphasizing the importance of location, scale and context. The contrary findings of those studies underline the urgency of understanding and distinguishing the immediate and specific responses of different ecosystems to drought events.

In addition to this gap in current knowledge, research on this topic concerning wetland/ riparian vegetation is particularly scarce. Although a great number of recent studies focuses on drought-related impacts on homogenous plant communities such as grasslands or forests (Schuldt et al. 2020; Rohner et al. 2021; Lindroth et al. 2020; Choat et al. 2012; Emadodin et al. 2021a; Cherwin and Knapp 2012), only few studies investigate these effects for water-associated, structurally rich ecosystems such as wetlands or floodplain areas (Kowalska et al. 2020; Mikac et al. 2018; Rinne et al. 2020). Some authors even excluded such habitats from their research due to difficulties in modelling wetlands or water-associated terrestrial ecosystems with (usually) high water tables (Bastos, Ciais, et al. 2020). Being acquainted of the vitality of floodplain areas, monitoring their reactions to drought events and investigating potential legacy effects is central in developing, prioritizing and adapting management approaches aiming to protect and enhance those sensitive ecosystems, which create and invaluable link between the terrestrial and the aquatic spheres. The unanswered questions concerning clear predictions on vitality responses of riparian vegetation to droughts result in an urgent call for action in this field.

Despite the reoccurrence of drought episodes over Central Europe throughout the last centuries, some episodes are, due to their severity, particularly noteworthy. Next to the record-breaking drought in 2003 (Hanel et al. 2018a; Garcia-Herrera et al. 2010; Schönwiese, Staeger, and Trömel 2004; Rebetez et al. 2006), have the climatic conditions occurring during the vegetative period (April till October) in 2018 been described as an exceptionally severe drought (Peters et al. 2020; Yiou et al. 2020; Schuldt et al. 2020; Buras, Rammig, and S. Zang 2020; Hanel et al. 2018a; Barriopedro et al. 2011). The mean growing season air temperature (MGT) during this season was reported to have been approx. 3.3°C higher over the DACH region (Germany, Austria and Switzerland) than the long-term average, recorded between 1961 and 1990 (Schuldt et al. 2020). The authors further noted that the mean growing season

air temperature (MGT) in 2018 was 1.2°C higher than during the drought event in 2003. The abnormally high temperatures in 2018 mark therefore yet another amplitude in the rising temperature trend. In addition to the positive anomaly in air temperature, the 2018 drought was characterized by a mean growing season precipitation rate (MGP) lower than the average long-term precipitation rate (1961-1990) and similar to rates recorded in 2003 or previous drought-affected years (Schuldt et al. 2020; Hanel et al. 2018a).

In this context and as no comparable studies exist for floodplain areas located in the DACH region, this master thesis aims at assessing the responses in plant vitality of riparian vegetation to the 2018 drought event. On five study areas located alongside the Isar River in Bavaria, Germany the following hypotheses are tested.

It is hypothesized, that

(i) drought-induced changes in air temperature are negatively linked to the vitality of riparian vegetation,
(ii) drought-induced alterations in precipitation patterns are negatively linked to the vitality of riparian vegetation,
(iii) changes in ground-water levels are negatively linked to the vitality of riparian vegetation and that
(iv) those impacts resulted in drought-legacy effects in the following year(s).

To investigate these hypotheses, this study will analyse whether the vitality of riparian vegetation during the drought year 2018 differed from the vitality in 2016, using remotely sensed data, geoprocessing tools, two derived vegetation indices and statistical analyses. The year 2016 is used as reference year for the NDVI and NDWI assessments. This is due to the fact that meteorological and hydrological conditions in 2016 can be considered as most representative for the long-term average, when compared to the other investigated years. Preceding and following years of 2018 are additionally considered, in order to better contextualize inter-annual changes of plant vitality with altering meteorological and hydrological site-conditions.

This work further targets to appraise the applicability of the two chosen vegetation indices, namely the Normalized Difference Vegetation Index (NDVI) and the Normalized Difference Water Index (NDWI), within the context of plant vitality assessments of riparian vegetation. channel

The gained insights will help to close the current gap in knowledge whether riparian vegetation directly responds to drought-induced anomalies in temperature regimes and precipitation patterns, which biotope types are more resilient to those alterations and whether legacy effects occur. The obtained results will be contextualized by examining them in contrast to other findings concerning the direct responses of similar ecosystems to drought-related impacts. The remainder of the paper will be structured as follows: Section 2 will detail the methodology, giving an overview of the current state of the art, clarifying matters of definition, explaining the choice of study areas and floodplain biotope types, describing data sources and the steps of the analysis conducted. In Section 3, the results are presented, which are then discussed in Section 4 and Section 5 concludes the findings.

2 Material and Methods

The following section provides a brief overview to the definitions at hand, an introduction to remote sensing data and techniques used in this assessment of land surface covers and plant vitality in particular, as well as a brief historical contextualisation of floodplain areas. The theoretical foundations of the methodology applied in this assessment are closely elaborated in this chapter. For this purpose, the basics of remote sensing and the underlying principles of vegetation indices are explained.

2.1 Drought

Depending on the topic at hand and the stakeholders involved, drought can be understood as a natural phenomenon during which abnormally dry and warm weather over an extended period of time results in water scarcity, causing activity restrictions for certain environmental related sectors or induces substantial detriments to natural and managed ecosystems, infrastructure or human health (Seneviratne et al. 2012). Various types of (physical) drought can be differentiated including hydrological, meteorological and soil moisture drought (Seneviratne et al. 2012; Wilhite and Glantz 1985). Hydrological drought, as the other two types, linked to shortages in precipitation rates, but is typified by ensuing anomalies in runoff regimes or supply deficits for surface and subsurface waters. This type of droughts is therefore closely related to the (in-)stability in conditions of wetlands and wetland habitats. This type of drought commonly occurs in a lag, subsequent to meteorological drought events (ibid.).

Meteorological droughts are associated with precipitation deficiencies, as well as above average temperatures, both resulting in shortfalls of infiltration or runoff rates, reduced groundwater recharge, lower relative humidity or increased evapotranspiration. Soil moisture droughts, oftentimes termed agricultural droughts, occur similar to hydrological droughts time lagged to meteorological droughts and are affiliated with the aspects of meteorological or hydrological droughts on soil moisture. Deficits in soil moisture, differences in actual and potential evapotranspiration and deficiencies of plant-available water in the topsoil layer impinge not only agroecosystems, but all other natural, near-natural or managed ecosystems, which is why the term agricultural drought remains unused in this thesis (Seneviratne et al. 2012). Particularly the latter is determinant for the health and growth of plants in early growth stages and therefore additionally relevant for vegetated areas in early succession, commonly found in floodplain areas. It is important to delimit drought, a climatic event, from aridity, which is the characteristic of a climatic region.

Against this backdrop, the drought occurring in 2018 over Central Europe can be specified as a drought event with exceptionally warm, but not exceptionally dry conditions at the outset of the vegetative period that, without respite, transitioned into an extreme summer drought (see Meteorological and Hydrological Data). Attributing this drought event to all of the abovementioned drought types leads to its common classification of a “global change-type drought”. As the aim of this paper is to analyse plant vitality of riparian vegetation, particularly exploring this topic within the context of a global-change type drought and its concomitant impacts by using remote sensing techniques, a clear definition of the subject matter is of fundamental importance. While floodplains are rather clearly defined as areas consisting of sedimentary material surrounding river courses (Baptista et al. 2014), that interact with both the surface and subsurface waterflow associated with respective rivers and which are flooded when river discharges are peaking (Bino et al. 2018), no such standard definition exists for plant vitality.

2.2 Plant Vitality

Plant vitality in general is conditional upon specific seasonal climate conditions which, when altering, adversely affect the native plant community. Changes in the hydrologic household, such as an increase in dryness, deficits in soil moisture and/ or differences in water availability, can exemplarily lead to severe impairments in plant vitality or ultimately to hydraulic failure, as a great amount of plant species engage within specific hydraulic margins (Rohner et al. 2021; Choat et al. 2012; Adams et al. 2017; Eamus et al. 2013). Next to hydraulic failure, carbon starvation (the discrepancy in carbohydrate demand and supply) is commonly named as another underlying mechanism in drought-induced deterioration of plant vitality (McDowell et al. 2008; Adams et al. 2017; Sevanto et al. 2014). This mechanism occurs when plants avoid hydraulic failure by stomata closing and rely upon carbohydrate reserves in order to maintain tissue (Adams et al. 2009). However, it is noted that carbon starvation accounts primarily for tree mortality rather than other types of vegetation (Allen and Breshears 2007). An additionally aggravating impact of global change-type droughts on vegetation is the increase in atmospheric vapour pressure deficit (VPD) due to overall higher global temperatures (Yuan et al. 2019; Eamus et al. 2013). An increase in VPD amplifies adverse effects of drought episodes on plants, compared to drought episodes combined with higher temperatures alone, by being accompanied by an increasing demand of water. This water demand needs then to be drawn through the roots, substantially affecting the transpiration rate and thereby the soil water content (Eamus et al. 2013; Yuan et al. 2019).

Droughts induce deterioration of plant vitality. This can appear in forested areas as premature leaf senescence (Schuldt et al. 2020), reduction foliage density (Rohner et al. 2021; Sousa-Silva et al. 2018), anomalies in foliage colour and discoloration (Schuldt et al. 2020; Rohner et al. 2021), abnormal yields or early fruit abortion (Nussbaumer et al. 2020) and can ultimately result in increased mortality rates (Breshears et al. 2005). Moreover, a variety of seasonal legacy effects can occur, including alterations in brush community composition and functioning (Zellweger et al. 2020) or detrimental alterations in the carbon cycle (Thompson et al. 2020; Rödenbeck et al. 2020; Smith et al. 2020). The latter can exemplarily be caused initially through abated photosynthetic performances following a reduction in foliage density. This in turn subsequently induced decreased growth rates and caused thereby a decline in the terrestrial net primary production (Zhao and Running 2010). This delineated cascade of consequential effects can ultimately lead to altered and reduced total carbon uptake for larger areas or entire ecosystems. Similar or even amplified responses to drought events were reported for ecosystems other than forested areas, including grass- and croplands. Alterations in yield rates, changes in either gross or net primary production and higher vulnerabilities to pest and disease incidences have been detected (Beillouin et al. 2020; van der Velde et al. 2012; Cherwin and Knapp 2012; Ciais et al. 2005; Barros, Thuiller, and Münkemüller 2018b; Emadodin et al. 2021b; Fu et al. 2020; Gharun et al. 2020). These responses oftentimes lead to similar legacy effects as observed in forested areas, such as alterations in carbon cycling, changes in water balance or shifts in the composition and functioning of native plant communities (Smith et al. 2020; Thompson et al. 2020; Barros, Thuiller, and Münkemüller 2018b; Gharun et al. 2020).

As described, plant vitality is influenced and determined by a variety of environmental conditions and can be understood or measured in various ways. In this thesis, vitality is understood as photosynthetic activity and plant productivity in the broad sense, as healthy vegetation contains more photosynthetically active in-leaf structures (chlorophyll-a) and a higher plant-water content than stress-affected vegetation. The reflectance percentages of certain intervals of the electromagnetic

spectrum are distinctly characterized by the content of in-leaf structures and intra-cellular water, which can be detected using remotely sensed data. This means, the more chlorphyll-a is present and the higher the intra-cellular water content is, the more vital the assessed vegetation is. Results on plant vitality in this study will be thus obtained by applying and amending an innovative, non-invasive, and resource-efficient remote sensing method to estimate the vitality of floodplain biotope types. This method allows to quickly assess the vitality state of (riparian) vegetation without the need for on-site measurements, thus enabling timely analysis even on larger scales.

2.3 Remote Sensing Techniques and Plant Vitality Assessment

Remote sensing is the acquisition of information on the physical conditions of the environment from distance, meaning that the measuring device is not being situated at the location measured. Remote sensors can be carried by drones, airplanes or satellites with the aim to provide information on the current state, as well as the changes the environment is subject to. Information is derived by detecting and recording reflected or emitted electromagnetic energy. The amount of energy reflected or absorbed is conditional upon the roughness of the surface and its albedo, resulting in unique spectral signatures of each surface type. Based on this fact, different types of features or conditions can be identified, as well as changes through time series analyses detected (NASA 2021).

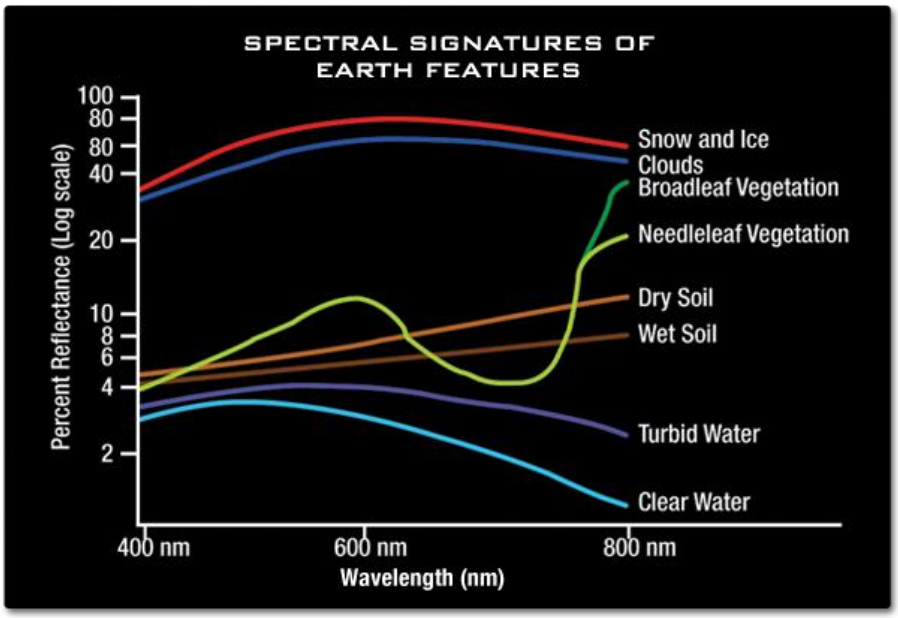

Figure 1. Spectral signatures of different Earth features within the visible light spectrum (NASA 2021).

Remotely sensed datasets from satellites are specified through four different types of resolution, which determine how data from respective sensors can be utilized. The size of each pixel within a remotely sensed image determines the spatial resolution. The finer the spatial resolution is, meaning the smaller the value, the higher the level of details that can be detected on the examined surface. Temporal resolution on the other hand is determined by the revisit time of a sensor, meaning the time a specific sensor needs to complete one orbit and reach the same area of observation. Depending on the number of spectral bands that can be detected and recorded by a specific sensor, one can differentiate between monochrome (1 band), RGB (3 bands), multispectral (4 – 15) or hyperspectral sensors (up to 1000s of bands). Each band contributes to an overall image. The more and the narrower the bands are, which can be detected by a specific sensor, the finer the spectral resolution is. Lastly, radiometric resolution is defined as the amount of information that each pixel consists of. The energy that sensors detect and record is represented through the number of bits, of which each captures an

exponent of power 2. Meaning, a 16-bit resolution for instance, indicates that this particular sensor is able to store information on light intensity of reflectance through (2^{16}) 65.536 digital values. The higher the radiometric resolution is, the greater the number of details, which can be detected within the observation area (NASA 2021).

When measuring biophysical vegetation characteristics, plant vitality or plant productivity, remote sensing-based techniques focusing on vegetation indices (VI) have been proven to function as fast, non-invasive and non-disturbing measurement options for larger scales (Rivero et al. 2009). Vegetation indices build on the fact that plants exhibit distinctive characteristics of reflecting and absorbing electromagnetic radiation along the electromagnetic spectrum, depending on their condition. Based on the amount of radiation reflected or absorbed, conclusions on the content of in-leaf structures or intracellular water content can be drawn and thus information on the current vitality status of plants derived (see Figure 2). Episodes of stress, which can be caused through nutrient deficiencies, water deficits or drought events for instance, have an impact on the regular, seasonal growth rates of plants. This can lead to visible symptoms as described in the previous section (e.g. discoloration/ dead tissue), but also to those that remain invisible to the human eye. These invisible symptoms can, however, be identified and monitored with multispectral sensors which can detect and record wavelengths beyond the spectrum of the human eye (Jones and Vaughan 2010). Before the NDVI and NDWI are closer elaborated, a brief overview of satellite data is enclosed in the following section.

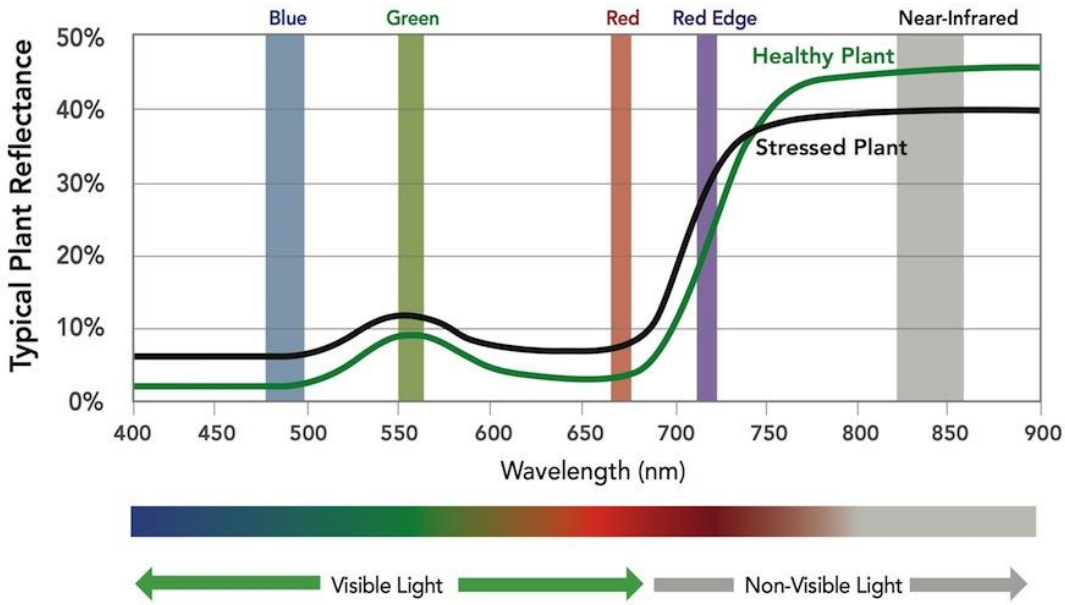

Figure 2. Reflected energy in the visible blue, green and red wavelengths as well as the non-visible red edge and near-infrared intervals of the electromagnetic spectrum (GISNOTE 2019).

2.4 Satellite Data

Remotely sensed imagery from the twin satellites Sentinel-2 is obtained and used in the context of this study. Sentinel-2 are part of the Copernicus Mission, operated by the European Space Agency (ESA). Data is provided with a relatively high temporal resolution with a minimum of a five-day global revisit time and is publicly available. The multispectral sensors carried by each satellite provide a wide spatial coverage with a swath width of 290 km and enable recording through 13 spectral bands with three different spatial resolutions, 10 m, 20 m or 60 m, respectively. Table 1 provides an overview of Sentinel-

2's spectral channels. The radiometric resolution of the Sentinel-2 sensor amounts to 12-bit, resulting in up to 4096 potential light intensity values (ESA 2021).

Table 1. Spectral bands and resolution of the Sentinel-2 MSI sensor. Highlighted are the bands used in this study (own amendmend; ESA 2021).

Spectral Band	Central Wavelength (nm)	Band Width (nm)	Spatial Resolution (m)
B1 Coastal aerosol	443	20	60
B2 Blue (B)	490	65	10
B3 Green (G)	560	35	10
B4 Red (R)	**665**	**30**	**10**
B5	705	15	20
B6	740	15	20
B7	783	20	20
B8	**842**	**115**	**10**
B8A	865	20	20
B9	945	20	60
B10	1380	30	60
B11	**1910**	**90**	**20**
B12	2190	180	20

Satellite imagery is obtained following a three-step process, which includes (1) specifying the times of investigation, (2) examining the existence of imagery encompassing the study areas for each time of investigation and (3) selecting high-quality imagery for respective time periods and study areas.

(1) Times of investigation per year are chosen considering three different stages of the growing season (spring, summer, and late autumn), allowing an identification of intra-annual and inter-annual changes in plant vigour (see Meteorological and Hydrological Data). Choosing three different stages which mark distinct points in the phenological cycle additionally ensure comparability between and within the vitality of each stage. By retrieving such time series, a reliable baseline in VI values per biotope type could be subsequently established and collated with information on temporal vegetation phenology (Rembold et al. 2019; Anyamba and Tucker 2012).

(2) The six study areas are encompassed in the Sentinel-2 tiles T32TPT, T32UPU, T32UQU, T32UQV, T33UUQ. Data for those tiles is acquired for each investigation time (Spring-T1, Summer-T2 and Autumn-T3) and per year, respectively. Data is obtained for temporarily comparable images only.

(3) The remaining data is subsequently sorted by selecting only high-quality imagery with less than 10% cloud coverage, resulting in 15 Sentinel-2 images per study area (2016-2017, respectively Spring-T1, Summer-T2 and Autumn-T3)

2.5 Drought Indices

A wide array of vegetation indices can be used to measure certain plant characteristics. The Normalized Difference Vegetation Index (NDVI), Normalized Difference Red Edge (NDRE) or Enhanced Vegetation Index (EVI) for example make use of the chlorophyll-a content in plant cells (Boelman et al. 2003; S. Szabó, Gácsi, and Balázs 2016a). Others, such as the Normalized Difference Water Index (NDWI) (Gao 1996), are commonly used as proxies for plant water stress, as it relates to the intra-cellular water

content in plants and instantly reacts to a shortage in water availability (JRC 2011). This study will apply the NDVI and NDWI for assessing the vitality of riparian vegetation. Both indices have proven to function as reliable measure for plant vigour within numerous contexts and across multiple climatic zones, confirming them to work as robust indices (Mancino et al. 2014; S. Szabó, Gácsi, and Balázs 2016a; Ogashawara and Bastos 2012; Griffith 2002; L Szabó et al. 2020).

2.5.1 Normalized Difference Vegetation Index

The Normalized Difference Vegetation index (NDVI) is based on the distinct spectral response of (healthy) vegetation, which causes the unique "red edge" characteristic within the plant spectral signature (see Figure 2). Vegetation absorbs and reflects electromagnetic radiance in a very specific manner, generating a drop in the reflectance of (visible) red light wavelengths (RED) followed by an extensive increase in the reflection percentage of near-infrared wavelengths (NIR) at around 680 nm-780 nm. Red light wavelengths are absorbed for the purpose of photosynthesis, while near-infrared wavelengths are scattered due to intracellular leaf structure. This "red edge" is caused by the intracellular structure of leaves and the content of chlorophyll-a and is therefore strongly correlated with the photosynthetic activity of plants (Rivero et al. 2009; Mancino et al. 2014). The NDVI serves thus as proxy for plant vitality and productivity, as healthy vegetation contains more photosynthetically active in-leaf structures, increasing the gradient in reflectance percentage. Moreover, other surface types such as soil or urban structures without vegetation, display a linear spectral signature, allowing a clear distinguishment between vegetated and non-vegetated areas.

The NDVI is defined as

$$NDVI = \frac{NIR - RED}{NIR + RED}$$

where NIR represents the value for a specific pixel at the near-infrared band and RED the value of respective pixel at the (visible) red light band. The NDVI ranges from -1 to 1. While negative values imply water bodies, values between -0.1 and 0.1 usually imply barren areas (e.g. sand or rock). NDVI values higher than 0.15 (usually) correspond to vegetated areas. High values (close to 1) are consequently an indicator for healthy and photosynthetically productive vegetation, whereas low values imply unhealthy vegetation or a change in intracellular structure due to chlorophyll reduction. Noteworthy is the difference in NDVI ranges between biotope types. A initially interpreted low NDVI does not necessarily refer to unhealthy vegetation, but may indicate less dense biotope types such as bushes compared to forested areas.

Following the abovementioned image preselection, the NDVI is calculated for each image using the NIR and the RED band, which in case of Sentinel-2 are Band 8 and Band 4, respectively. The equation for calculating the NDVI using Sentinel-2 imagery is thus

$$NDVI = \frac{Band\ 8 - Band\ 4}{Band\ 8 + Band\ 4}$$

2.5.2 Normalized Difference Water Index

The Normalized Difference Water Index (NDWI) makes use of the Short-Wave Infrared (SWIR) and the Near Infrared (NIR) intervals of the electromagnetic spectrum and is strongly related to the intra-cellular water content in plants (Gao 1996). The SWIR interval of the electromagnetic spectrum is sensitive to the amount of spectral reflectance controlled by the amount of liquid water molecules in

internal leaf structures, resulting in a negative correlation between SWIR reflectance and plant water content. The spectral reflectance in the NIR interval on the other hand is determined by internal leaf structures and leaf dry matter content but remains unpersuaded by water content. By combining the NIR and the SWIR channels, variations in reflectance due to dry matter content in leaves or leaf internal structures can be minimized, and the accuracy of plant water content estimations increased (Gao 1996; JRC 2011; Ceccato et al. 2001). The NDWI is therefore a sensitive indicator to changes in plant water content and thus, for water stress. Its equation is analogous to the one for calculating the NDVI and can be described as

$$NDVI = \frac{NIR - SWIR}{NIR + SWIR}$$

NDWI values range from -1 to 1, where values close to 1 indicate high water content in plants and low values relate to low water content in plants, resulting in decreasing NDWI values in case of water stress. The NDWI is calculated for each image using the NIR and the SWIR band, which in the case of Sentinel-2 are Band 8 and Band 11, respectively. The equation for calculating the NDWI using Sentinel-2 imagery is thus

$$NDVI = \frac{Band\ 8 - Band\ 11}{Band\ 8 + Band\ 11}$$

As data from Band 11 (SWIR) is provided in a spatial resolution of 20 m x 20 m, it is resampled to 10 x 10 m in order to match the spatial resolution of Band 8 and Band 4.

2.6 Meteorological and Hydrological Data

Site-specific meteorological and precipitation data is obtained from the Bavarian Waterways Information Service (Gewässerkundlicher Dienst, BayLfU) for measuring sites associated with either of the study areas. This data is used to determine the mean monthly air temperature, Mean Growing Season Air Temperature (MGT), mean monthly precipitation rate and Mean Growing Season Precipitation (MGP) for each investigated year (2016 – 2020) and study area, respectively. Groundwater levels are obtained for monitoring wells associated with either of the study areas for the same period. The data is acquired in pursuance of identifying changes in precipitation patterns, temperature variations and fluctuations of the groundwater level during the global change-type drought 2018, thereby being able to link alterations in plant vitality to drought-induced environmental stresses, as well as to identify potential legacy effects in the following years. Information on the locations of all meteorological sites and monitoring wells is depicted in Map 1 and detailed information of the data sets are attached under appendices.

2.6.1 Mean Growing Season Air Temperature and Mean Growing Season Precipitation

The phenological cycle is divided into two different phases, namely the vegetative period and the dormancy. This study focused particularly on the Mean Growing Season Air Temperature (MGT) and the Mean Growing Season Precipitation Rate (MGP), which are both premised on the vegetative period of the respective area. Following the definition given by the German Meteorological Service (Deutscher Wetterdienst, DWD), the growing season, or vegetative period, can be described as each years' period during which plants are photosynthetically active. Climatic conditions are limiting factors to this period, during which daily temperatures are required to be on average at least 5°C and during which a certain humidity or rainfall amount has to occur (DWD 2021b). Deficits in temperature and water availability determine the remaining period of the phenological cycle, named dormancy. Plants are

photosynthetically (mostly) inactive during this time, wherefore dormancy is disregarded in this paper, as both vegetation indices used in this thesis focus on intracellular characteristics primarily predominant during the vegetative period. Following the definition by the DWD, the vegetative period for the selected study areas spans from April to October (see appendices for source data), wherefore MGT and MGP are calculated by taking into account the temperature values of these months. As previously mentioned, the first investigation time per year was chosen to be Spring-T1, ideally in April. Summer-T2 would ideally be in August and Autumn-T3 in October. The gathering of data is always subject to data availability. Data analysis and data processing on both the meteorological and hydrological data are conducted using Microsoft Excel 365.

2.7 Analysis of Plant Vitality by applying the NDVI and NDWI

Image processing is conducted using Quantum GIS (QGIS) version 3.16.1 with GRASS 7.8.4., while Microsoft Excel 365 is used for the statistical analysis and computing time series graphics. QGIS is a free and open-source Geographic Information System for geoscientific data and analysis where satellite imagery in raster format can be obtained through the Semi-Automatic Classification Plug-in from a wide array of available sensors. As the NIR and RED bands are available with a spatial resolution of 10 m, the deviating resolution of the SWIR band with 20 m is resampled to match the other bands spatial resolution. Data is subsequently exported and further processed using QGIS version 3.16.1 for image mapping, geoprocessing, spatial analysis and Microsoft Excel 365 for statistical calculations.

NDVI and NDWI values are calculated based on the aforementioned equations for each investigation time (Spring-T1, Summer-T2, Autumn-T2 of 2016-2020), generating raster maps with a resolution of 10 m x 10 m. Preliminary to the actual data analysis all satellite images are clipped to the shapes of the study areas in order to minimize data redundancy and reduce computing time. This data is subsequently intersected with the boundaries of respective biotope types in QGIS in order to additionally obtain the VI values per biotope type. Mean VI values are calculated for each investigation time, per study area and per biotope type, enabling the analysis of intra-annual changes, as well as the identification of inter-annual alterations in NDVI and NDWI values. Image mapping and statistical time series analyses comprising of box and whisker plots, as well as line diagrams, allow to additionally establish a baseline in VI values for each stage of the vegetative period and thus, to identify drought-related deviations in plant vitality. The “Raster Calculator” allows to perform certain calculations and analyses based on existing raster pixel values. For increasing the accuracy of obtained results, NDVI values which represent non-vegetated areas are masked out using the following expression

$$(\text{“}rasterband\#\text{”} \geq 0.15) * \text{“}rasterband\#\text{”}$$

In other words, for each cell with a value greater or equal to 0.15, the conditional expression evaluates to 1, which keeps the original value by multiplying it by 1. Or else the conditional expression evaluates to 0, which sets the raster value to 0. By applying this step, most raster cells covering non-vegetated areas, such as water bodies or barren areas of rock, gravel or sand are excluded from statistical analysis of the NDVI. To reveal differences in plant vitality of each study area and biotope types between the investigated years in comparison to reference year 2016, the VI maps of 2017, 2018, 2019 and 2020 are intersected with the VI maps of 2016, respectively.

Inter-annual changes were calculated using the following expression

$$NDVI\_2016 - NDVI\_year\ x$$

and followingly categorized

Inter-annual Changes in NDVI		
Class	**Pattern of Damage**	**NDVI-Difference**
	High Increase in Plant Vitality	$x < -0.15$
	Low-moderate Increase in Plant Vitality	$-0.15 \leq x < -0.025$
	No Change	$-0.025 \leq x < 0.025$
	Low-moderate Decrease in Plant Vitality	$0.025 \leq x < 0.15$
	High Decrease in Plant Vitality	$0.15 < x$

As high NDVI values indicate healthy vegetation, negative differences between reference year 2016 and another investigated year indicate an increase in plant vitality. The VI results are subsequently linked to the corresponding meteorological and hydrological data, allowing a classification of VI values to specific climatologic conditions. In Chapter Results index values specified per investigation point (Spring-T1, Summer-T2 or Autumn-T3) and study area are mostly given as mean values in brackets.

2.8 Study Areas and Biotope Types

All study areas are located alongside the Isar River, whose catchment area of about 8965 km² lies partly within Austria, but mainly in Bavaria, Southern Germany. The Isar River sources in the Alpine region Karwendel, Tyrol (Austria) and feeds after approx. 295 km into the Danube River close to Deggendorf, Bavaria. It passes with a mean gradient of 2.9 ‰ in northerly direction through the Bavarian alpine foreland, before crossing the morainic landscape of the Alpine foothills and proceeding through the Munich Gravel Plain to its estuary, located in the tertiary hill country (WWA Landshut 2020). Numerous, species rich biotope types can be found in the Isar floodplain areas, including but not being limited to near-natural riparian woodlands, grasslands, forb stand or floodplain scrub vegetation (Manderbach 2020). The Isar floodplains are home to a great number of rare and protected species, as well as migrating species. However, natural or near-natural floodplain areas along the Isar are, as for most rivers in Germany, particularly hard to find, since nearly all river stretches underwent severe modifications throughout the last centuries and oftentimes resulted in heavy geomorphological, biogeochemical, hydrological and/ or biological changes (BMU 2021). Especially the building of the Sylvenstein reservoir close to Lenggries at the upper reaches of the Isar in the 1950's resulted in lasting alterations in discharge rate. Flood protection of the Isar River valley is its main function, the dam however also contributes to sufficient and reliable channel flow during drier/ drought episodes. Despite these modifications, some sections of the river course in the alpine area and the Isar estuary are particularly noteworthy, as these sections were or are still only very slightly modified compared to other German floodplain areas.

The selection of the study areas was based on a close evaluation of their ecological importance, their spatial extent, geographical distribution, as well the data availability. All study areas are incorporated in either the European transnational network of protected areas, the Natura-2000 network, or are designated as a conservation site. By selecting areas which are designated as protected sites, the influences of factors, other than drought-induced changes in precipitation rates, fluctuations in groundwater levels or altered temperature patterns, are minimised. External factors would

exemplarily include influences resulting from direct or indirect land use changes, (diffuse) substance inputs through the use of fertilizers, herbicides and pesticides or changes in management measures.

The selection of biotope types investigated in this thesis is not based on the respective category of protected zone, however, but derived from data provided by the Bavarian State Ministry of the Environment (BayLfU) in the Bavarian Biotope Mapping ("Biotopkartierung Bayern"). The biotope mapping of Bavaria records ecologically valuable habitats that are worthy of protection. The acquisition of those biotopes focuses on the biotopes legally protected under §30 of the Federal Nature Conservation Act (BNatSchG) and Article 23 of the Bavarian Nature Conservation Act (BayNatSchG), as well as on the habitat types listed under the "Fauna-Flora-Habitat Directive" (FFH-RL). The selection of biotope types is based on the main type of vegetation as indicated in the Bavarian Biotope Mapping and narrowed down to suitable biotope type groups, if necessary. A list of all biotope types occurring in the analysed study areas are summarised in Table 2, while site-specific biotope types can be found in each study areas descriptive map, respectively. Map 1 depicts the location of all study areas, as well as the monitoring sites from which the meteorological and hydrological data was obtained. By choosing five different study areas, one in the upper, two in middle and two lower course of the Isar River, this thesis aims to ensure a better comparability of the results obtained. Furthermore, choosing study areas in different river sections, meteorological and hydrological site specifications can be more adequately assessed and compared. Site-specific descriptions, as well as the results of the VI assessments are enclosed in Chapter 3 – Results.

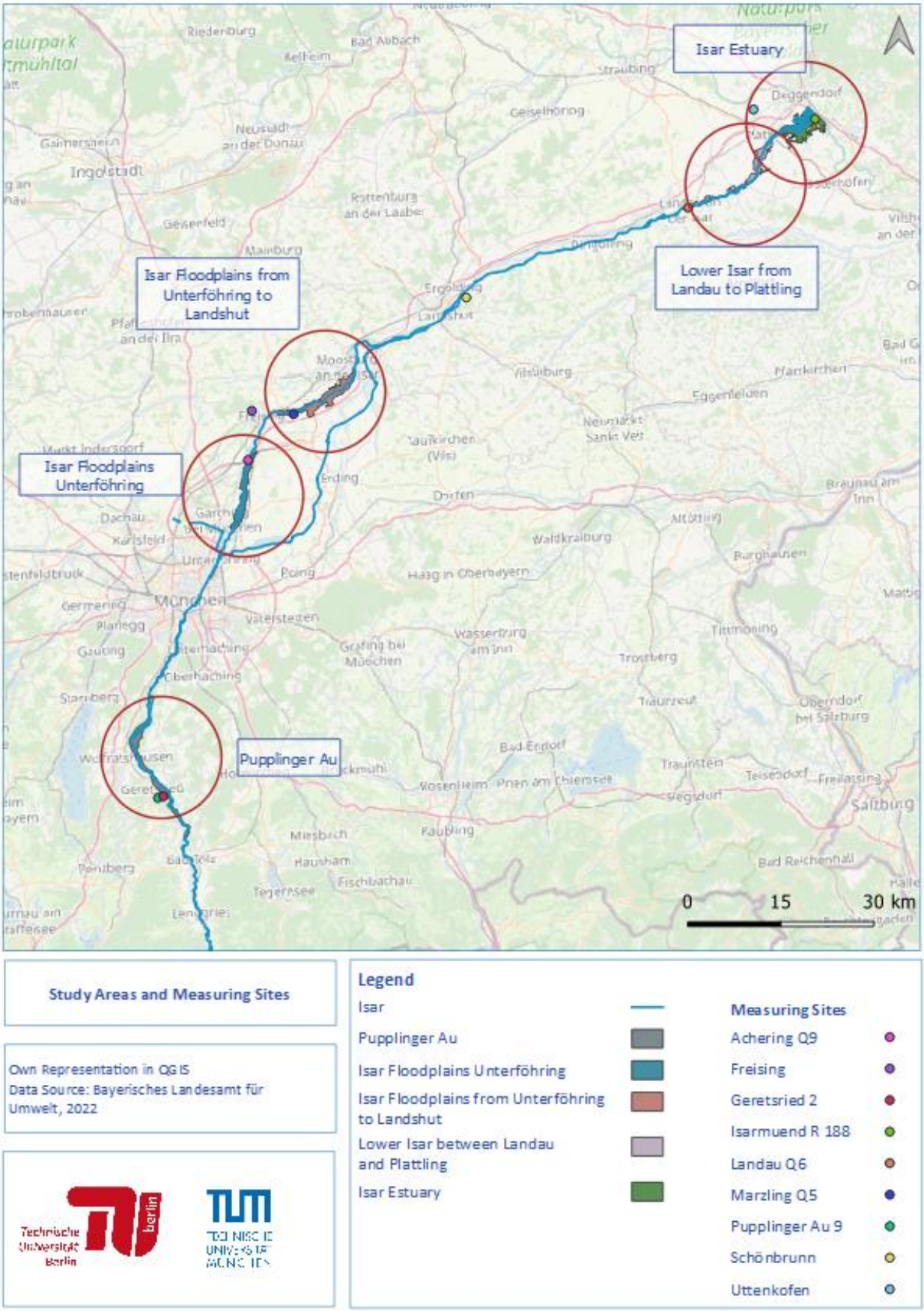

Map 1. Overview study areas and meteorological and hydrological monitoring sites.

Table 2. Biotope types of all study areas (own amendment; BayLfU 2021).

	ID	Name	Translation
Forested Areas	WA	Auwald	Floodplain forest
	WL	Laubwälder, mesophil	Deciduous forests
	WJ	Schlucht- und Schuttwald	Canyon forests
	WE	Kiefernwälder, basenreich	Pine forests
Shrubs, Hedges, Bushes	WD	Wärmeliebende Gebüsche	Thermophilic bushes
	WG	Feuchtgebüsch	Moist bushes
	WH	Hecken, naturnah	Hedges
	WI	Initiale Gebüsche und Gehölze	Initial bushes and shrubs
	WN	Gewässer-Begleitgehölze	Shrubs associated with streams
	WO	Feldgehölz	Field shrubs
	WX	Mesophile Gebüsche, naturnah	Mesophilic shrubberies
Wet Habitats of the Open Landscape	GG	Großseggenriede außerhalb der Verlandungszone	Sedges fen offside the siltation area
	GH	Feuchte und nasse Hochstaudenfluren, planar bis montan	Moist and wet tall forb communities
	GJ	Schneidriedsümpfe	Marshland dominated by Great fen sedge (Cladium mariscum)
	GN	Seggen- oder binsenreiche Nasswiesen, Sümpfe	Welands/ Wet meadows dominated by sedges and rushes
	GP	Pfeifengraswiesen	Meadows dominated by moor grass
	GR	Landröhrichte	Reeds
	MF	Flachmoore	Fen
	MF	Flachmoor, Streuwiese	Fen, straw meadow
	ST	Initalvegetation	Inital vegetation
Dry Habitats of the Open Landscape	GB	Magere Altgrasbestände und Grünlandbrachen	Nutrient-poor grassland and green fallow
	GC	Zwergstrauch- und Ginsterheiden	Dwarfshrub and broom heath
	GE	Artenreiches Extensivgrünland	Species-rich grassland
	GT	Magerrasen, basenreich	Nutrient-poor meadow / meagre meadow
	GW	Wärmeliebende Säume	Thermophilic fringe communities
	SG	Schuttfluren und Blockhalden	Scree plant communities
	ST	Initalvegetation, trocken	Initial vegetation on dry patches
Alpine Biotope Types	AR	Alpine Rasen	Alpine grassland
Others	RF	Ruderalflur	Ruderal meadows
	XR	Rohboden	Raw soil
Water ways	VC	Großseggenried der Verlandungszone	Sedges fen of the siltation area
	VH	Großröhrichte	Reeds

Following the Köppen-Geiger climate classification, the climate of the catchment area can be in average described as temperate continental, humid with warm summers, with an average annual air temperature range around 8.1°C (DWD 2020; ClimateData 2021). Considering the period from 1881 till 2020, the average annual air temperature ranged between the minimum of 5.9°C in 1887 and the maximum of 9.9°C in 2018, showing a clear upward trend (Figure 3) of 1.8 K in 2020 relative to the start of climate documentation in 1881 (DWD 2020). Depending on the model, predictions state an increase of approx. 4.5 K in the average annual air temperature in 2100 compared to 1881 (A1B emission scenario), if the current trend continuous (DWD 2021a). Average precipitation rates for the catchment area range from 700 mm – 2000 mm per year (BayLfU 2020c). The runoff regime, described as the yearly course of the mean runoff, is classified as Nival regime. This regime is dominated by the presence of extensive seasonal snow cover, as precipitation in winter is mainly accumulated in the form of snow. As a result, the lowest runoff rates occur during this season, whereas snowmelt in spring and early summer is superimposed by (liquid) precipitation, causing usually maximum runoff rates during these seasons (BayLfU 2020a). Site-specific meteorological and hydrological conditions are specified under each study area in Chapter 3 – Results.

a)

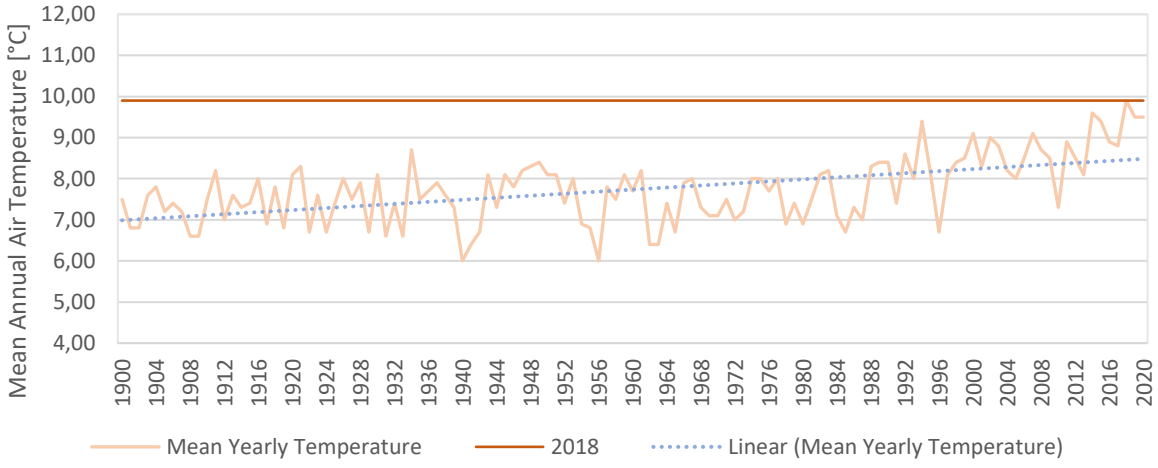

b)

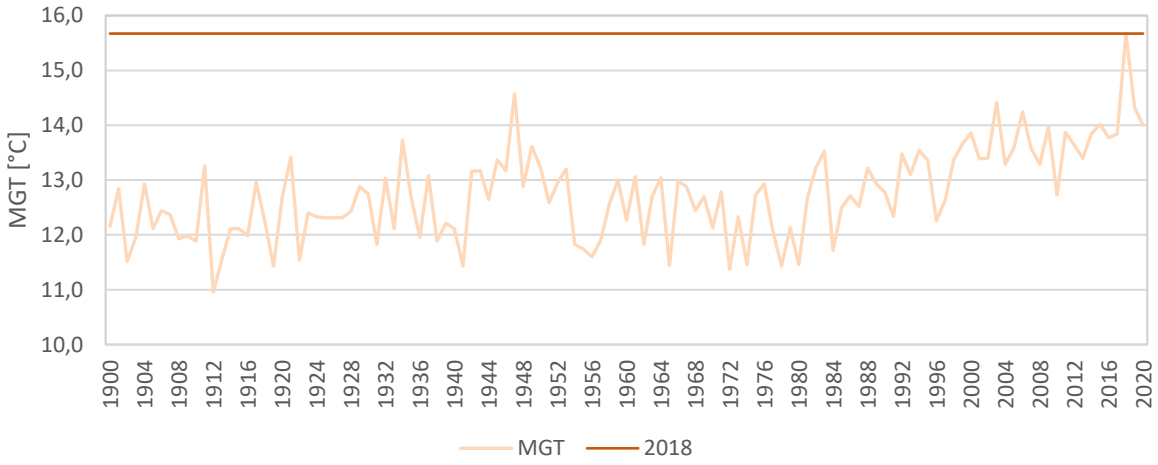

Figure 3. Mean annual air temperature (a) and mean growing season air temperature (MGT; b) of the Isar catchment area. The growing season encompasses the months April to October. Long-term average of MGT for the depicted period is at 12.64°C. The horizontal red lines denote the corresponding values of 2018, respectively (DWD 2020).

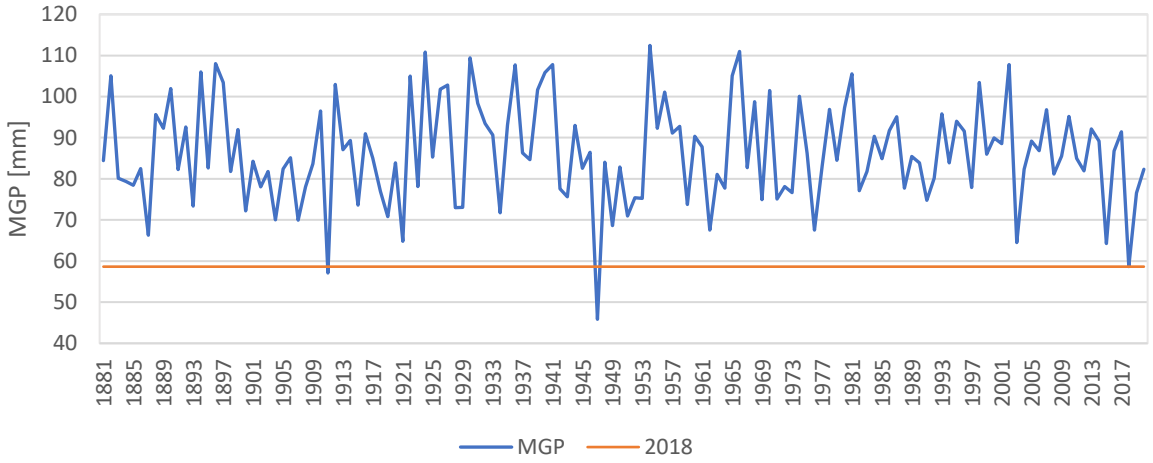

Figure 4. Mean growing season precipitation rate (MGP) of the Isar catchment area. The growing season encompasses the months April to October. Long-term average of MGP for the depicted period amounts to 86 mm. The horizontal orange line denotes the corresponding value of 2018 (DWD 2020).

3 Results

3.1 Study Area Upper Course – Pupplinger Au

The borders of this study area are derived from the conservation area “Isar floodplains from Schäftlarn to Bad Tölz”, former “Pupplinger and Ascholdinger floodplain” (“Naturschutzgebiet Isarauen zwischen Schäftlarn und Bad Tölz”) which encompasses at date approximately 1657 hectares and lies at about 576 m above sea level. Cyclic erosion and sedimentation create repeatedly new riverbeds in this area, which are subsequently populated by pioneer plants including alpine toadflax (*Linaria alpina*) or fairies' thimbles (*Campanula cochleariifolia*) and result in various stages of riparian vegetation development. Tamarisk stands or winter flowering heather-pine forests successively develop when conditions stabilize for instance. Gravel banks, oftentimes designated as bird protection areas serve as breeding grounds for rare bird species and are particularly protected during spring and summer months. Main risks to this area and its specialised communities are changes in the hydrological regime, recreation and tourism (ACADEMIC, n.d.; Manderbach 2020).

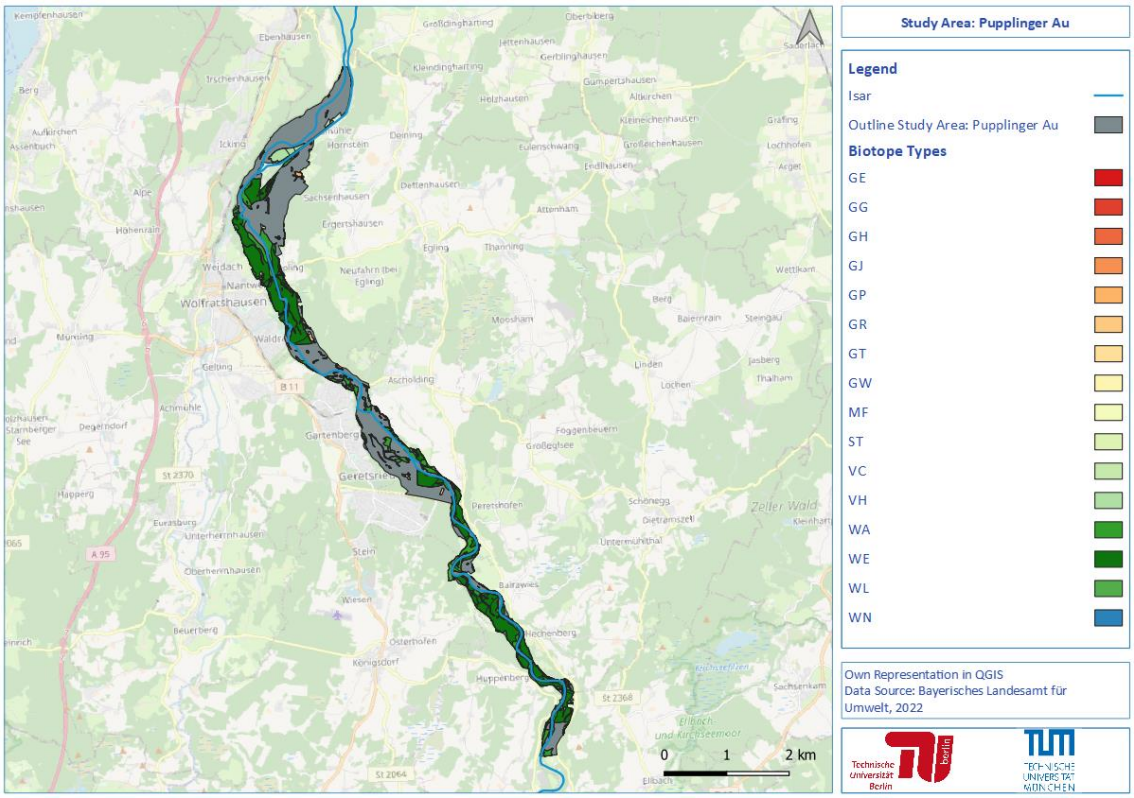

Map 2. Outline of study area Pupplinger Au with biotope types derived from the Bavarian Biotope Mapping.

Meteorological data was obtained from the station “Geretsried” and the monitoring well “Pupplinger Au 9”, both located in the immediate surroundings of this study area. Mean Growing Season Air Temperature (MGT) was lowest in 2016 (13.46°C), followed by 2017 (14.30°C), 2020 (14.50°C), 2019 (14.80°C) and 2018 (16.02°C) in increasing order. 2018 was characterized by above-average hot and dry conditions, ranking highest in mean monthly air temperatures for April, May, July and August compared to the other years. Mean Growing Season Precipitation Rates (MGP) differed significantly among the years and were highest in 2016 (149 mm). Similar values were recorded for 2017 (132 mm), 2019 (130 mm) and 2020 (137 mm), but were substantially lower in 2018 (77 mm) (see Apendices). Groundwater fluctuations remained mostly imperceptible throughout the investigation period, but experienced a flattening in spring 2018.

Site-specific Meteorological and Hydrological Conditions

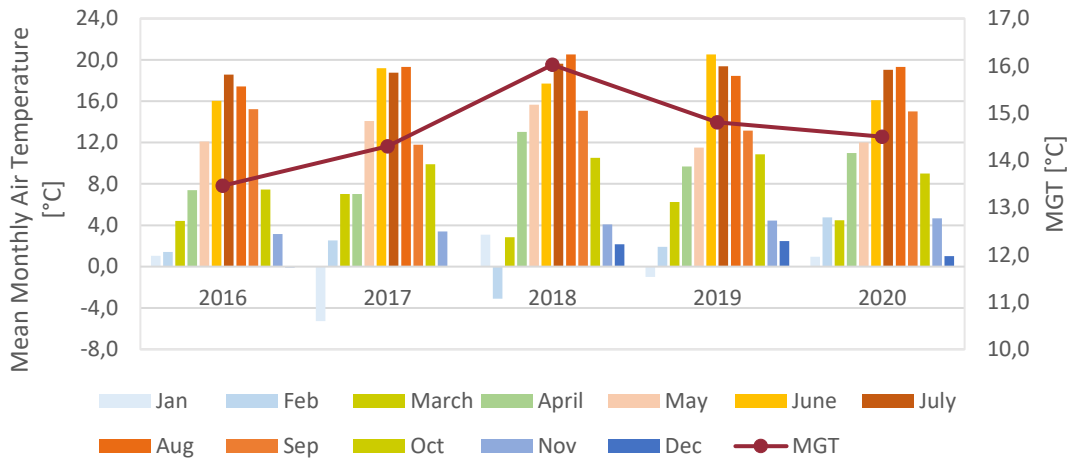

(a)

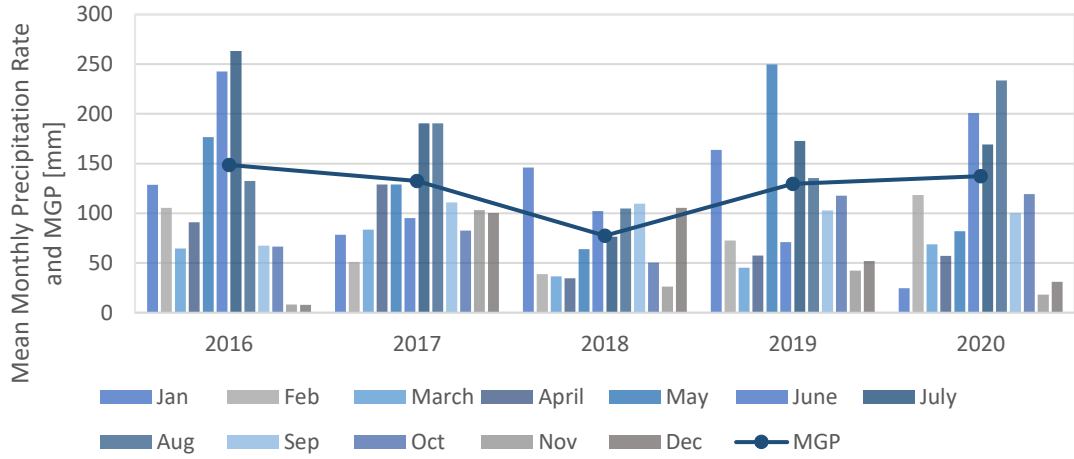

(b)

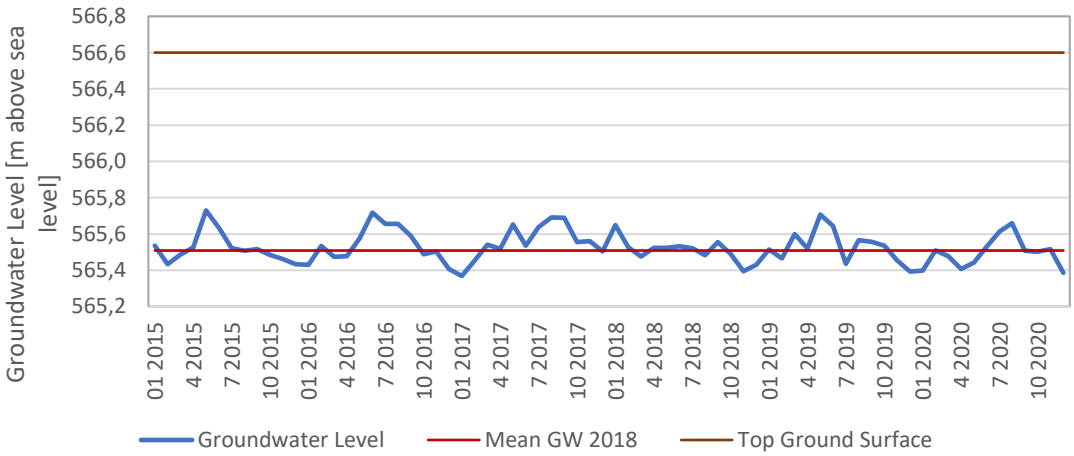

(c)

Figure 5. Mean monthly air temperature and mean growing season air temperature (MGT; a), mean monthly precipitation rate and mean growing season precipitation rate (MGP; b), as well as groundwater level and groundwater-surface distance (c) of study area Pupplinger Au. The growing season encompasses the months April to October (BayLfU 2020b; 2020d; 2020c; 2020e).

3.1.1 NDVI – Pupplinger Au

Satellite Data

Table 3. Satellite imagery used in the NDVI assessment of study area Pupplinger Au. Differences in investigation times arose from data availability limitations. Greyed out times are disregarded in the analysis by reason of undue temporal deferral.

Time	2016	2017	2018	2019	2020
T1	29 April	17 May	07 April	19 April	08 April
T2	27 August	25 August	22 August	30 August	21 August
T3	16 October	16 October	16 October	29 September	15 September

Intra-annual Alterations in NDVI Values

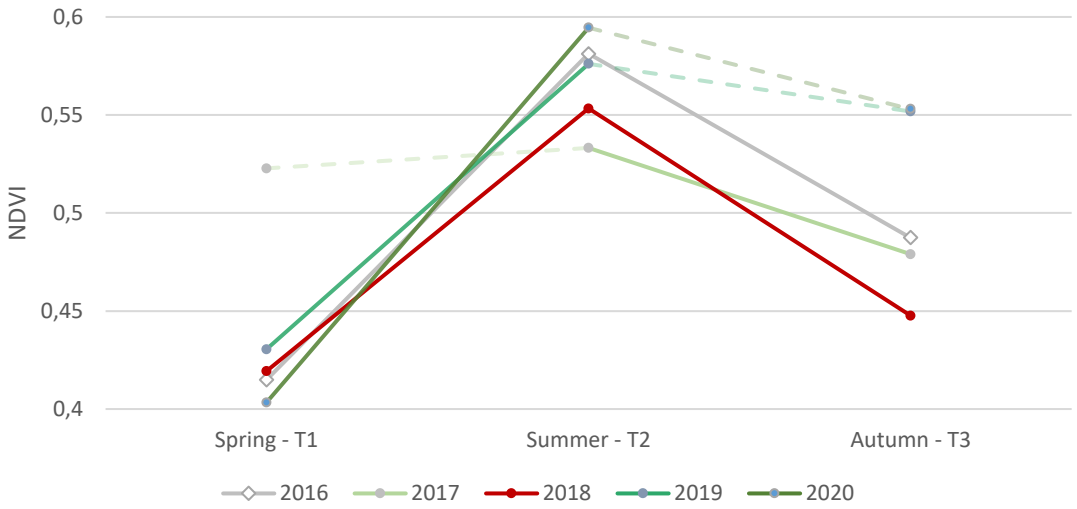

Figure 6. Intra-annual alterations in NDVI values for all investigated years (2016-2020) of Pupplinger Au. Dashed lines indicate the disregarded values, as outliers in investigation times can cause incomparability of obtained results.

Intra-annual alterations in NDVI values are depicted in Figure 6 for the entire study area Pupplinger Au. For all investigated years the NDVI, corresponding to plant vitality, peaks during investigation time Summer-T2. NDVI values for all investigated years subsequently decline to Autumn-T3. This characteristic development in NDVI values can be explained by the annual increase and decline in plant biomass and therefore chlorophyll-a content throughout the phenological cycle. However, steepness of increase and decrease in NDVI values varies for each year. Interesting results were obtained for Spring-T1 in 2018 compared to the reference year 2016. The NDVI for this investigation point is higher in 2018 (0.42) than in 2016 (0.41). This can be connected to earlier development of leaves/ plant biomass due to a shift in the growing season, caused by warmer climatic conditions in spring 2018. This is particularly noteworthy when considering the (moderate) difference in investigation times (29th April 2016 and 07th April 2018). However, NDVI values fall significantly back for Summer-T2 (0.55) and Autumn-T3 (0.45) in 2018 compared to Summer-T2 (0.58) and Autumn-T3 (0.49) in 2016, indicating impaired plant vitality. These declines in seasonal NDVI values can be linked to the contrasting meteorological and hydrological conditions between 2016 and 2018. The year 2018 has been, as previously described, significantly hotter than the reference year 2016 and with a MGP approx. 70 mm lower in comparison to 2016. Interestingly, the year 2020 exhibits highest NDVI for Summer-T2 (0.59), although having started with the lowest NDVI in Spring-T1 (0.40). (see Appendices).

The following two maps (Map 3 and Map 4) exemplarily display the intra-annual NDVI regime of study area Pupplinger Au for the reference year 2016 and the drought year 2018, respectively. Those two years are exemplarily chosen, as this thesis primarily aims at investigating the differences in plant vitality caused by the drought 2018. Pupplinger Au is displayed as sample for floodplain areas alongside the upper reaches of the Isar River.

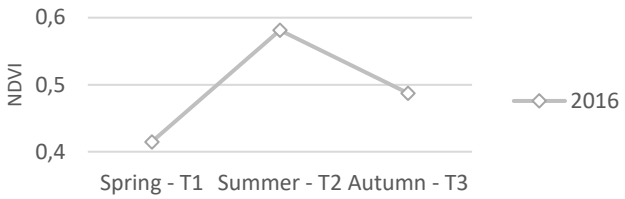

Figure 7. Intra-annual alterations of the NDVI in 2016 for the entire study area Pupplinger Au with Spring-T1 (0.41), Summer-T2 (0.58) and Autumn-T3 (0.49). The following map visualizes this course in NDVI values.

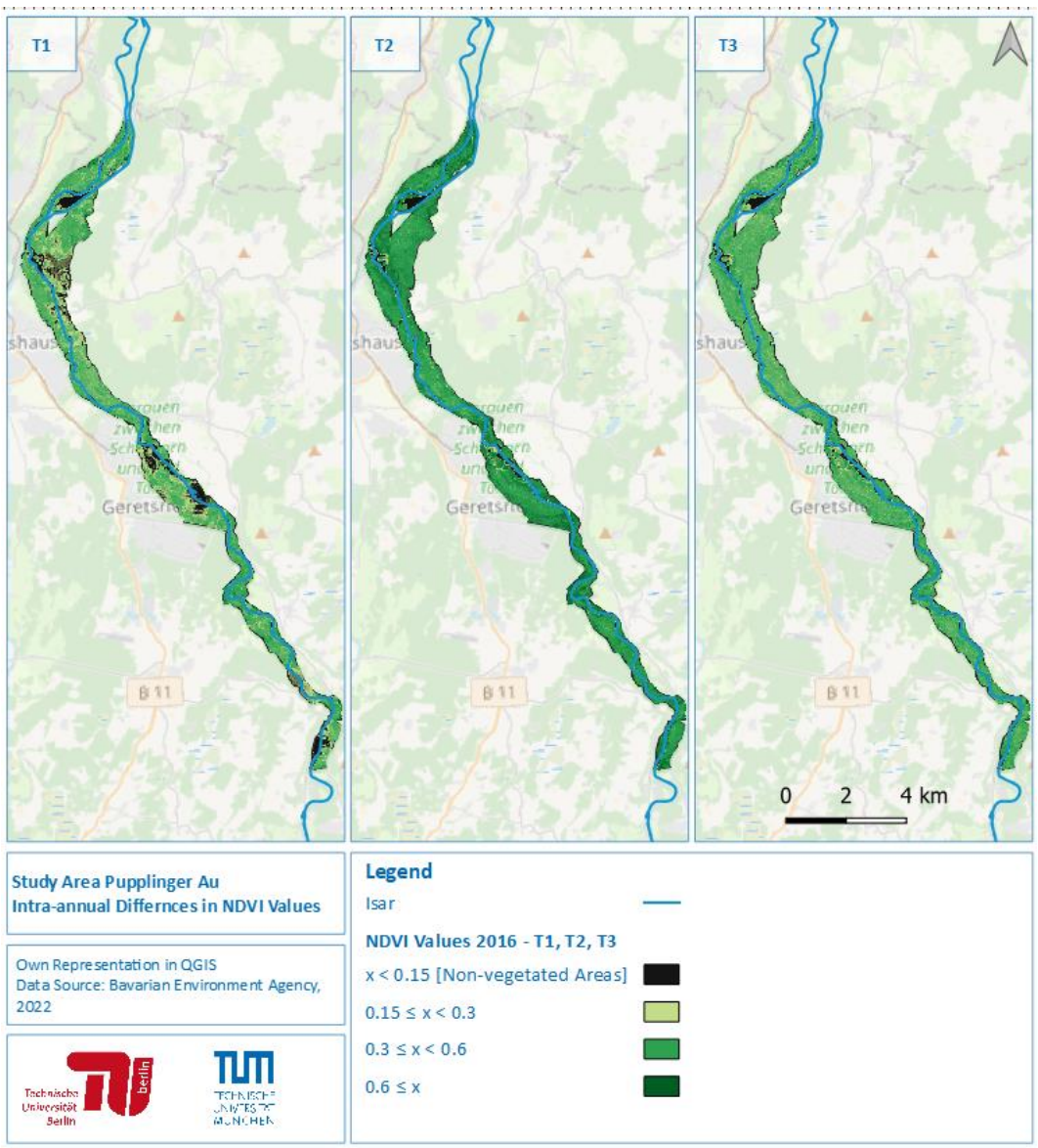

Map 3. NDVI throughout the year 2016 for study area Pupplinger Au. Darker green nuances indicate higher NDVI values, as detectable in Summer-T2, whereas lighter shades depict lower NDVI values. Black parts indicate non-vegetated areas or masked out cloud coverage.

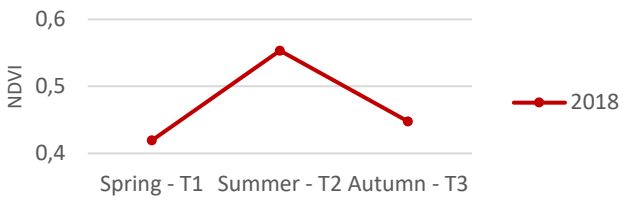

Figure 8. Intra-annual NDVI regime of 2018 for the entire study area Pupplinger Au with Spring-T1 (0.42), Summer-T2 (0.55) and Autumn-T3 (0.45). The following map visualizes those results.

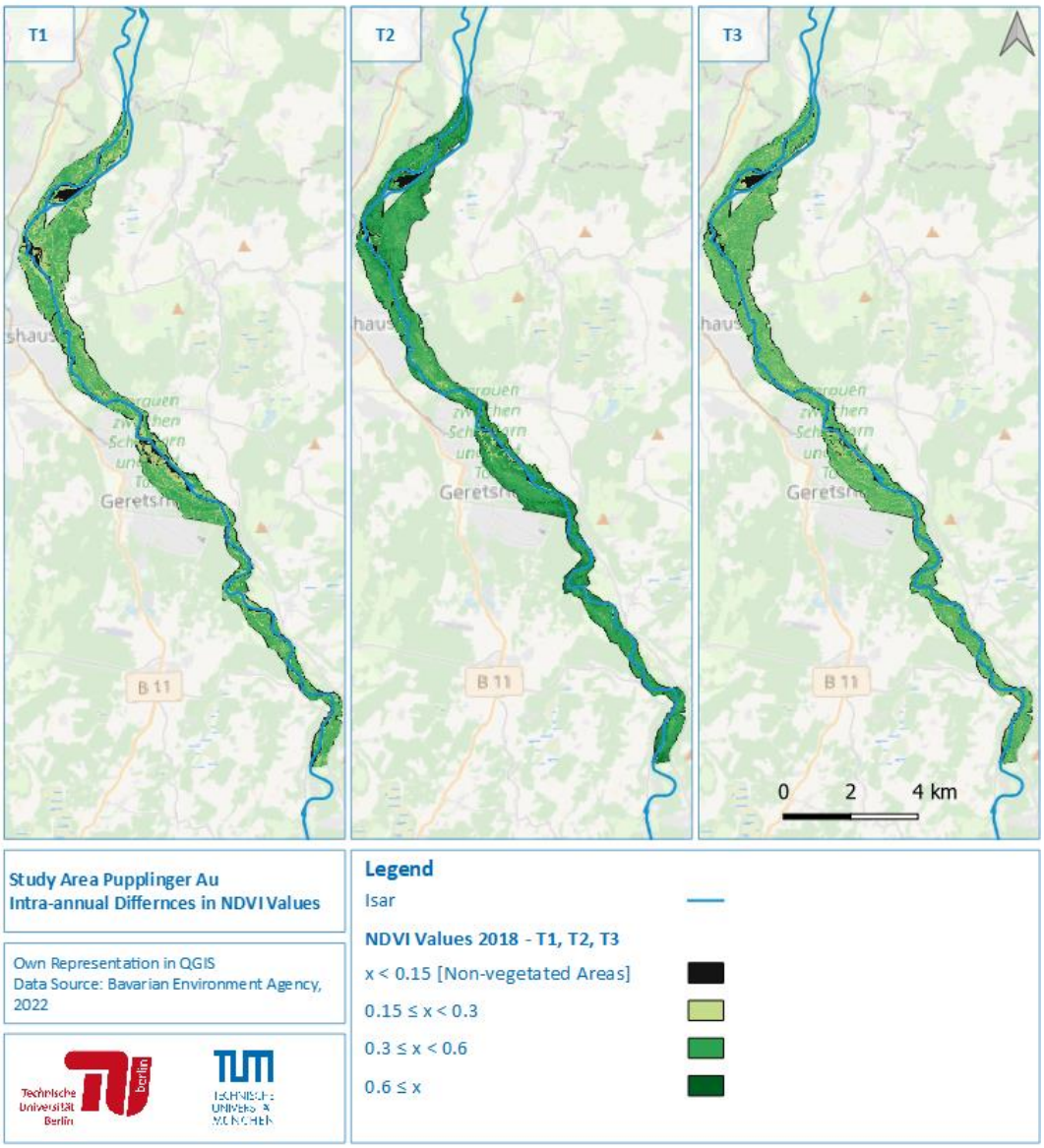

Map 4. NDVI throughout the year 2018 for Pupplinger Au. Darker green nuances indicate higher NDVI values, as detectable in Summer-T2, whereas lighter shades depict lower NDVI values. Black parts indicate non-vegetated areas or masked out cloud coverage.

Intra-annual alterations in NDVI values per biotope type and investigated year are depicted in Figure 8. The NDVI of all investigated biotope types peaks during investigation point Summer-T2 and subsequently declines to Autumn-T3. However, steepness of increase and decrease in NDVI values varies for each year and biotope type, respectively. For all four biotope types the NDVI regime in 2018 is the lowest out of all investigated years.

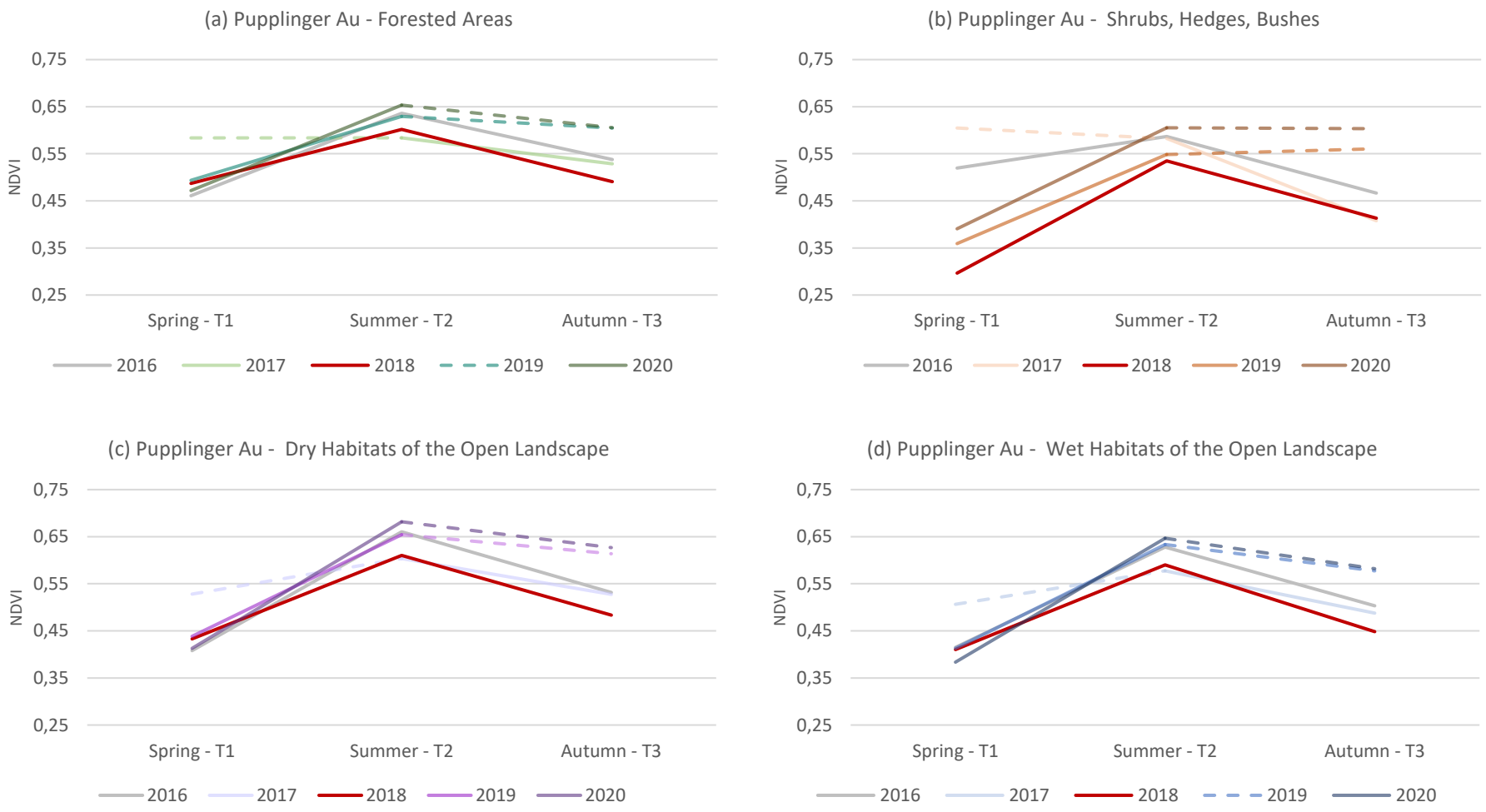

Figure 9. Intra-annual alterations of the NDVI values per biotope type and investigated year. NDVI regimes display specific signatures for (a) Forested Areas (NDVI 0.46-0.65), (b) Shrubs, Hedges and Bushes (NDVI 0.30-0.61), (c) Dry Habitats of the Open Landscape (NDVI 0.41-0.68) and (d) Wet Habitats of the Open Landscape (NDVI 0.38-0.65). The 2018 NDVI regimes are, in comparison to the other investigated years, in average lowest for all biotope types. Especially by contrast with the reference year 2016, all biotope types display significantly lower NDVI regimes in 2018. These results can be connected to the meteorological and hydrological conditions, meaning that all biotope types experienced plant vitality decreases following the drought event 2018.

Inter-annual Differences in NDVI Values for Study Area Pupplinger Au and per Biotope Type

The following maps display the inter-annual differences in NDVI values between the reference year 2016 and the other investigated years (2017, 2018, 2019 and 2020). Differences were calculated using the equation found under Materials and Methods. Changes in plant vitality were derived thereof and are depicted in the legend. The alleged increases in plant vitality for all T1 can be traced back to partial cloud coverage in obtained satellite imagery for Spring-T1 2016. Images of higher quality with lesser cloud coverage were not obtainable for this time and sensor.

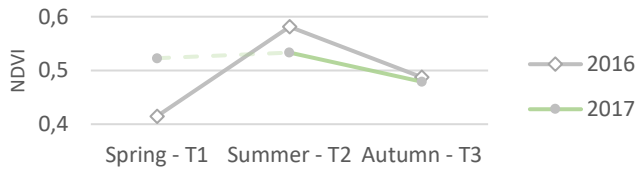

Figure 10. Mean intra-annual alterations of the NDVI 2016 and NDVI 2017 for the entire study area. Summer-T2 (0.53) of 2017 is significantly lower than Summer-T2 of 2016 (0.58). Both NDVI regimes decline in Autumn-T3 to 2017 (0.48) and 2016 (0.49). Spring-T1 of 2017 is disregarded, as data was obtained May 17th, causing incomparability of the obtained results Those differences in NDVIs are visualized in Map 5.

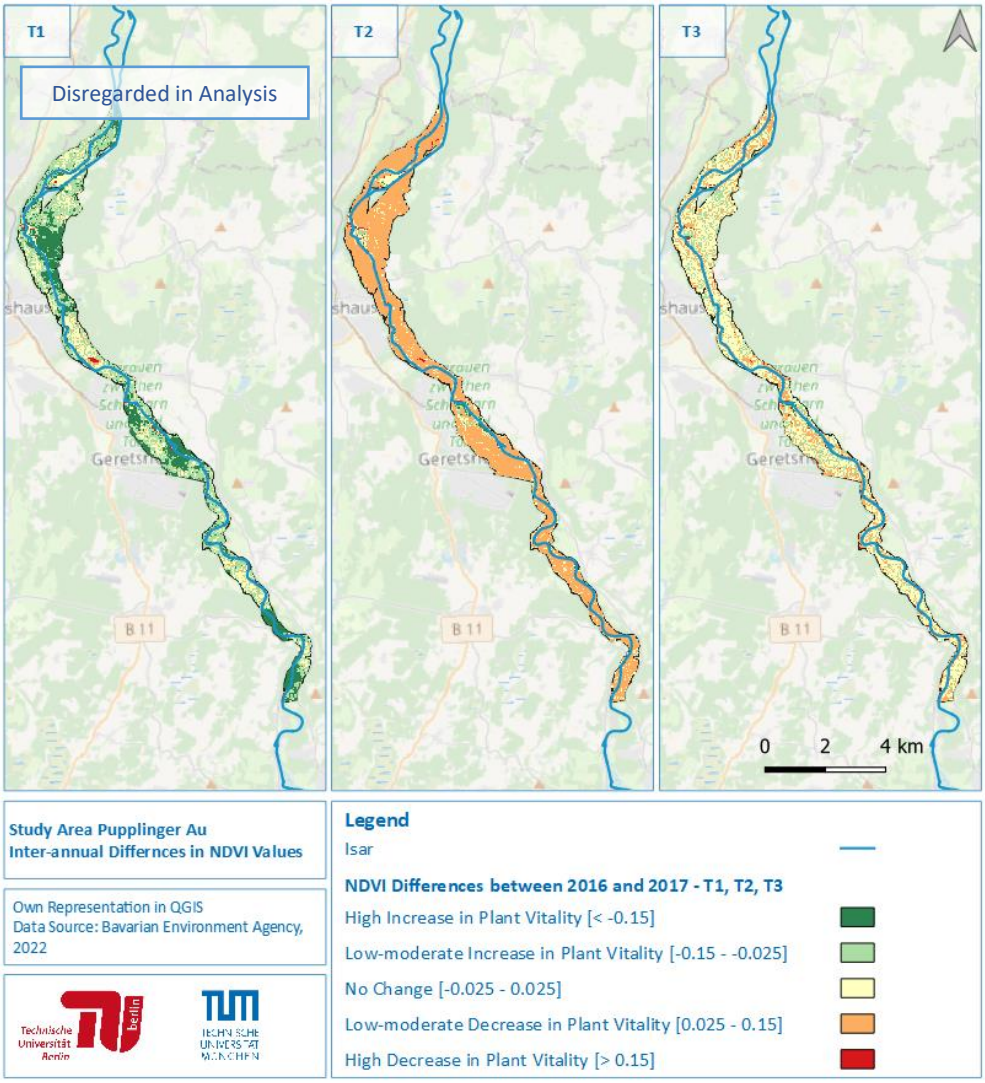

Map 5. Inter-annual differences in NDVI values Pupplinger Au. A comprehensive low-moderate decrease in plant vitality can be observed between 2016-2017 at Summer-T2, whereas almost no change is detected for 2016-2017 at Autumn-T3. Results depict a fragmentation of small plots for the latter, displaying various changes, most likely depending on biotope types.

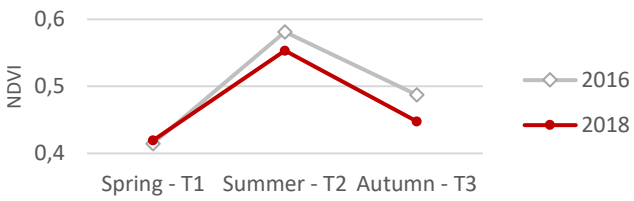

Figure 11. Mean intra-annual alterations of the NDVI 2016 and NDVI 2018 for the entire study area Pupplinger Au. Spring-T1 of 2016 and 2018 have almost the same NDVI value (0.41) and (0.42) respectively, while Summer-T2 (0.55) and Autumn-T3 (0.45) of 2018 depict reduced NDVI values compared to Summer-T2 (0.58) and Autumn-T3 (0.49) of 2016. Those differences in NDVI values are visualized in Map 6.

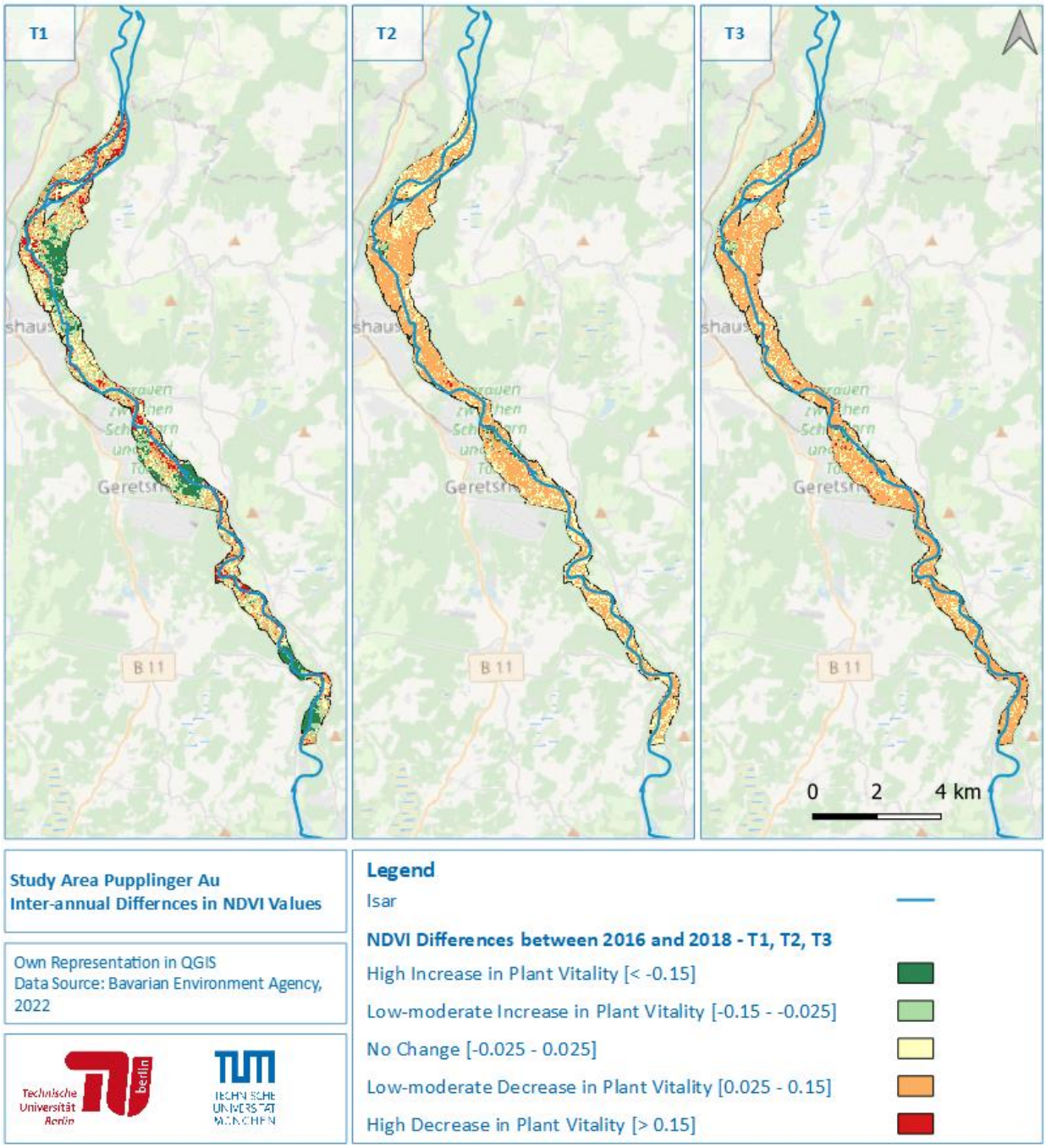

Map 6. Inter-annual differences in NDVI Pupplinger Au. Disregarding the erroneous display of plant vitality increase due to cloud coverage in Spring-T1, the remaining surfaces depict low-moderate and partially high decreases in plant vitality for this investigation point (2016-2018 Spring-T1). Exhaustive low-moderate decreases in plant vitality can be observed between 2016-2018 both at Summer-T2 and Autumn-T3.

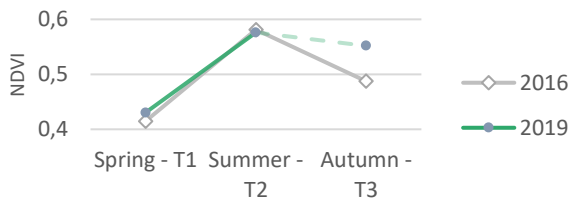

Figure 12. Mean intra-annual alterations of the NDVI regimes of 2016 and 2019 for the entire study area Pupplinger Au. Spring-T1 of 2019 (0.43) is slightly higher than Spring-T1 of 2016 (0.41), while the same NDVIs are recorded for Summer-T2 of 2016 and 2019 (0.58). Autumn-T3 is disregarded in this analysis as data was obtained September 29th, 2019. Distortions stemming from temporal deferral in the NDVI difference between 2016 and 2019 could therefore not be excluded. NDVI Differences are visualized in Map 7.

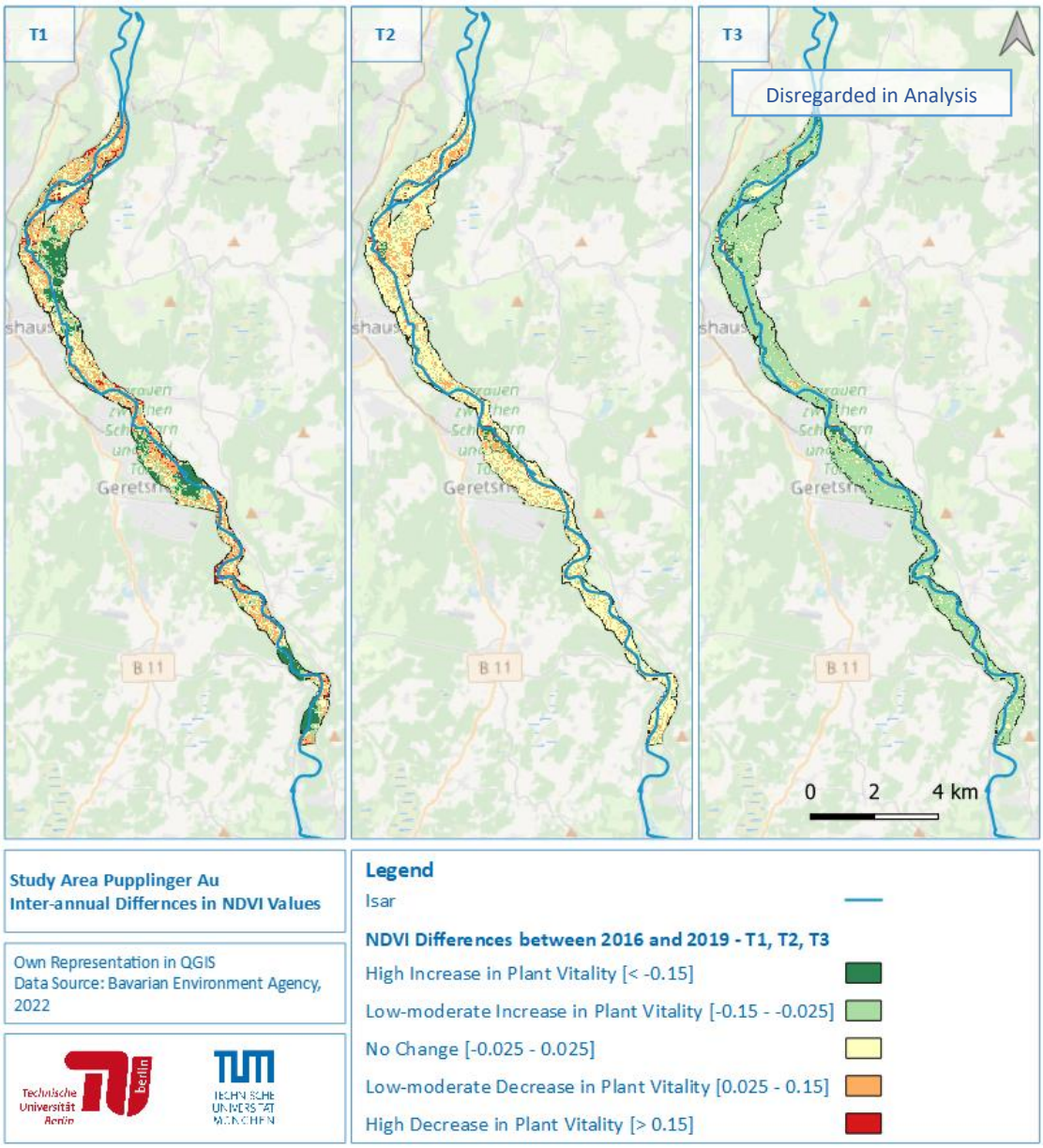

Map 7.Inter-annual differences in NDVI Pupplinger Au.Disregarding the erroneous display of plant vitality increase due to cloud coverage in T1, the remaining surface exposes low-moderate decreases in plant vitality for the investigation point Spring-T1 (2016-2019). Minor low-moderate decreases in plant vitality are detected in the comparison between 2016-2019 for Summer-T2, but plant vitality was subject to no change for the most part at this investigation point. Low-moderate increases in plant vitality are detected for Autumn-T3 (2016-2019), but are disregarded in the analysis as high quality satellite imagery was only obtainable for Sep. 2019 and not Oct. 2019.

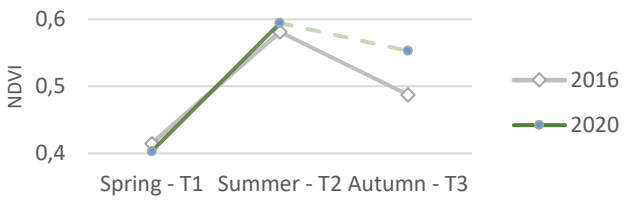

Figure 13.Mean intra-annual alterations of the NDVI 2016 and NDVI 2020 for the entire study area Pupplinger Au. Spring-T1 of 2020 (0.40) is slightly lower than Spring-T1 of 2016 (0.41), while a slightly higher NDVI value was recorded for Summer-T2 of 2020 (0.59) compared to Summer-T2 of 2016 (0.58). Autumn-T3 of 2020 is disregarded in this analysis as data was obtained Sep. 15th, causing incomparability of the obtained results by reason of undue temporal deferral. NDVI Differences are visualized in Map 8.

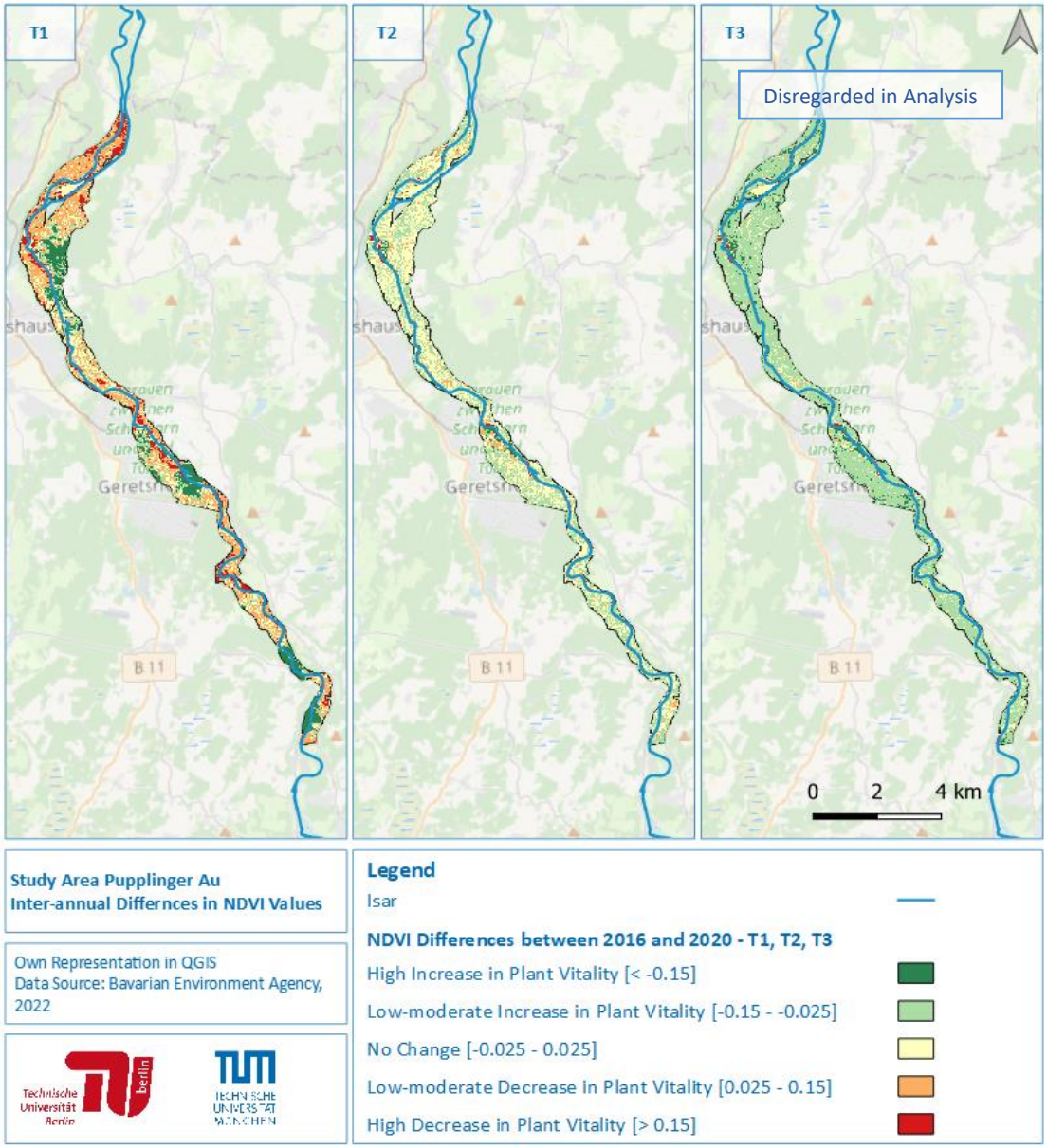

Map 8.Inter-annual differences in NDVI Pupplinger Au. Disregarding the erroneous display of plant vitality increase due to cloud coverage at Spring-T1, the remaining surface exposed fragmented low-moderate and high decreases in plant vitality for this investigation point (2016-2020). Minor low-moderate decreases in plant vitality were detected in the comparison between 2016-2020 for Summer-T2, but plant vitality was subject to no change for the most part. Low-moderate increases in plant vitality were detected for Autumn-T3 (2016-2020), but are disregarded in the analysis as high quality satellite imagery was only obtainable for Sep. 2020. Distortions in the NDVI results can therefore not be excluded. This map adequately visualizes the results depicted in Figure 13.

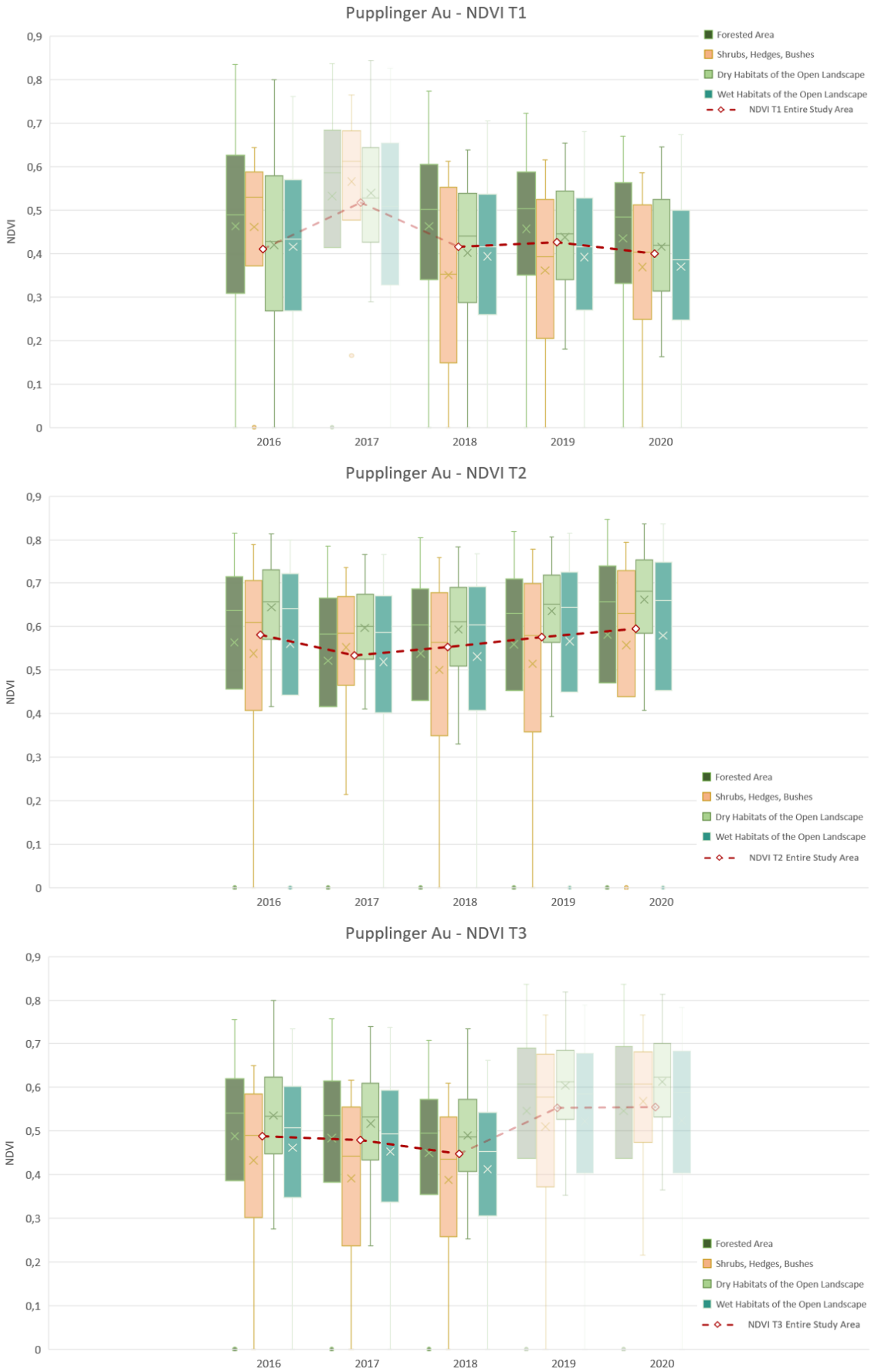

Figure 14. Inter-annual differences in NDVI values per biotope type and year of study area Pupplinger Au.

Box and whisker plots describe the variability of NDVI value distribution within each biotope type and depict the scatter range. Scattering is highest for Shrubs, Hedges and Bushes, followed by Dry Habitats of the Open Landscape, Wet Habitats of the Open Landscape and are lowest for Forested Areas. Dotted red lines indicate the mean NDVI values for the entire study area in relation to each biotope type. All biotope types exhibit lower mean NDVI values for each investigation point (Spring-T1, Summer-T2 and Autumn-T3) for the drought year 2018, when compared to the refernce year 2016. The only exeption are Forested Areas, which display a lower mean NDVI at Spring-T1 in 2016 than at Spring-T1 in 2018.

By contrast with all investigated years, however, Forested Areas exhibt the lowest mean NDVI at Summer-T2 in 2017 (0.58) out of all investigated years and the lowest mean NDVI at Autumn-T3 in 2018(0.49). Shrubs, Hedges and Bushes depict the lowest mean NDVI for all investigation points (Spring-T1, Summer-T2 and Autumn-T3) in 2018. Contrary to this, Dry Habitats of the Open Landscape display the lowest mean NDVIs at Spring-T1 in 2016 and 2020 with equal values (0.41), the lowest mean NDVI at Summer-T2 in 2017 (0.60) and the lowest mean NDVI at Autumn-T3 in 2018 (0.48). Wet Habitats of the Open Landscape exhibit lowest mean NDVI at Spring-T1 in 2018 (0.41), the lowest mean NDVI at Summer-T2 in 2017 (0.58) and the lowest mean NDVI at Autumn-T3 in 2018 (0.45). These results indicate the importance of considering regional site conditions, as well as differentiating between different biotope types.

3.1.2 NDWI – Pupplinger Au

Satellite Data

Table 4. Satellite imagery used in the NDWI assessment of Study Area Pupplinger Au. Differences in investigation times arose from limitations in data availability. Greyed out times are disregarded in the analysis by reason of undue temporal deferral.

Time	2016	2017	2018	2019	2020
T1	29 April	24 April	07 April	19 April	08 April
T2	27 August	25 August	22 August	30 August	21 August
T3	16 October	16 October	16 October	29 September	15 September

Intra-annual Alterations in NDWI Values

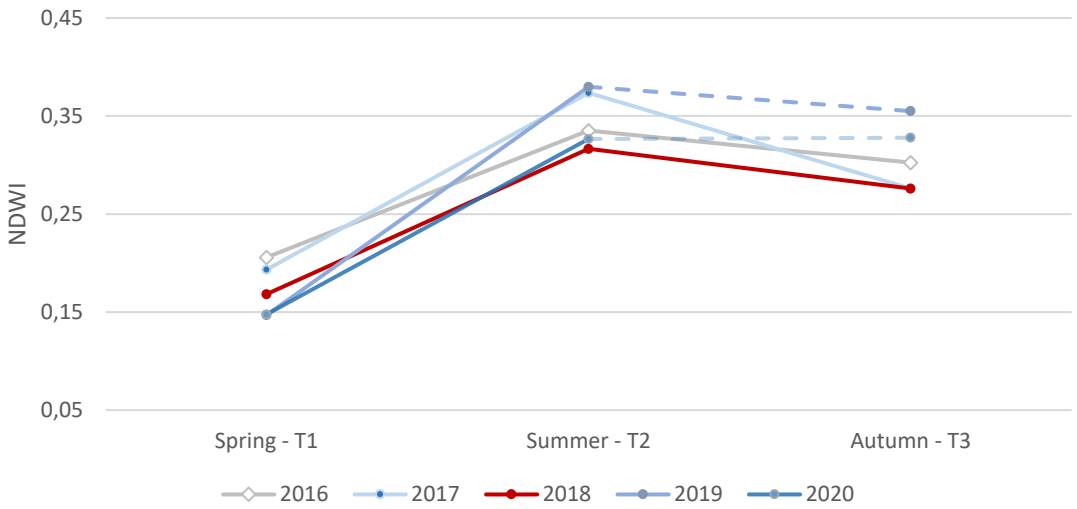

Figure 15. Intra-annual alterations in NDWI for the entire study area Pupplinger Au. Dashed lines indicate the (disregarded/ excluded) values, as outliers of investigation times may cause incomparability in obtained results.

Intra-annual alterations in NDWI values are depicted in Figure 15 for the entire study area Pupplinger Au. For all investigated years, the NDWI peaks during investigation point Summer-T2 of respective year. NDWI values for all investigated years subsequently decline to Autumn-T3. This characteristic development in NDWI values can be explained by the positive correlation between plant biomass and intracellular water content with regards to the normal course of the phenological cycle. However, steepness of increase and decrease in NDWI values varies for each year. The NDWI regime in 2019 increases with the steepest gradient, followed by 2017, 2020, 2018 and 2016 in decreasing order. The NDWI regimes of 2016 and 2018 run almost parallel to each other, where the 2018 NDWI constantly lies below the 2016 NDWI. Spring-T1 (0.17), Summer-T2 (0.32) and Autumn-T3 (0.28) during 2018 are significantly lower in comparison to Spring-T1 (0.21), Summer-T2 (0.34) and Autumn-T3 (0.30) during 2016. The disparate meteorological conditions within the investigation period (2016-2020) are closely tied to the obtained differences in NDWI regimes, where both temperature and precipitation rate in 2018 heavily deviated from the ones of the reference year 2016. This results in impediments for plant growth and thus, reduced plant water content measured by the NDWI. The NDWI regimes of 2019 and 2020 start with quite low values at Spring-T1 (both 0.15), but recover at Summer-T2 (0.38 and 0.33).

The following figures (16 and 17) and maps (Map 9 and Map 10) exemplarily display the intra-annual course in NDWI values of this study area for the reference year 2016 and the drought year 2018, respectively. These depictions are enclosed for comprehension and overview reasons. Pupplinger Au is chosen and plotted as example for floodplain areas alongside the upper reaches of the Isar River. Figures and maps depicting the intra-annual NDWI regimes of study area Isar Floodplains from Unterföhring to Landshut (middle reaches) and Isar Estuary (lower reaches) are enclosed in the following subchapters.

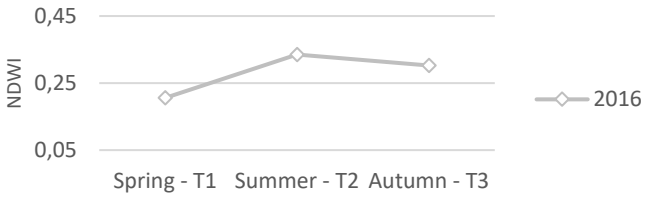

Figure 16. Mean intra-annual alterations of the NDWI 2016 for Pupplinger Au with Spring-T1 (0.21), Summer-T2 (0.33) and Autumn-T3 (0.30). The following Map 9 visualizes the intra-annual alterations.

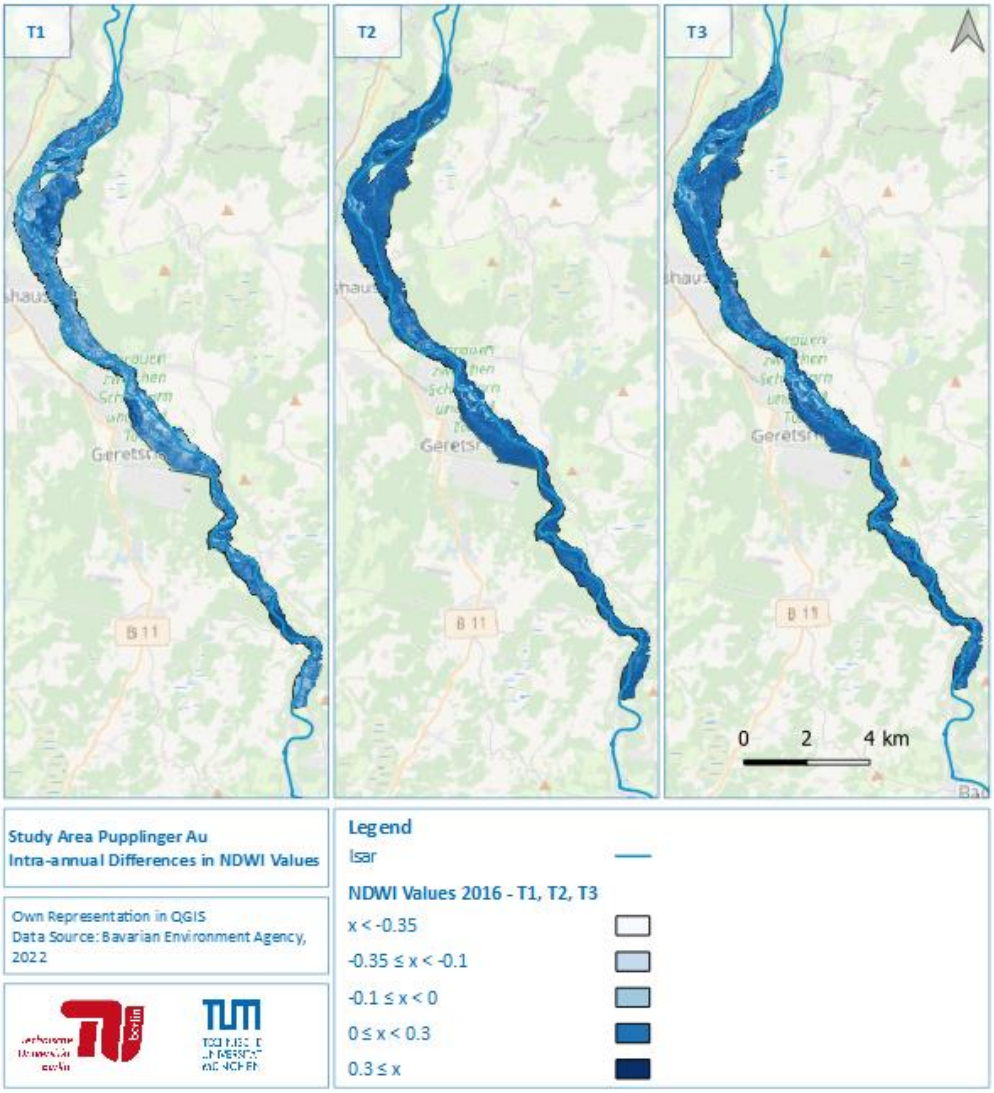

Map 9. Intra-annual differences in NDWI values of Pupplinger Au. A clear increase in NDWI is visible for the investigation point Summer-T2, adequately displayed by darker nuances in blue compared to investigation point Spring-T1. Minor differences are noticebale between Summer-T2 and Autumn-T3, indicating slow decreases in NDWI and thus plant water content between summer and autumn of respective year.

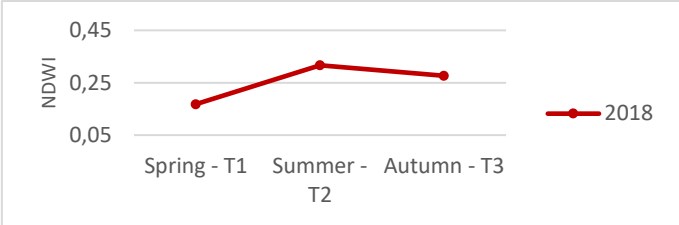

Figure 17. Mean intra-annual alterations of the NDWI 2018 for the entire study area with Spring-T1 (0.17), Summer-T2 (0.32) and Autumn-T3 (0.28). Intra-annual alterations throughout 2018 are visualized in Map 10.

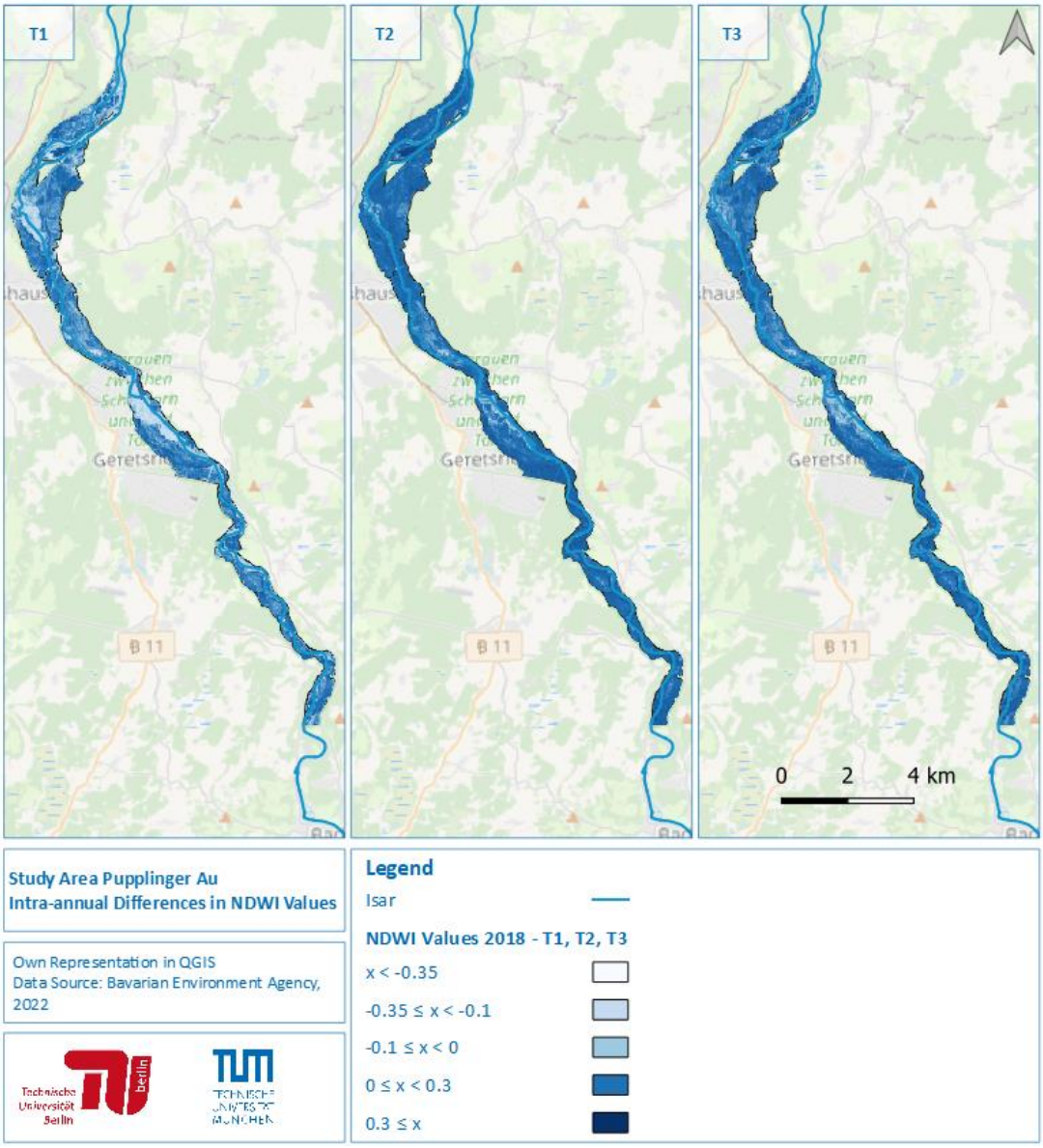

Map 10. Intra-annual differences in NDWI values for study area Pupplinger Au. A clear increase in NDWI is visible for the investigation point Summer-T2, adequately displayed by darker nuances in blue compared to investigation point Spring-T1. Minor differences are noticebale between Summer-T2 and Autumn-T3, caused by lasting accumulation of intra-cellular water content.

Intra-annual alterations in NDWI values per biotope type and investigated year are depicted in Figure 17. For all biotope types, NDWI peaks during investigation point Summer-T2 and subsequently declines to Autumn-T3. However, steepness of increase and decrease in NDWI varies for each year and biotope type, respectively. For all four biotope types the NDWI regime in 2018 is in average the lowest out of all investigated years.

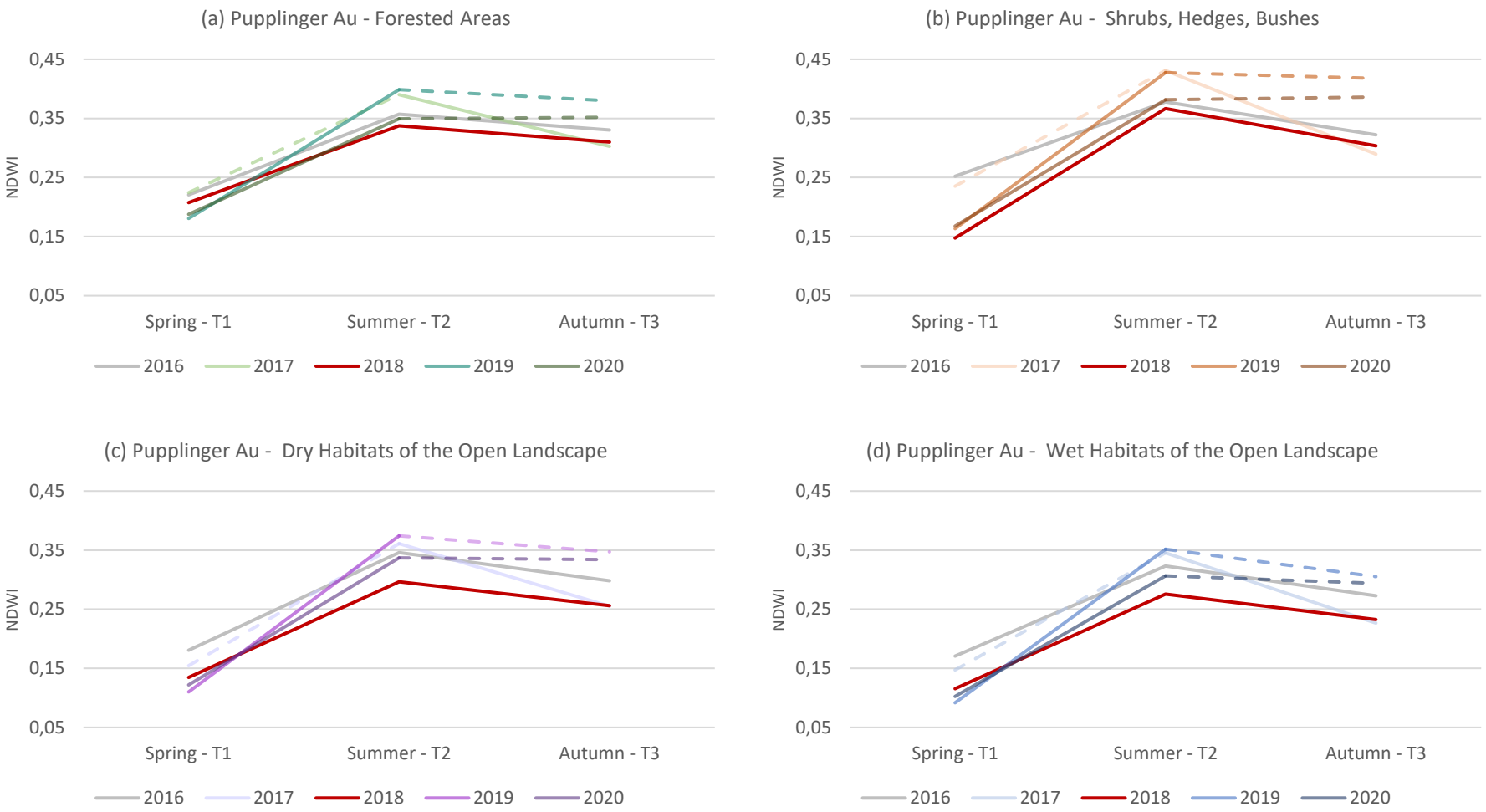

Figure 18. Intra-annual alterations of the NDWI values per biotope type and investigated year. NDWI regimes display specific signatures for (a) Forested Areas (NDWI 0.18-0.40), (b) Shrubs, Hedges and Bushes (NDWI 0.15-0.43), (c) Dry Habitats of the Open Landscape (NDWI 0.11-0.37) and (d) Wet Habitats of the Open Landscape (NDWI 0.09-0.35). The 2018 NDWI regimes are, in comparison to the other investigated years, in average lowest for all biotope types. Particularly in contrast to the NDWI regimes of 2016 exhibit the NDWI regimes of 2018 significantly lower values These results can be connected to the meteorological and hydrological conditions, meaning that all biotope types experienced decreases in NDWI following the drought event 2018. This reflects plant water stress throughout 2018.

Inter-annual Differences in NDWI Values and per Biotope Type

The following figures and maps display the inter-annual NDWIs for all years per investigation point (T1, T2, T3), respectively. Change detection cannot be visualized for NDWI due to calculation restrictions, as NDWI values range from negative values to positive values. Inter-annual changes are visualized by depicting maps of each investigation point (T1, T2, T3) for all years, respectively (Maps 11 – 13). (Unlike NDVI values, negative NDWI values cannot be excluded as some vegetated surfaces/areas display negative NDWI values). Figures and maps are depicted only for study area Pupplinger Au, Isar Floodplains between Unterföhring and Landshut and Isar Estuary and for comprehension purposes. They do not incorporate Change Detection as for the NDVI.

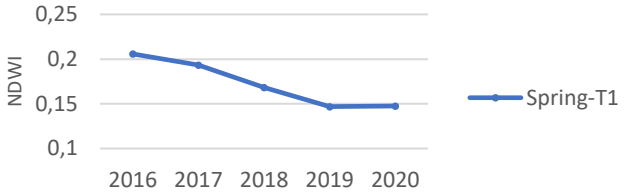

Figure 19. Inter-annual alterations of the NDWI throughout the investigation period (2016-2020) for Pupplinger Au at Spring-T1. NDWI values are highest in 2016 (0.21), followed by 2017 (0.19), 2018 (0.17) and 2019 and 2020 (0.15) in decreasing order. Map 11 visualizes the inter-annual alterations of Spring-T1 for all investigated years.

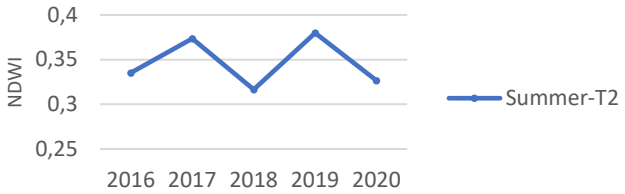

Figure 20. Inter-annual alterations of the NDWI throughout the investigation period (2016-2020) for Pupplinger Au at Summer-T2. NDWI values are highest in 2019 (0.38), followed by 2017 (0.37), 2016 (0.34), 2020 (0.33) and 2018 (0.32) in decreasing order. Map 12 visualizes the inter-annual alterations of Summer-T2 for all investigated years.

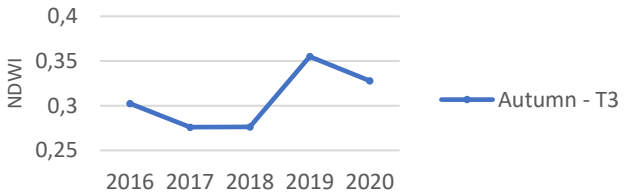

Figure 21. Inter-annual alterations of the NDWI throughout the investigation period (2016-2020) for Pupplinger Au at Autumn-T3. NDWI values are highest in 2019 (0.35), followed by 2020 (0.33), 2016 (0.30) and 2017 and 2018 (0.28) in decreasing order. 2019 and 2020 are, however, disregarded in the analysis as high-quality satellite imagery was only obtainable for September 2019 and 2020, respectively. Distortions in the NDWI results can therefore not be excluded. Map 13 visualizes the inter-annual alterations of Autumn-T3 for all investigated years.

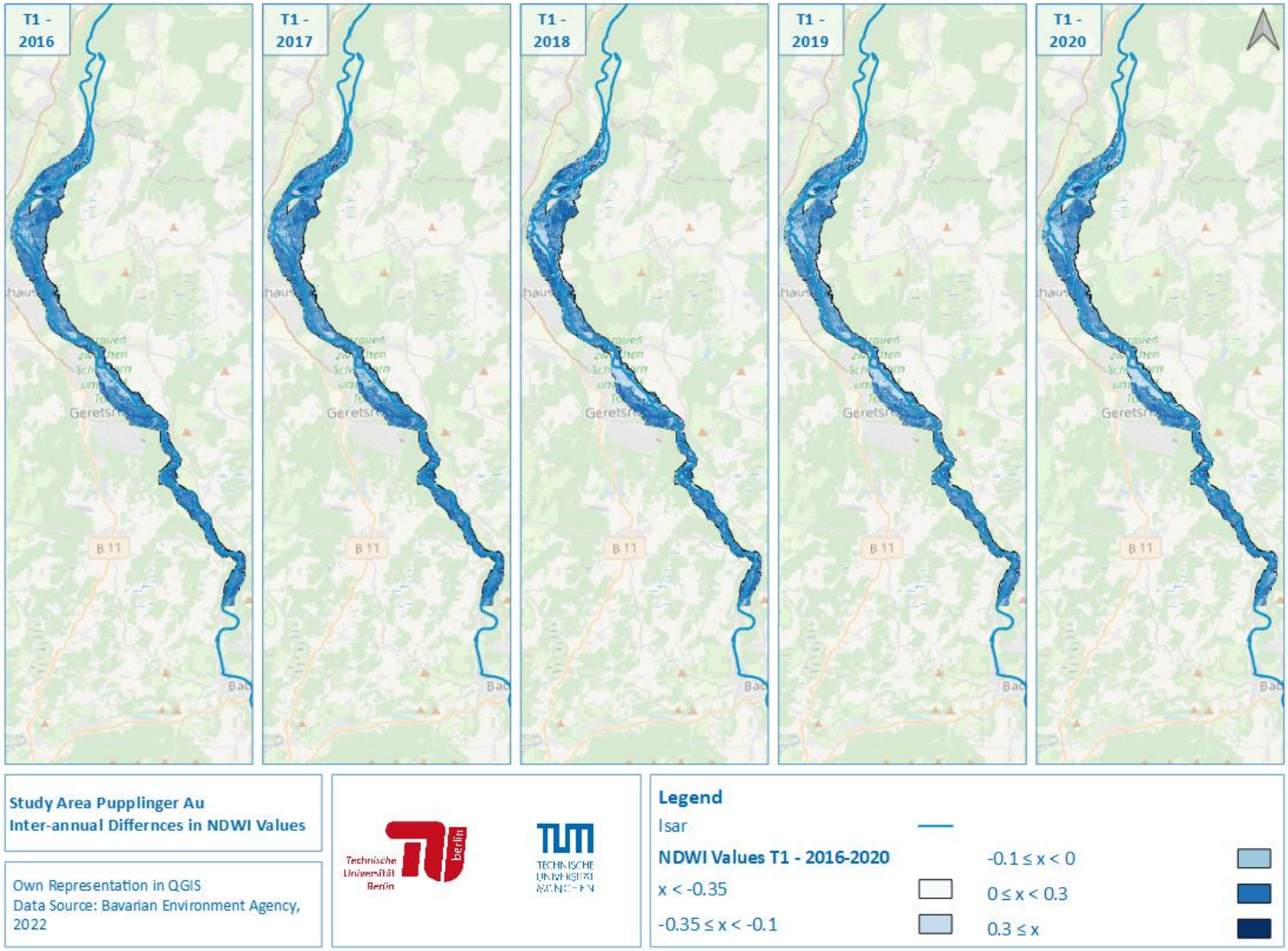

Map 11. Inter-annual differences in NDWI values. Differences in NDWI values can be visually detected between all years for investigation point Spring-T1. Brightest nuances depict low NDWI values, whereas darker shades indicate higher NDWI values. This map adequately reflects the results as seen in Figure 19.

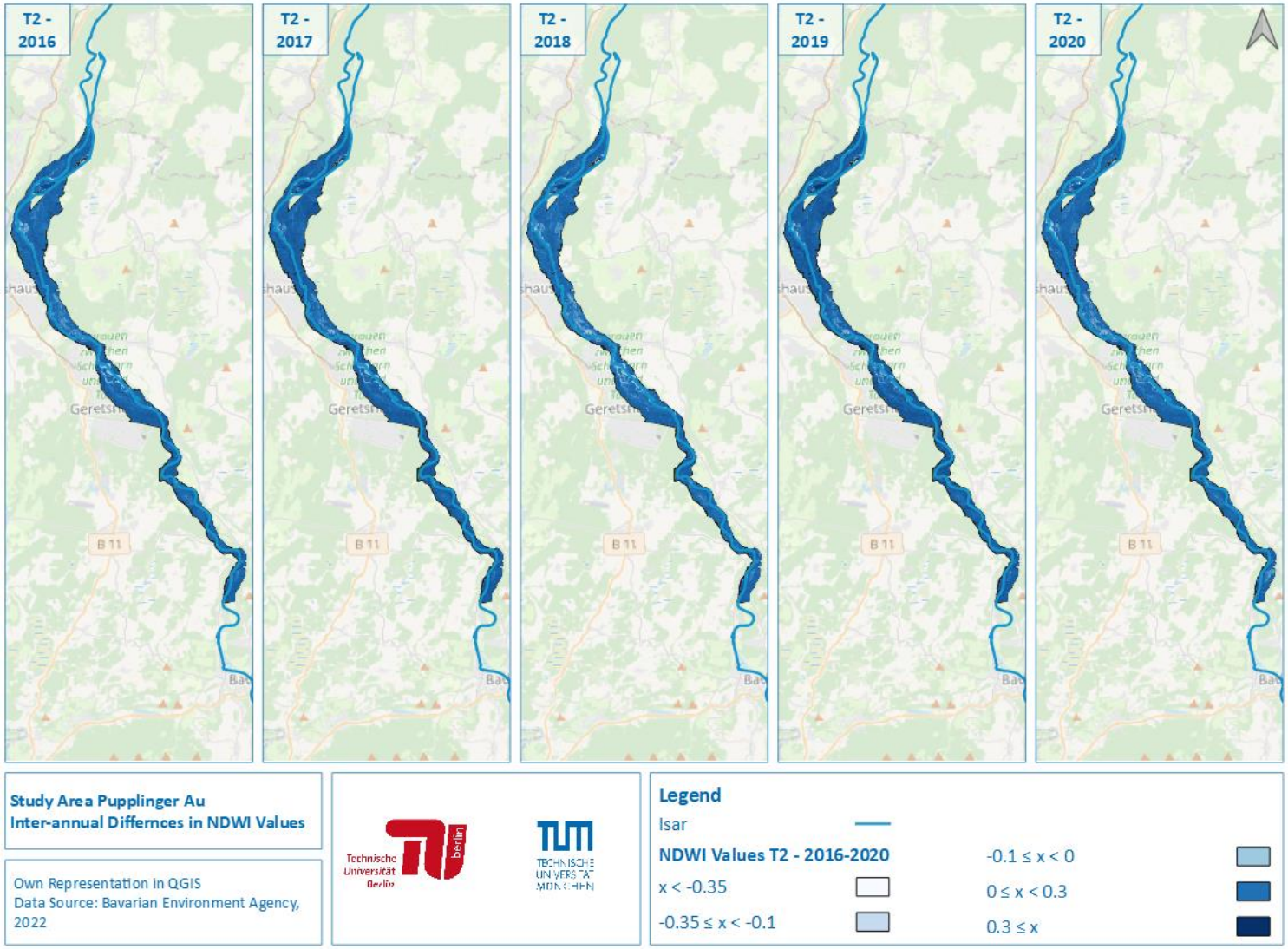

Map 12. Inter-annual differences in NDWI values. Differences in NDWI values can be visually detected between all years for investigation point Summer-T2. Brightest nuances depict low NDWI values, whereas darker shades indicate higher NDWI values. This map adequately reflects the results depicted in Figure 20.

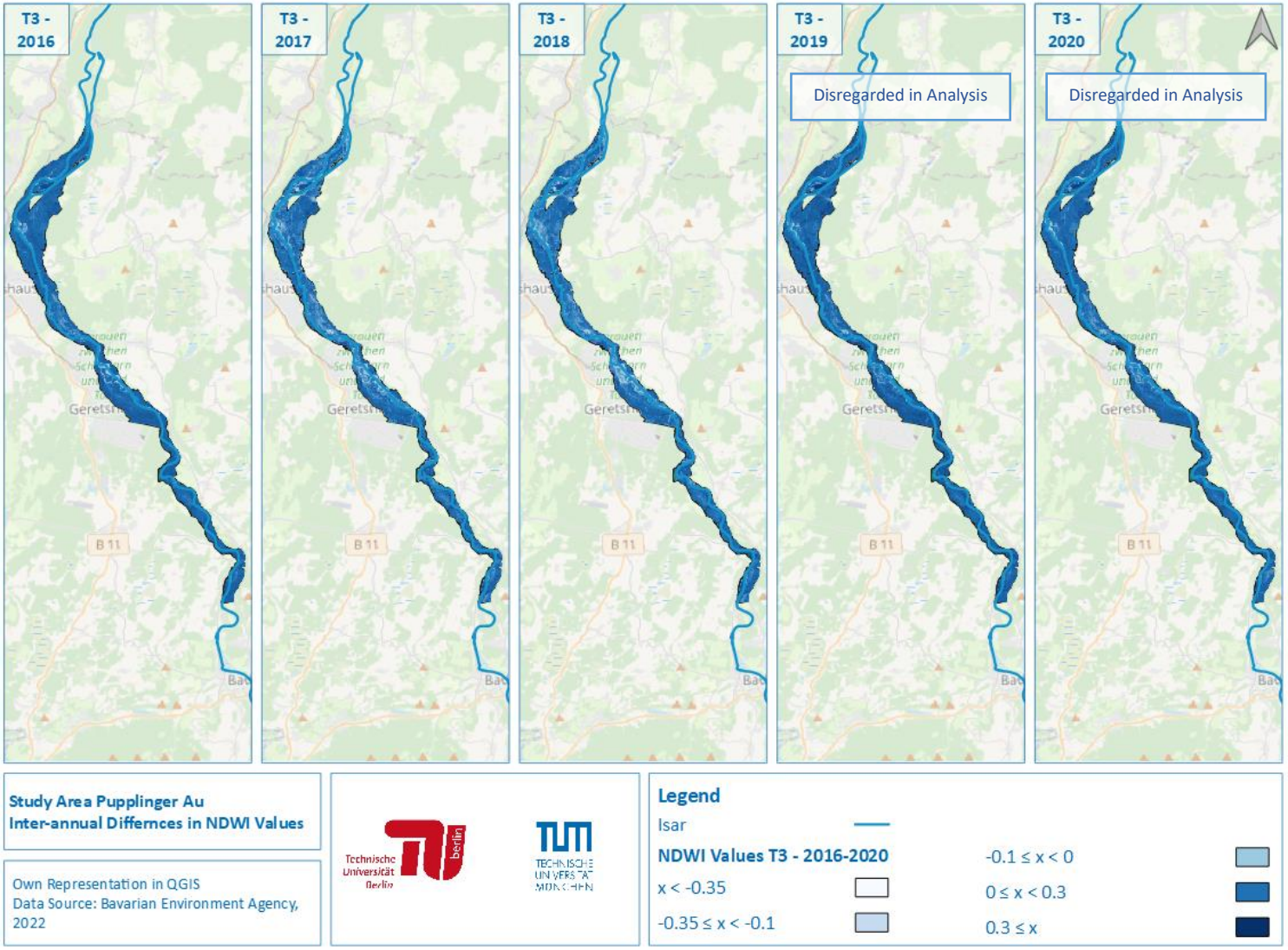

Map 13. Inter-annual differences in NDWI values for Pupplinger Au. Differences in NDWI values can be visually detected between all years for investigation point Autumn-T3. Brightest nuances depict low NDWI values, whereas darker shades indicate higher NDWI values. This map adequately reflects the results as seen in Figure 21.

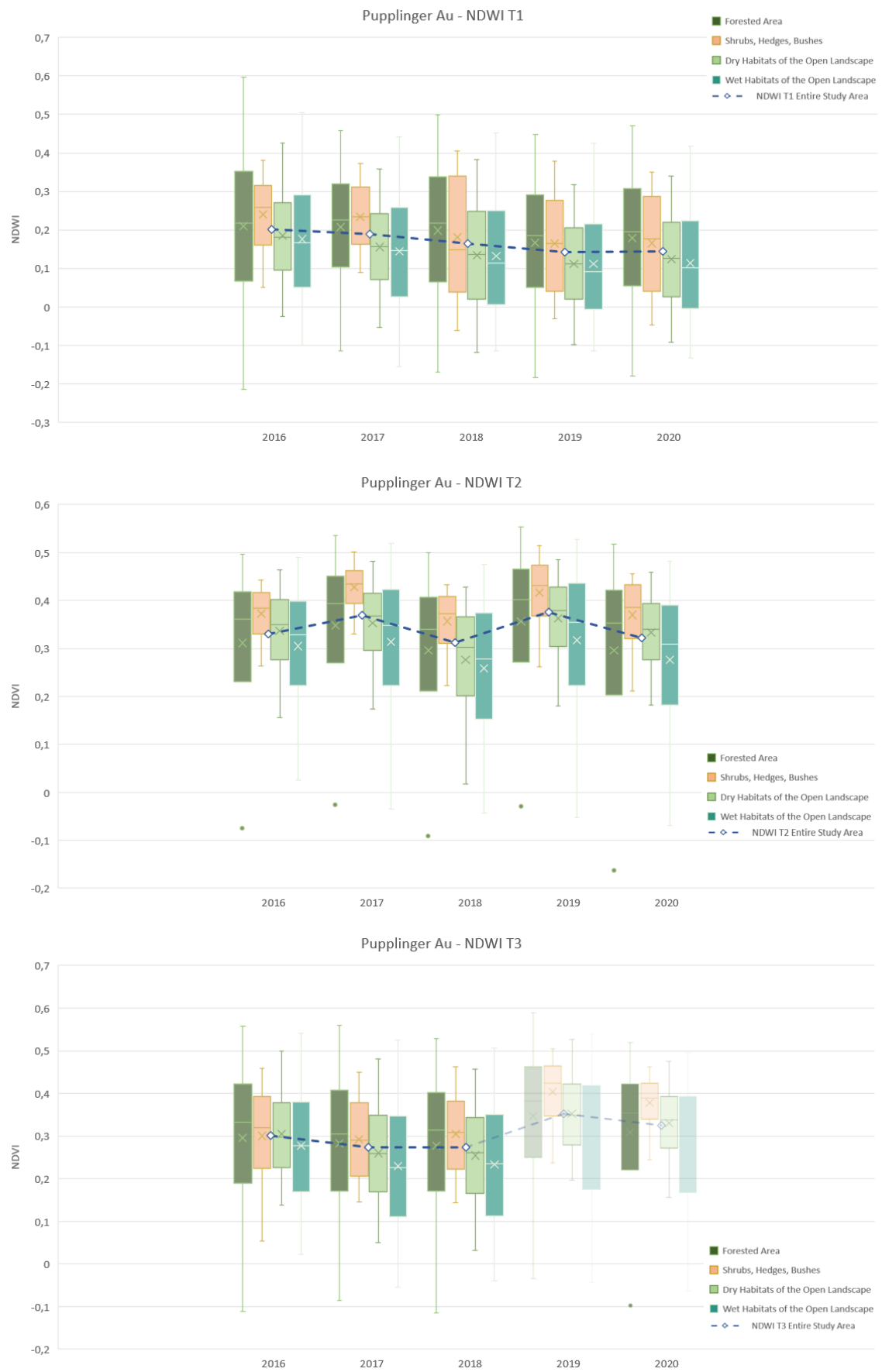

Figure 22. Inter-annual diffences in NDWI values per biotope type and year of study area Pupplinger Au.

Box and whisker plots describe the variability of NDWI value distribution within each biotope type and depict the scatter range. Scattering is, contrary to the NDVI, lowest for Forested Areas, followed by Wet Habitats of the Open Landscape, Shrubs, Hedges and Bushes and Dry Habitats of the Open Landscape in increasig order (see Appendix X). Dotted blue lines indicate the mean NDWI values for the entire study area in relation to each biotope type. All biotope types experienced decreases in NDWI values for all investigation points (Spring-T1, Summer-T2 and Autumn-T3) in 2018 when compared to 2016. This indicates lessened intra-cellular water content and thereby water stress, following the abnormally dry and warm spring 2018.

By contrast with all investigated years, however, Forested Areas exhibt the lowest mean NDWI at Spring-T1 (0.18) in 2019, at Summer-T2 in 2018 and 2020 with equal value (0.35) the lowest mean NDWI at Autumn-T3 (0.30) in 2017. Shrubs, Hedges and Bushes depict the lowest mean NDWI for all investigation points (Spring-T1, Summer-T2 and Autumn-T3) in 2018. Contrary to this, Dry Habitats of the Open Landscape display the lowest mean NDWIs at Spring-T1 (0.11) in 2019 , the lowest mean NDWI at Summer-T2 in 2018 (0.30) and the lowest mean NDWI at Autumn-T3 in 2017 and 2018 with equal value (0.26). Wet Habitats of the Open Landscape exhibit lowest mean NDWI at Spring-T1 in 2019 (0.09), the lowest mean NDWI at Summer-T2 in 2018 (0.28) and the lowest mean NDWI at Autumn-T3 in 2017 (0.23). Similar to the results obtained for the NDVI, these results indicate the importance of considering regional site conditions, as well as differentiating between different biotope types.

3.2 Study Areas Middle Course – Isar Floodplains Unterföhring

The study areas located alongside the middle reaches of the Isar river are both incorporated in the FFH conservation site “Isar floodplains from Unterföhring to Landshut” (“Isarauen von Unterföhrung bis Landshut”) but are spatially separated. This first study area of the middle reaches will followingly be addressed as “Isar Floodplains Unterföhring”, while the second study area of the middle reaches will be addressed by the original name “Isar Floodplains from Unterföhring to Landshut” for differentiation reasons. Located at 392 m – 500 m above sea level, those contiguous dealpine floodplain landscapes with an overall extent of 1272 ha and 1791 ha respectively, function as significant connectivity axes of (large-scale) biotopes between the Alps and the Danube River. Both include extensive floodplain habitats, such as semi-natural dry grasslands and nutrient-poor dry sites, but are primarily dominated by ash-elm alluvial forests with black alder (*Alnus glutinosa*) and ash (*Fraxinus excelsior*). The two sites are associated with the Continental biogeographic region, (Manderbach 2020).Main risks these study area face are lowering groundwater tables, disturbances of flood dynamics caused by hydraulic engineering measures, tourism and other recreational activities, uncontrolled grazing by sheep and disruptions by the nearby airport (Manderbach 2020).

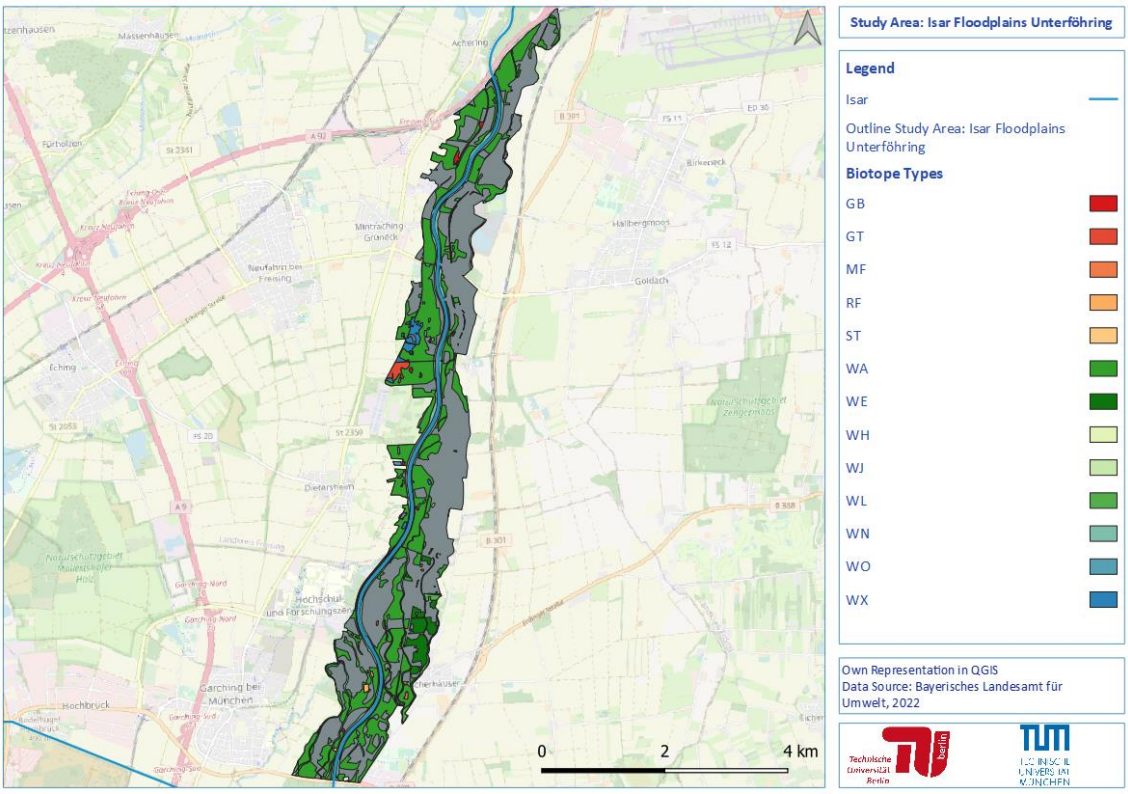

Map 14. Study area Isar Floodplains Unterföhring with biotope types plotted in the Bavarian Biotope Mapping.

Meteorological data was obtained from the station “Freising” and hydrological data from the monitoring well “Achering Q9”, both located close to the northern border of this study area. Mean Growing Season Air Temperature (MGT) was lowest in 2016 (13.92°C), followed by 2017 (14.10°C), 2020 (14.13°C), 2019 (14.57°C) and 2018 (15.84°C) in increasing order. 2018 was characterized by above-average hot and dry conditions, ranking highest in mean monthly air temperatures for April, May, July, August and September compared to the other years. Mean Growing Season Precipitation Rates (MGP) however differed only slightly among the years and were highest in 2017 (83 mm). In decreasing order, MGPs were recorded with (74 mm) in 2020, (73 mm) in 2016 and (68 mm) in 2018. Lowest MGP was recorded for 2019 with 62 mm (see Appendices). Groundwater fluctuations remained

mostly imperceptible throughout the investigation period but recorded the absence of the usual peak in spring 2018.

Site-specific Meteorological and Hydrological Conditions

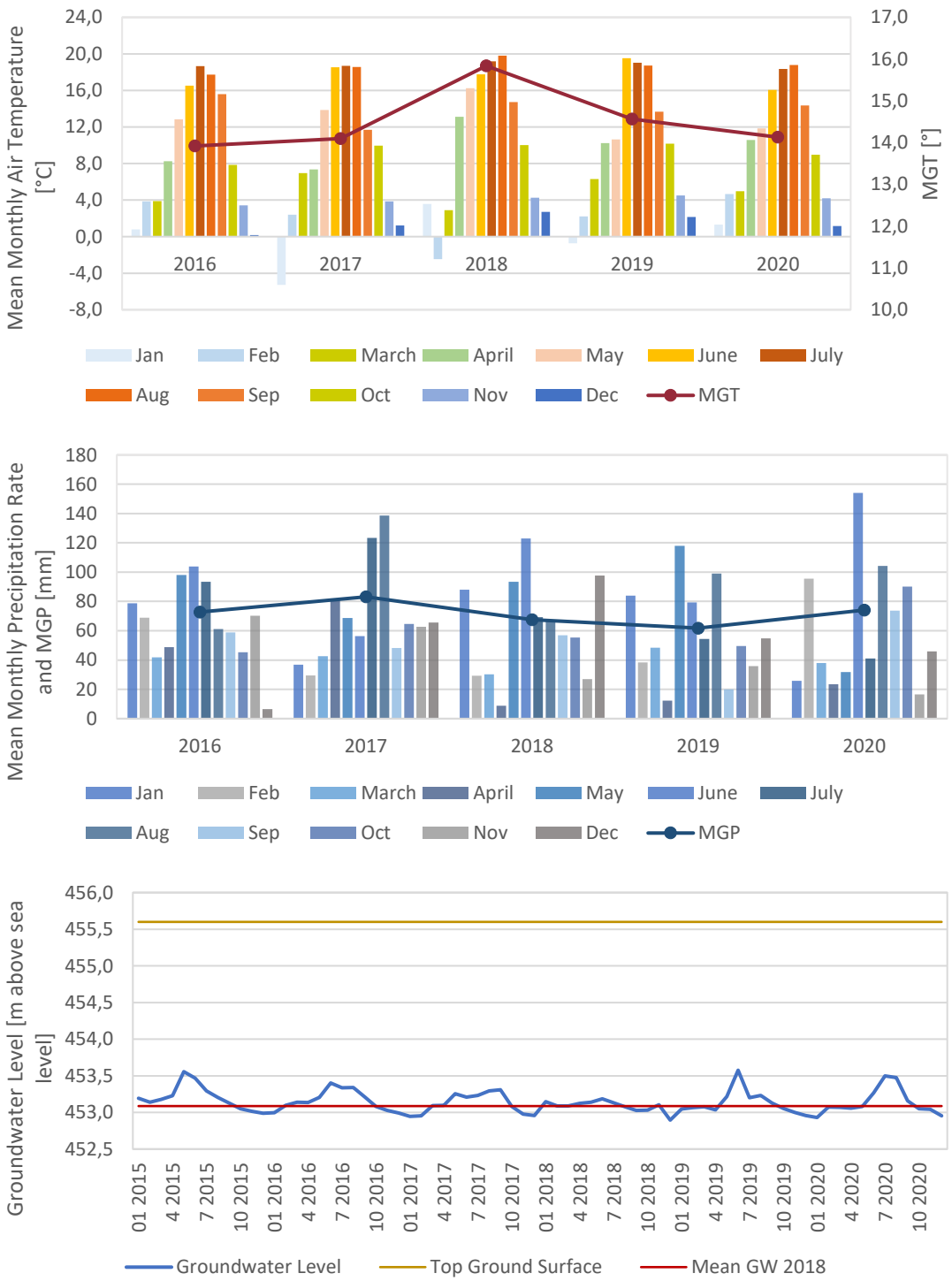

Figure 23. Mean monthly air temperature and mean growing season air temperature (MGT; a), mean monthly precipitation rate and mean growing season precipitation rate (MGP; b), as well groundwater level and groundwater-surface distance (c) of study area Isar Floodplains Unterföhring. The growing season encompasses the months April to October. (BayLfU 2020b; 2020d; 2020c; 2020e).

3.2.1 NDVI – Isar Floodplains Unterföhring

Satellite Data

Table 5. Satellite imagery used in the NDVI assessment of study area Isar Floodplains Unterföhring. Differences in investigation times arose from limitations in data availability. Greyed out times are disregarded in the analysis by reason of undue temporal deferral.

Time	2016	2017	2018	2019	2020
T1	29 April	17 May	07 April	19 April	08 April
T2	27 August	25 August	22 August	30 August	21 August
T3	16 October	16 October	16 October	29 September	15 September

Intra-annual Alterations in NDVI Values

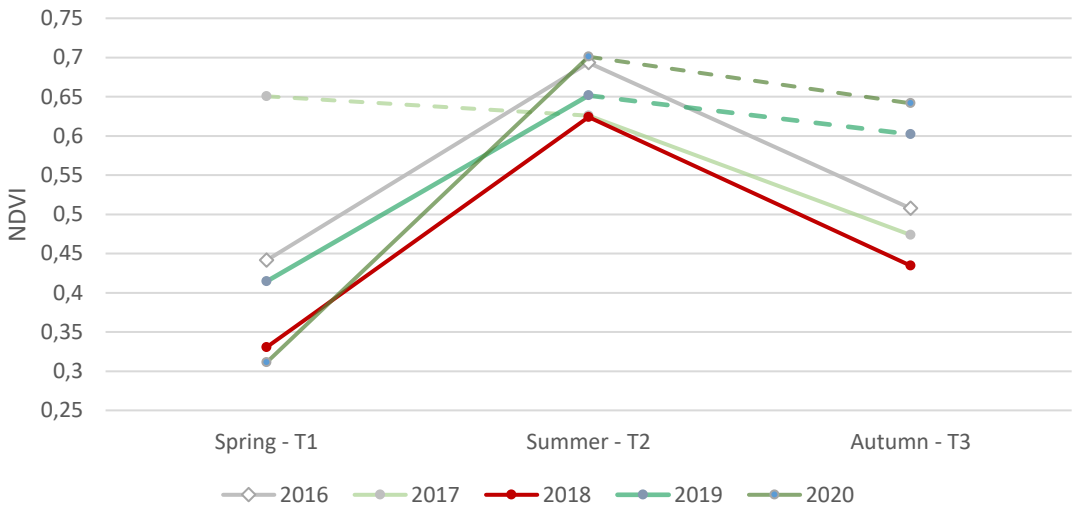

Figure 24. Intra-annual alterations in NDVI values for all investigated years (2016-2020) for study area Isar Floodplains Unterföhring. Dashed lines indicate the disregarded values, as outliers in investigation times may cause incomparability of obtained results.

Intra-annual alterations in NDVI values are depicted in Figure 24 for the entire study area Isar Floodplains Unterföhring. Similar to Pupplinger Au, steepness of increase and decrease in NDVI values vary for each year. The NDVI regime adequately reflects the phenological cycle, more specifically the chlorophyll-a content, here too. The NDVI values for Spring-T1 (0.33), Summer-T2 (0.62) and Autumn-T3 (0.43) of drought year 2018 run almost parallel to the NDVI regime of the reference year 2016 with Spring-T1 (0.44), Summer-T2 (0.69) and Autumn-T3 (0.51) but remain notably and consistently below it. The significantly different meteorological and hydrological conditions between 2016 and 2018 can be linked to these results. Climatic conditions in 2018 have been, as previously described, significantly hotter than the other investigated years, but not significantly drier for this particular study area. MGP was recorded to have been only 5 mm lower in 2018, compared to 2016. Interestingly, as for Pupplinger Au, the year 2020 exhibited the highest NDVI for Summer-T2 (0.70) out of all investigated years, although having started with the lowest NDVI in Spring-T1 (0.31). Maps visualising the intra-annual NDVI regimes of 2016 and 2018 are only incorporated for study areas Pupplinger Au, Isar Floodplains between Unterföhring and Landshut and Isar Estuary, which exemplarily represent the upper, middle and lower reaches.

Intra-annual alterations in NDVI regimes per biotope type and investigated year are depicted in Figure 25. For all four biotope types the NDVI regime in 2018 is the lowest out of all investigated years.

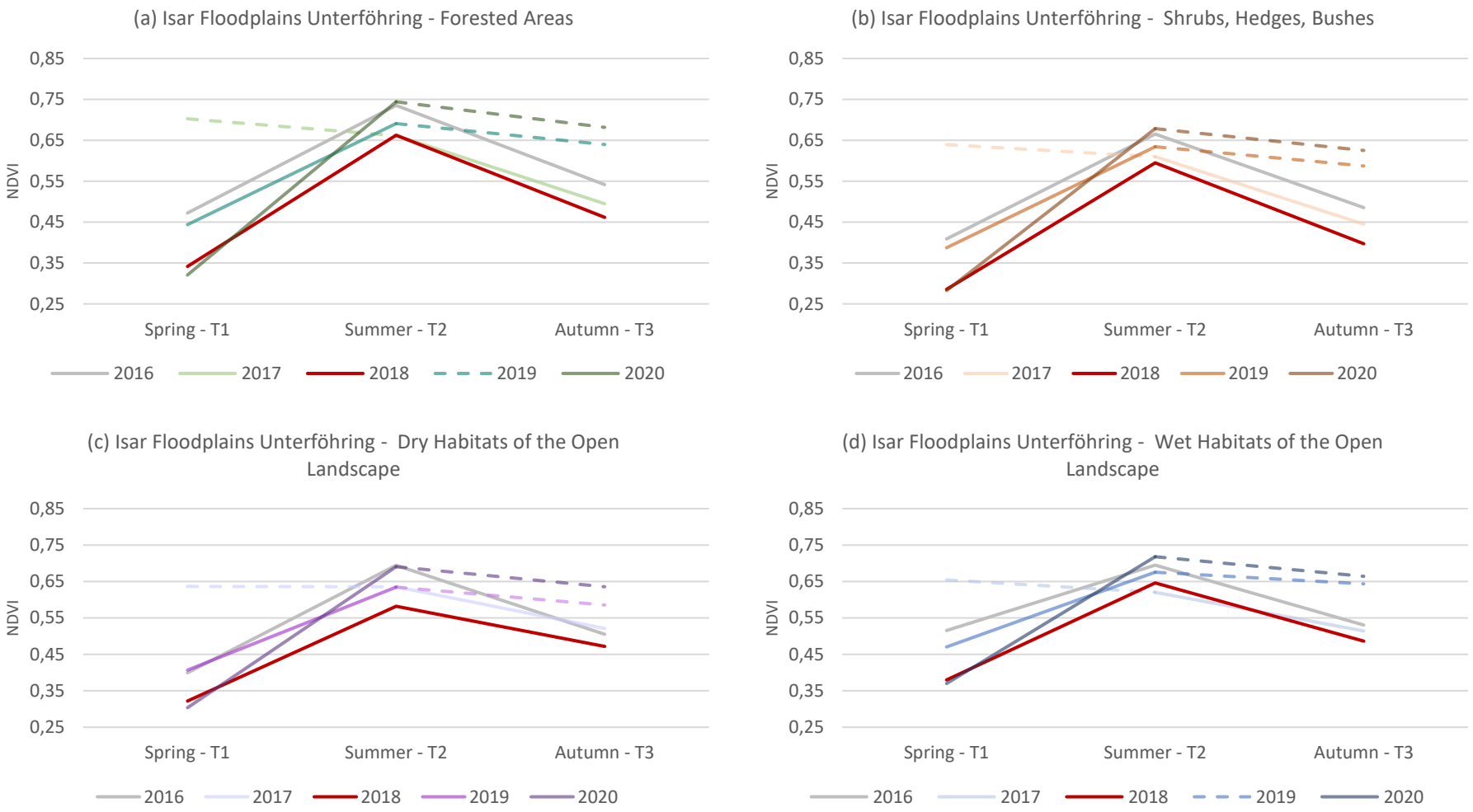

Figure 25. Intra-annual alterations of the NDVI values per biotope type and investigated year. NDVI regimes display specific value ranges with highest values for (a) Forested Areas (0.32-0.74), followed by (d) Wet Habitats of the Open Landscape (0.37-0.72), (c) Dry Habitats of the Open Landscape (0.30-0.69) and (c) Shrubs, Hedges and Bushes (0.28-0.68) in decreasing order. The 2018 NDVI regimes are, in comparison to the other investigated years, in average lowest for all biotope types. Especially in comparison to the NDVI regimes of reference year 2016, the NDVI regimes of 2018 remain significantly lower for all investigated biotope types. These results can be connected to the meteorological and hydrological conditions, meaning that all biotope types experienced plant vitality decreases following the drought event 2018.

Inter-annual Difference in NDVI Values per Biotope Type

The following maps display the inter-annual differences in NDVI values between the reference year 2016 and the other investigated years (2017, 2018, 2019 and 2020). Differences were calculated using the equation found under Materials and Methods. Changes in plant vitality were derived thereof and are depicted in the legend. Cloud coverage causes minor distortions in some maps.

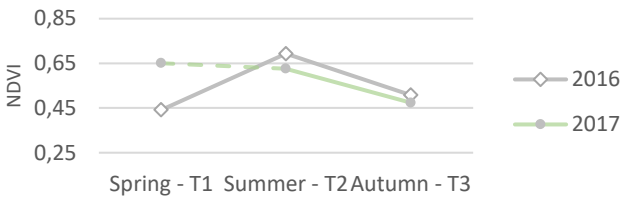

Figure 26. Mean intra-annual alterations of the NDVI 2016 and NDVI 2017 for Isar Floodplains Unterföhring. Summer-T2 (0.69) and Autumn-T3 (0.51) in 2016 are higher than Summer-T2 (0.63) and Autumn-T3 (0.47) in 2017. Spring-T1 differs significantly between these two years but can be led back to the data obtained for Spring-T1 2017. Recording date was May 17th, resulting in indue temporal deferral and thus, incomparability of the obtained results. These differences in NDVI regimes are visualized in Map 15.

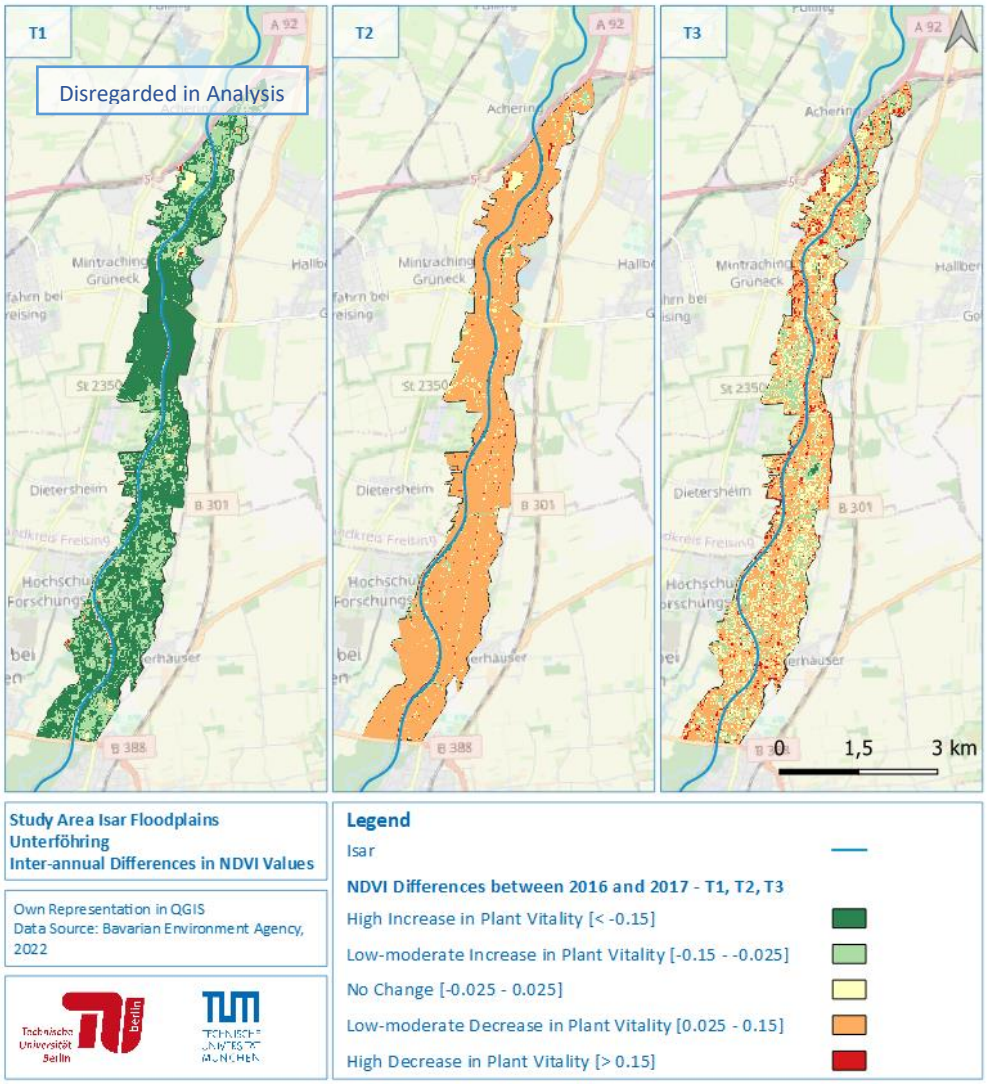

Map 15. Extensive low-moderate decreases in plant vitality, and some negligible small areas with high decreases in plant vitality were observed between 2016-2017 at Summer-T2. Autumn-T3 displays very disparate results with fragmented plots of all possible differences in plant vitality, causing the overall similarity in NDVI values depicted in Figure 26. Spring-T1 is disregarded due to undue temporal deferral of obtained data.

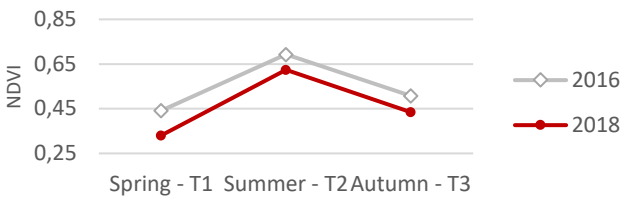

Figure 27. Mean intra-annual alterations of the NDVI 2016 and NDVI 2018 for Isar Floodplains Unterföhring. The NDVI regime of 2018 depicts consistent reductions in NDVI values for Spring-T1 (0.33), Summer-T2 (0.62) and Autumn-T3 (0.43) in comparison to 2016, with Spring-T1 (0.44), Summer-T2 (0.69) and Autumn-T3 (0.51). Those differences are visualized in Map 16.

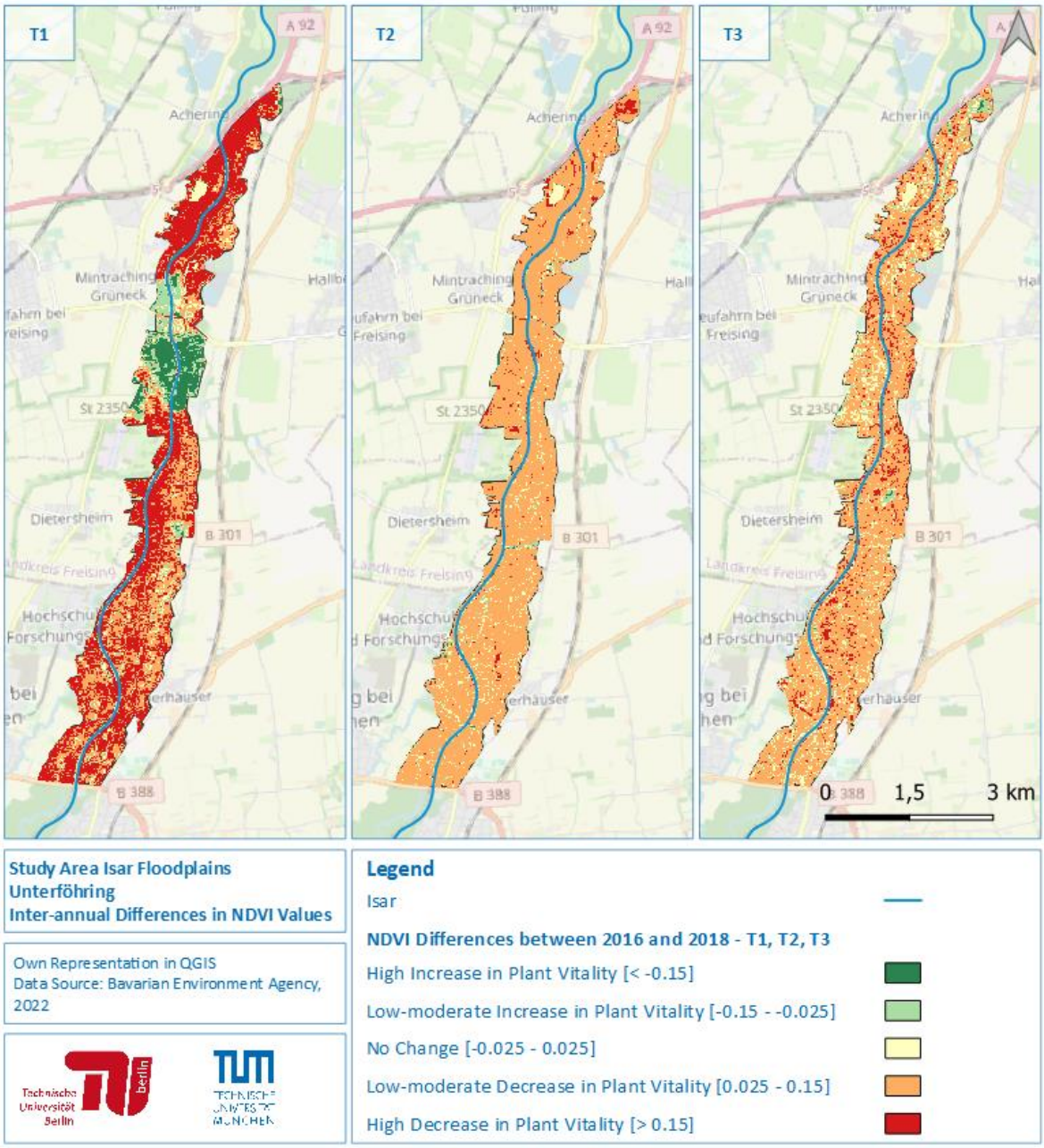

Map 16. Exhaustive high decreases in plant vitality were detected for Spring-T1 between 2016 and 2018, while similar extents of low-moderate decreases in plant vitality were detected for this study area in the comparison between 2016-2018 at Summer-T2. Autumn-T3 show more fragmented changes in plant vitality, but resulted in overall similar differences in NDVI values between 2016 and 2018 as for Summer-T2. Cloud coverage in the satellite imagery obtained for Spring-T1 2016 causes distortions in the central part of the study area, resulting in overall smaller NDVI differences than actually occurring, seen in Figure 27.

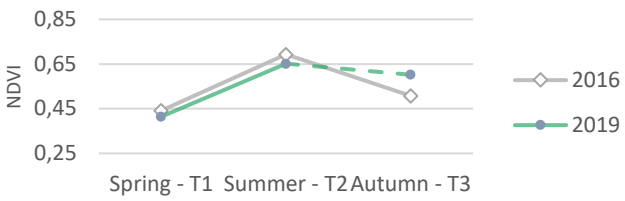

Figure 28. Mean intra-annual alterations of the NDVI 2016 and NDVI 2019 for Isar Floodplains Unterföhring. NDVI regimes of those two years displayed strong similarities with Spring-T1 (0.44) and Summer-T2 (0.69) of 2016 and Spring-T1 (0.41) and Summer-T2 (0.65) of 2019. Autumn-T3 (0.60) for 2019 is disproportionately higher, which can be traced back to the recording date of satellite imagery and will be disregarded in this analysis. Scope of inter-annual NDVI differences between those years are visualized in Map 17.

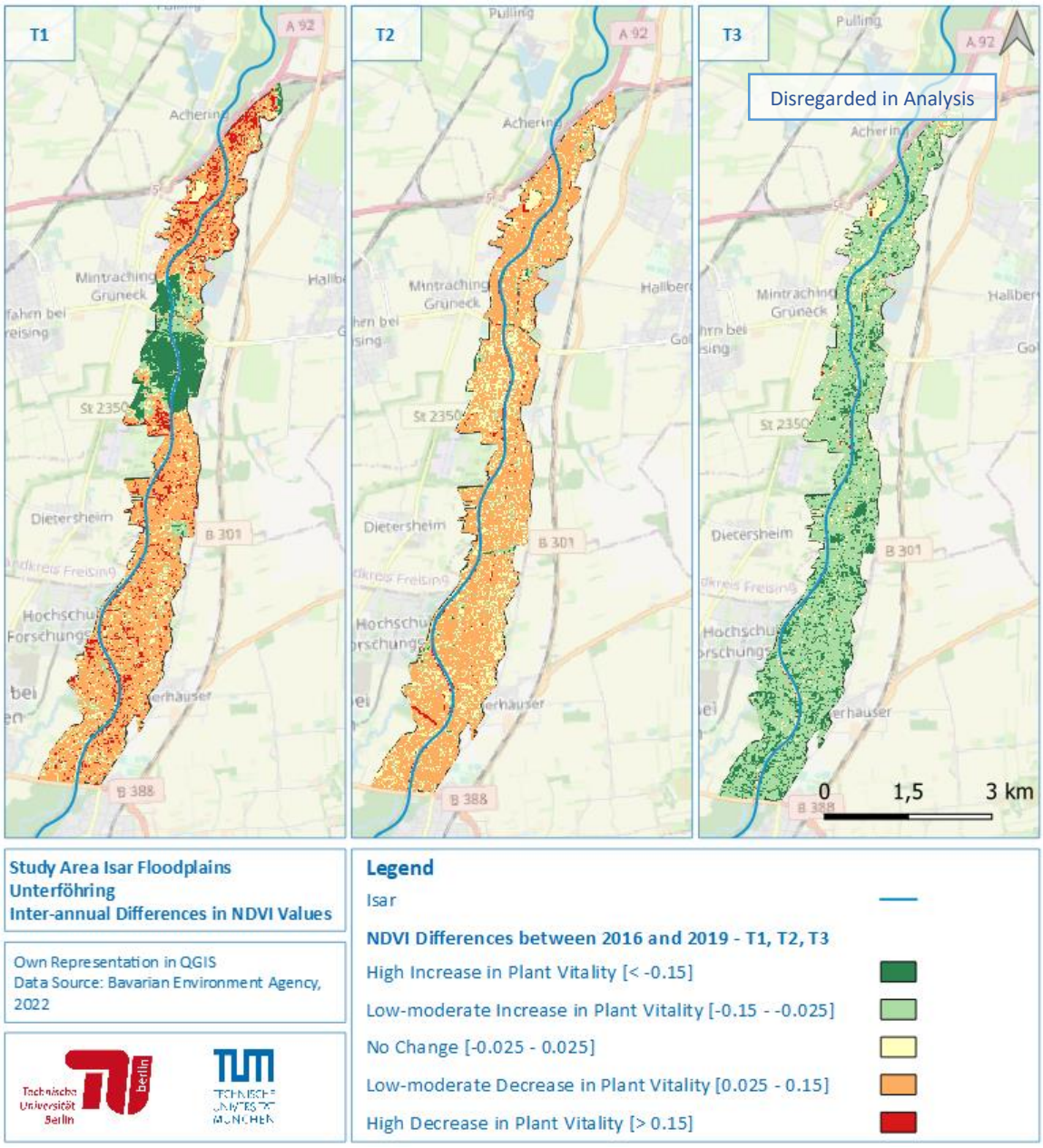

Map 17. Disregarding the small erroneous display of plant vitality increase due to cloud coverage in Spring-T1, the remaining surface exposed fragmented low-moderate and high decreases in plant vitality for the investigation point Spring-T1 (2016-2019). Exhaustive low-moderate decreases and minor high decreases in plant vitality were detected in the comparison between 2016-2019 for Summer-T2. Low-moderate increases in plant vitality, however, were detected for Autumn-T3 (2016-2019). These results have to be critically regarded in this analysis, as data was obtained September 29th in 2019, potentially resulting in spuriously high NDVI values for 2019-T3.

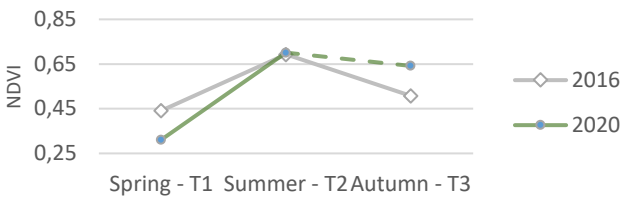

Figure 29. Mean intra-annual alterations of the NDVI 2016 and NDVI 2020 for Isar Floodplains Unterföhring. Spring-T1 of 2020 (0.31) is significantly lower than Spring-T1 of 2016 (0.44), while almost the same NDVI was recorded for Summer-T2 of 2020 (0.70) and 2016 (0.69). Autumn-T3 of 2020 (0.64) is disregarded in this analysis as data was obtained 15th September 2020, resulting in incomparability of obtained result by reason of undue temporal deferral. The scope in NDVI differences is visualized in Map 18.

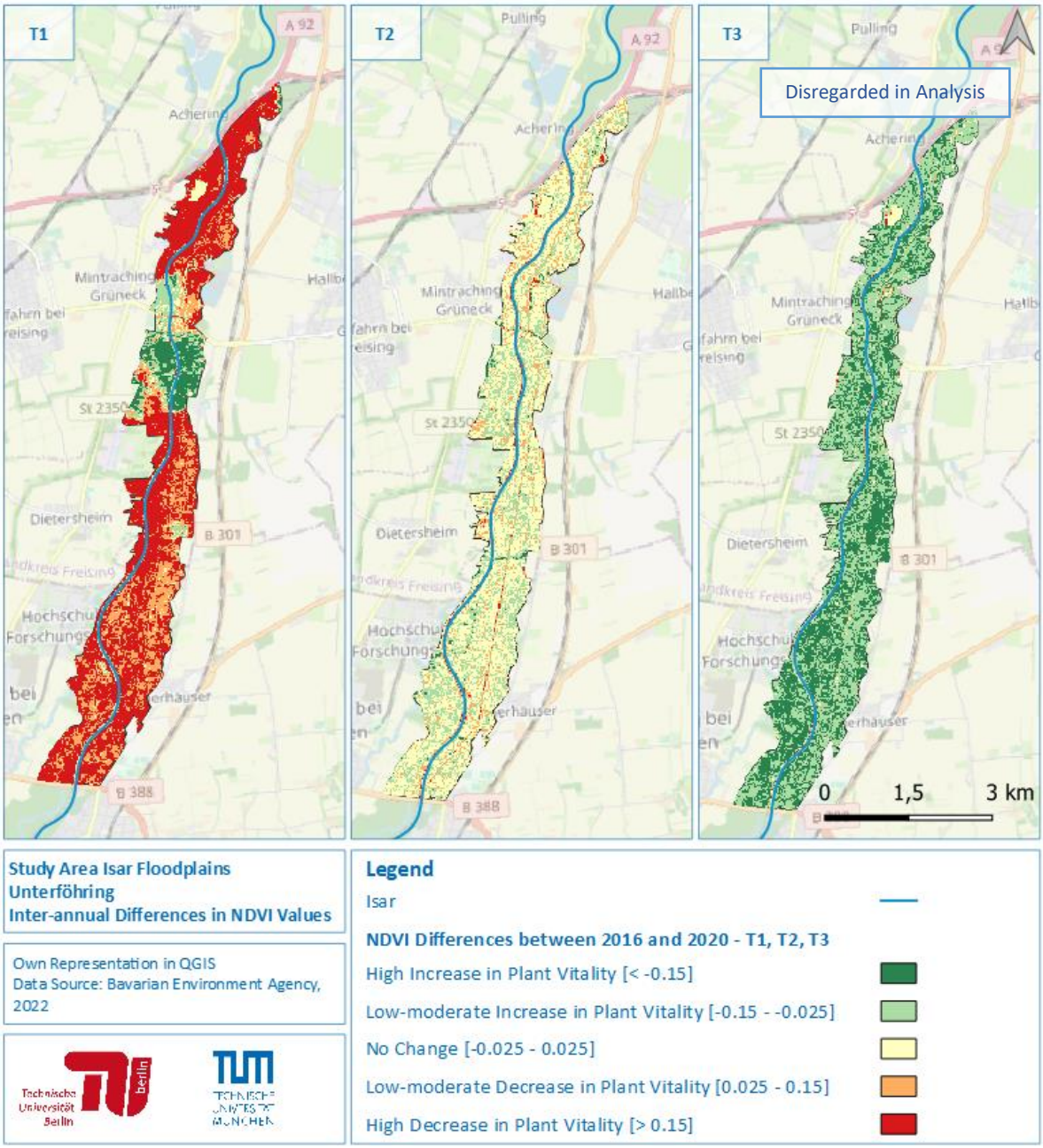

Map 18. High decreases in NDVI values and thus, plant vitality, were observed for Spring-T1 between 2016 and 2020 with extensive scope, whereas almost no change was detected between 2016 and 2020 at Summer-T2. Fragmented areas display NDVI differences of all categories for this investigation time. Autumn-T3 is disregarded, as data for 2020-T3 was obtained September 15th, creating an undue temporal deferral.

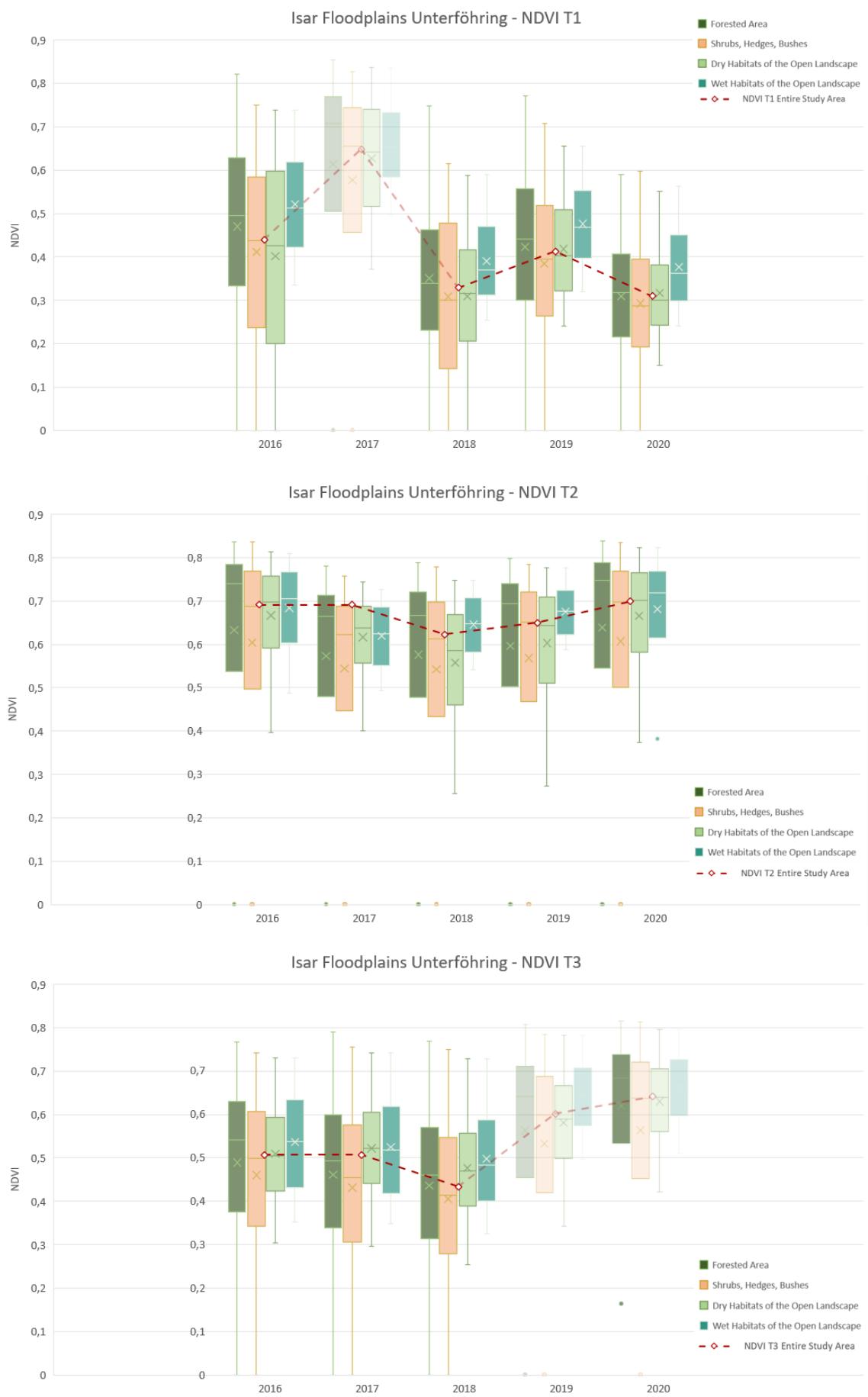

Figure 30. Inter-annual diffences in NDVI values per biotope type and year for Isar Floodplains Unterföhring.

Box and whisker plots describe the variability of NDVI value distribution within each biotope type and depict the scatter range. Scattering of the NDVI ranges was lowest for Wet Habitats of the Open Landscape, followed by Dry Habitats of the Open Landscape, Shrubs, Hedges and Bushes and Forested Areas in increasing order. Dotted red lines indicate the mean NDVI values for the entire study area. All biotope types exhibit significantly lower NDVI values during drought year 2018 in comparison to the reference year 2016 for all investigation points (Spring-T1, Summer-T2 and Autumn-T3).

Variations are displayed by contrast with all investigated years. While NDVI at Spring-T1 was lowest for Forested Areas (0.34) in 2018, Shrubs, Hedges and Bushes exhibited the lowest NDVI in 2020 (0.28) for this investigation point. When comparing all years, Dry Habitats of the Open Landscape display lowest value at Spring-T1 in 2020 (0.30) and Wet Habitats of the Open Landscape with equal value in 2018 and 2020 (0.37). At Summer-T2, lowest NDVI is exhibited by Forested Areas in 2017 and 2018 with equal value (0.66), by Shrubs, Hedges and Bushes in 2018 (0.59), by Dry Habitats of the Open Landscape in 2018 (0.58) and by Wet Habitats of the Open Landscape in 2017 (0.62). These results indicate the importance of considering regional site conditions, as well as differentiating between different biotope types.

3.2.2 NDWI – Isar Floodplains Unterföhring

Satellite Data

Table 6. Satellite imagery used in the NDWI assessment of Study Area Isar Floodplains from Unterföhring to Landshut. Differences in investigation times arose from limitations in data availability. Greyed out times are disregarded in the analysis by reason of undue temporal deferral.

Time	2016	2017	2018	2019	2020
T1	29 April	24 April	07 April	19 April	08 April
T2	27 August	25 August	22 August	30 August	21 August
T3	16 October	16 October	16 October	29 September	15 September

Intra-annual Alterations in NDWI Values

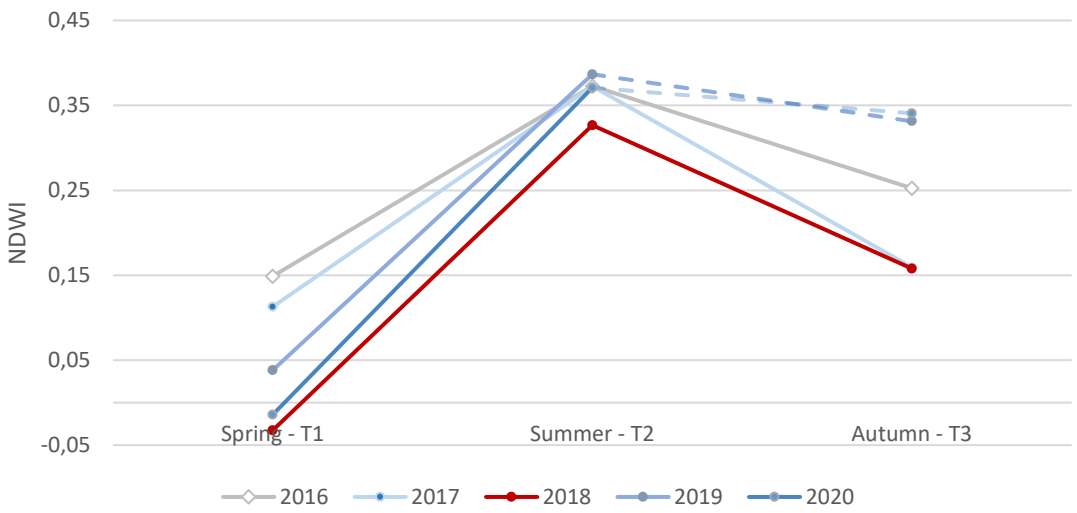

Figure 31. Mean intra-annual alterations in NDWI for study area Isar Floodplains Unterföhring. Dashed lines indicate the disregarded values, as outliers of investigation times may cause incomparability in obtained results.

Intra-annual alterations in NDWI values are depicted in Figure 31 for the entire study area "Isar Floodplains Unterföhring". For all investigated years, the NDWI peaks during investigation point Summer-T2 of respective year. As for study area Pupplinger Au in the upper course of the Isar river, the NDWI regimes of this study area adequately reflect the relation between the phenological cycle and the intracellular water content. The NDWI regime of 2018 is significantly lower than the NDWI regime of 2016, where the difference is highest at Spring-T1 (-0.03 and 0.15). Summer-T2 (0.33) and Autumn-T3 (0.16) are nevertheless substantially diminished for 2018, when compared to Summer-T2 (0.37) and Autumn-T3 (0.25) of 2016. All other NDWI regimes (2017, 2019, 2020) depict lower values at Spring-T1 than 2016, but recover at Summer-T2 and reach similar values (see Appendices). Intra-cellular water content decreases with the steepest gradient between Summer-T2 and Autumn-T3 in 2017. Contrasting climatic site conditions within the investigation period (2016-2020) are closely tied to the obtained differences in NDWI regimes. Particularly the above-normal temperature profile of 2018 deviated from the one of reference year 2016.

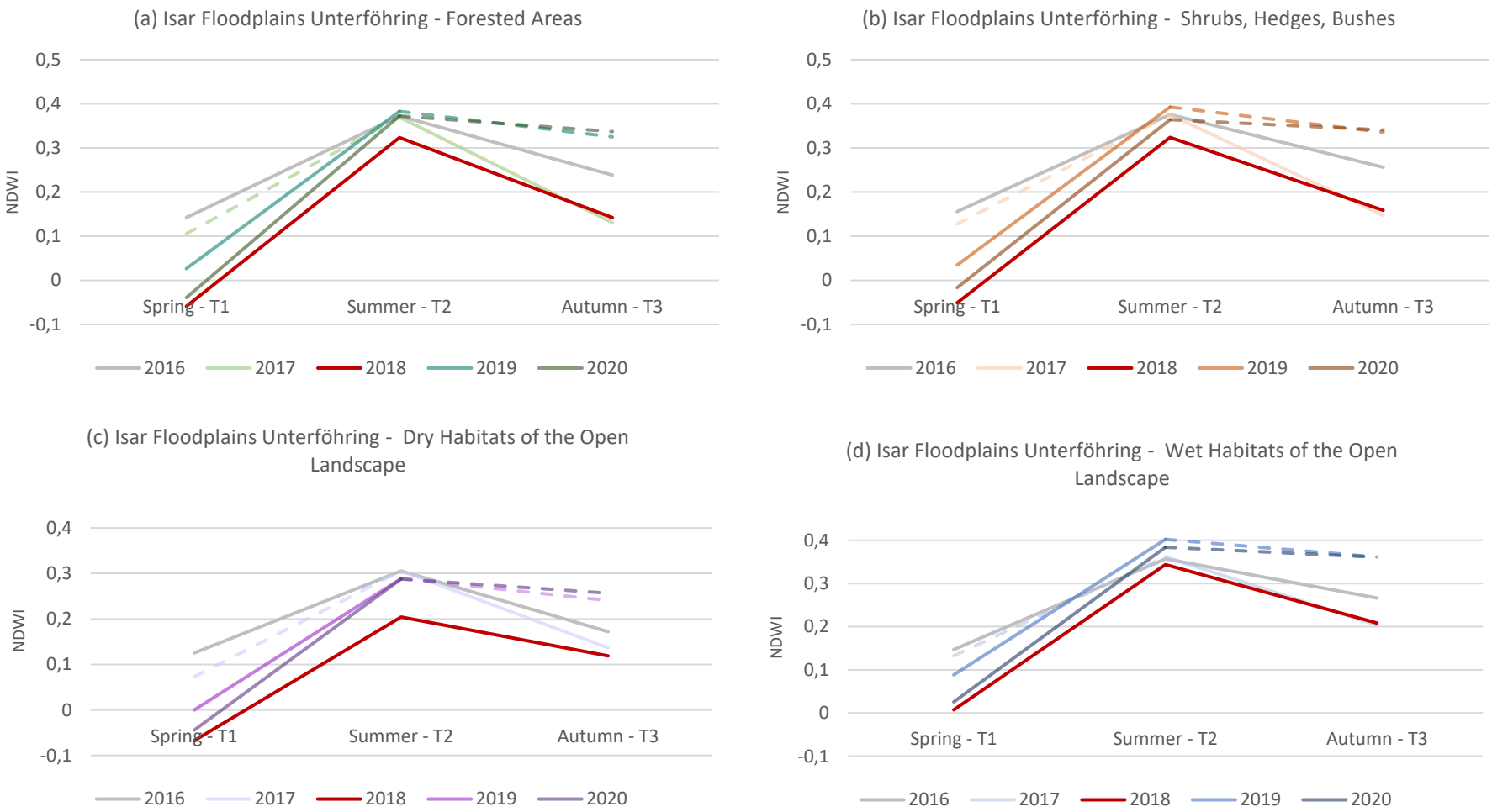

Figure 32. Intra-annual alterations of the NDWI values per biotope type and investigated year. NDWI regimes display specific signatures for (a) Forested Areas (NDWI -0.05 -0.38), (b) Shrubs, Hedges and Bushes (NDWI -0.05-0.39), (c) Dry Habitats of the Open Landscape (NDWI -0.07-0.30) and (d) Wet Habitats of the Open Landscape (NDWI 0.01-0.40). The 2018 NDWI regimes are, in comparison to the other investigated years and especially the reference year 2016, lowest for all biotope types. These results can be linked to the meteorological and hydrological conditions. All biotope types depict reduced intra-cellular water content throughout 2018, most likely caused by above-normal air temperature and reduced precipitation rates during this year.

Inter-annual Differences in NDWI Values and per Biotope Type

Figure 33. Inter-annual diffences in NDWI values per biotope type and year for Isar Floodplains Unterföhring.

Box and whisker plots describe the variability of NDWI value distribution within each biotope type and depict the scatter range. Scattering is, lowest for Dry Habitats of the Open Landscape, followed by Wet Habitats of the Open Landscape, Forested Areas and Shrubs, Hedges and Bushes in increasing order. Dotted blue lines indicate the mean NDWI values for the entire study area in relation to each biotope type. NDWI values are lowest for Forested Areas (-0.05), Shrubs, Hedges and Bushes (-0.05) and Wet Habitats of the Open Landscape (0.01) at Spring-T1 in 2018. Dry Habitats of the Open Landscape are lowest at Spring-T1 in 2020 (-0.04), although the difference is negigible. At Summer-T2, all biotope types exhibit lowest values in 2018. At investigation point Autumn-T3, lowest values were measured for Forested Areas (0.13), Shrubs, Hedges and Bushes (0.15), and Wet Habitats of the Open Landscape (0.20) in 2017, but diplayed only slighlty higher values in 2018 (0.14, 0.16, 0.21). Dry Habitats of the Open Landscape at Autumn-T3 are lowest in 2018 (0.12).

However, comparing solemnly the results of drought year 2018 and reference year 2016, all biotope types experienced significant decreases in NDWI values at all investgation points in 2018. This indicates lessened intra-cellular water content and thereby water stress, following the abnormally dry and warm spring 2018.

3.3 Study Areas Middle Course – Isar Floodplains from Unterföhring to Landshut

Descriptions on the location and site specifications of this study area are detailed in the previous section. Study area Isar Floodplains from Unterföhring to Landshut is the second study area located alongside the middle reaches of the Isar River and part of the FFH conservation site "Isar floodplains from Unterföhring to Landshut", which consists of multiple, spatially separated areas. With 1791 ha this study area functions similar to the other areas as significant connectivity axes of (large-scale) biotopes between the Alps and the Danube River.

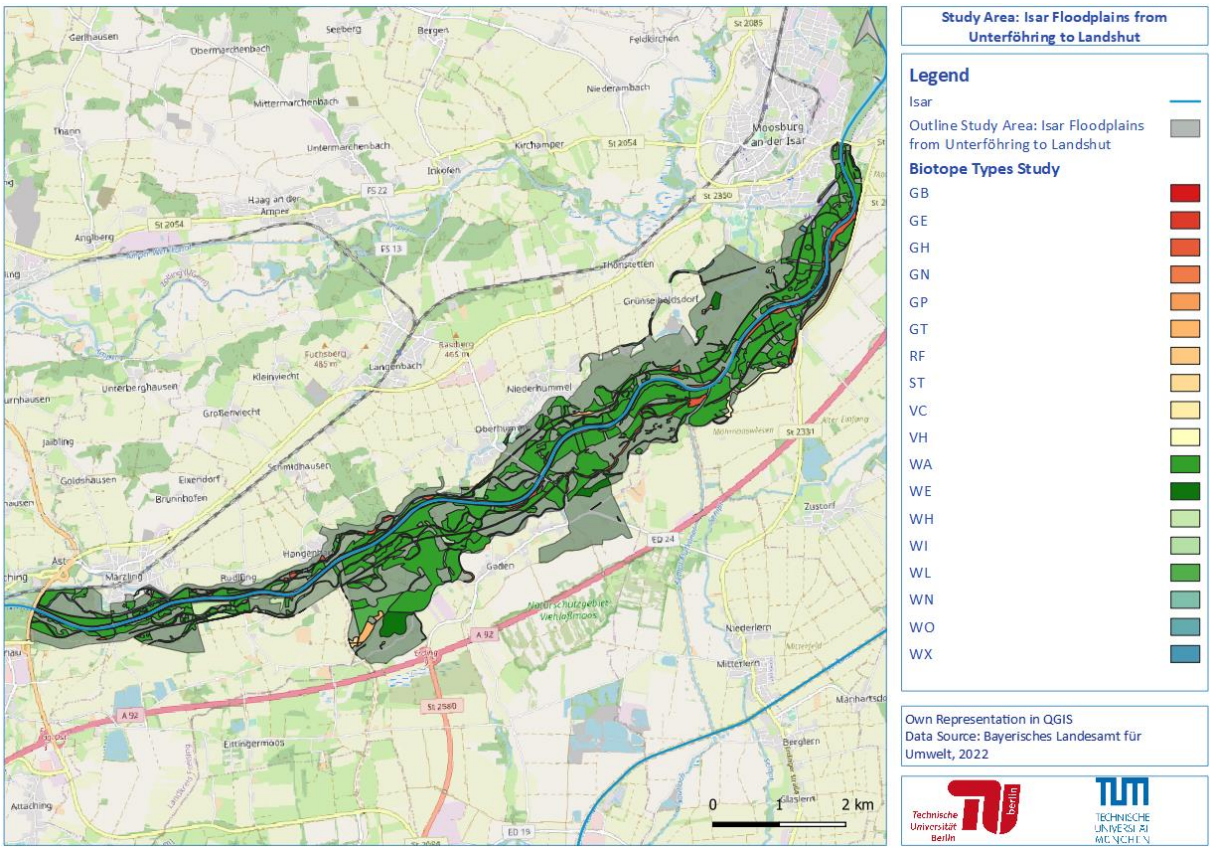

Map 19. Study area Isar Floodplains from Unterföhring to Landshut with biotope types derived from the Bavarian Biotope Mapping.

Meteorological data was obtained from the station "Schönbrunn" located west of this study area, while hydrological data was gathered from the monitoring well "Marzling Q5" located in the immediate eastern surroundings of this study area. Mean Growing Season Air Temperature (MGT) was lowest in 2016 (14.60°C), followed by 2017 and 2020 (14.72°C), 2019 (15.25°C) and 2018 (16.50°C) in increasing order. 2018 was characterized by above-average hot and dry conditions, ranking highest in mean monthly air temperatures for April, May, July, August and September compared to the other years. Mean Growing Season Precipitation Rates (MGP) differed among the years and were highest in 2017 (83 mm). In decreasing order, MGPs were recorded with (74 mm) in 2020, (73 mm) in 2016 and (68 mm) in 2018. Lowest MGP was recorded for 2019 with 62 mm (see Appendices). Groundwater fluctuations remained mostly imperceptible throughout the investigation period, with only a minor flattening in spring 2018.

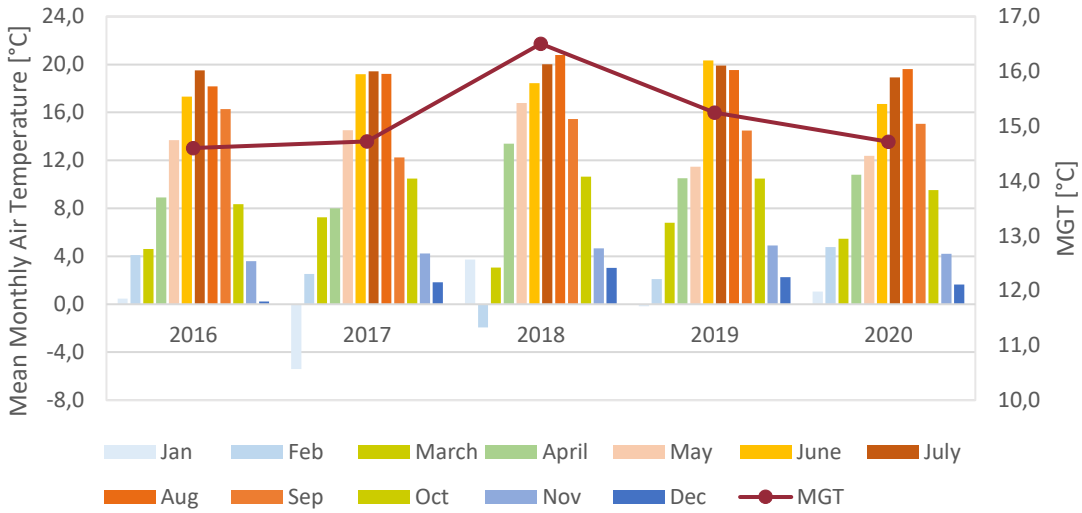

(a)

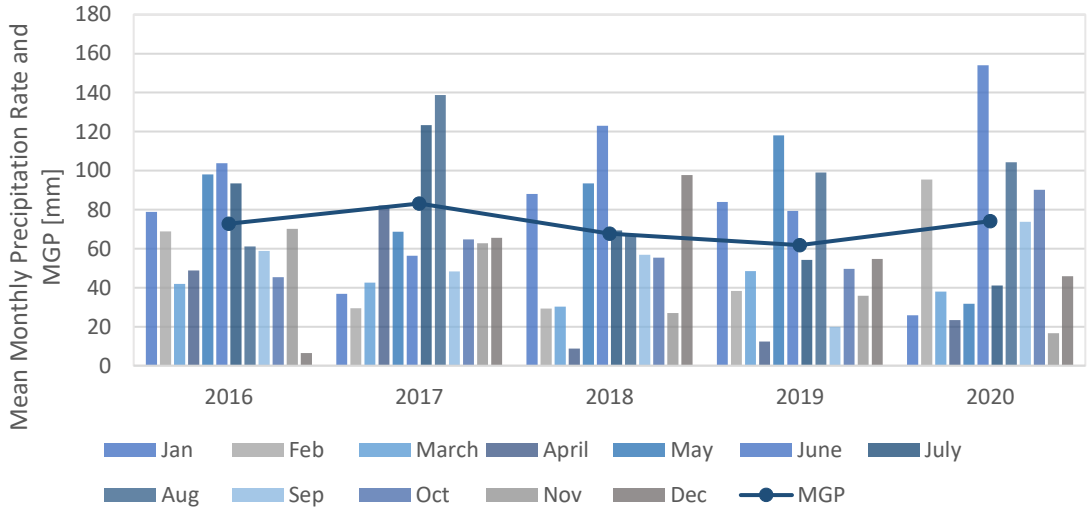

(b)

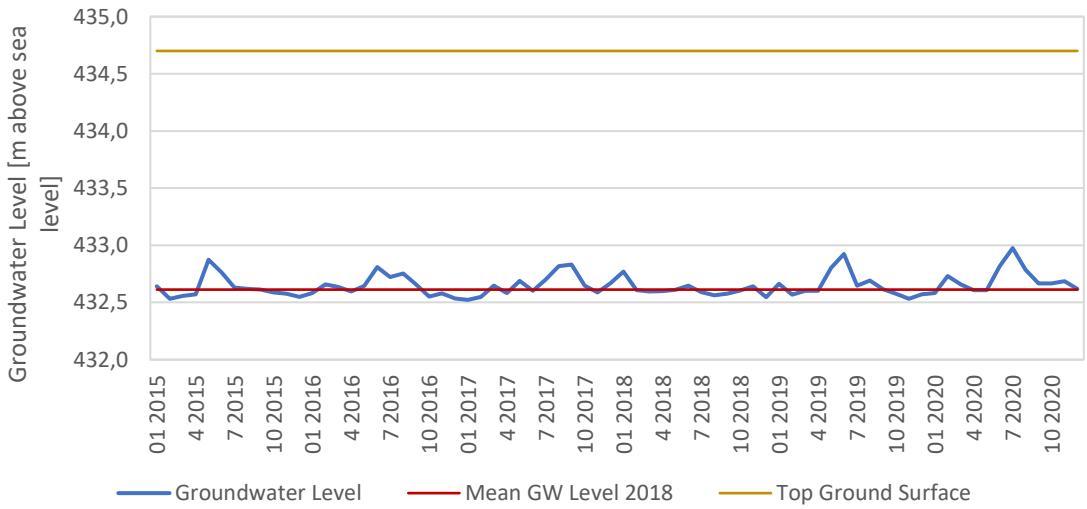

(c)

Figure 34. Mean monthly air temperature and mean growing season air temperature (MGT; a), mean monthly precipitation rate and mean growing season precipitation rate (MGP; b), as well as groundwater level and groundwater-surface distance (c) of study area Isar Floodplains from Unterföhring to Landshut. The growing season encompasses the months April to October. Data was obtained from the meteorological station Freising and monitoring well "Marzling Q5". (BayLfU 2020b; 2020d; 2020c; 2020e).

3.3.1 NDVI – Isar Floodplains from Unterföhring to Landshut

Satellite Data

Table 7. Satellite imagery used in the NDVI assessment of Study Area Pupplinger Au. Differences in investigation times arose from data availability limitations. Greyed out times are disregarded in the analysis by reason of undue temporal deferral.

Time	2016	2017	2018	2019	2020
T1	29 April	24 April	07 April	19 April	08 April
T2	27 August	25 August	22 August	27 August	21 August
T3	16 October	16 October	16 October	01 October	15 September

Intra-annual Alterations in NDVI Values

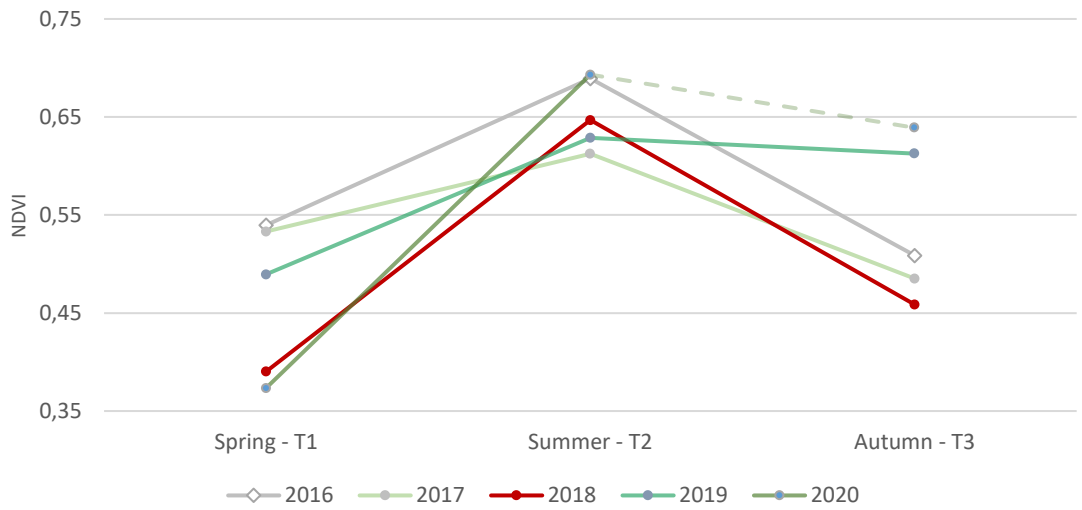

Figure 35. Intra-annual alterations in NDVI values of all investigated years for study area Isar Floodplains from Unterföhring to Landshut (2016-2020). Dashed lines indicate the disregarded excluded values, as outliers in investigation times may cause incomparability of obtained results.

Intra-annual alterations in NDVI values are depicted in Figure 35 for the entire study area Isar Floodplains from Unterföhring to Landshut. As for the previous two study areas, NDVI regimes adequately display the phenological cycle peaking in Summer-T2. However, steepness of increase and decrease in NDVI values vary for each year. NDVI for Spring-T1 (0.39), Summer-T2 (0.65) and Autumn-T3 (0.46) of drought year 2018 remain consistently below the NDVI regime of the reference year 2016 with Spring-T1 (0.54), Summer-T2 (0.69) and Autumn-T3 (0.51). This evenly reduced intra-annual NDVI regime of 2018 can be linked to the significantly different meteorological and hydrological conditions between 2016 and 2018. The latter has been, as previously described, substantially hotter than the other investigated year, but MGP differed only sightly between 2016 and 2018 (approx. 5mm). As for the study areas Pupplinger Au and Isar Floodplains Unterföhring, did the year 2020 exhibit the highest NDVI for Summer-T2 (0.69) out of all investigated years, although having started with the lowest NDVI in Spring-T1 (0.37). Maps visualising the intra-annual NDVI of 2016 and 2018, respectively, are included for this study area in the following section, as representative of areas alongside the middle reaches

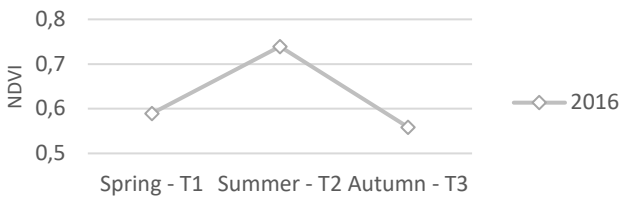

Figure 36. Intra-annual alterations of the NDVI in 2016 for Isar Floodplains from Unterföhring to Landshut with Spring-T1 (0.54), Summer-T2 (0.69) and Autumn-T3 (0.51). The following map visualizes this course in NDVI.

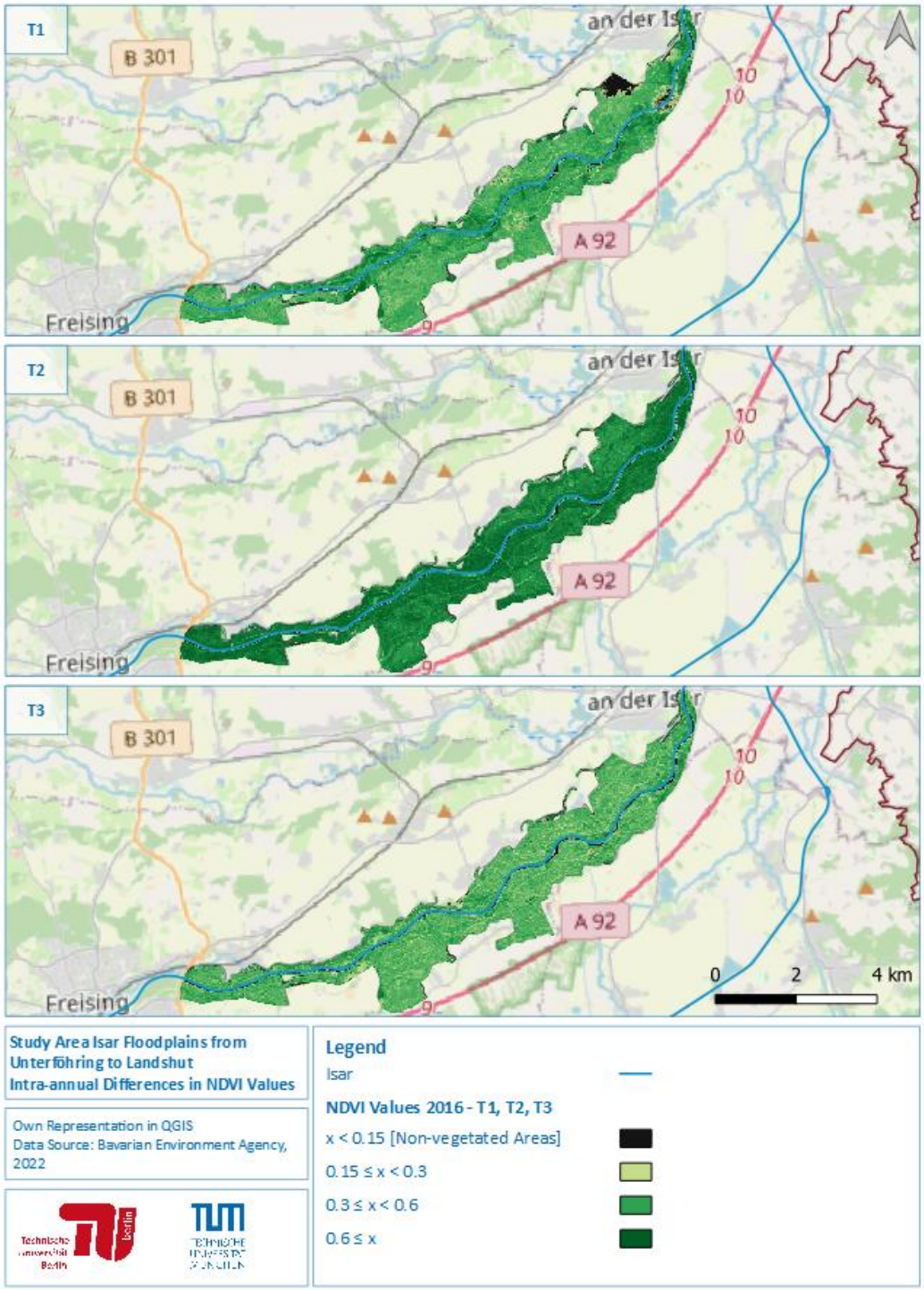

Map 20. NDVI throughout the year 2016. Darker green nuances indicate higher NDVI values, as detectable in Summer-T2, whereas lighter shades depict lower NDVI values. Black parts indicate non-vegetated areas or masked out cloud coverage.

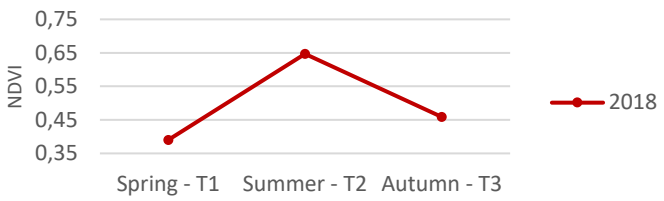

Figure 37. Intra-annual NDVI regime of 2018 for Isar Floodplains from Unterföhring to Landshut with Spring-T1 (0.39), Summer-T2 (0.65) and Autumn-T3 (0.46). The following map visualizes those results.

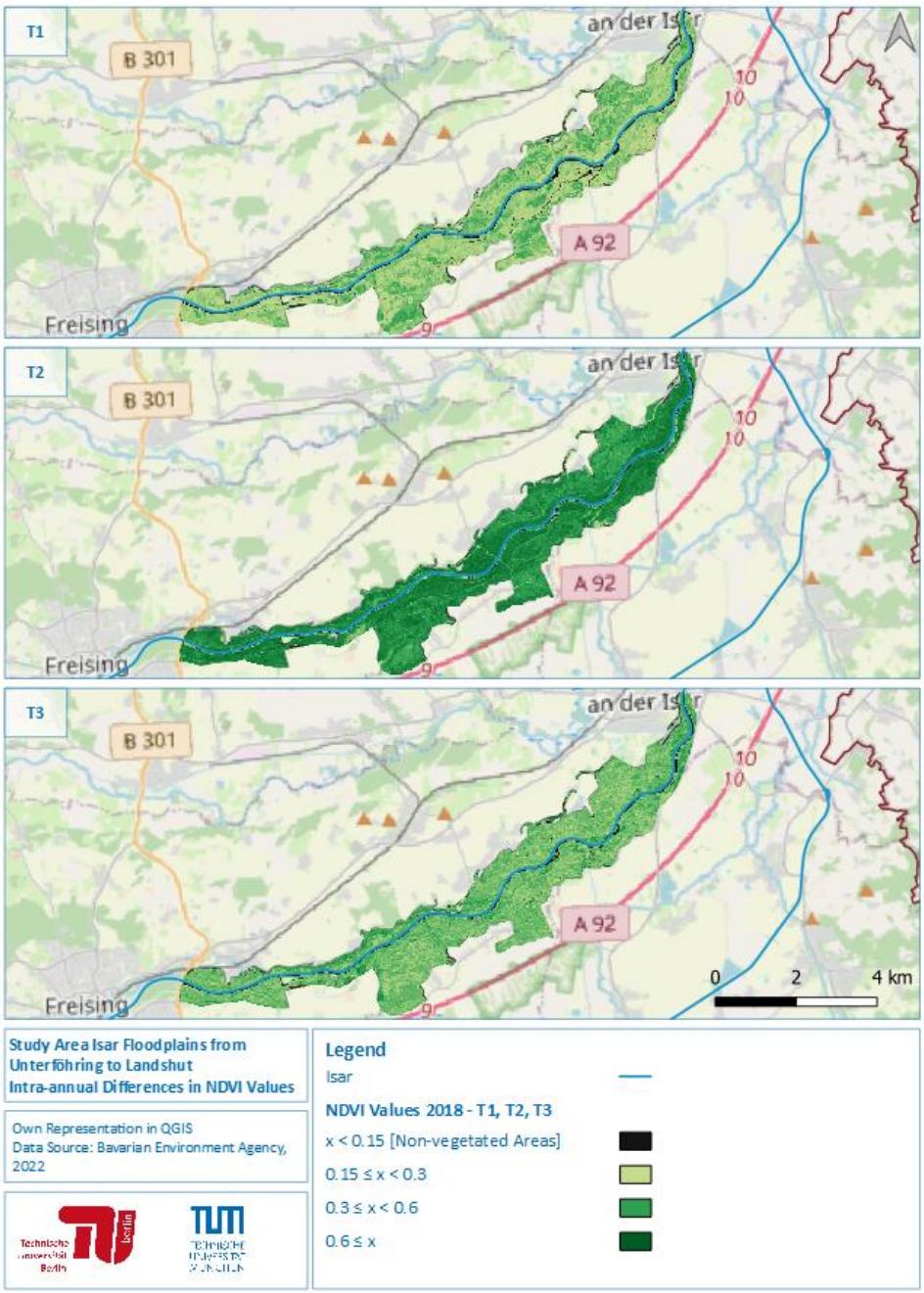

Map 21. NDVI throughout the year 2018. Darker green nuances indicate higher NDVI values, as detectable in Summer-T2, whereas lighter shades depict lower NDVI values. Black parts indicate non-vegetated areas or masked out cloud coverage.

Intra-annual alterations in NDVI values per biotope type and investigated year are depicted in Figure 38. Here too does the NDVI reflect the phenological cycle, by being directly related with chlorophyll-a content and thus, plant biomass. NDVI regimes of 2018 are in average lowest for all biotope types.

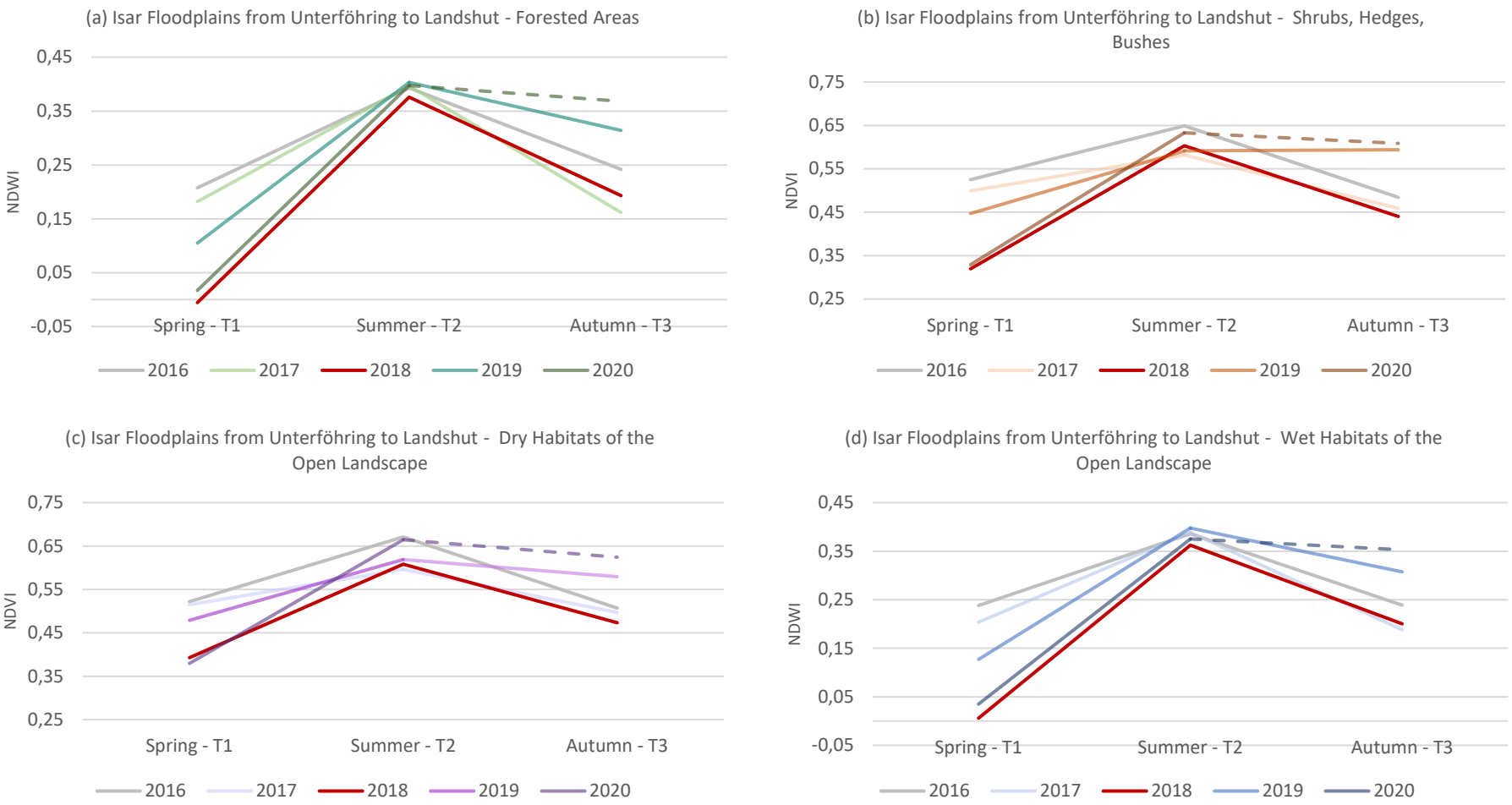

Figure 38. Intra-annual alterations of the NDVI values per biotope type and investigated year. NDVI regime reaches highest values for (a) Forested Areas (0.37-0.73), followed by (d) Wet Habitats of the Open Landscape (0.34-0.70), (c) Dry Habitats of the Open Landscape (0.38-0.67) and (c) Shrubs, Hedges and Bushes (0.32-0.65) in decreasing order. The 2018 NDVI regimes are, in comparison to the other investigated years, in average lowest for all biotope types. Particularly in comparison to the NDVI regimes of 2016, the 2018 NDVI regimes remain significantly lower for all investigation points (Sprin-T1, Summer-T2 and Autumn-T3) throughout the entire period (2016-2020) and for all biotope types. These results can be connected to the meteorological and hydrological conditions, meaning that all biotope types experienced plant vitality decreases following the drought event 2018.

Inter-annual Differences in NDVI Values for Study Area Isar Floodplains from Landshut to Unterföhring and per Biotope Type

The following maps display the inter-annual differences in NDVI values between the reference year 2016 and the other investigated years (2017, 2018, 2019 and 2020). Differences were calculated using the equation found under Materials and Methods. Changes in plant vitality were derived thereof and are depicted in the legend. Cloud coverage causes minor distortions in some maps.

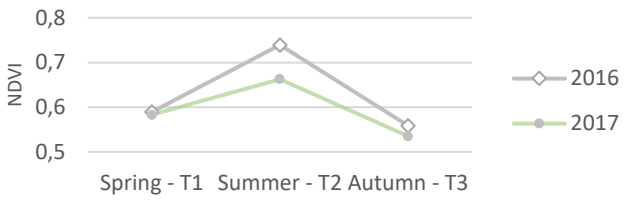

Figure 39. Mean intra-annual alterations of the NDVI 2016 and NDVI 2017 for the entire study area Isar Floodplains from Unterföhring to Landshut. Spring-T1 of 2016 and 2017 exhibit almost the same values (0.54) and (0.53), while Summer-T2 of 2017 (0.61) is significantly lower than Summer-T2 of 2016 (0.69). Both NDVI regimes decline in Autumn-T3 to 2017 (0.49) and 2016 (0.51). Those differences are visualized in Map 22.

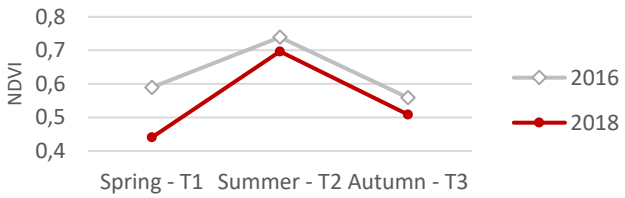

Figure 40. Mean intra-annual alterations of the NDVI 2016 and NDVI 2018 for the entire study area Isar Floodplains from Unterföhring to Landshut. Spring-T1 of 2016 (0.54) and 2018 (0.39) differ significantly from each other, whereas Summer-T2 and Autumn-T3 of 2018 (0.65 and 0.46) and 2016 (0.69 and 0.51) slightly converge. Nevertheless, the 2018 NDVI regime remains consistently lower than the NDVI regime of 2016. Those differences are visualized in Map 23.

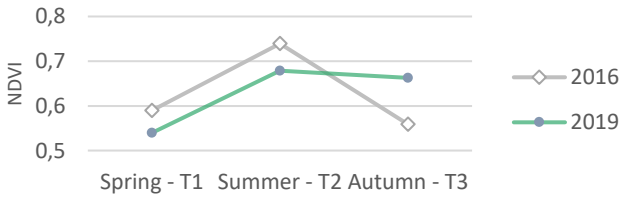

Figure 41. Mean intra-annual alterations of the NDVI 2016 and NDVI 2019 for the entire study area. Spring-T1 and Summer-T2 of 2016 (0.54 and 0.69) and 2019 (0.49 and 0.63) differ from each other by (0.05) and (0.06) respectively. Autumn-T3 of 2019 (0.61) is to be critically assessed in this analysis, as data was obtained October 1st, 2019, causing a quite high NDVI value. Scope of NDVI differences for those years are visualized in Map 24.

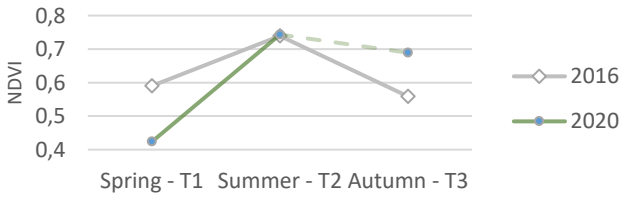

Figure 42. Mean intra-annual alterations of the NDVI 2016 and NDVI 2020 for the entire study area. Spring-T1 of 2020 (0.37) is significantly lower than Spring-T1 of 2016 (0.54), while the same NDVI was recorded for Summer-T2 of 2020 (0.69) and 2016 (0.69). Autumn-T3 of 2020 (0.64) is disregarded in this analysis as data was obtained 15th September 2020, resulting in undue temporal deferral. The scope in NDVI differences is visualized in Map 25.

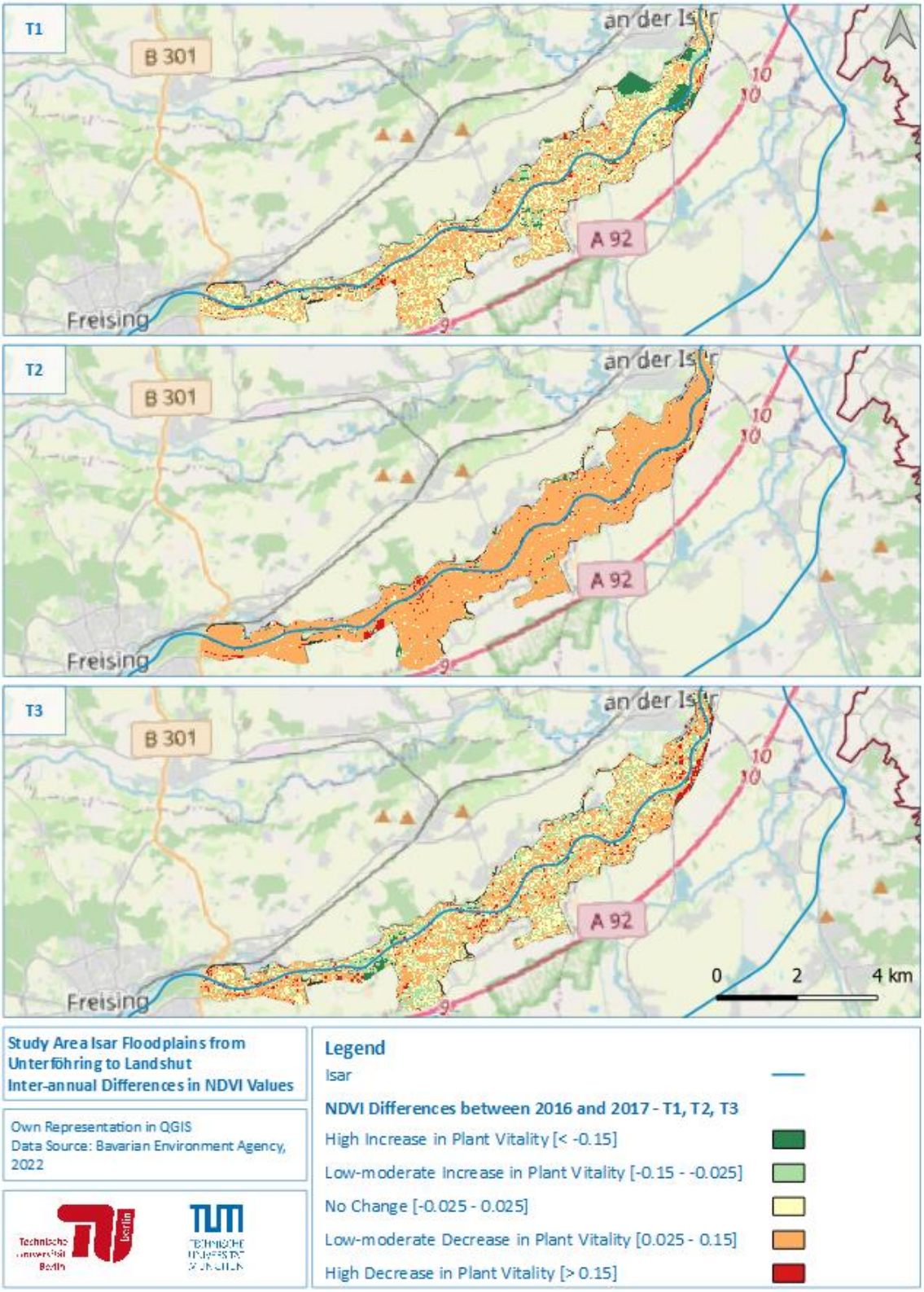

Map 22. Extensive low-moderate decreases in plant vitality, and some areas with high decreases in plant vitality were observed for 2016-2017 at Summer-T2. Both Spring-T1 and Autumn-T3 display very disparate results with fragmented plots of all possible differences in plant vitality, causing the similarity in NDVI values depicted in Figure 39.

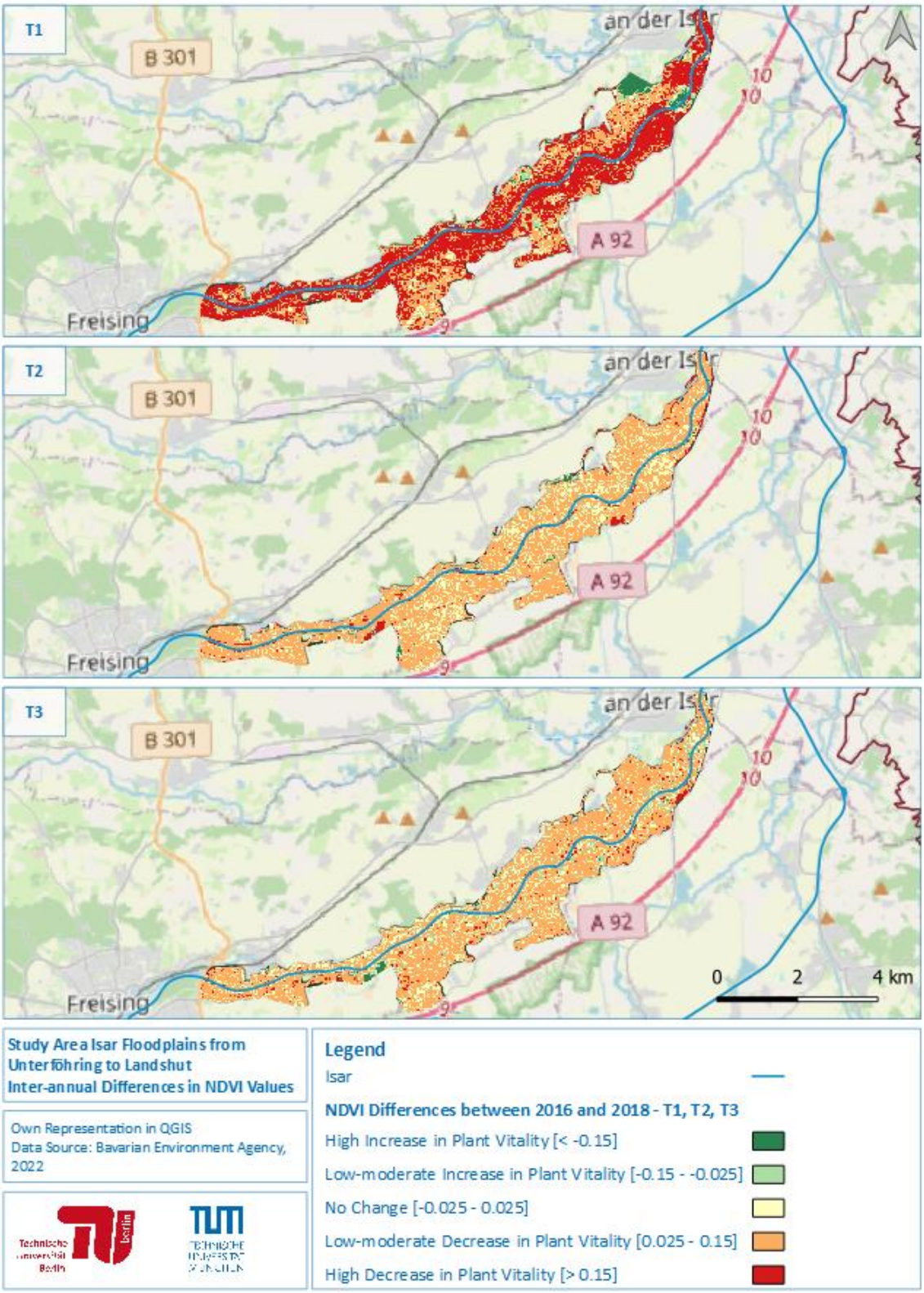

Map 23. Exhaustive high decreases in plant vitality are arevealed for Spring-T1 between 2016 and 2018, while similar extents of low-moderate decreases in plant vitality were detected for this study area in the comparison between 2016-2018 both at T2 and T3. Those depictions accurately reflect the NDVI regimes in Figure 40.

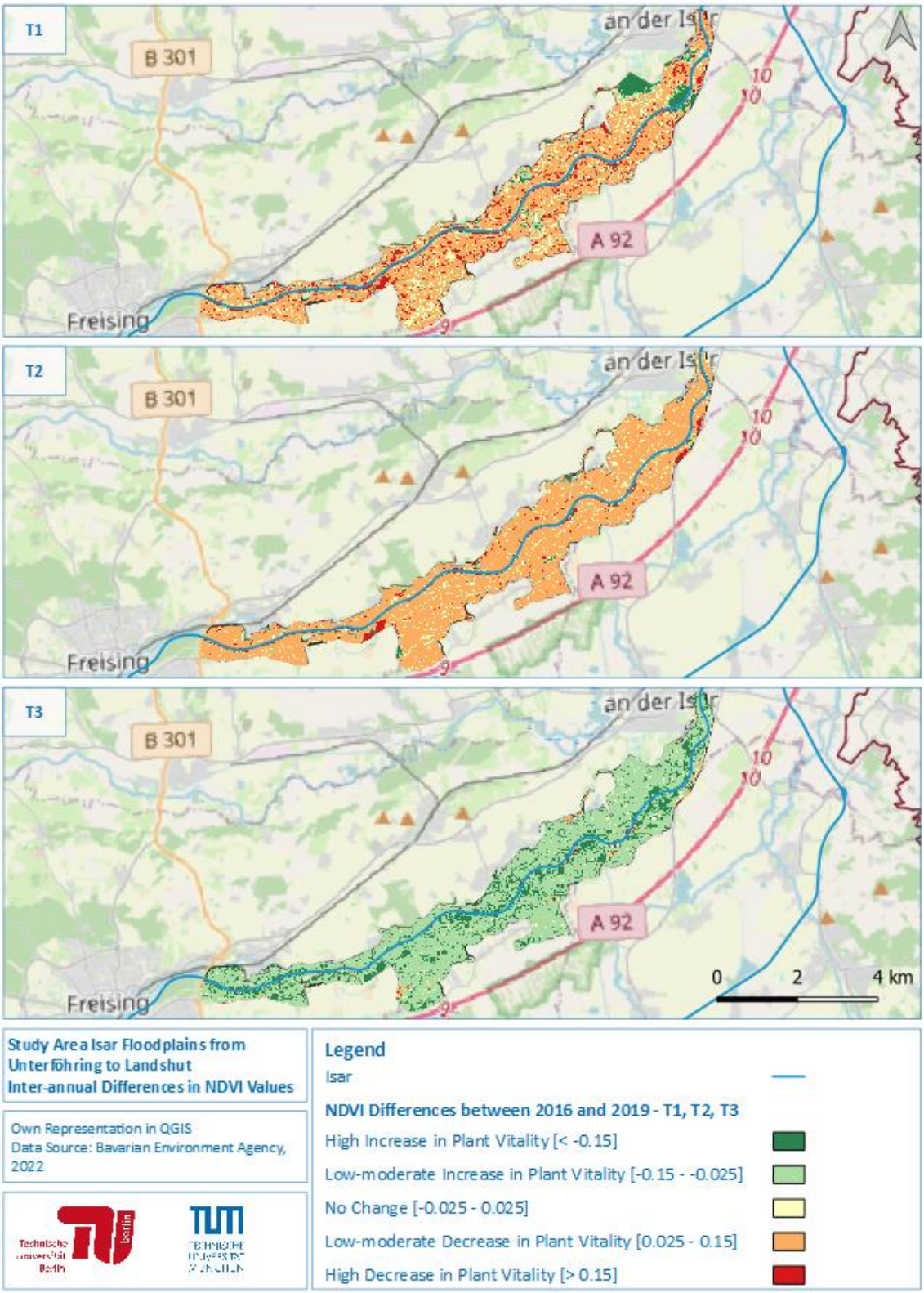

Map 24. Disregarding the small erroneous display of plant vitality increase due to cloud coverage in T1, the remaining surface exposed fragmented low-moderate and high decreases in plant vitality for the investigation point Spring-T1 (2016-2019). Exhaustive low-moderate decreases and minor high decreases in plant vitality were detected in the comparison between 2016-2019 for Summer-T2. Low-moderate increases in plant vitality, however, were detected for Autumn-T3 (2016-2019). These results have to be critically regarded in this analysis, as data was obtained October 1st 2019, potentially resulting in spuriously high NDVI values for 2019-T3. See Figure 41.

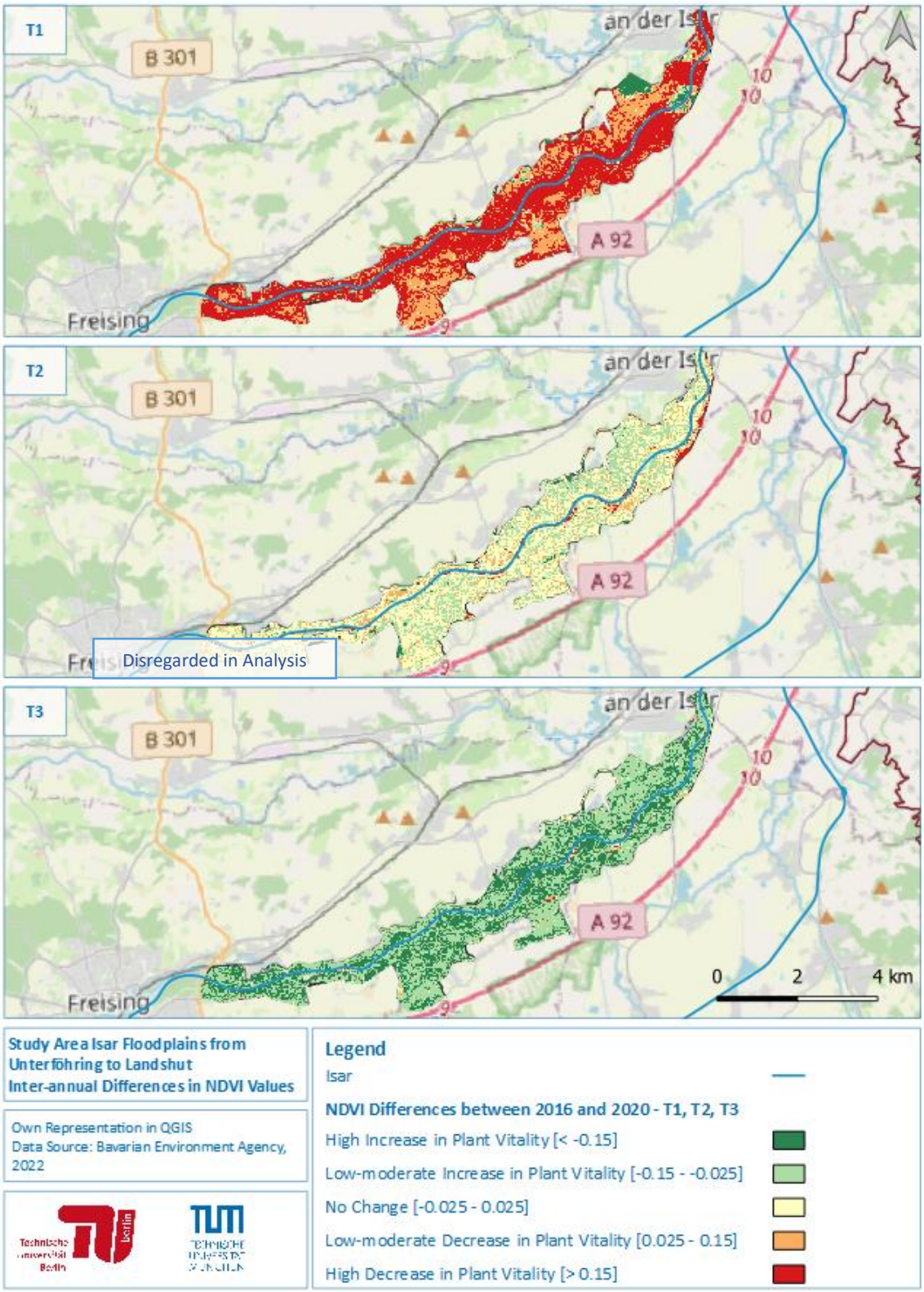

Map 25. High decreases in NDVI values and thus, plant vitality, were observed for Spring-T1 between 2016 and 2020 with extensive scope, whereas almost no change was detected between 2016 and 2020 at Summer-T2. Fragmented areas display NDVI differences of all categories. Autumn-T3 is disregarded, as data for 2020-T3 was obtained September 15th, creating an undue temporal deferral. Those depictions adequately reflect the results as displayed in Figure 42.

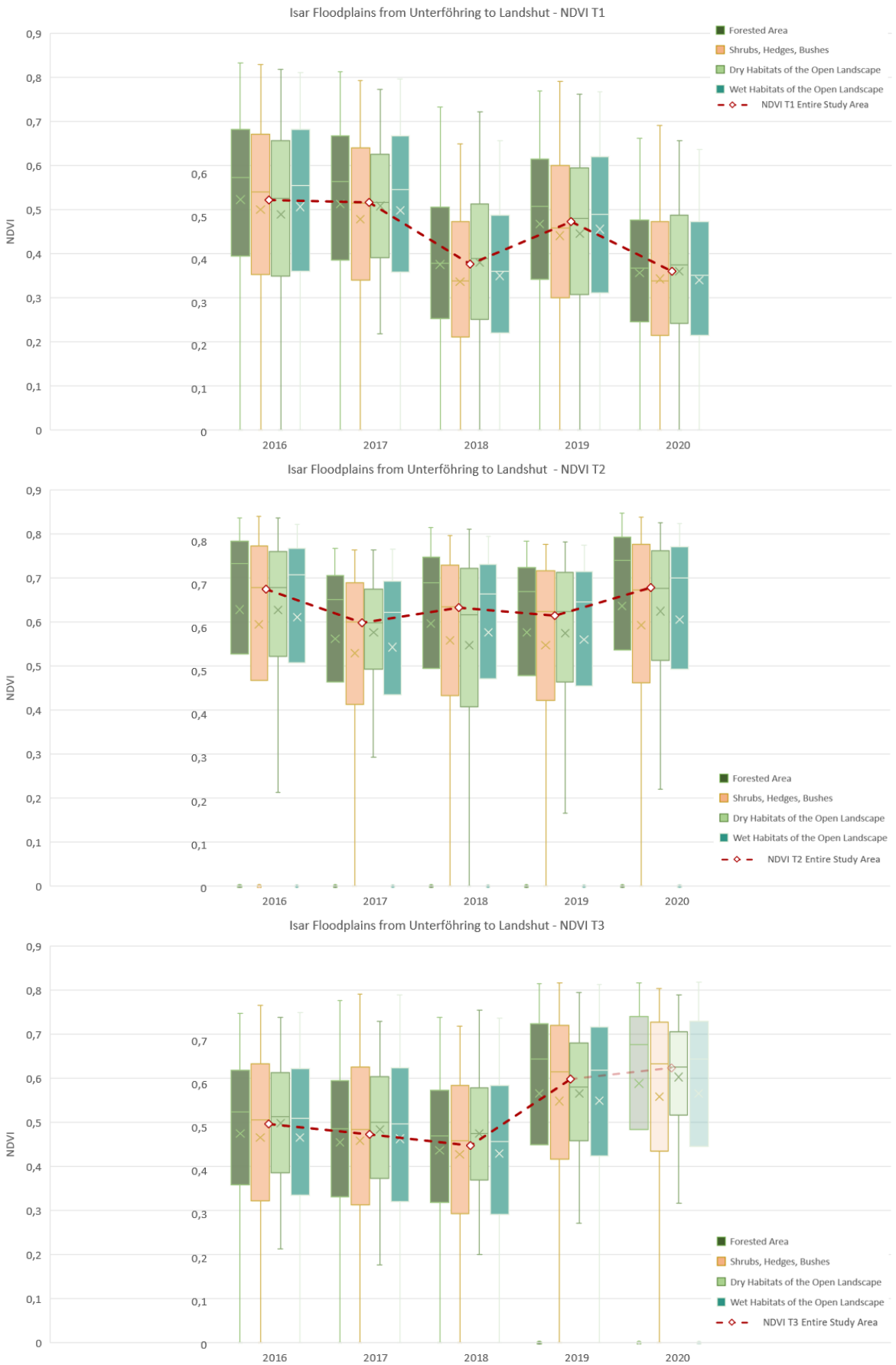

Figure 43. Inter-annual diffences in NDVI values per biotope type and year for Isar Floodplains from Unterföhring to Landshut.

Box and whisker plots describe the variability of NDVI value distribution within each biotope type and depict the scatter range. Scattering of the NDVI ranges in increasing order: Dry Habitats of the Open Landscape, Shrubs, Hedges and Bushes, Wet Habitats of the Open Landscape and Forested Areas. Dotted red lines indicate the mean NDVI values for the entire study area in relation to each biotope type. All biotope types exhibit lower mean NDVI values at each investigation point (Spring-T1, Summer-T2 and Autumn-T3) for the drought year 2018, when compared to the refernce year 2016.

By contrast with all investigated years, however, Forested Areas exhibt the lowest mean NDVI at Spring-T1 in 2020 (0.37), Shrubs Hedges and Bushes in 2018 (0.32), Dry Habitats of the Open Landscape in 2020 (0.38) and Wet Habitats of the Open Landscape in 2010 (0.34). For Summer-T2 , Forested Areas display the lowest mean NDVI in 2017 (0.64), Shrubs Hedges and Bushes in 2017 (0.58) , Dry Habitats of the Open Landscape in 2017 and 2018 with equal value (0.60)and Wet Habitats of the Open Landscape in 2017 (0.61). For Autumn-T3, all biotope types exhibit the lowest mean NDVI in 2018 - Forested Areas (0.47), Shrubs Hedges and Bushes (0.44), Dry Habitats of the Open Landscape (0.47) and Wet Habitats of the Open Landscape (0.44).These results indicate the importance of considering regional site conditions, as well as the differentiation between different biotope types.

3.3.2 NDWI – Isar Floodplains from Landshut to Unterföhring and per Biotope Type

Satellite Data

Table 8. Satellite imagery used in the NDWI assessment of Study Area Isar Floodplains from Landshut to Unterföhring. Differences in investigation times arose from limitations in data availability. Greyed out times are disregarded in the analysis by reason of undue temporal deferral.

Time	2016	2017	2018	2019	2020
T1	29 April	24 April	07 April	19 April	08 April
T2	27 August	25 August	22 August	27 August	21 August
T3	16 October	16 October	16 October	01 October	15 September

Intra-annual Alterations in NDWI Values

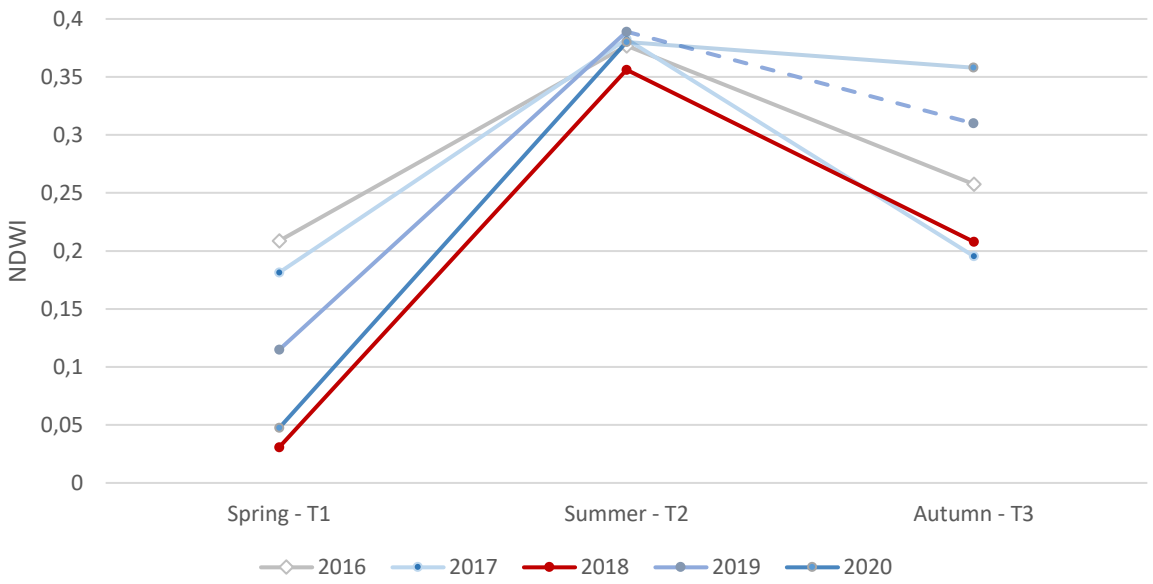

Figure 44.Mean intra-annual alterations in NDWI for study area Isar Floodplains from Unterföhring to Landshut. Dashed lines indicate the disregarded values, as outliers of investigation times may cause incomparability in obtained results.

Intra-annual alterations in NDWI values are depicted in Figure 44 for the entire study area Isar Floodplains from Unterföhring to Landshut. The positive correlation between plant biomass and intracellular water content with regards to the normal course of the phenological cycle is adequately reflected be the NDWI regimes of this study area or all investigated years. As for the other study areas, steepness of increase and decrease in NDWI values varies for each year. The NDWI regime in 2019 increases with the steepest gradient, followed by 2017, 2020, 2018 and 2016 in decreasing order. The NDWI regime of 2018 remains significantly lower than the NDWI regime of 2016 for all investigated years. Spring-T1 (0.03), Summer-T2 (0.36) and Autumn-T3 (0.21) during 2018 are substantially lower in comparison to Spring-T1 (0.21), Summer-T2 (0.38) and Autumn-T3 (0.26) during 2016. The above-described disparate meteorological conditions within the investigation period (2016-2020) are closely tied to the obtained differences in NDWI regimes, where both temperature and precipitation rate in 2018 deviated from the ones of the reference year 2016, resulting in impediments for plant growth and thus, reduced plant water content.

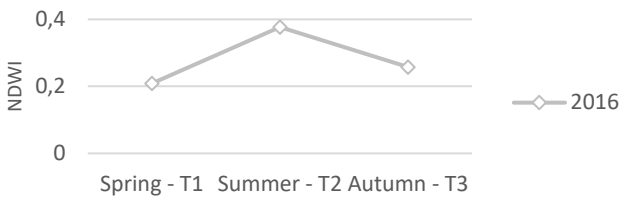

Figure 45. Mean intra-annual alterations of the NDWI 2016 for Isar Floodplains from Unterföhring to Landshut with Spring-T1 (0.21), Summer-T2 (0.38) and Autumn-T3 (0.26). The following map visualizes the intra-annual alterations of 2016.

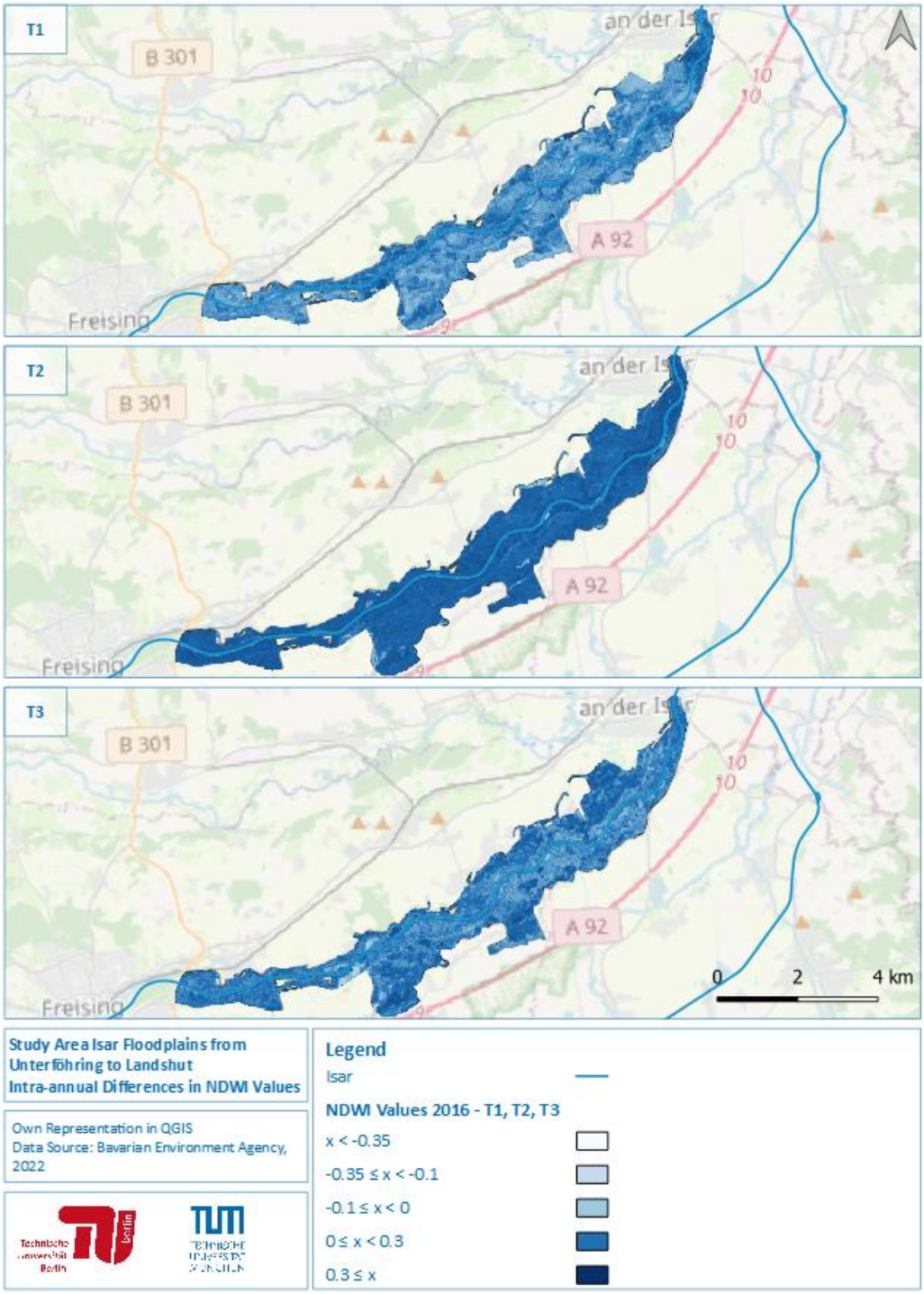

Map 26. A clear increase in NDWI is visible for the investigation point Summer-T2, adequately displayed by darker nuances in blue compared to investigation point Spring-T1. Decreasing NDWI between Summer-T2 and Autumn-T3 are visible for the entire study area.

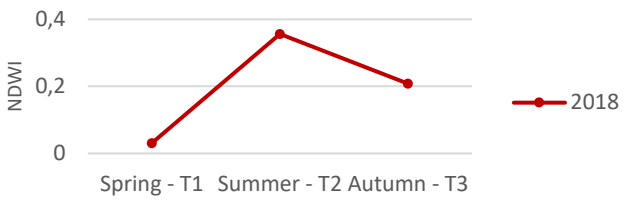

Figure 46. Mean intra-annual alterations of the NDWI 2018 for the entire study area with Spring-T1 (0.03), Summer-T2 (0.36) and Autumn-T3 (0.21). The following map visualizes the intra-annual alterations of 2018.

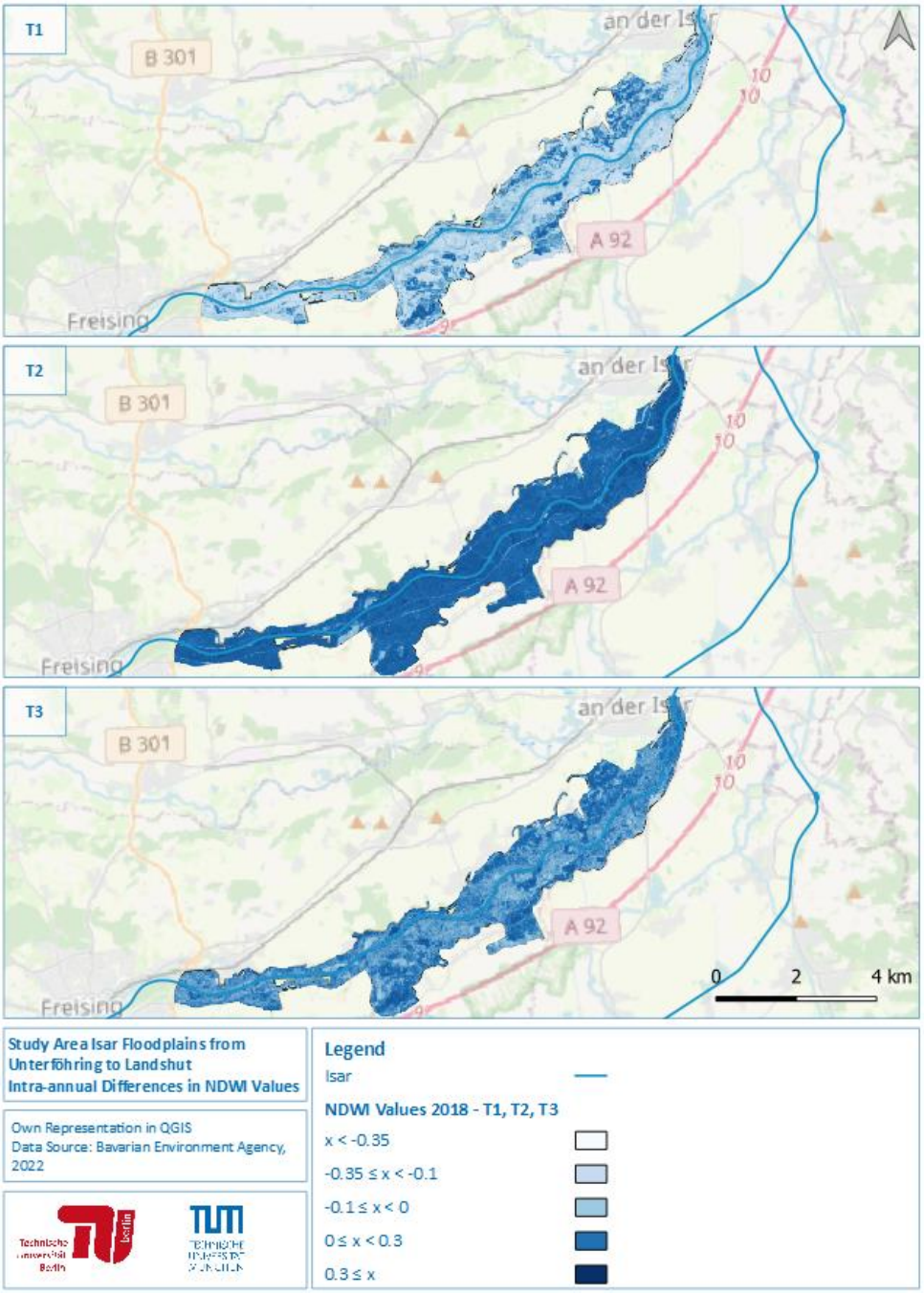

Map 27. A clear increase in NDWI is visible for the investigation point T2, adequately displayed by darker nuances in blue compared to investigation point T1. Minor differences are noticebale between T2 and T3.

Intra-annual alterations in NDWI values per biotope type and year, respectively, are depicted in Figure 47. For all four biotope types the NDWI regime in 2018 is in average the lowest out of all investigated years.

Figure 47. Intra-annual alterations of the NDWI values per biotope type and investigated year. NDWI regimes display specific signatures for (a) Forested Areas (NDWI -0.06 -0.40), (b) Shrubs, Hedges and Bushes (NDWI 0.01-0.40), (c) Dry Habitats of the Open Landscape (NDWI 0.0-0.31) and (d) Wet Habitats of the Open Landscape (NDWI 0.01-0.40). The 2018 NDWI regimes are, in comparison to the other investigated years, lowest for all biotope types. These results can be connected to the meteorological and hydrological conditions, meaning that all biotope types experienced significantly decreases in NDWI throughout 2018, being directly linked to plant water stress following the 2018 drought.

Inter-annual Differences in NDWI Values and per Biotope Type

The following graphs and maps display the mean inter-annual NDWIs for all years per investigation point (T1, T2, T3), respectively. Change detection cannot be displayed for NDWI due to calculation restrictions, as NDWI values range from negative values to positive values. Inter-annual changes are visualized by depicting maps of each investigation point (T1, T2, T3) for all years, respectively (Maps 28 – 30). (Unlike NDVI values, negative NDWI values cannot be excluded from calculations as some vegetated surfaces/areas display negative NDWI values). They do not incorporate Change Detection as for the NDVI.

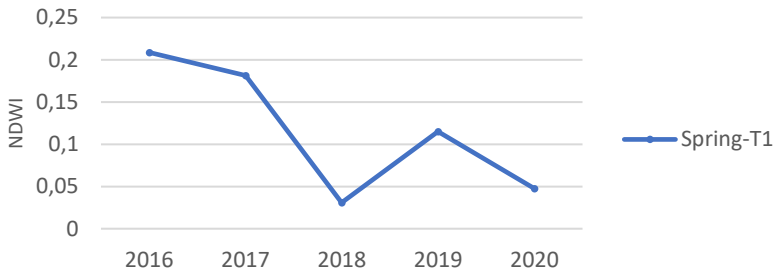

Figure 48. Mean inter-annual alterations of the NDWI throughout the investigation period (2016-2020) for the entire study area at Spring-T1. NDWI values are highest in 2016 (0.21), followed by 2017 (0.18), 2019 (0.11), 2020 (0.05) and 2018 (0.03) in decreasing order. Map 28 visualizes the NDWI for Spring-T1 of all investigated years.

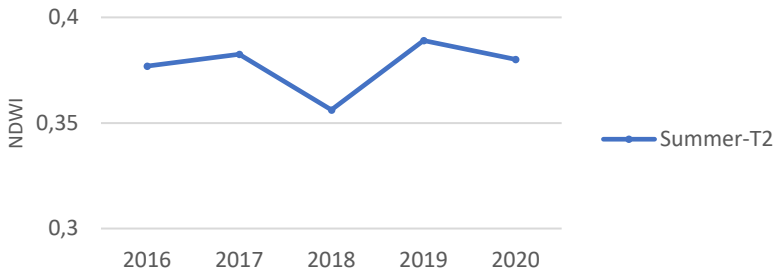

Figure 49. Mean inter-annual alterations of the NDWI throughout the investigation period (2016-2020) for the entire study area at Summer-T2. NDWI values are highest in 2019 (0.39), followed by 2017 (0.38), 2016 (0.38), 2020 (0.38) and 2018 (0.36) in decreasing order. Map 29 visualizes the NDWI for Summer-T2 of all investigated years.

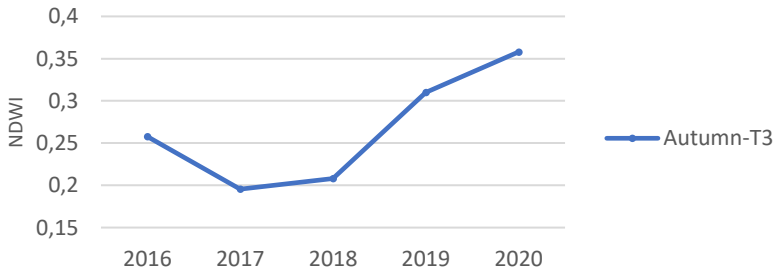

Figure 50. Mean inter-annual alterations of the NDWI throughout the investigation period (2016-2020) for the entire study area at Autumn-T3. NDWI values are highest in 2020 (0.36), followed by 2019 (0.31), 2016 (0.26) and 2018 (0.21) and 2017 (0.20) in decreasing order. 2019 and 2020 are, however, disregarded in the analysis as high-quality satellite imagery was only obtainable for September 2019 and 2020, respectively. Distortions in the NDWI results can therefore not be excluded. Map 30 visualizes the NDWI for Autumn-T3 of all investigated years.

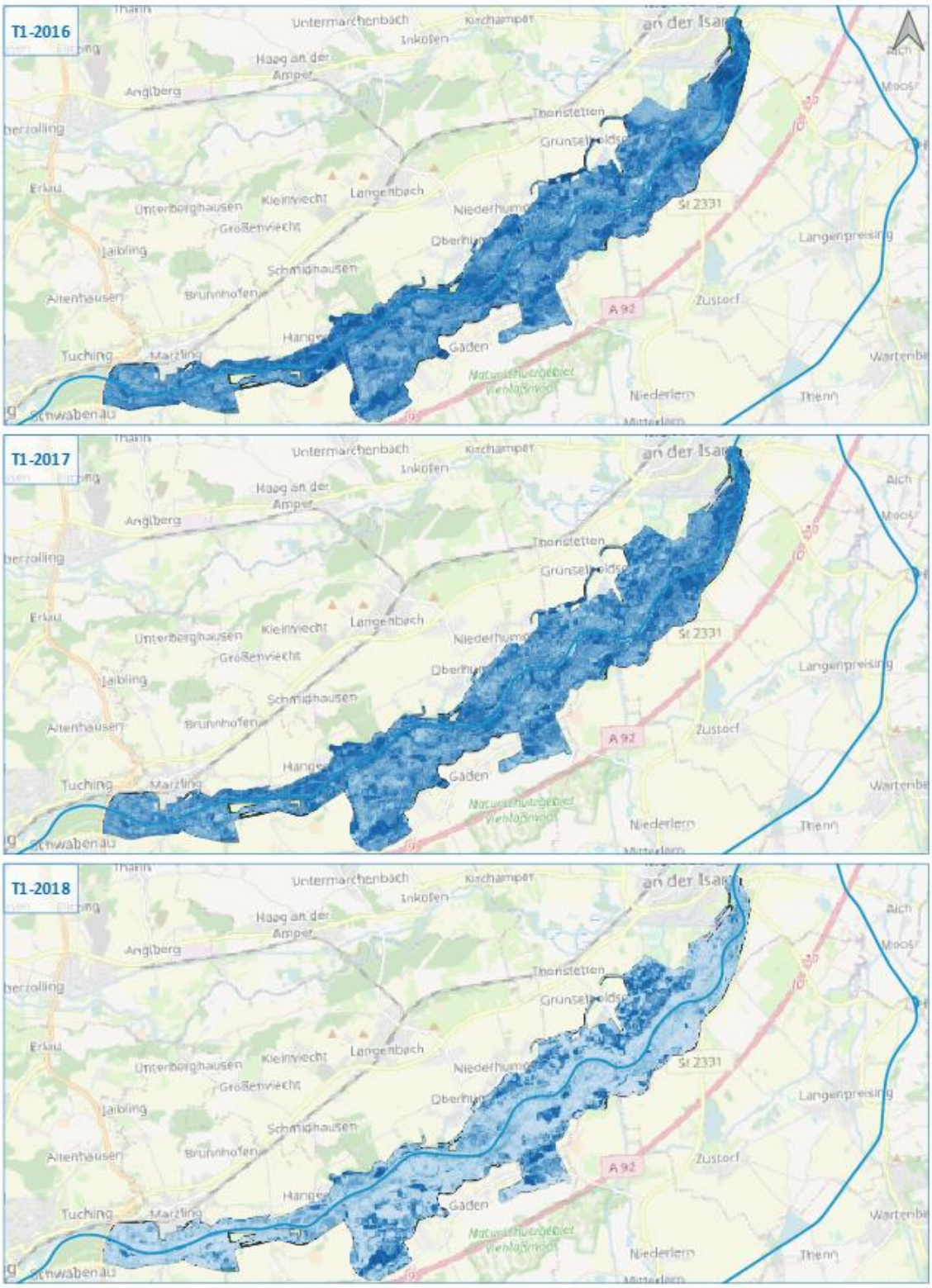
T1-2016
T1-2017
T1-2018
Untermarchenbach
Kirchampfer
Inkofen
Haag an der Amper
Angiberg
Thonstetten
Grunsel
Langenbach
Kleinwiecht
Unterberghausen
Großenwiecht
Niederhum
Oberhum
St 2331
Langenpreising
Jaibling
Schmidhausen
Altenhausen
Brunnhofen
Zustorf
A 92
Tuching
Marzling
Gaden
Niederlern
Thenn
Erlau
Aich
Moos

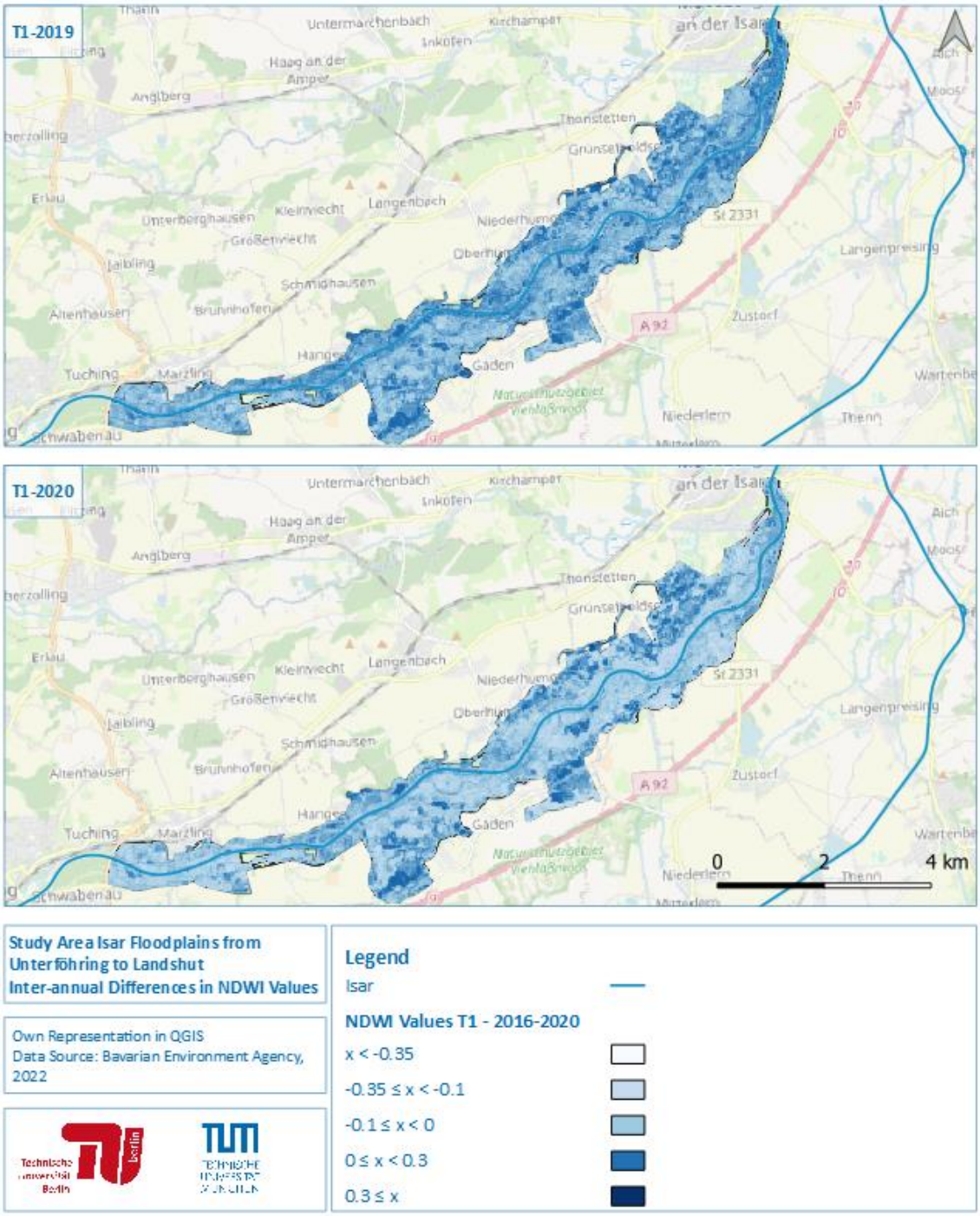

Map 28. NDWI for study area Isar Floodplains from Unterföhring to Landshut of all investigated years at Spring-T1. This map visualized the results as seen in Figure 48.

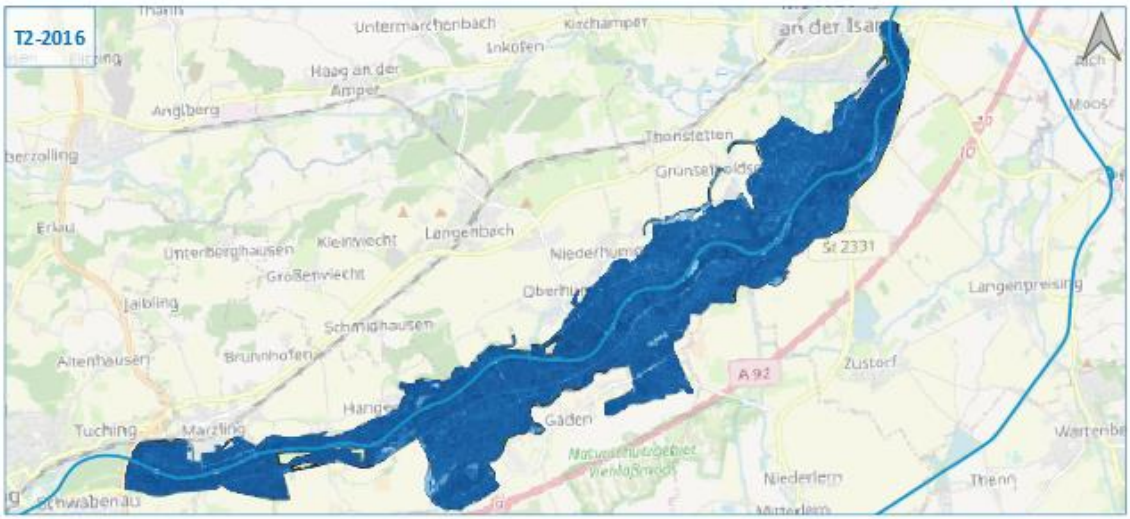
T2-2016
Untermarchenbach
Kirchamper
Inkofen
an der Isar
Haag an der Amper
Anglberg
Thonstetten
Grunsel
Erkau
Unterberghausen
Kleinwiecht
Langenbach
Niederhum
St 2331
Großenwiecht
Oberhum
Langenpreising
Jaibling
Schmidhausen
Altenhausen
Brunnhofen
Zustorf
A 92
Hange
Tuching
Marzling
Gaden
Niederlern
Thenn

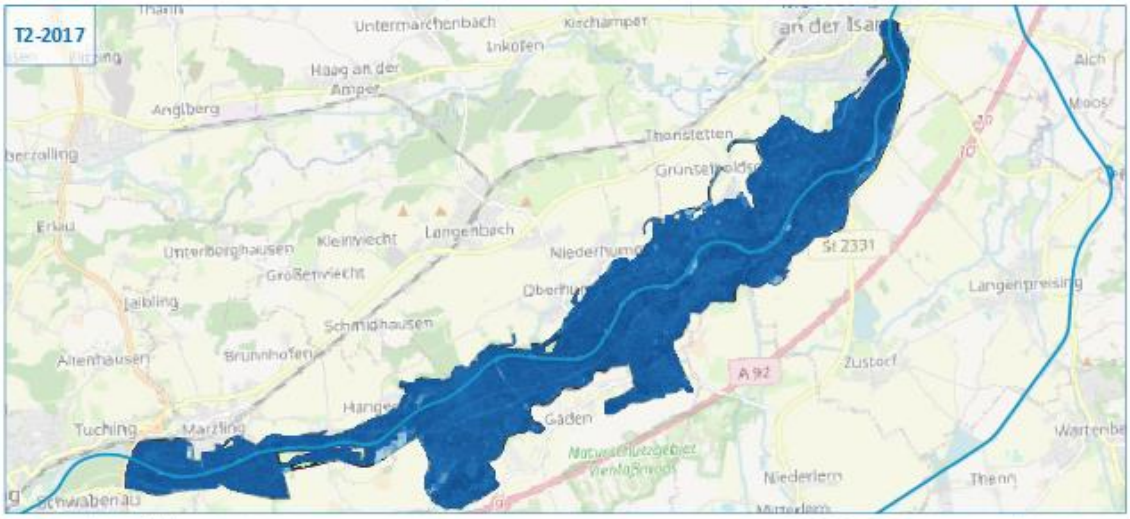
T2-2017
Untermarchenbach
Kirchamper
Inkofen
an der Isar
Haag an der Amper
Anglberg
Thonstetten
Grunsel
Erkau
Unterberghausen
Kleinwiecht
Langenbach
Niederhum
St 2331
Großenwiecht
Oberhum
Langenpreising
Jaibling
Schmidhausen
Altenhausen
Brunnhofen
Zustorf
A 92
Hange
Tuching
Marzling
Gaden
Niederlern
Thenn

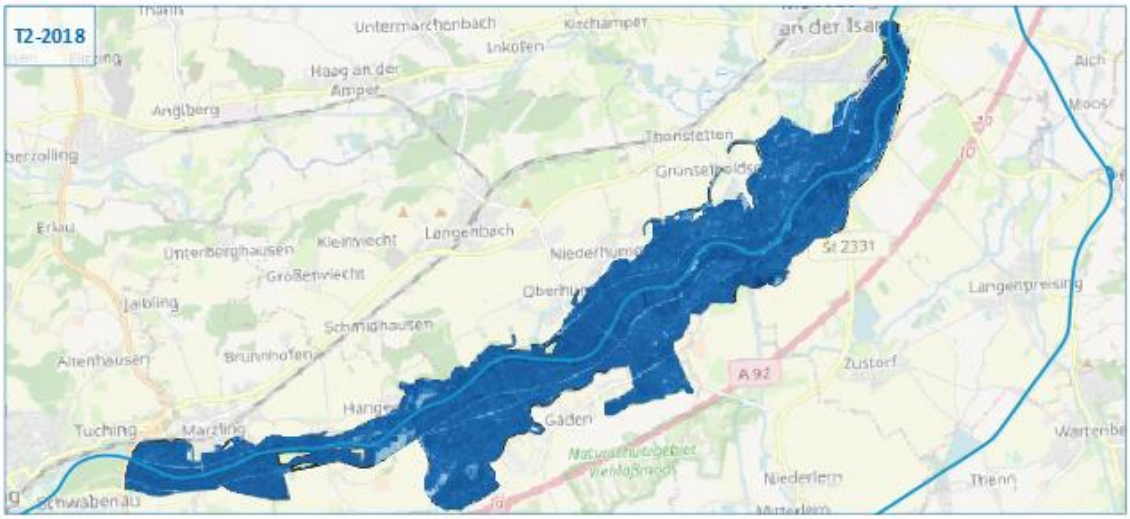
T2-2018
Untermarchenbach
Kirchamper
Inkofen
an der Isar
Haag an der Amper
Anglberg
Thonstetten
Grunsel
Erkau
Unterberghausen
Kleinwiecht
Langenbach
Niederhum
St 2331
Großenwiecht
Oberhum
Langenpreising
Jaibling
Schmidhausen
Altenhausen
Brunnhofen
Zustorf
A 92
Hange
Tuching
Marzling
Gaden
Niederlern
Thenn

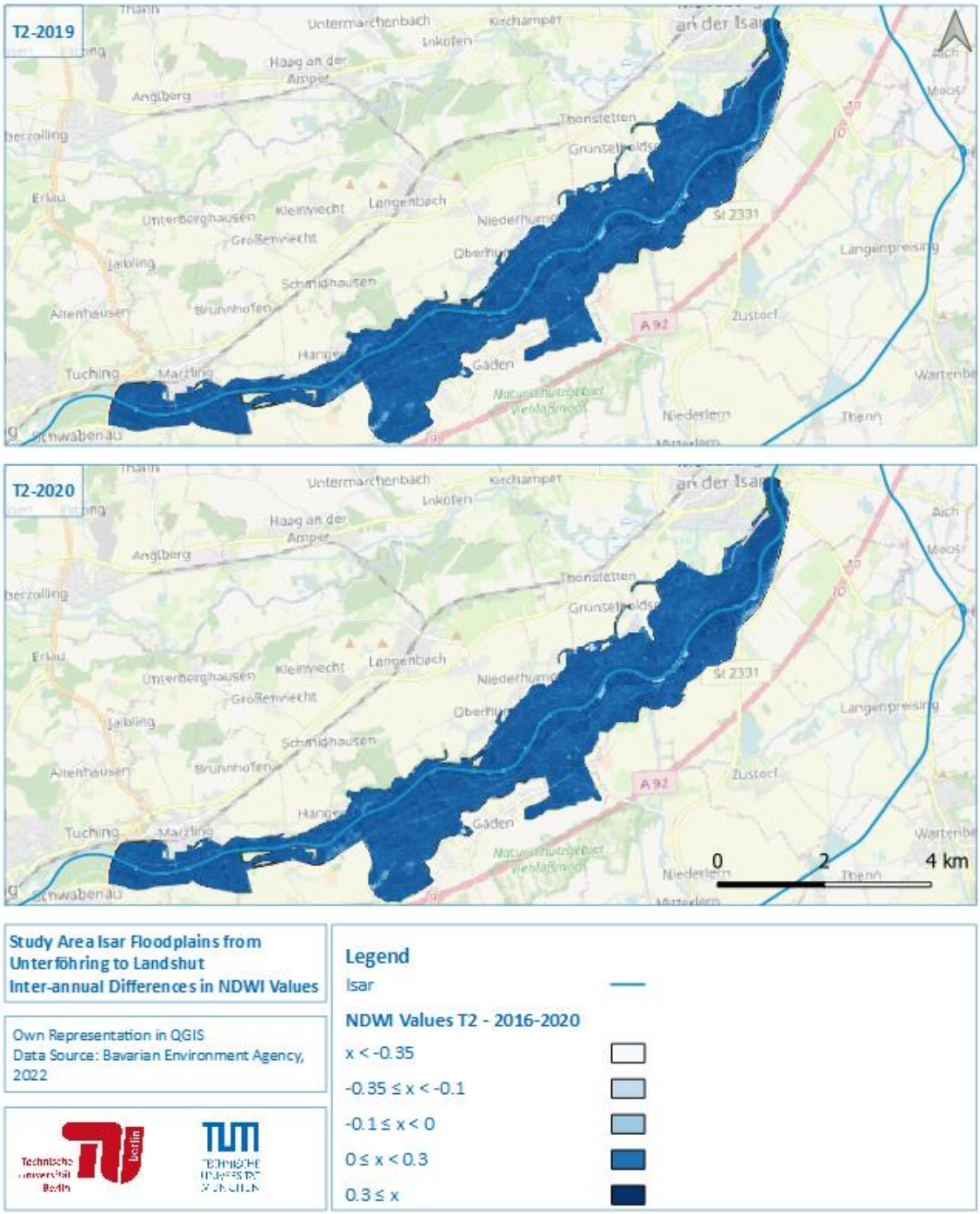

Map 29. NDWI for study area Isar Floodplains from Unterföhring to Landshut of all investigated years at Summer-T2. This map visualized the results as seen in Figure 49.

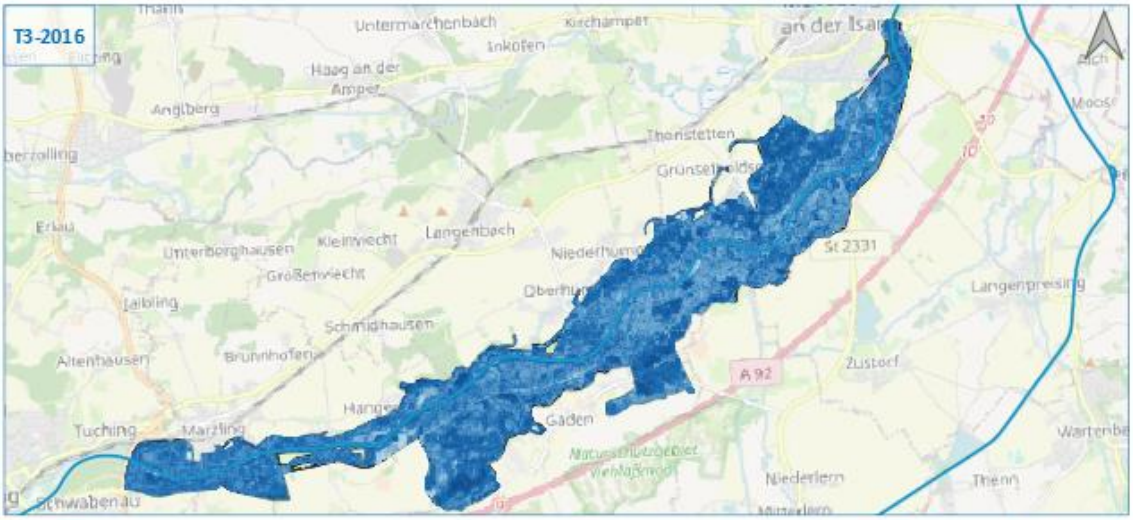
T3-2016
Untermarchenbach
Kirchampet
Inkofen
an der Isar
Haag an der Amper
Anglberg
Thonstetten
Grünseiboldsdorf
Erlau
Unterberghausen
Kleinwiecht
Langenbach
Niederhummel
St 2331
Großenwiecht
Oberhummel
Langenpreising
Laibling
Schmidhausen
Altenhausen
Brunnhofen
A 92
Zustorf
Hangenham
Tuching
Marzling
Gaden
Niederlern
Thenn

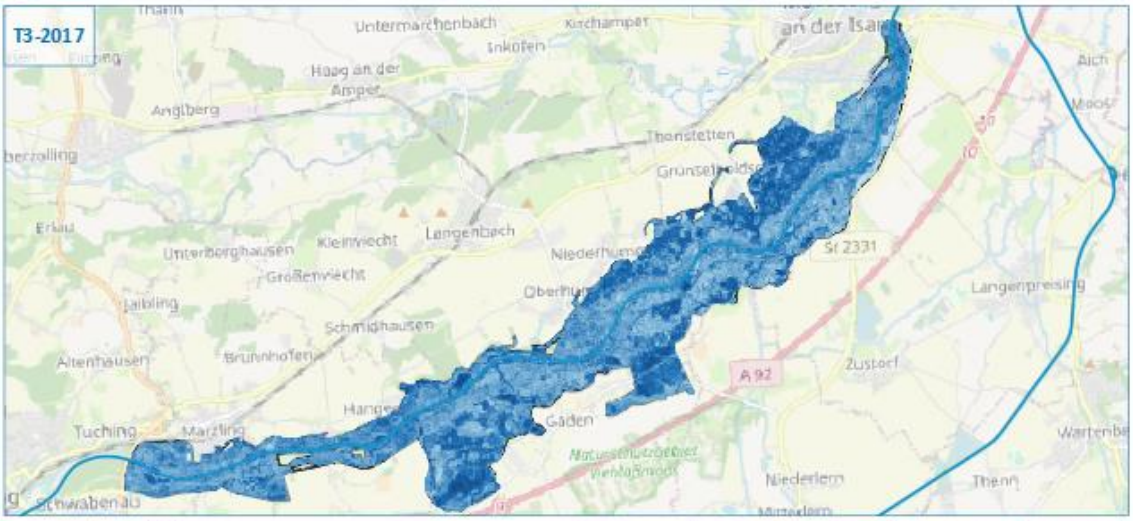
T3-2017
Untermarchenbach
Kirchampet
Inkofen
an der Isar
Haag an der Amper
Anglberg
Thonstetten
Grünseiboldsdorf
Erlau
Unterberghausen
Kleinwiecht
Langenbach
Niederhummel
St 2331
Großenwiecht
Oberhummel
Langenpreising
Laibling
Schmidhausen
Altenhausen
Brunnhofen
A 92
Zustorf
Hangenham
Tuching
Marzling
Gaden
Niederlern
Thenn

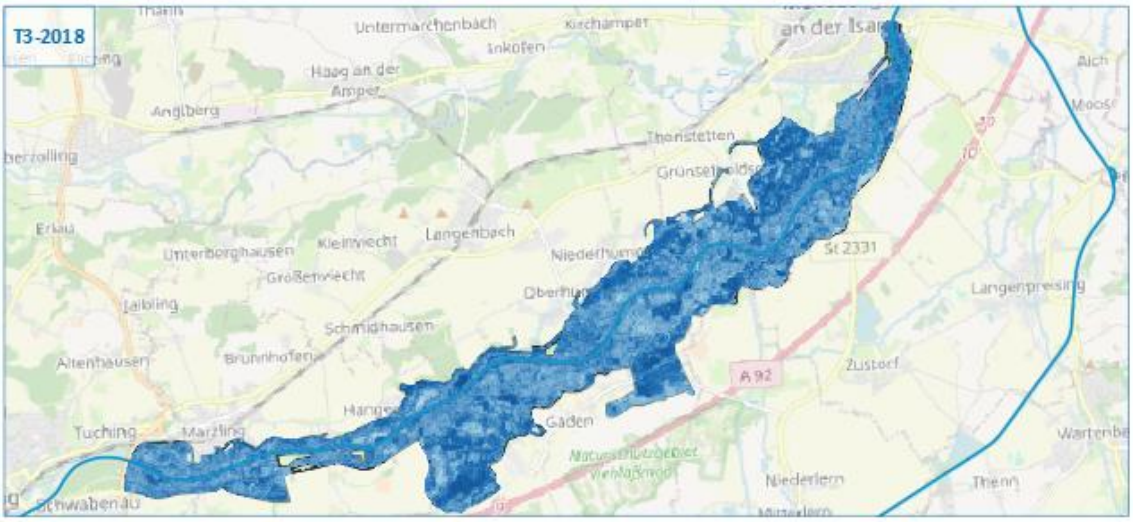
T3-2018
Untermarchenbach
Kirchampet
Inkofen
an der Isar
Haag an der Amper
Anglberg
Thonstetten
Grünseiboldsdorf
Erlau
Unterberghausen
Kleinwiecht
Langenbach
Niederhummel
St 2331
Großenwiecht
Oberhummel
Langenpreising
Laibling
Schmidhausen
Altenhausen
Brunnhofen
A 92
Zustorf
Hangenham
Tuching
Marzling
Gaden
Niederlern
Thenn

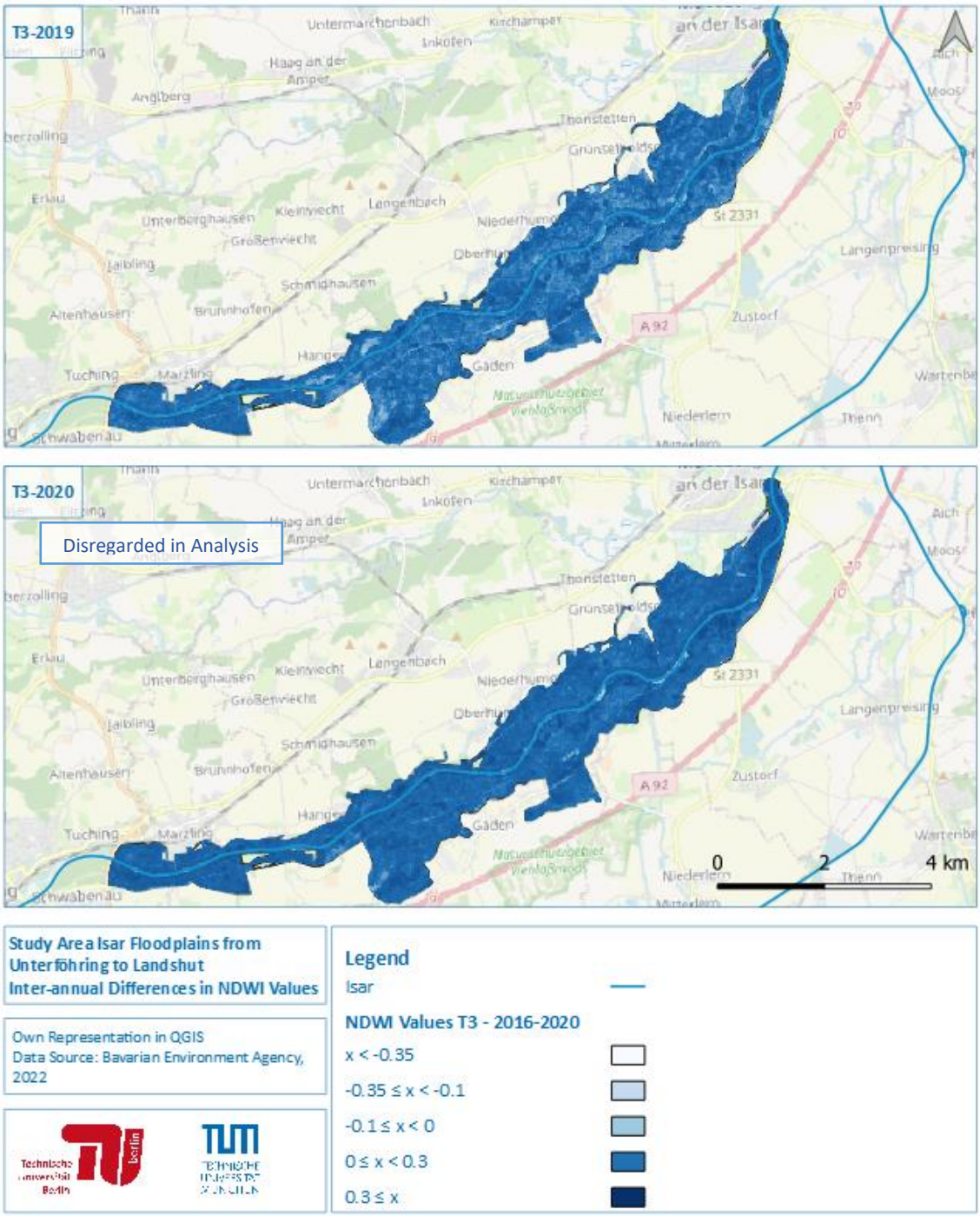

Map 30. NDWI for study area Isar Floodplains from Unterföhring to Landshut of all investigated years at Autumn-T3. This map visualized the results as seen in Figure 50.

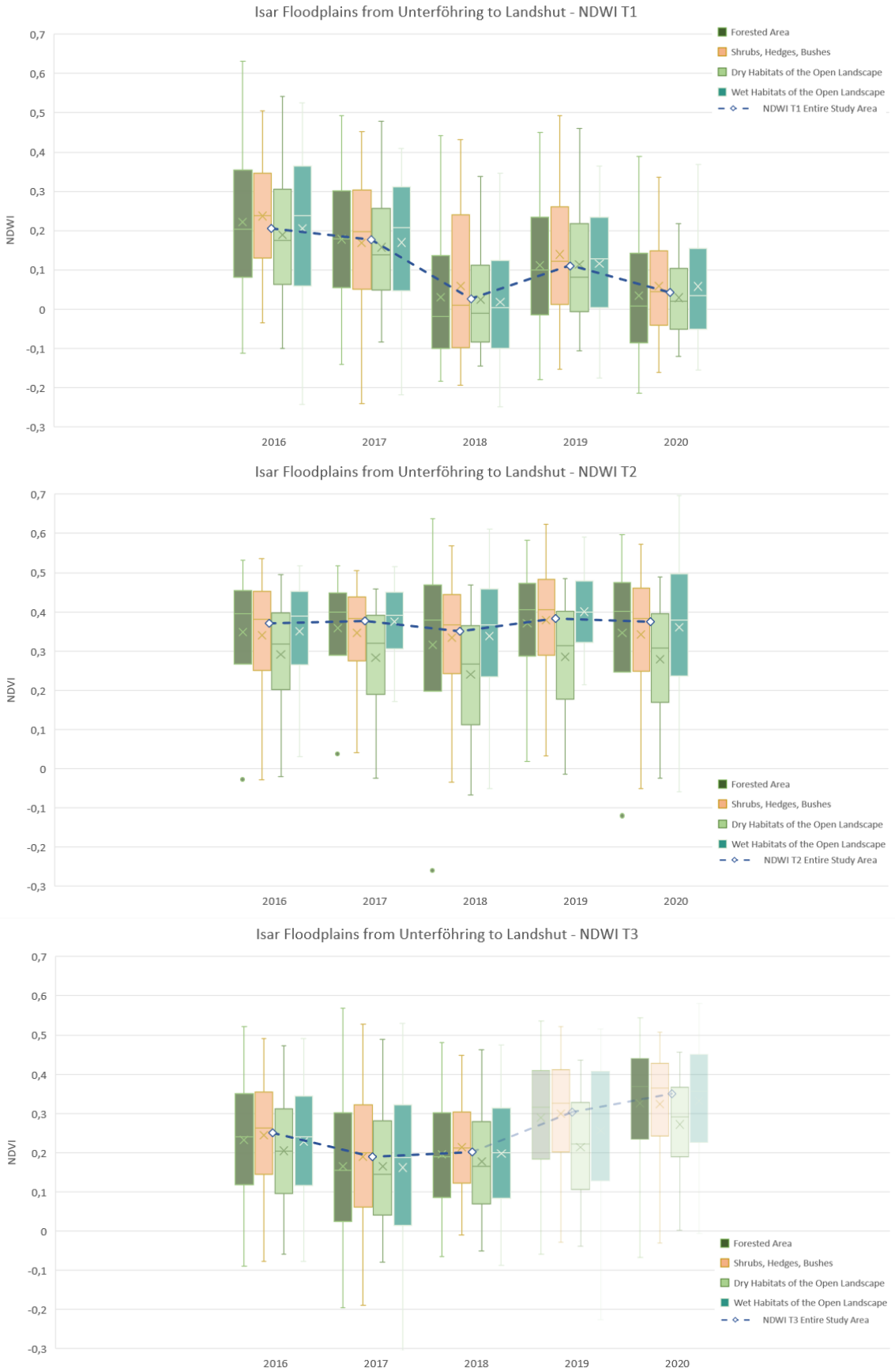

Figure 51. Inter-annual diffences in NDWI values per biotope type and year for study area Isar Floodplains from Unterföhring to Landshut.

Box and whisker plots describe the variability of NDWI value distribution within each biotope type and depict the scatter range. Scattering is, contrary to NDVI, lowest for Dry Habitats of the Open Landscape, followed by Wet Habitats of the Open Landscape, Shrubs, Hedges and Bushes and Forested Areas in increasing order. Dotted blue lines indicate the mean NDWI values for the entire study area in relation to each biotope type. All biotope types exhibut siginificantly lower NDWI values for all investigation points (Spring-T1, Summer-T2 and Autumn-T3) in 2018 when compared to 2016. This indicates lessened intra-cellular water content and thereby water stress, following the abnormally dry and warm spring 2018.

In comparison to the other investigated years, mean NDWI values of each biotope type during 2018 are not invariably lowest. Forested Areas exhibt the lowest mean NDWI at Spring-T1 (0.0) in 2018, at Summer-T2 in 2018 (0.38) and the lowest mean NDWI at Autumn-T3 (0.16) in 2017. Shrubs, Hedges and Bushes depict the lowest mean NDWI for all investigation points (Spring-T1, Summer-T2 and Autumn-T3) in 2018. Contrary to this, Dry Habitats of the Open Landscape display the lowest mean NDWIs at Spring-T1 (0.0) in 2018 , the lowest mean NDWI at Summer-T2 in 2018 (0.25) and the lowest mean NDWI at Autumn-T3 in 2017 (0.15). Wet Habitats of the Open Landscape exhibit lowest mean NDWI at Spring-T1 in 2018 (0.01), the lowest mean NDWI at Summer-T2 in 2018 (0.36) and the lowest mean NDWI at Autumn-T3 in 2017 (0.18). Similar to the results obtained for the NDVI, these results indicate the importance of considering regional site conditions, as well as differentiating between different biotope types.

3.4 Study Areas Lower Course - Lower Isar between Landau and Plattling

This study area is oriented towards the outline of the FFH Area “Lower Isar between Landau and Plattling” (“Untere Isar zwischen Landau und Plattling”) and covers an area of approx. 1290 hectares at 325 m – 337 m above sea level. The area is a representative section of the lower Isar valley with extensive alluvial forests and oxbow lakes consisting of reeds, sedges and banks of tall herbaceous vegetation, as well as dams with partly limestone grasslands. No direct existing risks are named for this area, which is categorized as part of the continental biogeographic region (Manderbach 2020).

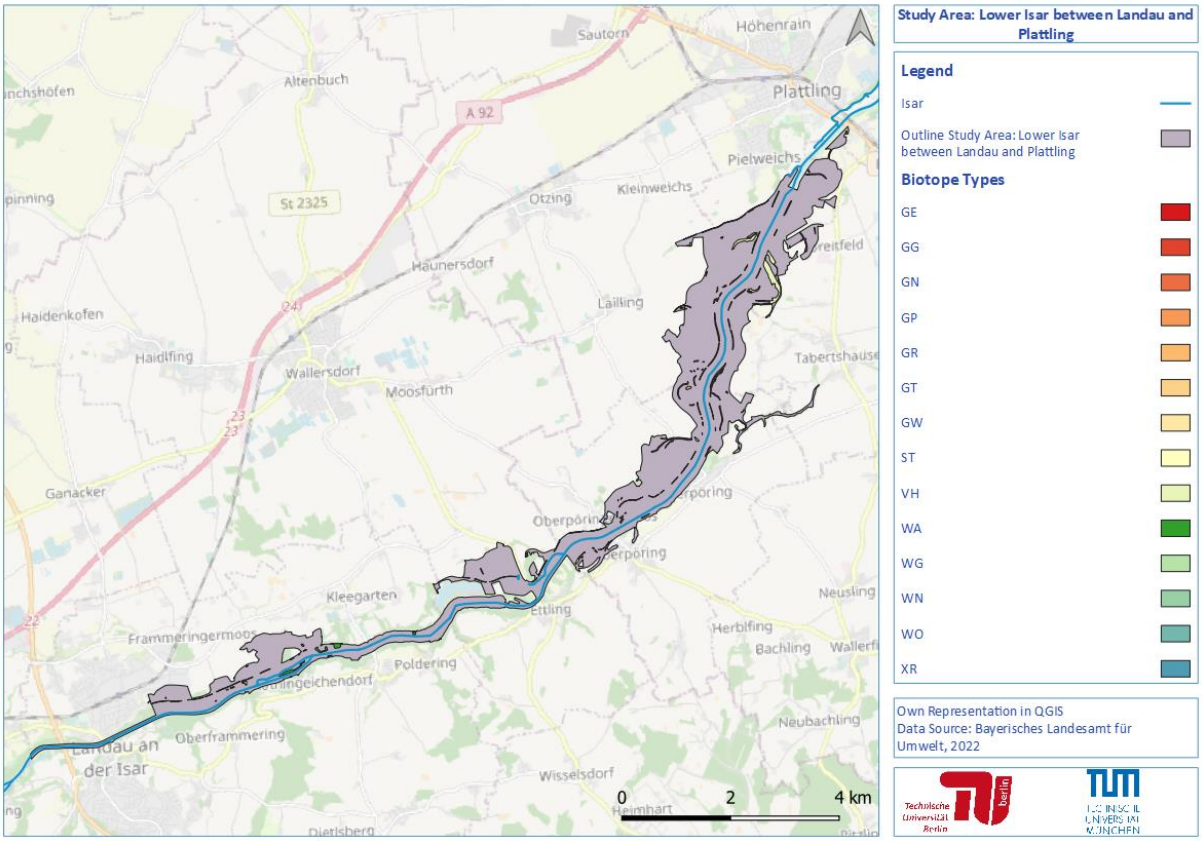

Map 31. Study area Lower Isar between Landau and Plattling, as well as plotted biotope types from the Bavarian Biotope Mapping.

Meteorological data was obtained from the station “Schönbrunn”, while hydrological data from the monitoring well “Landau Q6”. Both monitoring sites are located west of this study area. Mean Growing Season Air Temperature (MGT) was lowest in 2016 (14.60°C), followed by 2017 and 2020 (14.72°C), 2019 (15.25°C) and 2018 (16.50°C) in increasing order. 2018 was characterized by above-average hot and dry conditions, ranking highest in mean monthly air temperatures for April, May, July, August and September compared to the other years. Mean Growing Season Precipitation Rate (MGP) differed among the years and was highest in 2016 (71 mm), followed by 2020 (70 mm), 2017 (65 mm) and 2018 (49 mm). Lowest MGP was recorded for 2019 with 48 mm (see Appendices). Overall, Groundwater fluctuations remained mostly imperceptible throughout the investigation period, but displayed decreases in summer 2018 and late 2019. Noteworthy here is that the groundwater table is with about 5.5 m below the surface quite deep, compared to the other study areas.

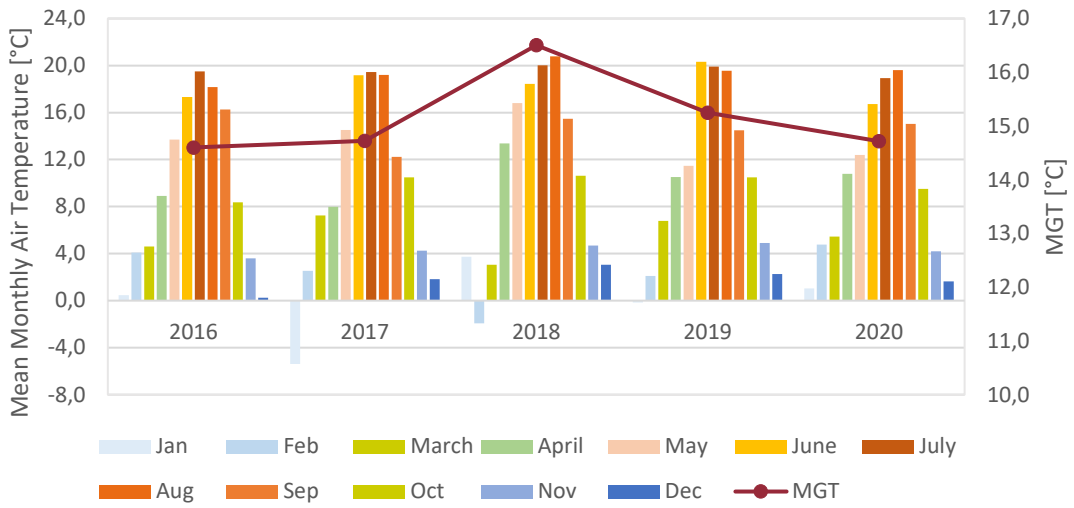

(a)

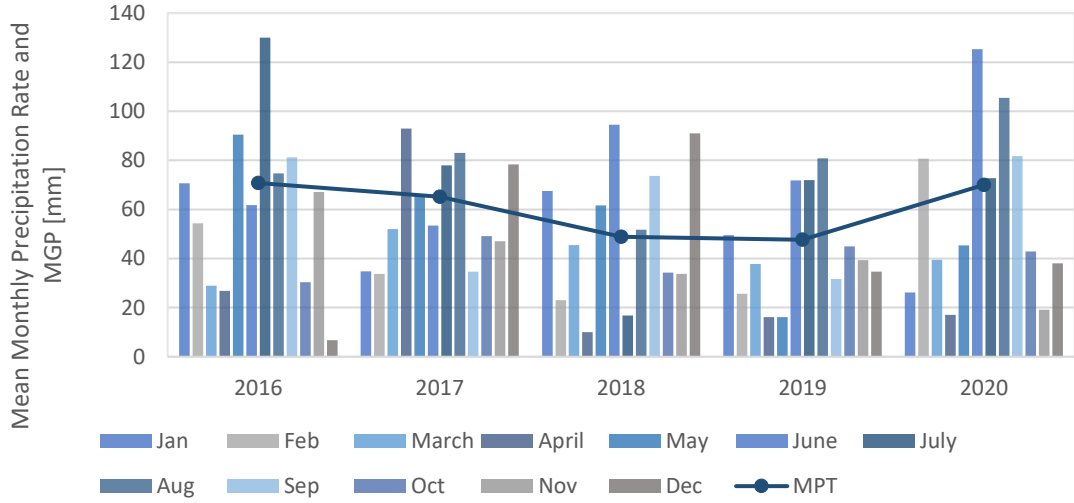

(b)

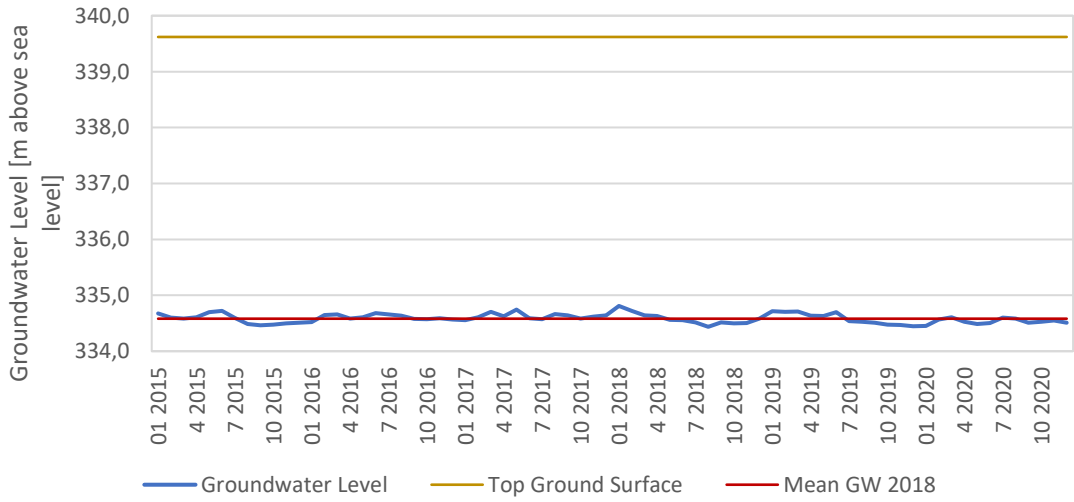

(c)

Figure 52. Mean monthly air temperature and mean growing season air temperature (MGT; a), mean monthly precipitation rate and mean growing season precipitation rate (MGP; b), as well as groundwater level and groundwater-surface distance (c) of study area Lower Isar between Landau and Plattling. The growing season encompasses the months April to October (BayLfU 2020b; 2020d; 2020c; 2020e).

3.4.1 NDVI – Lower Isar between Landau and Plattling

Satellite Data

Table 9. Satellite imagery used in the NDVI assessment of study area Lower Isar between Landau and Plattling. Differences in investigation times arose from limitations in data availability. Greyed out times are disregarded in the analysis by reason of undue temporal deferral.

Time	2016	2017	2018	2019	2020
T1	09 May	24 April	19 April	24 April	08 April
T2	27 August	13 July	27 August	27 August	21 August
T3	16 October	16 October	16 October	31 October	20 September

Intra-annual Alterations in NDVI Values

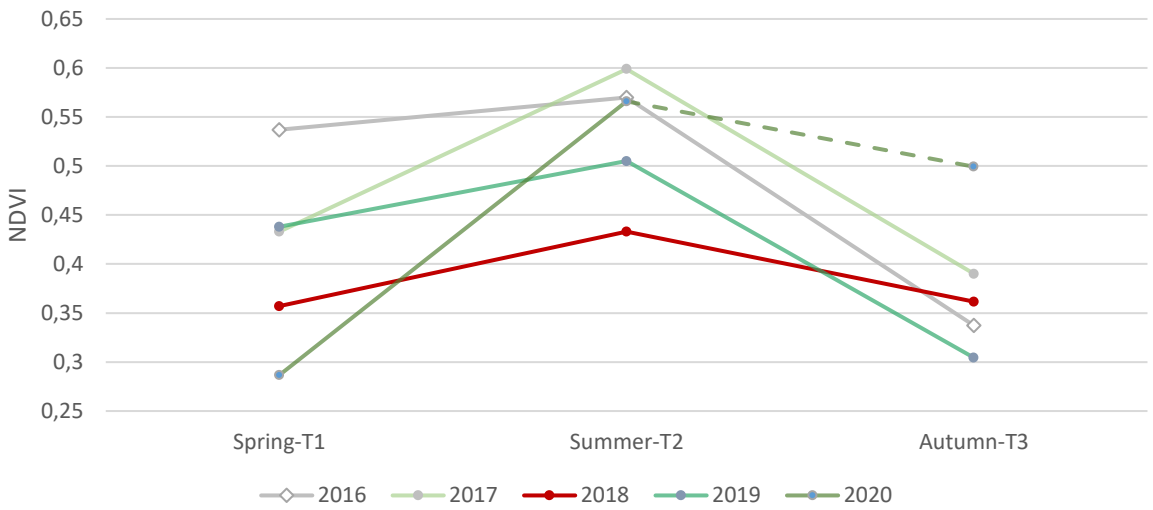

Figure 53. Intra-annual alterations in NDVI values of study area Lower Isar between Landau and Plattling for all investigated years (2016-2020). Dashed lines indicate the disregarded values, as outliers in investigation times may cause incomparability of obtained results.

Intra-annual alterations in NDVI values are depicted in Figure 53 for the entire study area Lower Isar between Landau and Plattling. Spring-T1 2018 (0.36) differs significantly from Spring-T1 2016 (0.54) and is equally lower at Summer-T2 2018 (0.43) than Summer-T2 2016(0.57). Shortly before Autumn-T3, the NDVI regimes of 2018 and 2016 cross and 2018-T3 (0.36) remains higher compared to Autumn-T3 in 2016 (0.34). The NDVI regime of 2017 depicts the highest Summer-T2 (0.60) and Autumn-T3 (0.39) values out of the investigated years, while the NDVI regime of 2020 displays the steepest increase between Spring-T1 (0.29) and Summer-T2 (0.57). Comparing the reference year 2016 and the drought year 2018, a clear reduction in NDVI and thus plant vitality is observable. This can be connected with the meteorological and hydrological site conditions, where the air temperature of the vegetative period in 2018 was significantly hotter than the one in 2016. MGP however, differed only moderately by 22 mm.

By reason of scope, maps depicting the intra-annual alterations in NDVI are enclosed solemnly for the next study area (Isar Estuary) as representative for floodplains alongside the lower reaches of the Isar River. Intra-annual alterations in NDVI values per biotope type and investigated year are depicted in Figure 54. For all four biotope types incorporated in this study area, the NDVI regime 2018 is, in average, the lowest out of all investigated years.

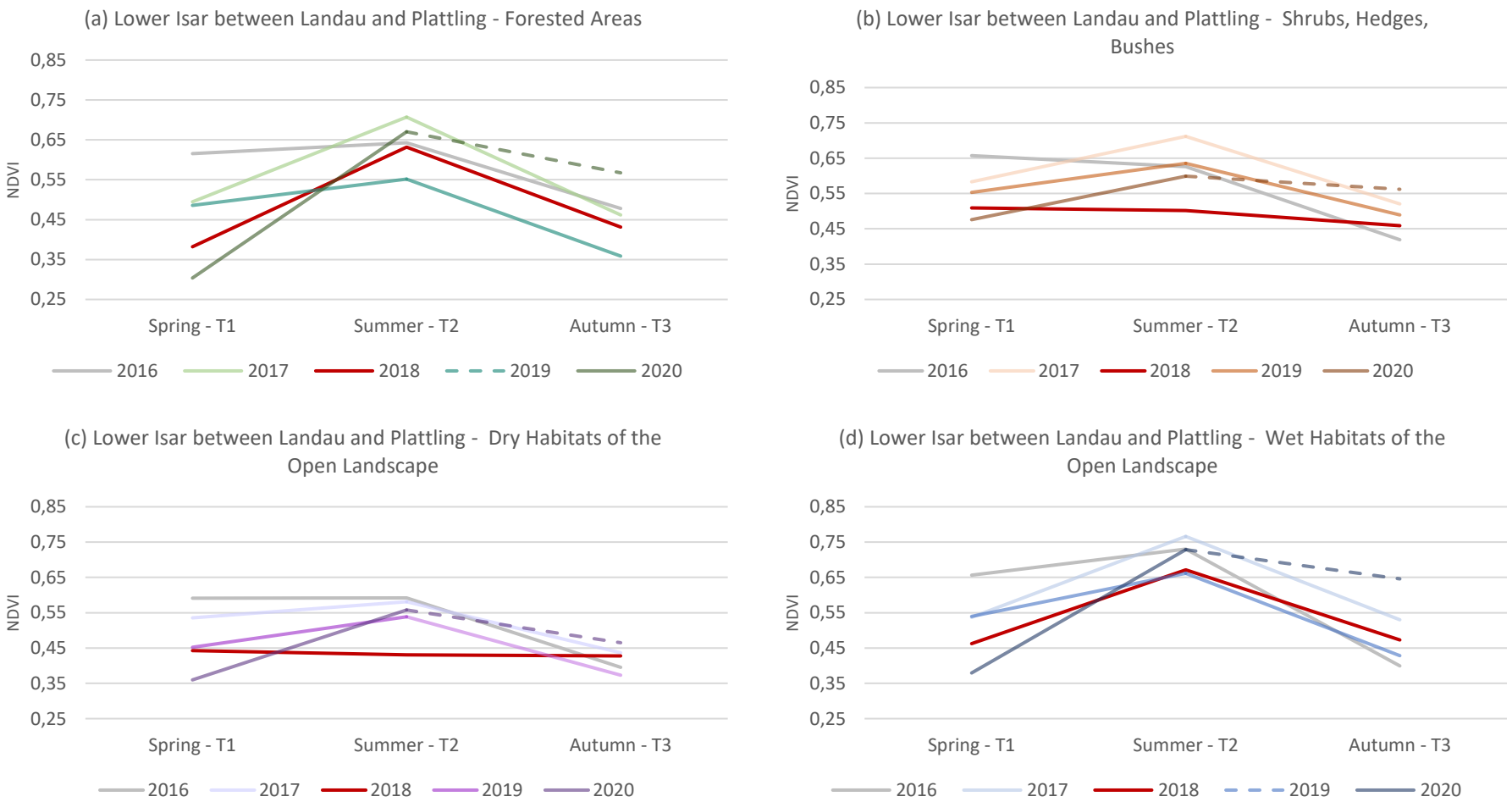

Figure 54. Intra-annual alterations of the NDVI values per biotope type and investigated year. NDVI regimes display specific signatures for (a) Forested Areas (NDVI 0.30-0.71), (b) Shrubs, Hedges and Bushes (NDVI 0.41-0.71), (c) Dry Habitats of the Open Landscape (NDVI 0.36-0.59) and (d) Wet Habitats of the Open Landscape (NDVI 0.38-0.77). The 2018 NDVI regimes are, in comparison to the other investigated years, in average lowest for all biotope types but show more divergences than the other study areas. Comparing the reference year 2016 and the drought year 2018, reveal that the 2018 NDVI regimes of all biotope types remain lower than the NDVI regimes of 2016. These results can be connected to the disparate meteorological and hydrological site conditions, meaning that all biotope types experienced plant vitality decreases following the abnormally warm and moderately drier spring 2018.

Inter-annual Difference in NDVI Values per Biotope Type

The following maps display the inter-annual differences in NDVI values between the reference year 2016 and the other investigated years (2017, 2018, 2019 and 2020). Differences were calculated using the equation found under Materials and Methods. Changes in plant vitality were derived thereof and are depicted in the legend.

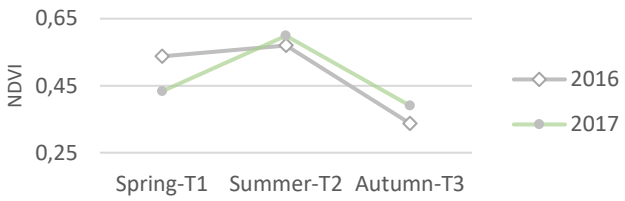

Figure 55. Mean intra-annual alterations of the NDVI 2016 and NDVI 2017 for study area Lower Isar between Landau and Plattling. Spring-T1 of 2017 (0.43) is significantly lower than Spring-T1 of 2016 (0.54). This can be led back to the temporal deferral of obtained data for Spring-T1 in 2016 (7th May). Summer-T2 (0.60) and Autumn-T3 (0.39) of 2017 are unexpectedly higher, compared to Summer-T2 (0.57) and Autumn-T3 (0.34) of 2016. NDVI differences between 2016 and 2017 for study area Isar Estuary are visualized in Map 32.

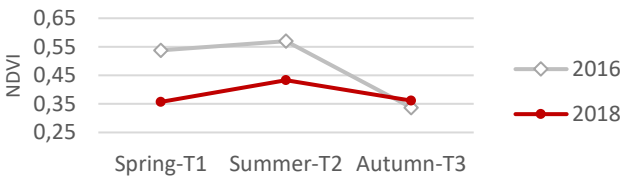

Figure 56. Mean intra-annual alterations of the NDVI 2016 and NDVI 2018 for study area Lower Isar between Landau and Plattling. Spring-T1 of 2016 (0.54) and 2018 (0.36) differ significantly but converge slightly at Summer-T2 (0.57 and 0.43) before exhibiting similar values at Autumn-T3 (0.34 and 0.36). Differences in NDVI regimes are visualized in Map 33.

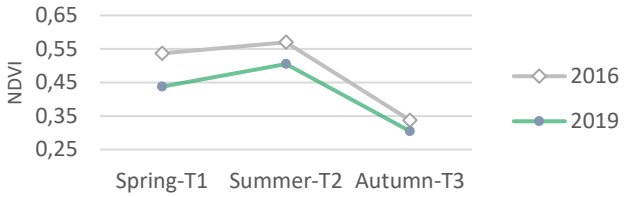

Figure 57. Mean intra-annual alterations of the NDVI regimes of 2016 and 2019 for study area Lower Isar between Landau and Plattling. Spring-T1 of 2019 (0.44) is significantly lower than Spring-T1 of 2016 (0.54). NDVIs for Summer-T2 (0.51) and Autumn-T3 (0.30) in 2019 remain lower than Summer-T2 (0.57) and Autumn-T3 (0.34) in 2016, but present lower disparities than at Spring-T1. The scope of NDVI differences between 2016 and 2019 are visualized in Map 34.

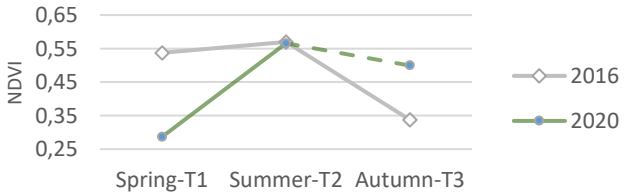

Figure 58. Mean intra-annual alterations of the NDVI 2016 and NDVI 2020 for study area Lower Isar between Landau and Plattling. Spring-T1 of 2016 (0.54) was significantly higher than Spring-T1 of 2020 (0.29), while NDVI values for Summer-T2 of 2020 (0.57) and Summer-T2 of 2016 (0.57) are equally high. Autumn-T3 of 2020 is disregarded in this analysis as data was obtained September 20th, causing incomparability between the obtained results. NDVI differences between 2016 and 2020 are visualized in Map 35.

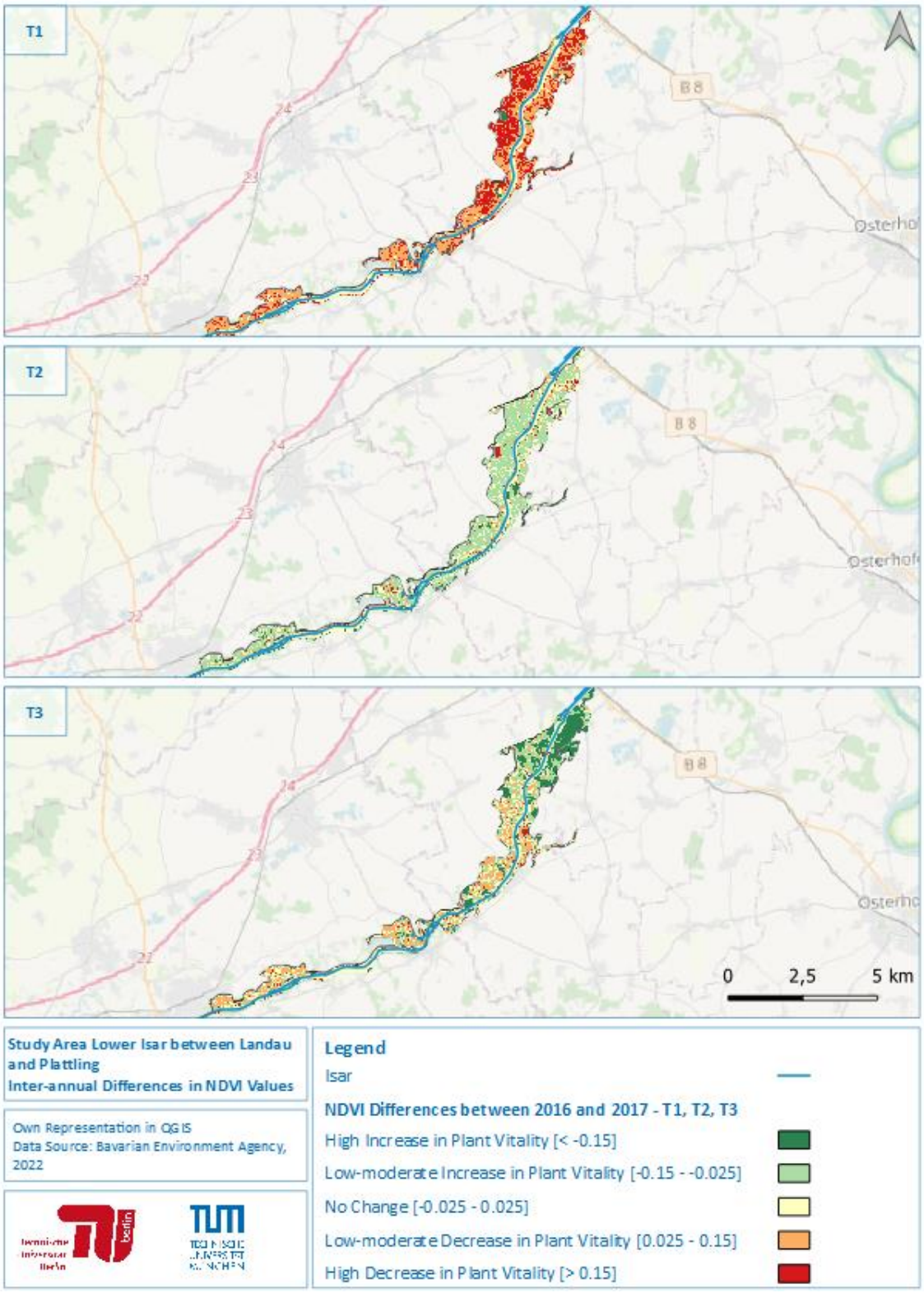

Map 32. Exhaustive low-moderate and high decreases in NDVI can be observed for 2016-2017 at Spring-T1, whereas low-moderate increases in NDVI and thus, plant vitality were detected between 2016-2017 at Summer-T2 and Autumn-T3. Fragmented NDVI changes adequately depict the differences in biotope types, which need to be considered for impacts of the 2018 drought on individual biotope types. See Figure 55.

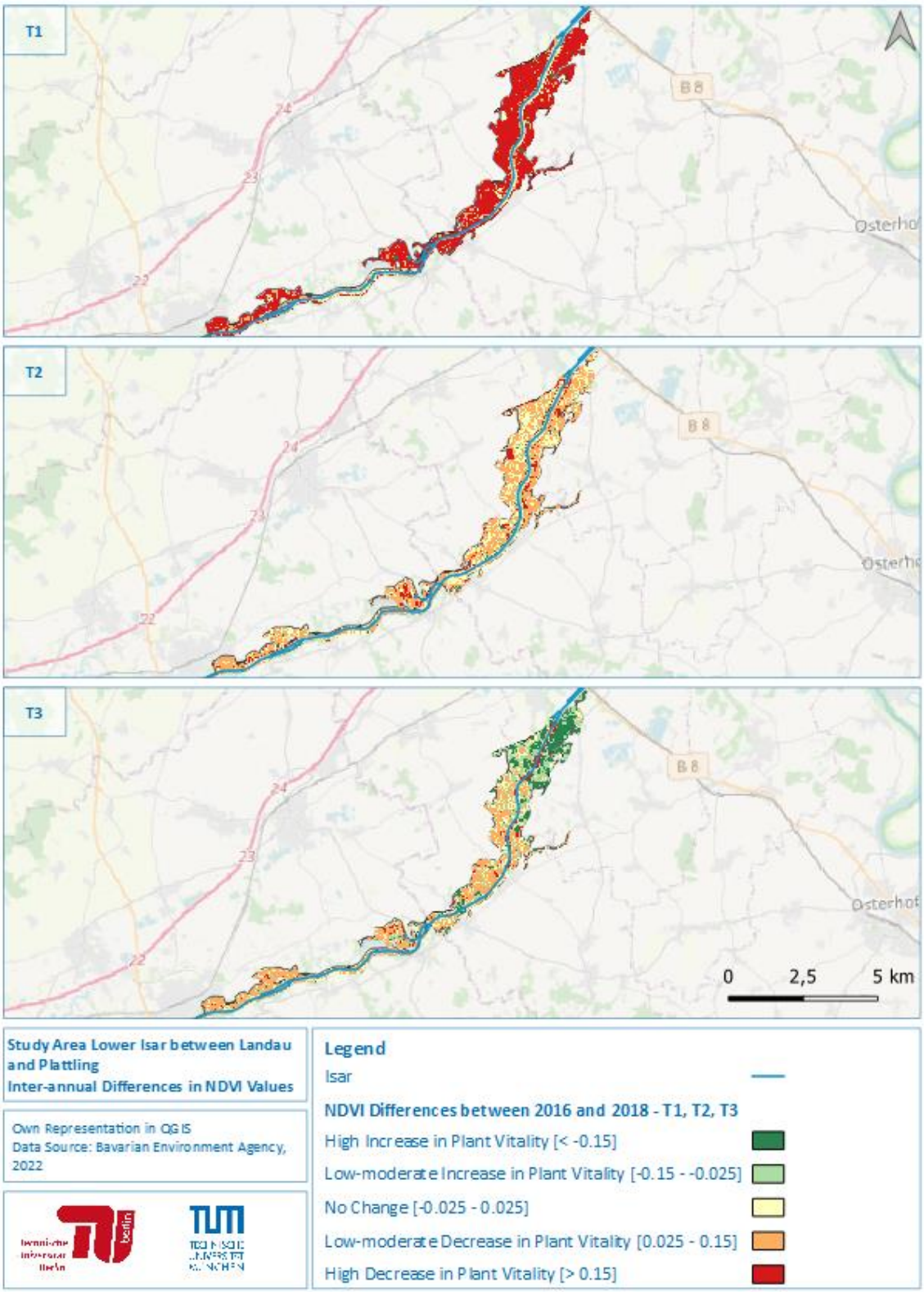

Map 33. Comprehensive high and low-moderate decreases in NDVI are predominant at Spring-T1, when comparing 2016 and 2018 at this investigation point. Summer-T2 and Autumn-T3 display quite fragmented areas within all categories of NDVI Changes, indicating the importance of investigating individual biotope types when necessary. Autumn-T3 depicts distortions in NDVI values caused by cloud coverage in the northern parts of the study area, leading to the unexpected slightly higher NDVI value at Autumn-T3 in 2018 compared to Autumn-T3 in 2016 as depicted in Figure 56).

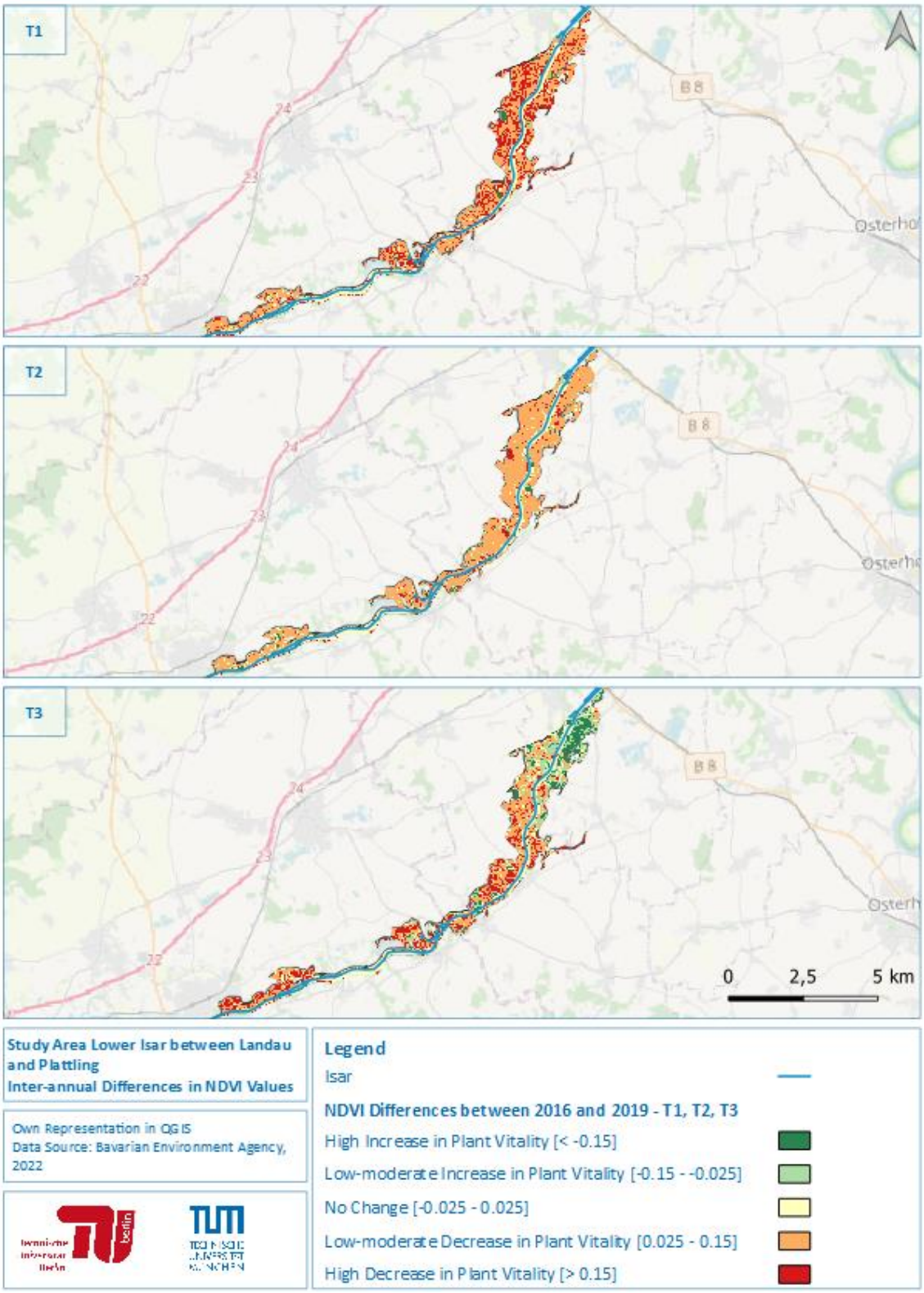

Map 34. Exhaustive low-moderate decreases and partial high decreases in NDVI and therefore plant vitality are recorded for all investigation points between 2016 and 2019. Spring-T1 and Autumn-T3 however depicted the most extensive decreases, encompassing considerable extents with high reductions in plant vitality. The distribution however shifted from the more northern parts at Spring-T1 to the southwestern parts at Autumn-T3. These visualized results adequately reflect Figure 57.

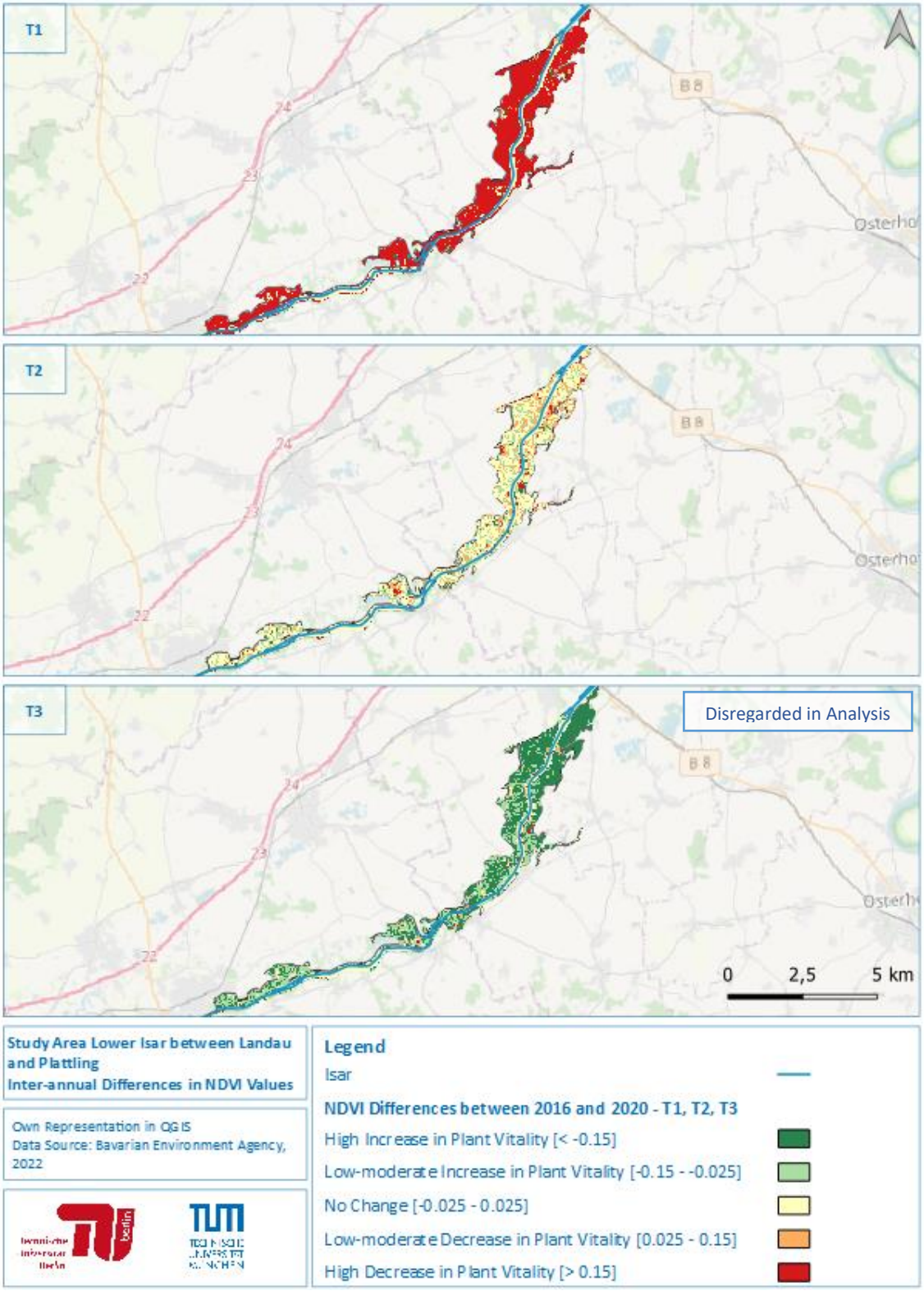

Map 35. Almost the entire scope of study area Lower Isar between Landau and Plattling experienced high decreases in plant vitality between 2016 and 2020 at Spring-T1. Fragmented areas of decreases and increases in plant vitality, but majorly areas with no change in NDVI values caused the levelled NDVI values in Figure 58. Here the spatial distributions are adequately depicted. High and low-moderate increases in plant vitality were detected for T3 (2016-2020) but are disregarded in the analysis, as high-quality satellite imagery was only obtainable for September 2020. Distortions in the NDVI results can therefore not be excluded.

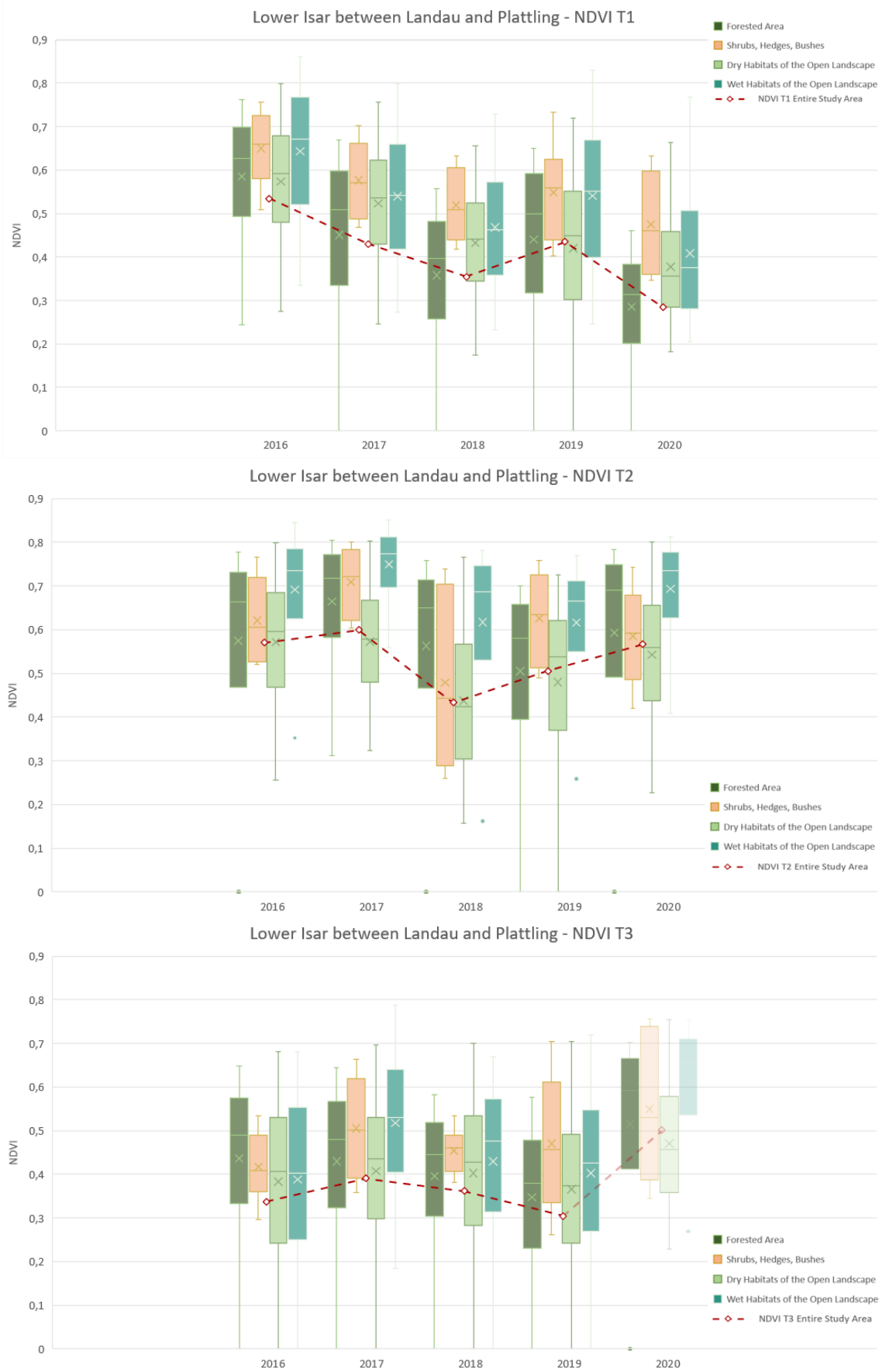

Figure 59. Inter-annual diffences in NDVI values per biotope type and year of study area Lower Isar between Landau and Plattling.

Box and whisker plots describe the variability of NDVI value distribution within each biotope type and depict the scatter range. Scattering is lowest for Dry Habitats of the Open Landscape, followed by Shrubs, Hedges and Bushes, Wet Habitats of the Open Landscape and Forested Areas in increasing order. Dotted red lines indicate the mean NDVI values for the entire study area in relation to each biotope type. Mean NDVI course deviates slightly more for this study area compared to the other study areas, as biotop coverage from the Bavarian Biotope Mapping exists only to a minor extent. Therefore the mean NDVI course for the entire study area deviates from the NDVI values for particular biotope types. Compared to Spring-T1 and Summer-T2 of reference year 2016, the NDVI values for Spring-T1 and Summer-T2 of drought year 2018 are significantly lower for all biotopte types assessed. This indicates considerable decreases in plant vitality during spring and summer of 2018, following the abnormally dry and warm conditions in spring 2018. At Autumn-T3 however, only Forested Areas display a decrease in mean NDVI values in 2018 (0.43) compared to 2016 (0.47). Shrubs, Hedges and Bushes, Dry Habitats of the Open Landscape and Wet Habitats of the Open Landscape exhibit lower values at Autumn-T3 in 2016, than in 2018.

In comparison to all investigated years, the NDVI results of this study area show higher variations. NDVI is lowest for all biotopte types at Spring-T1 in 2020. For Summer-T2 the different biotope types depict varying results. Forested Areas (0.55) and Wet Habitats of the Open Landscape (0.66) exhibit lowest values in 2019 for this investigation point, whereas Shrubs, Hedges and Bushes (0.50) and Dry Habitats of the Open Landscape (0.43) exhibit lowest values for Summer-T2 in 2018. Variations in NDVI values are recoreded for Autumn-T3 as well. Here, Forested Areas (0.36) and Dry Habitats of the Open Landscape (0.37) are lowest in 2019. Shrubs, Hedges and Bushes (0.42) and Wet Habitats of the Open Landscape (0.40) on the other hand exhibit lowest values in 2016. These variations display the importance of considering regional/ local differences in meteorologcial and hydrological conditions.

3.4.2 NDWI – Lower Isar between Landau and Plattling

Satellite Data

Table 10. Satellite imagery used in the NDWI assessment of study area Lower Isar between Landau and Plattling. Differences in investigation times arose from data availability limitations. Greyed out times are disregarded in the analysis by reason of undue temporal deferral.

Time	2016	2017	2018	2019	2020
T1	09 May	24 April	19 April	24 April	08 April
T2	27 August	13 July	27 August	27 August	21 August
T3	16 October	16 October	16 October	31 October	20 September

Intra-annual Alterations in NDWI Values

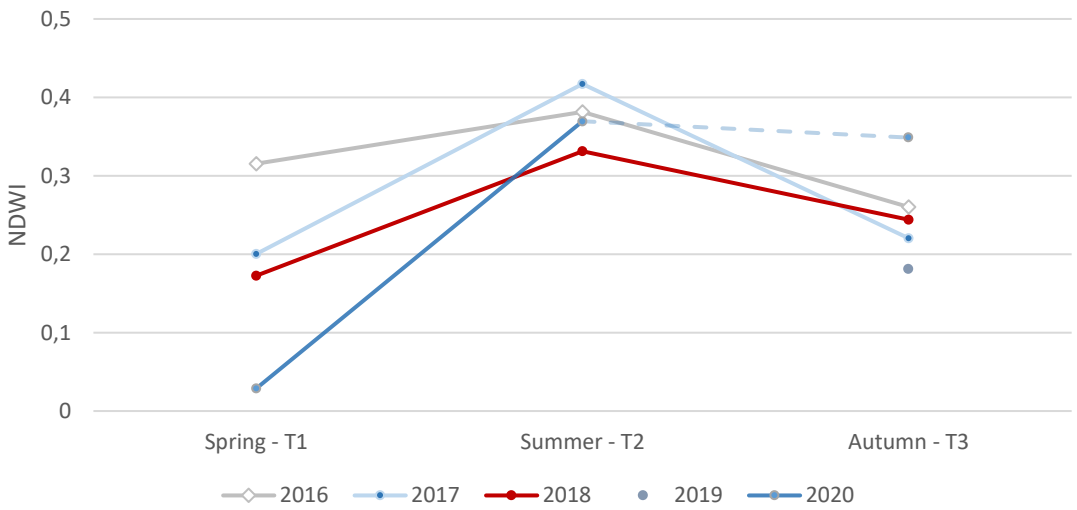

Figure 60, Intra-annual alterations in NDWI for the entire study area Lower Isar between Landau and Plattling. Dashed lines indicate the (disregarded/ excluded) values, as outliers of investigation times may cause incomparability in obtained results.

Intra-annual alterations in NDWI values are depicted in Figure 60 for the entire study area Lower Isar between Landau and Plattling. Summer-T2 displays the highest values of each year, respectively, but as for the other study areas, steepness of increase and decrease in NDWI values vary for each year. The NDWI regime in 2020 increases with the steepest gradient, followed by 2017 and 2018. As for reasons of errors occurring during procession, no results could be calculated with the obtained satellite imagery for Spring-T1 and Summer-T2 2019. Spring-T1 is significantly higher for the reference year 2016 (0.32), compared to 2018 (0.17), but converges slightly at Summer-T2 (0.38 and 0.33) and Autumn-T3 (0.26 and 0.24). The high difference between Spring-T1 in 2016 and Spring-T1 2018 can be explained by the fact that Spring-T1 for 2016 was obtained early May, causing the NDWI to be at an already quite high value for this investigation point compared to the other years. Nevertheless, the NDWI regime of 2018 remains significantly lower than the 2016 regime throughout the entire vegetation period. This links reduced intra-cellular water content during the growing season 2018 to the contrasting meteorological and hydrological conditions of 2016 and 2018. Adverse meteorological and hydrological conditions in early 2020 probably caused the exorbitantly low NDVI at Spring-T1 (0.29), before the NDVI regime fully recovers at Summer-T2 (0.57) for this year.

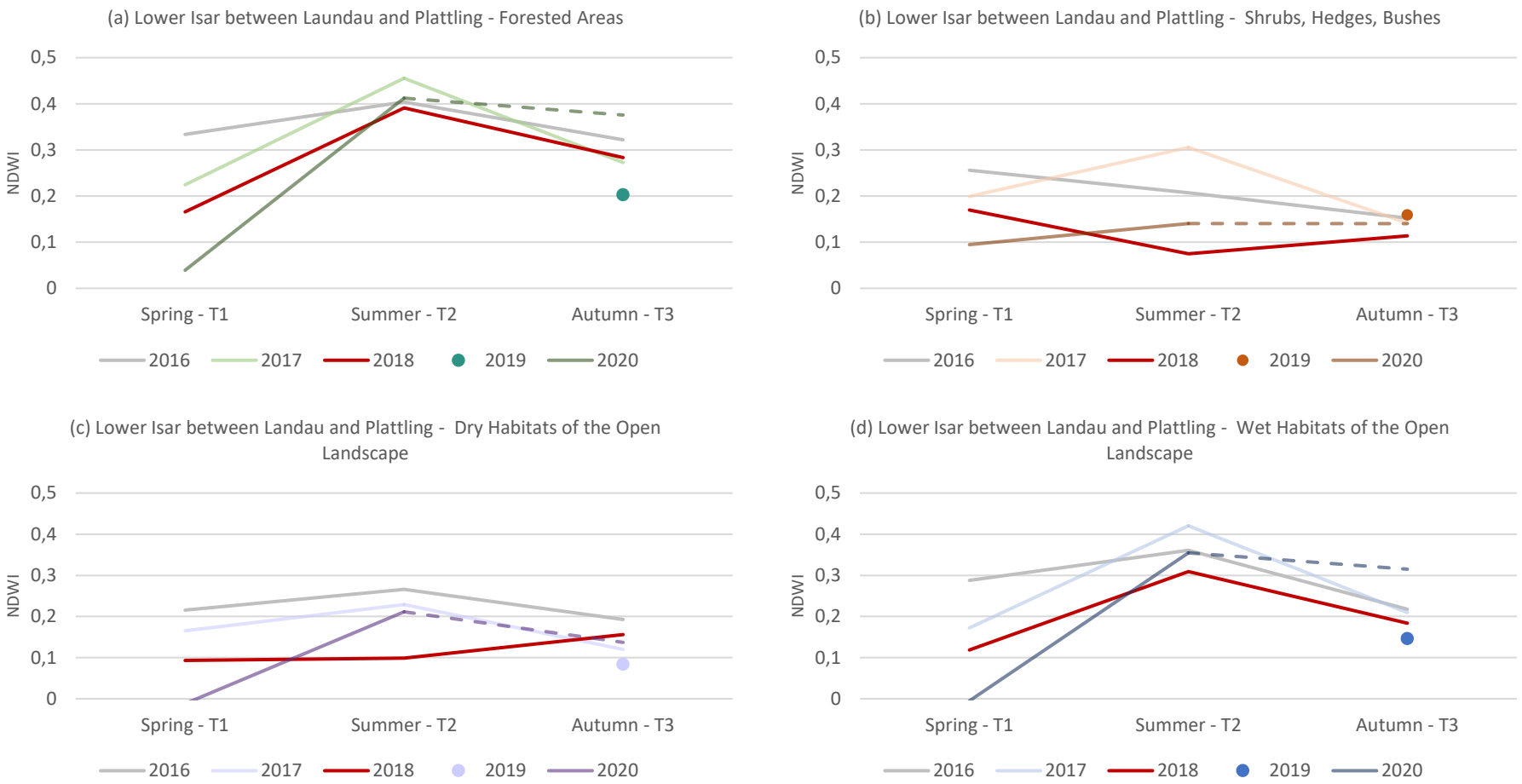

Figure 61. Intra-annual alterations of the NDWI values per biotope type and investigated year. NDWI regimes display specific signatures for (a) Forested Areas (NDWI 0.04-0.46), (b) Shrubs, Hedges and Bushes (NDWI 0.07-0.31), (c) Dry Habitats of the Open Landscape (NDWI -0.01-0.27) and (d) Wet Habitats of the Open Landscape (NDWI 0.0-0.42). The NDWI regimes of 2018 for Shrubs, Hedges and Bushes (b) and Dry Habitats of the Open Landscape (c) display interesting courses, starting with the high values at Spring-T1 and then decreasing to Summer-T2, before accelerating to Autumn-T3. The 2018 NDWI regimes of all biotope types are significantly lower in comparison to the NDWI regimes of reference year 2016 and in average lower than the NDWI regimes of the other investigated years. These results can be connected to the adverse meteorological and hydrological conditions in 2018, causing all biotope types to reflect decreases in NDWI values and thus plant water content following the drought 2018.

Inter-annual Differences in NDWI Values and per Biotope Type

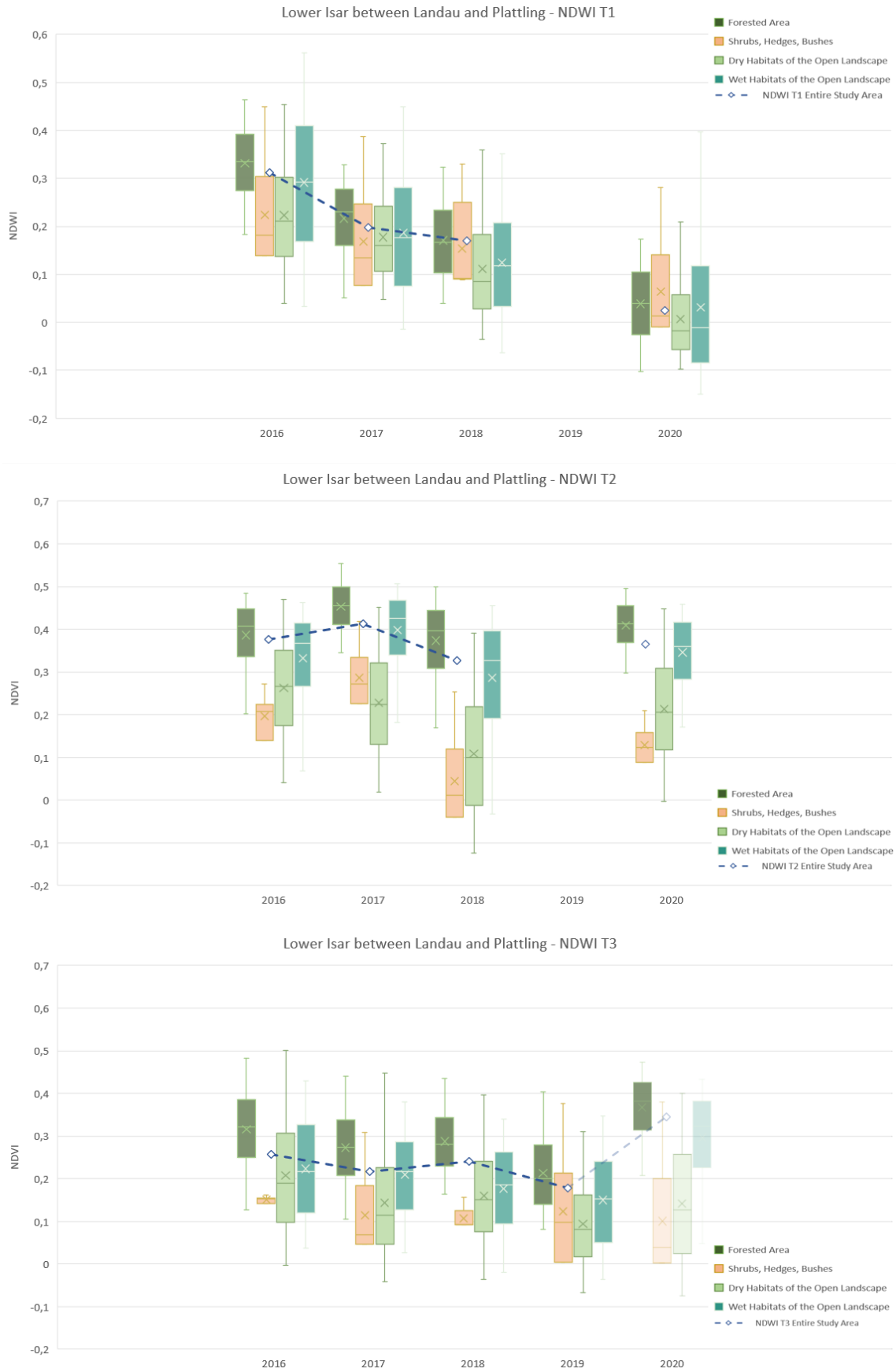

Figure 62. Inter-annual diffences in NDWI values per biotope type and year of study area Lower Isar between Landau and Plattling.

Box and whisker plots describe the variability of NDWI value distribution within each biotope type and depict the scatter range. Scattering is lowest for Shrubs, Hedges and Bushes, followed by Dry Habitats of the Open Landscape, Forested Areas and Wet Habitats of the Open Landscape in increasing order. Dotted blue lines indicate the mean NDWI values for the entire study area in relation to each biotope type. NDWI values are lowest for all biotope types at Spring-T1 in 2020. For Summer-T2 the results show overly diverse NDWI ranges between the biotope types throughout the investigation period (2016-2020). Nevertheless, NDWI values for Summer-T2 are lowest in 2018 for all biotope types. At Autumn-T3, NDWI is lowest for Shrubs, Hedges and Bushes in 2018 (0.11), while the other three investigated biotope types display lowest values in 2019. Comparing the reference year 2016 and the drought year 2018 in particular, all biotope types depict significantly lower values for 2018 at all investigation points. These results connect the evident decrease in intra-cellular water content to the anomalous meteorological and hydrological conditions in early 2018. Similar to the results obtained for the NDVI, these results indicate the importance of considering regional site conditions, as well as differentiating between different biotope types.

3.5 Study Area Lower Course – Isar Estuary

This last study area, which lies at 309 m – 319 m above sea level, is dominated by extensive and structurally rich alluvial forests, reed beds, floodplain meadows and occurrences of several, for floodplain areas typical protected (bird) species. After its renaturation between 1981 and 2001, it is the singular largely intact estuary of two major rivers in Germany and provides numerous habitat types to a wide variety of species (BfN 2021). The main risk to this internationally significant estuary are changes in natural floodplain dynamics (Manderbach 2020; BMUB 2015). The 2132 hectares of this study area are not only influenced by discharge rates of the Isar River, but additionally from flow rates of the Danube River. This study area belongs to the Continental biogeographic region and is the second of two study areas alongside the lower reaches of the Isar River.

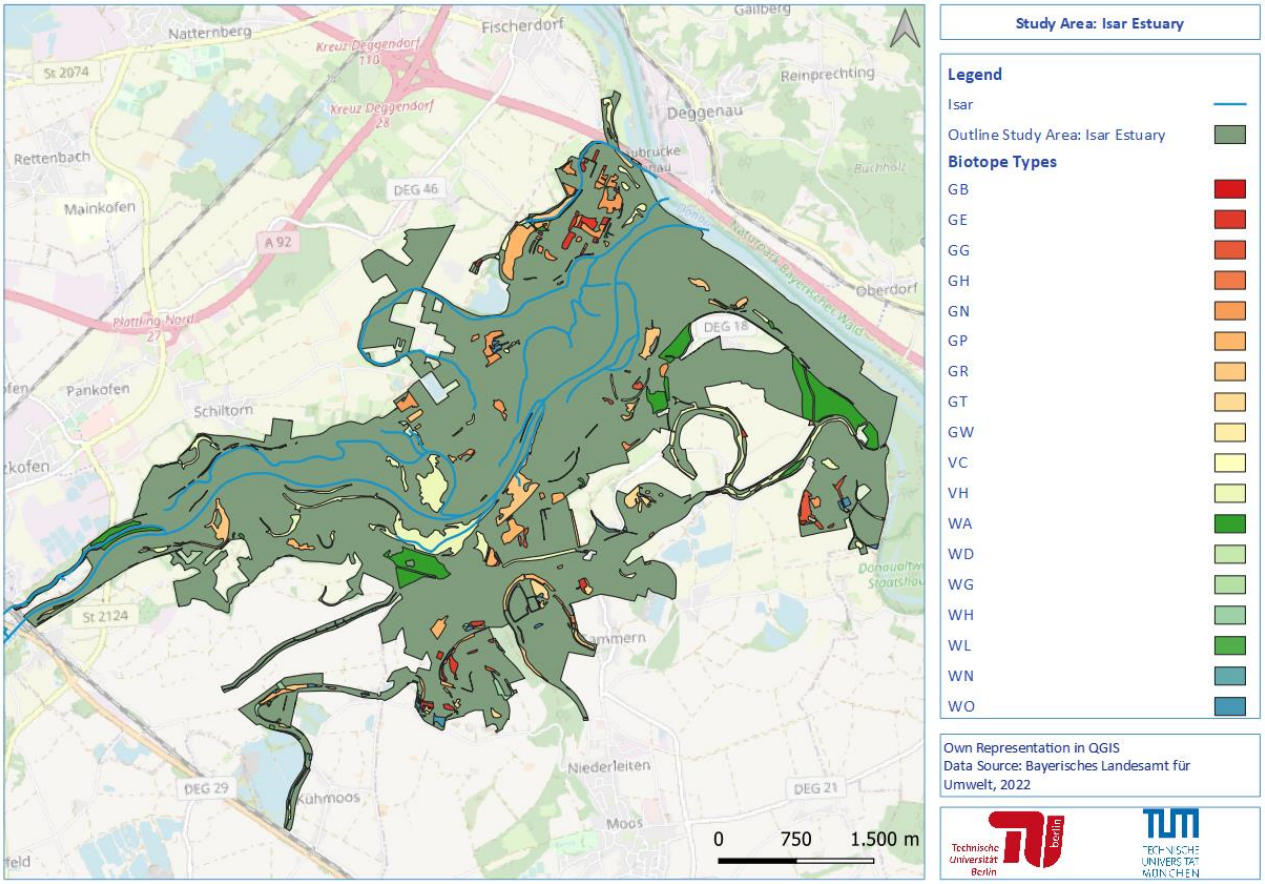

Map 36. Study area Isar Estuary with biotope types plotted in the Bavarian Biotope Mapping.

Mean Growing Season Air Temperature (MGT) was lowest in 2016 (14.94°C), followed by 2017 (15.03°C), 2020 (15.15C), 2019 (15.73°C) and 2018 (17.04°C) in increasing order. 2018 was characterized by above-average hot and dry conditions, ranking highest in mean monthly air temperatures for April, May, July, August and September compared to the other years. Mean Growing Season Precipitation Rates (MGP) differed among the years and were highest in 2016 (84 mm). In decreasing order, MGP was recorded with 75 mm in 2017 and 68 mm in 2020. MGP was equal in 2018 and 2019 (52 mm) (see Appendices). Groundwater fluctuations remained mostly imperceptible throughout the investigation period but peaked distinctly in early 2018 and decreased in autumn 2018, resulting in a moderate mean GW level 2018. No GW data could be obtained for this monitoring well after March 2020.

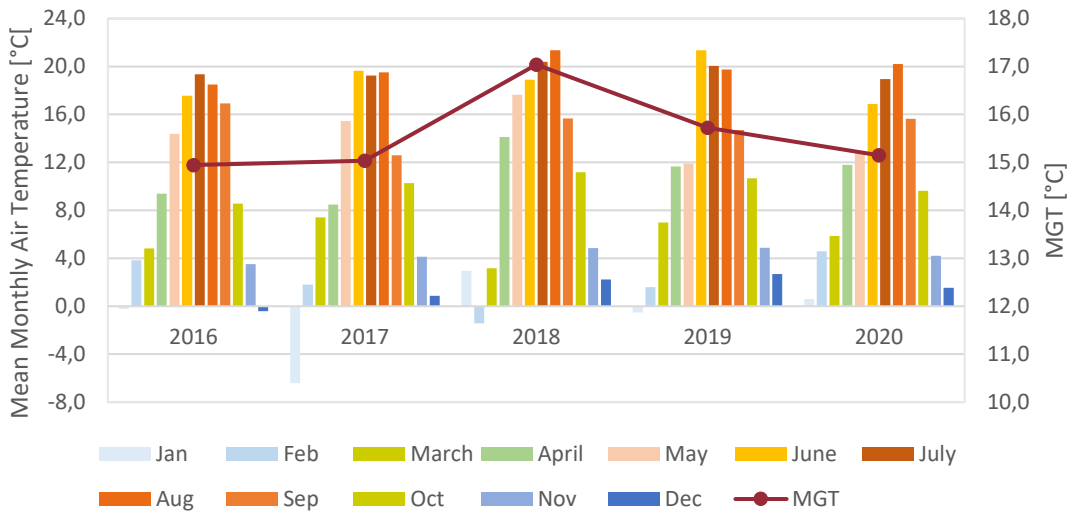

(a)

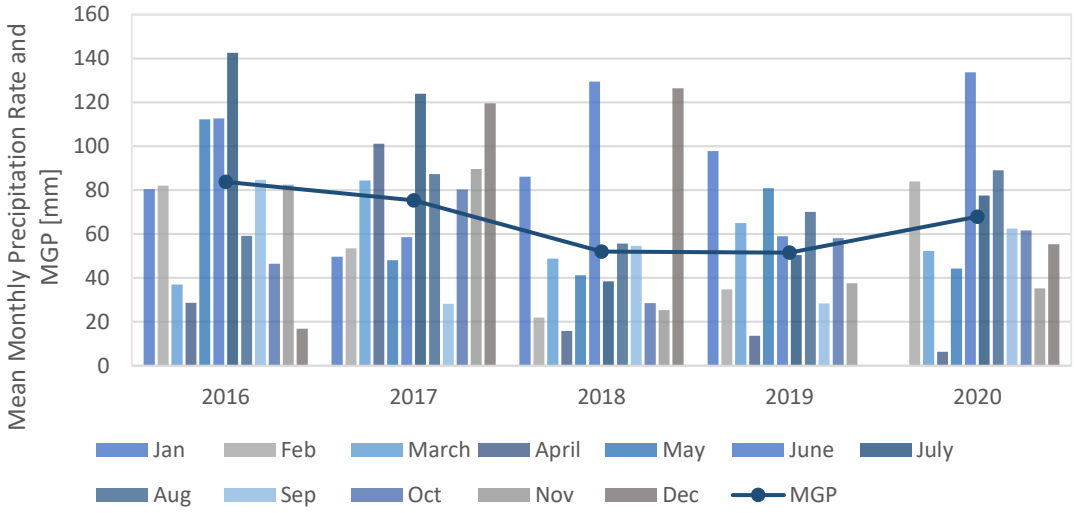

(b)

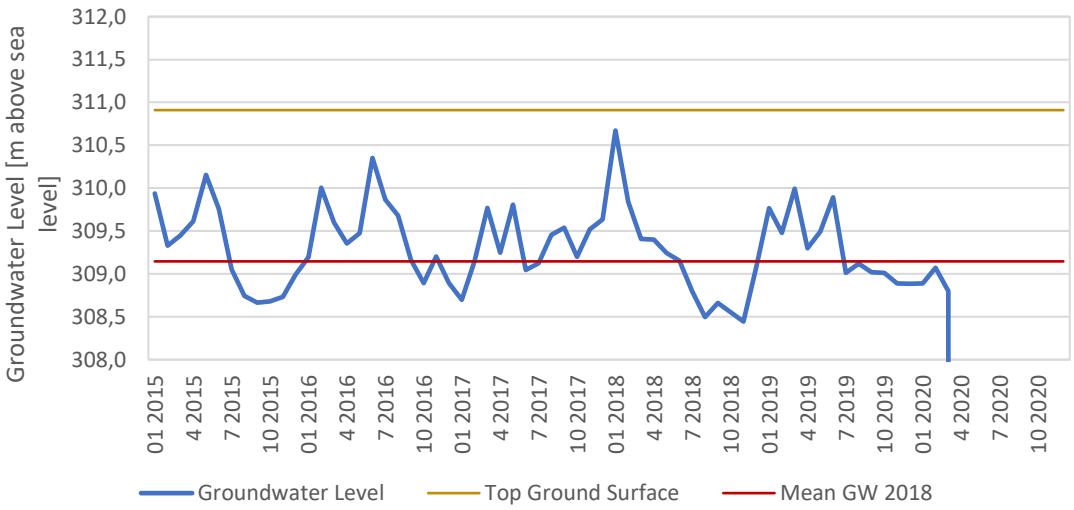

(c)

Figure 63 Mean monthly air temperature and mean growing season air temperature (MGT; a), mean monthly precipitation rate and mean growing season precipitation rate (MGP; b), as well as groundwater level and groundwater-surface distance (c) of study area Isar Estuary. The growing season encompasses the months April to October. Data was obtained from the meteorological station Uttenkofen and monitoring well "Isarmuend R 188". (BayLfU 2020b; 2020d; 2020c; 2020e).

3.5.1 NDVI – Isar Estuary

Satellite Data

Table 11. Satellite imagery used in the NDVI assessment of Study Area Isar Estuary. Differences in investigation times arose from data availability limitations. Greyed out times are disregarded in the analysis by reason of undue temporal deferral.

Time	2016	2017	2018	2019	2020
T1	09 May	24 April	19 April	24 April	08 April
T2	27 August	13 July	27 August	27 August	21 August
T3	16 October	16 October	16 October	31 October	20 September

Intra-annual Alterations in NDVI Values

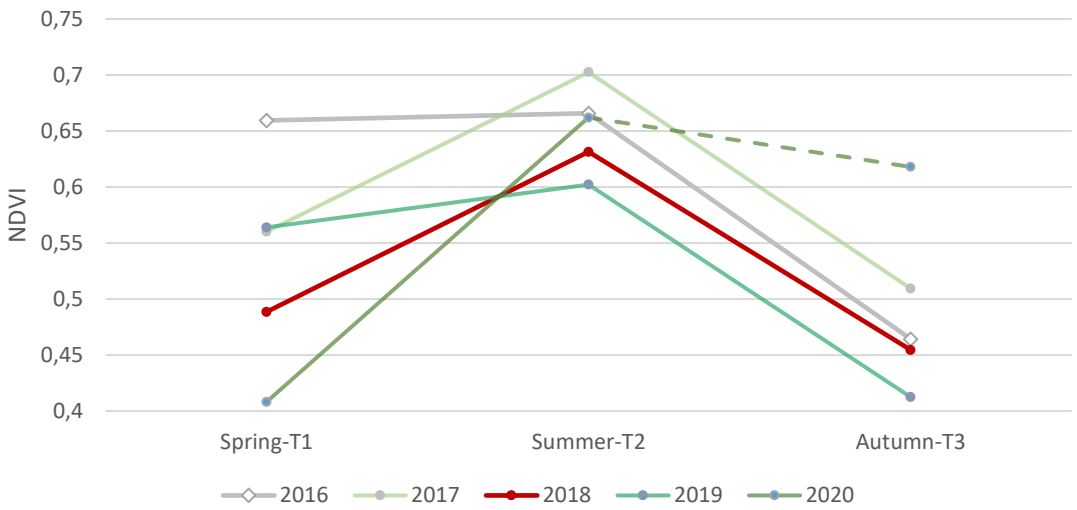

Figure 64. Intra-annual alterations in NDVI values of study area Isar Estuary for all investigated years (2016-2020). Dashed lines indicate the disregarded values, as outliers in investigation times may cause incomparability of obtained results.

Intra-annual alterations in NDVI values are depicted in Figure 64 for the entire study area Isar Estuary. As for the other study areas, the NDVI, corresponding to plant vitality, peaks during investigation time Summer - T2. NDVI values subsequently decline to Autumn – T3. However, steepness of increase and decrease in NDVI values vary for each year. NDVI at Spring-T1 in 2016 is relatively high, as cloud free imagery was only obtainable for May 9th during this period. NDVI for 2018 is significantly lower at Spring-T1 (0.49) in comparison to 2016 (0.66). Although NDVI regimes of 2018 and 2016 slightly converge for the other two investigation points, NDVI at Summer-T2 (0.63) and Autumn-T3 (0.45) in 2018 remain lower than Summer-T2 (0.67) and Autumn-T3 (0.46) in 2016. This indicates substantially impaired plant vitality in early 2018 and moderately impaired plant vitality in later 2018. These consistent reductions in NDVI values can be linked to the contrasting meteorological and hydrological conditions within the investigated period (2016-2020). The year 2018 has been significantly hotter and drier compared to the reference year 2016 for this particular study area. MGT was recorded to be 2°C higher in 2018 and the MGP 32 mm lower than the MGT and MGP of 2016. Interestingly, similar to the other study areas, the year 2020 exhibited the highest gradient in NDVI increase between Spring-T1 (0.41) and Summer-T2 (0.66).

The following figures (65 and 66) and maps (Map 37 and Map 38) exemplarily display the intra-annual NDVI alterations of study area Isar Estuary for the reference year 2016 and the drought year 2018, respectively, as representative flooplain area alongside the lower reaches of the Isar River.

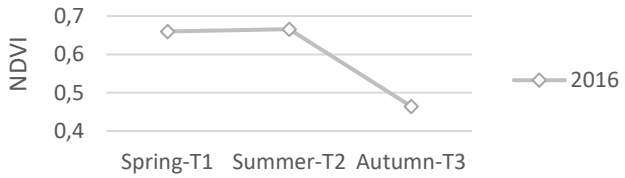

Figure 65. Intra-annual alterations of the NDVI in 2016 for the entire study area Isar Estuary with Spring-T1 (0.66), Summer-T2 (0.67) and Autumn-T3 (0.46). The following map visualizes this course in NDVI values.

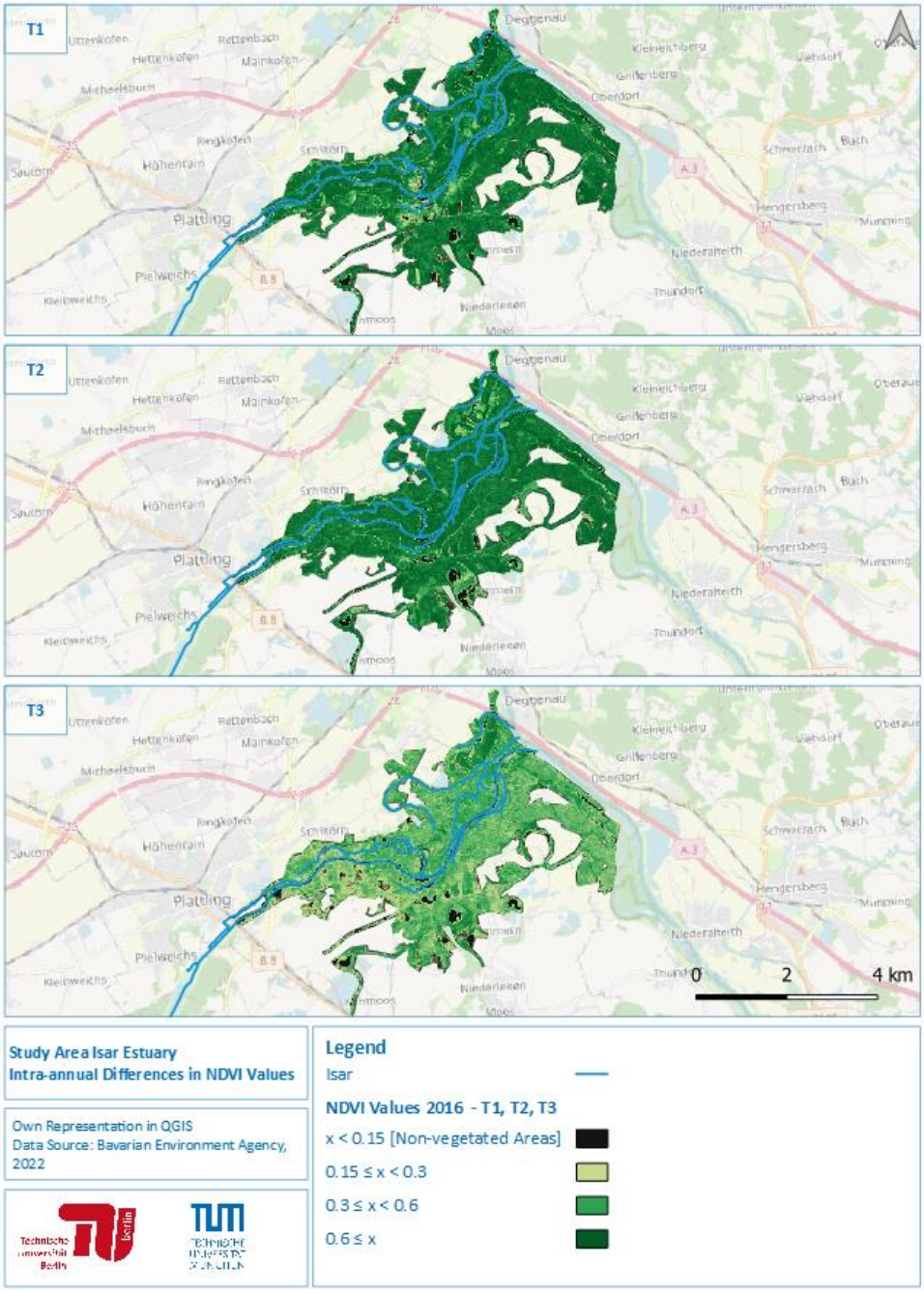

Map 37. NDVI throughout the year 2016 for study area Isar Estuary. Darker green nuances indicate higher NDVI values, as detectable in Summer-T2, whereas lighter shades depict lower NDVI values. Black parts indicate non-vegetated areas or masked out cloud coverage.

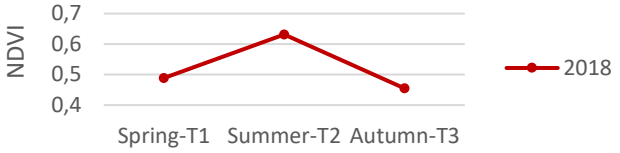

Figure 66. Intra-annual NDVI regime of 2018 for the entire study area Isar Estuary with Spring-T1 (0.49), Summer-T2 (0.63) and Autumn-T3 (0.45). The following map visualizes those results.

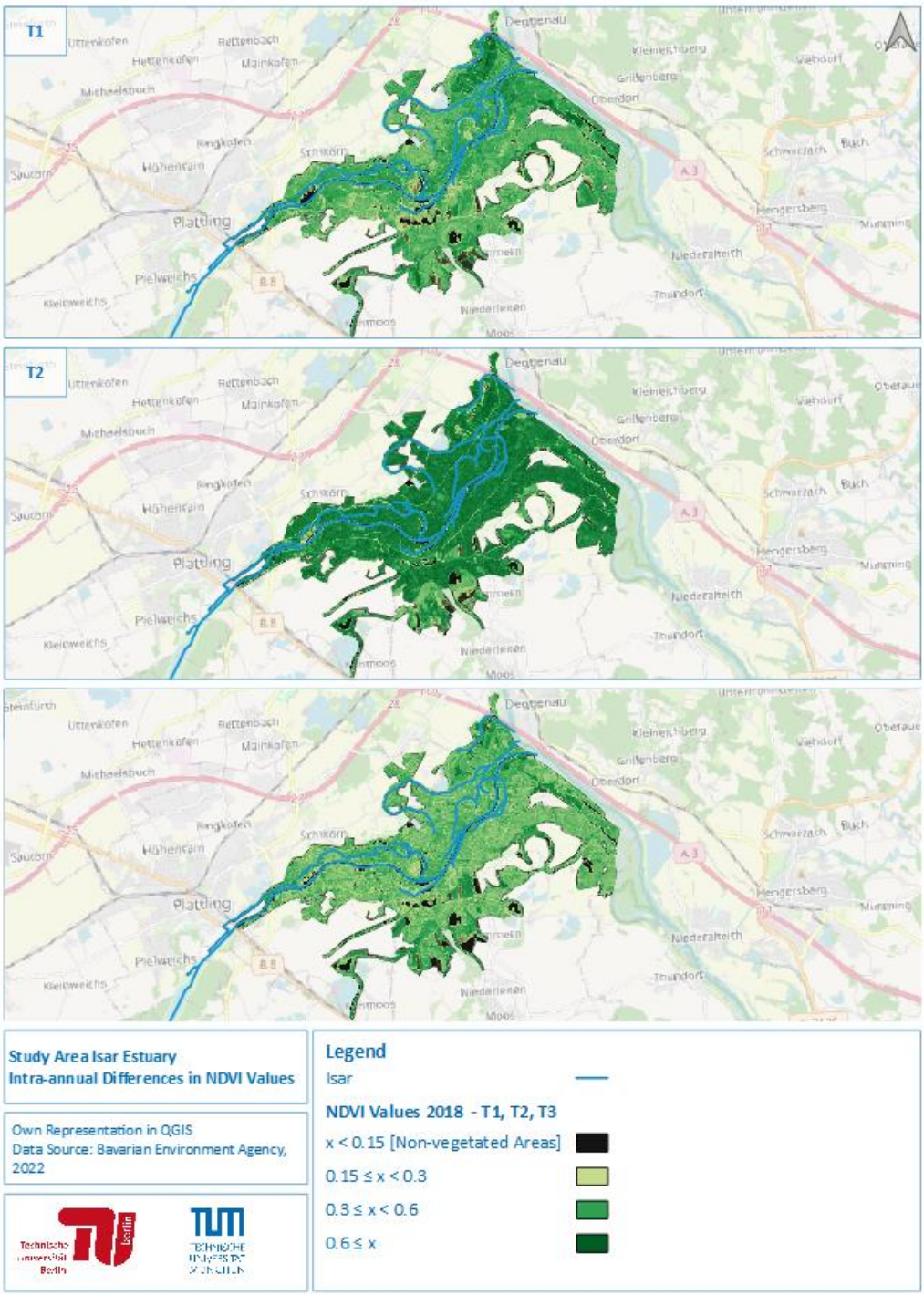

Map 38. NDVI throughout the year 2018. Darker green nuances indicate higher NDVI values, as detectable in Summer-T2, whereas lighter shades depict lower NDVI values. Black parts indicate non-vegetated areas or masked out cloud coverage.

Intra-annual alterations in NDVI values per biotope type and investigated year are depicted in Fig. 67.

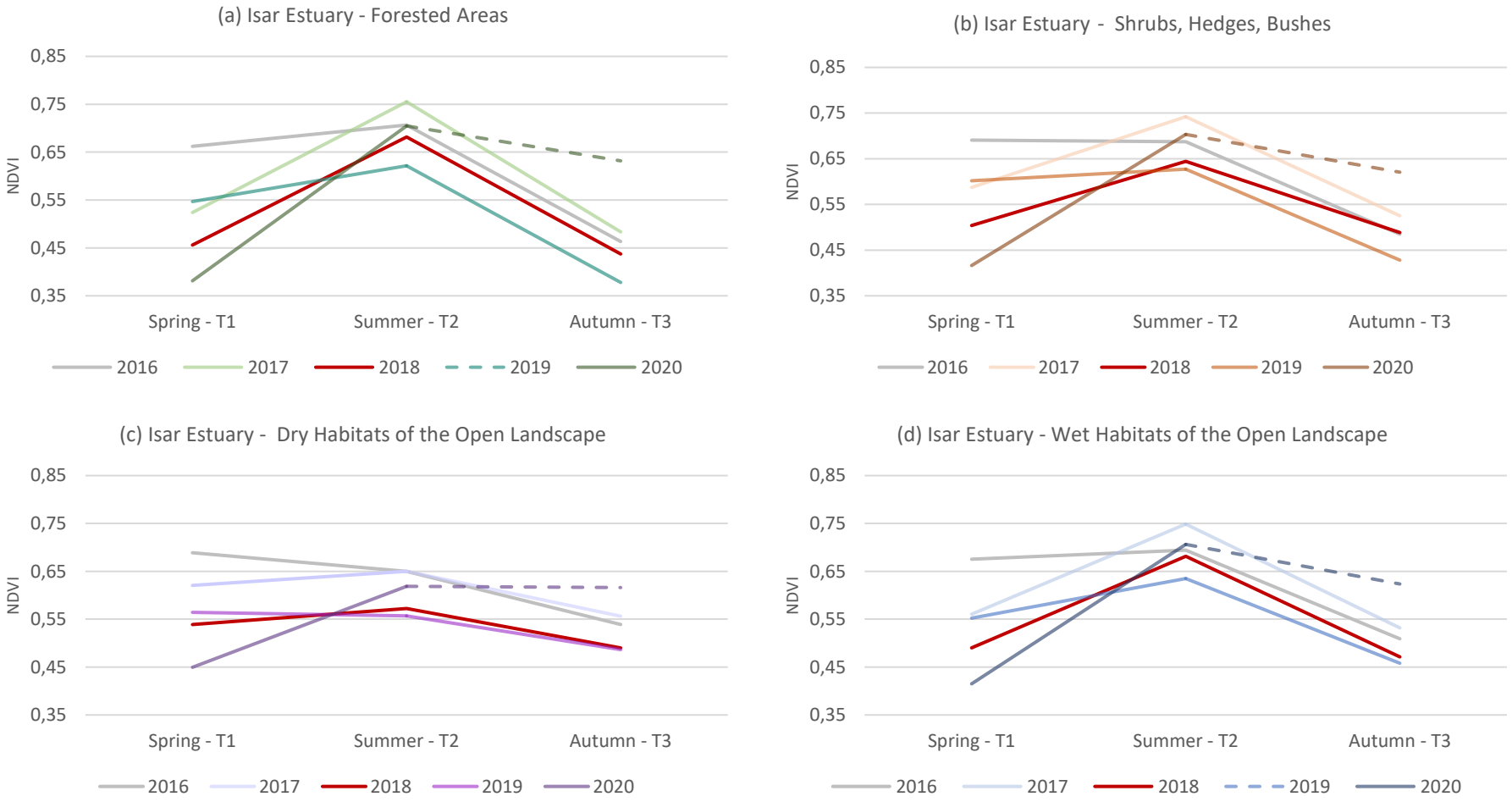

Figure 67. Intra-annual alterations of the NDVI values per biotope type and investigated year. NDVI regimes display specific signatures for (a) Forested Areas (NDVI 0.38-0.76), (b) Shrubs, Hedges and Bushes (NDVI 0.42-0.74), (c) Dry Habitats of the Open Landscape (NDVI 0.45-0.65) and (d) Wet Habitats of the Open Landscape (NDVI 0.42-0.75). The 2018 NDVI regimes are, in comparison to the reference year2016 significantly for all biotope types. These results can be connected to the meteorological and hydrological conditions, meaning that all biotope types experienced plant vitality decreases following the drought event 2018. However, in contrast to the other investigated years, the NDVI regimes of 2018 are not prominently lower. All four biotope types exhibit very low NDVI regimes in 2019 for instance. Particularly noteworthy are the investigation points Summer-T2 and Autumn-T2 of 2019, where the NDVI of all biotope types remains lower than the NDVI values of 2018 for these investigation points.

Inter-annual Difference in NDVI Values for Study Area Isar Estuary and per Biotope Type

The following maps display the inter-annual differences in NDVI values between the reference year 2016 and the other investigated years (2017, 2018, 2019 and 2020). Differences were calculated using the equation found under Materials and Methods. Changes in plant vitality were derived thereof and are depicted in the legend.

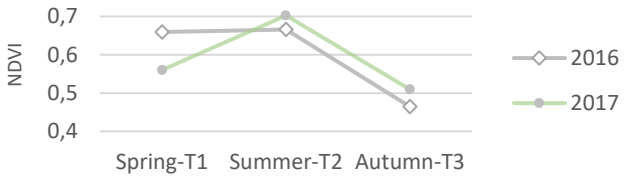

Figure 68. Mean intra-annual alterations of the NDVI 2016 and NDVI 2017 for study area Isar Estuary. Spring-T1 (0.56) of 2017 is significantly lower than Spring-T1 of 2016 (0.66). This can be led back to the temporal deferral of obtained data for Spring-T1 in 2016 (7th May). Summer-T2 (0.70) and Autumn-T3 (0.51) of 2017 are unexpectedly higher, compared to Summer-T2 (0.67) and Autumn-T3 (0.46) of 2016. NDVI differences between 2016 and 2017 for study area Isar Estuary are visualized in Map 39.

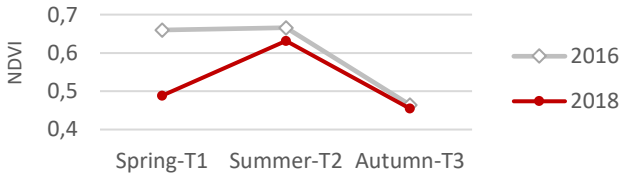

Figure 69. Mean intra-annual alterations of the NDVI 2016 and NDVI 2018 for study area Isar Estuary. Spring-T1 of 2016(0.66) and 2018 (0.49) differ significantly but converge in Summer-T2 (0.67 and 0.63) and are almost the same for Autumn-T3 (0.46 and 0.45). The differences in those NDVI regimes are visualized in Map 40.

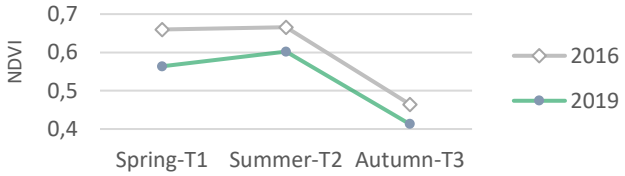

Figure 70. Mean intra-annual alterations of the NDVI regimes of 2016 and 2019 for study area Isar Estuary. Spring-T1 of 2019 (0.56) is significantly lower than Spring-T1 of 2016 (0.66). NDVIs for Summer-T2 (0.60) and Autumn-T3 (0.41) in 2019 remain lower than Summer-T2 (0.67) and Autumn-T3 (0.46) in 2016, but show lower differences than at Spring-T1. The scope of NDVI differences between 2016 and 2019 are visualized in Map 41.

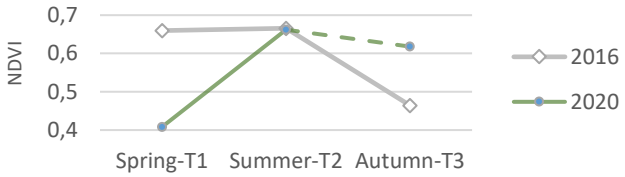

Figure 71. Mean intra-annual alterations of the NDVI 2016 and NDVI 2020 for study area Isar Estuary. Spring-T1 of 2016 (0.66) was significantly higher than Spring-T1 of 2020 (0.41), while NDVI values for Summer-T2 of 2019 (0.66) and Summer-T2 of 2016 (0.67) were almost the same. Autumn-T3 of 2020 is disregarded in this analysis as data was obtained September 20th, resulting in undue temporal deferral. NDVI Differences between those years are visualized in Map 42.

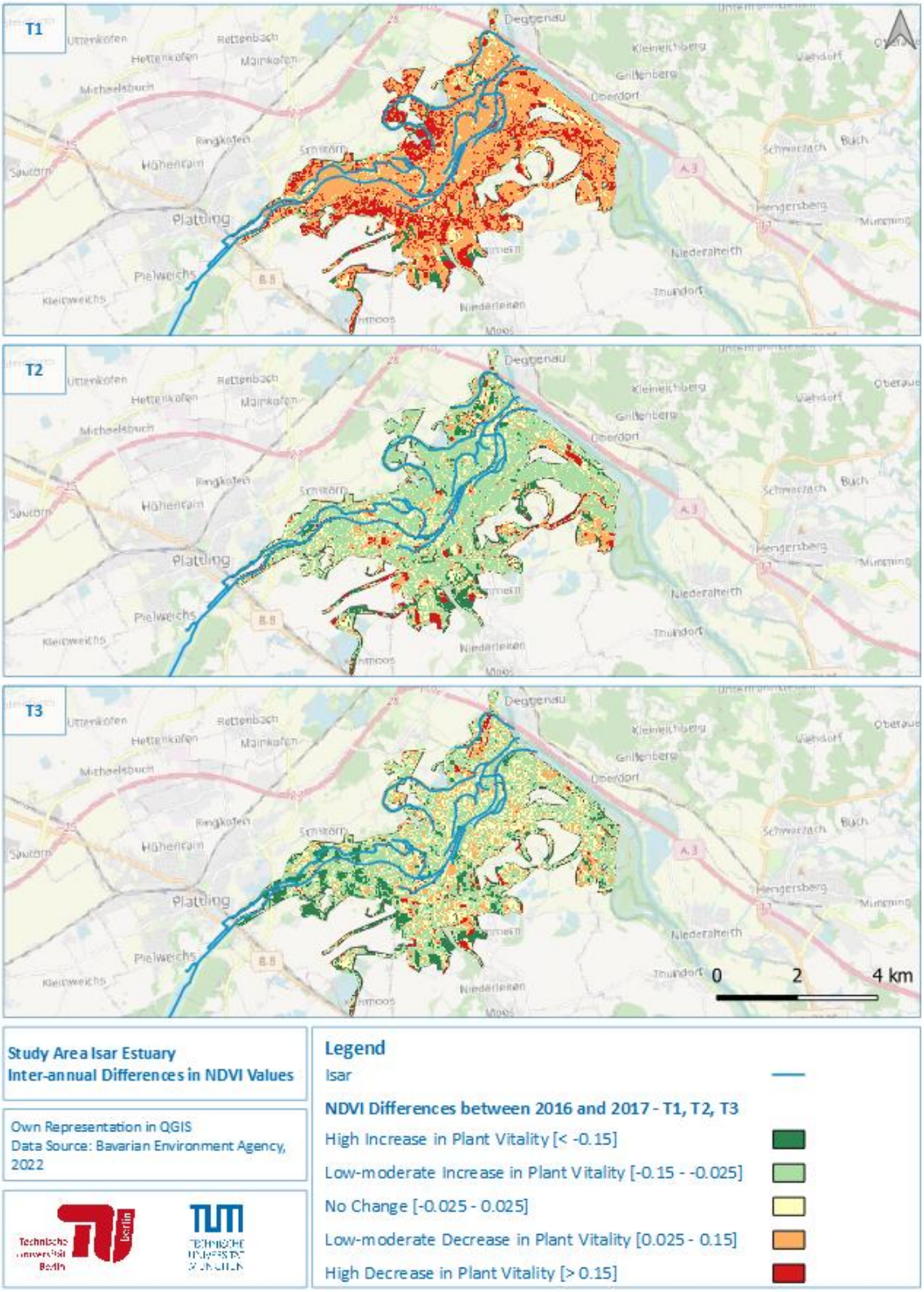

Map 39. Exhaustive low-moderate and high decreases in NDVI can be observed for 2016-2017 at Spring-T1, whereas low-moderate increases in NDVI and thus, plant vitality, are detected between 2016-2017 for Summer-T2 and Autumn-T3. These maps reflect the NDVI regimes depicted in Figure 68. Fragmented NDVI changes adequately depict the differences in biotope types, which need to be considered for impacts of the 2018 drought on individual biotope types.

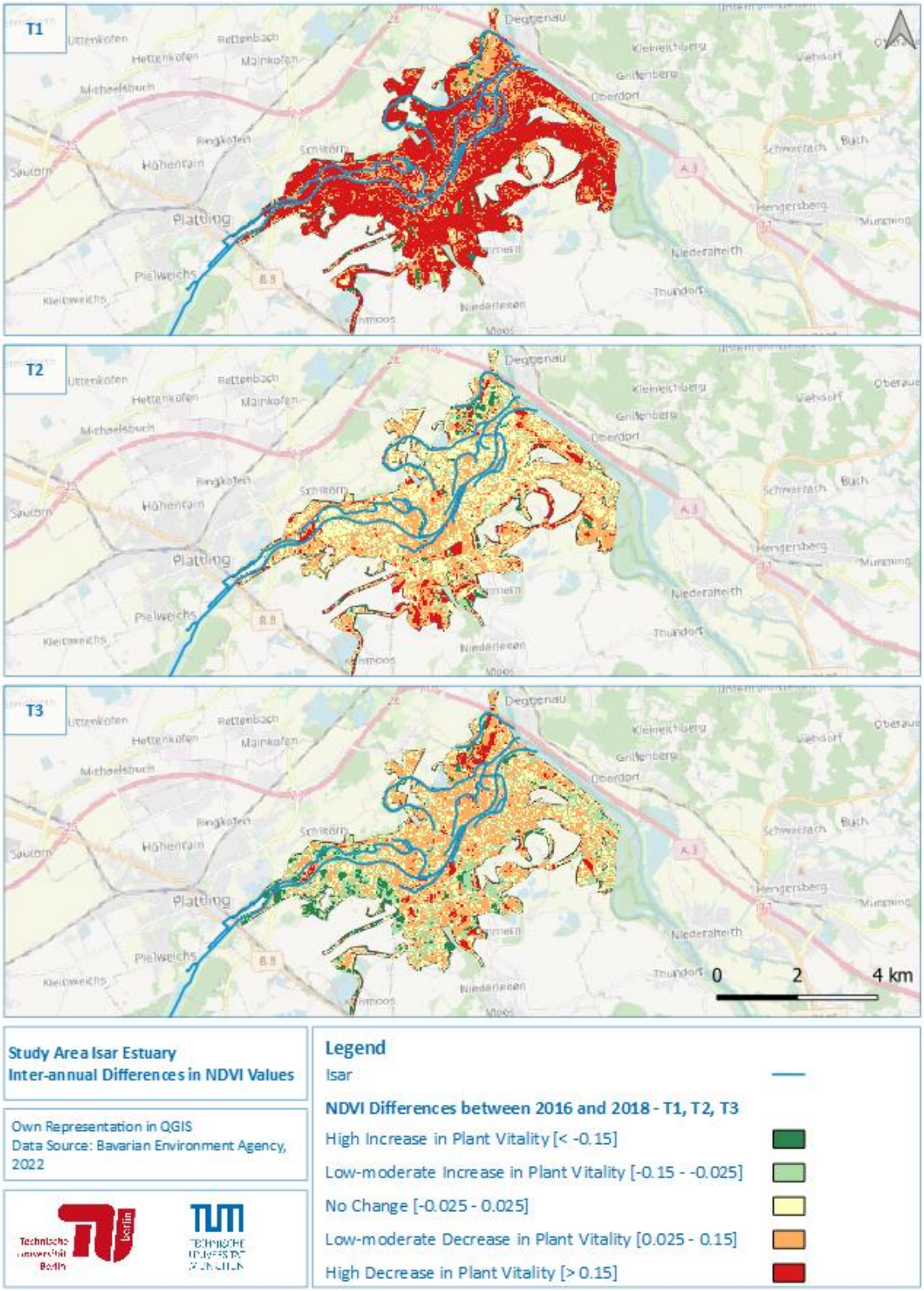

Map 40. High and low-moderate decreases in NDVI are predominant at Spring-T1, when comparing 2016 and 2018 at this investigation point. Summer-T2 and Autumn-T3 display quite fragmented areas within all categories of NDVI Changes, indicating the importance of investigating individual biotope types when necessary. Especially the southwestern fringes of this study area display partial low-moderate/high increases in NDVI for Summer-T2 and Autumn-T3. Overall, NDVI and therefore plant vitality, still remain lower at Summer-T2 and Autumn-T3 for 2018 than in 2016 as depicted in Figure 69.

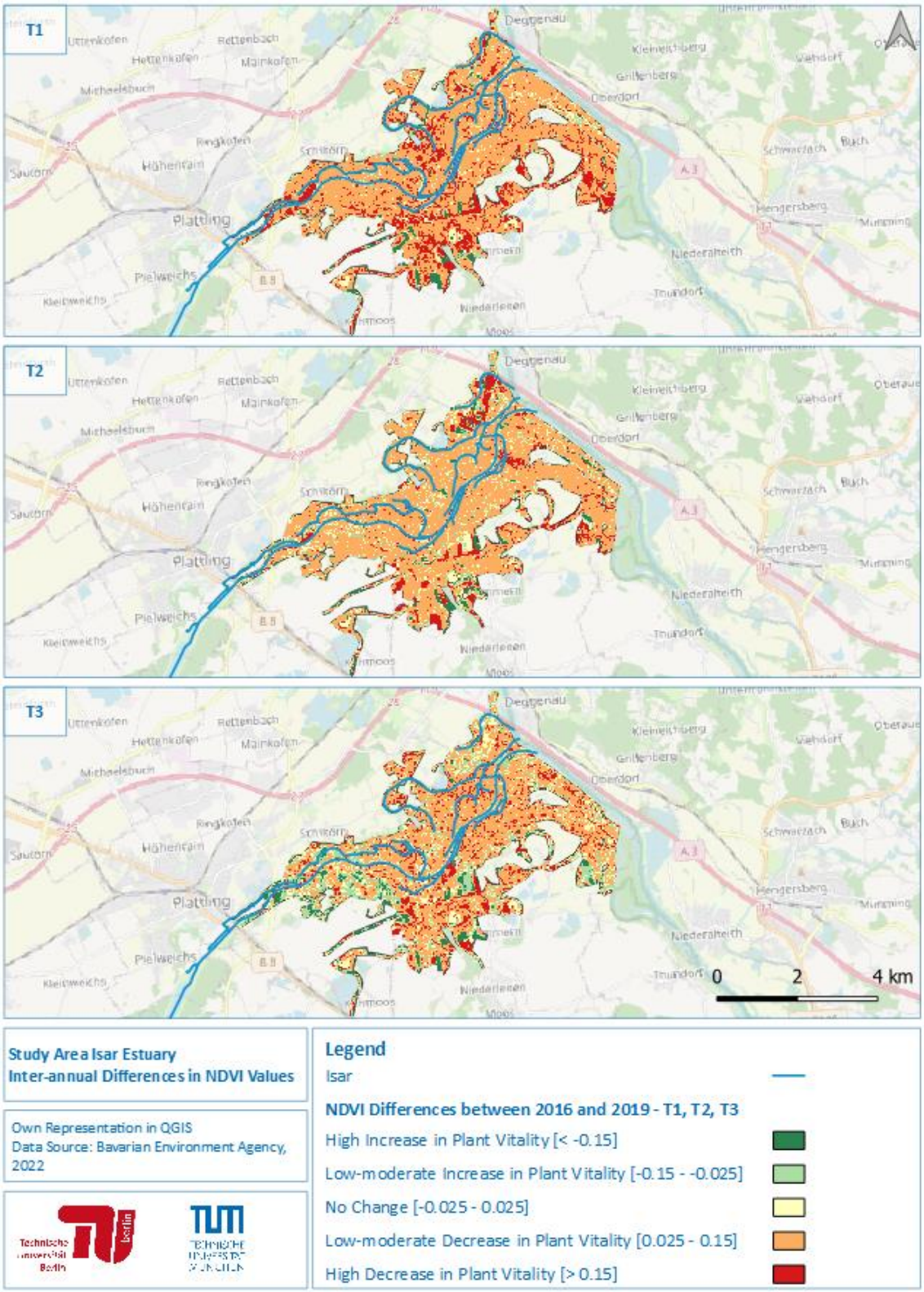

Map 41. Exhaustive low-moderate decreases in NDVI and therefore plant vitality were recorded for all investigation points between 2016 and 2019. Spring-T1 however depicted the most extensive decreases, encompassing several areas with high reductions in plant vitality. Autumn-T3 incorporated NDVI changes of all categories in similar extents, although low-moderate decreases in plant vitality were predominant. These maps adequately visualize the differences in index values as seen in Figure 70.

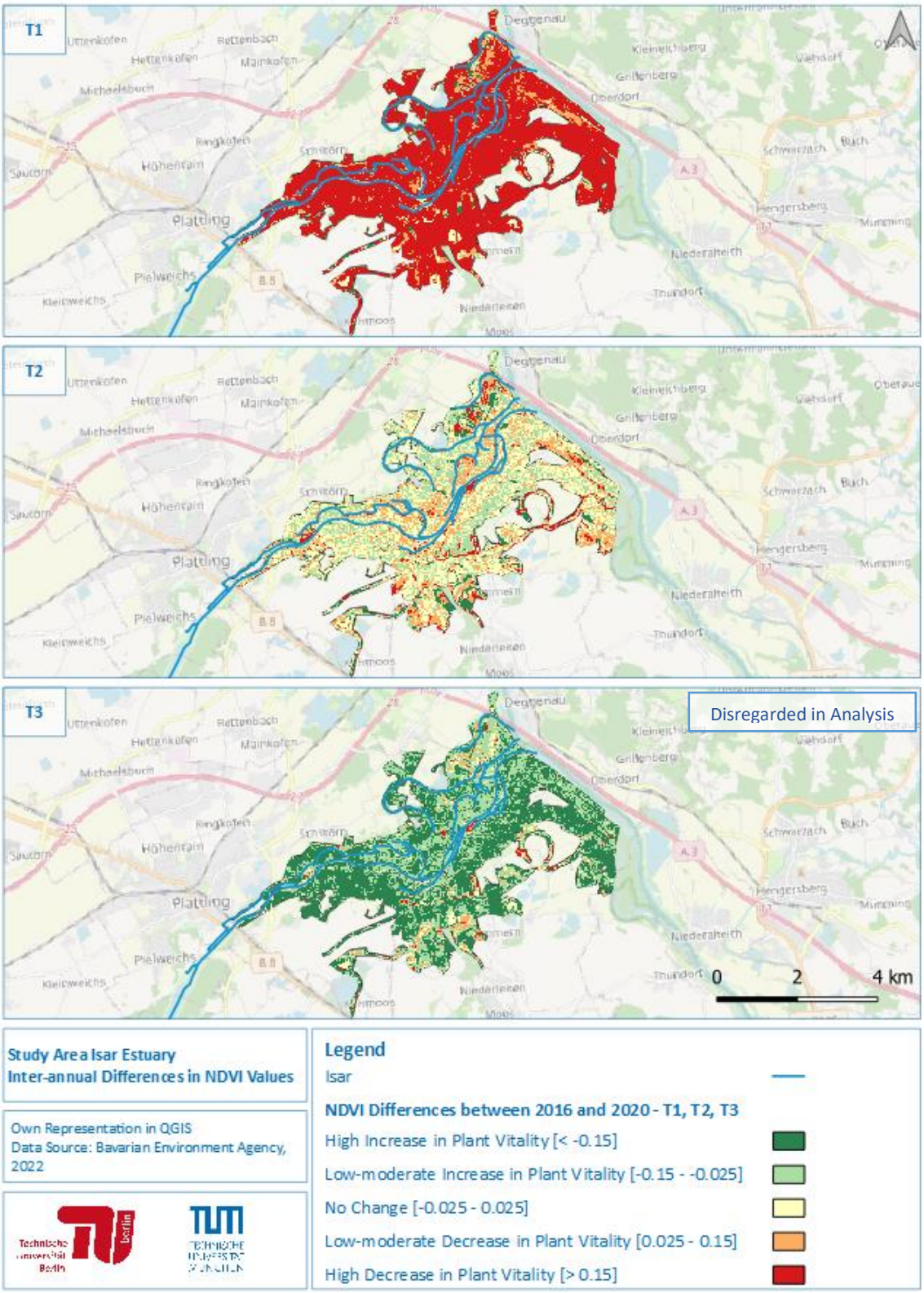

Map 42. Almost the entire scope of study area Isar Estuary experienced high decreases in plant vitality between 2016 and 2020 at Spring-T1. Balanced extents of decreases and increases in plant vitality caused the levelled NDVI values in Figure 71. Here the spatial distributions are adequately depicted. High and low-moderate increases in plant vitality were detected for T3 (2016-2020) but are disregarded in the analysis, as high-quality satellite imagery was only obtainable for September 2020. Distortions in the NDVI results can therefore not be excluded.

Figure 72. Inter-annual diffences in NDVI values per biotope type and year for study area Isar Estuary.

Box and whisker plots describe the variability of NDVI value distribution within each biotope type and depict the scatter range. Scattering is lowest for Dry Habitats of the Open Landscape, followed by Shrubs, Hedges and Bushes, Wet Habitats of the Open Landscape and Forested Areas in increasing order. Dotted red lines indicate the mean NDVI values for the entire study area in relation to each biotope type. All biotope types exhibit lower NDVI at Spring-T1 and Summer-T2 in 2018 than at Spring-T1 and Summer-T2 in 2016. This indicates, that all investigated biotope types experienced decreases in NDVI, and thus plant vitality during spring and summer 2018, following the abnormally warm and dry spring 2018. At Autumn-T3, however, only Forested Areas (0.44), Dry Habitats of the Open Landscape (0.49) and Wet Habitats of the Open Landscape (0.47) record lower values at Spring-T1 in 2018 than in 2016 (0.46, 0.54 and 0.51 respectively). Shrubs, Hedges and Bushes are lower at Spring-T1 in 2016 (0.48) than in 2018 (0.49).

In comparison to all investigated years, however, the NDVI results of this study area show higher variations. Similar to study area Lower Isar between Landau and Plattling, NDVI is lowest for all biotopte types at Spring-T1 in 2020. NDVI at Summer-T2 and Autumn-T3 on the other hand are lowest for all biotope types in 2019. These results emphasise the contextualization of NDVI assessments for time series and in comparison to more recent drought periods especially in the beginning of the vegetative period, as seen in 2020.

3.5.2 NDWI – Isar Estuary

Satellite Data

Table 12. Satellite imagery used in the NDWI assessment of study area Isar Estuary. Differences in investigation times arose from data availability limitations. Greyed out times are disregarded in the analysis by reason of undue temporal deferral.

Time	2016	2017	2018	2019	2020
T1	09 May	24 April	19 April	24 April	08 April
T2	27 August	13 July	27 August	27 August	21 August
T3	16 October	16 October	16 October	31 October	20 September

Intra-annual Alterations in NDWI Values

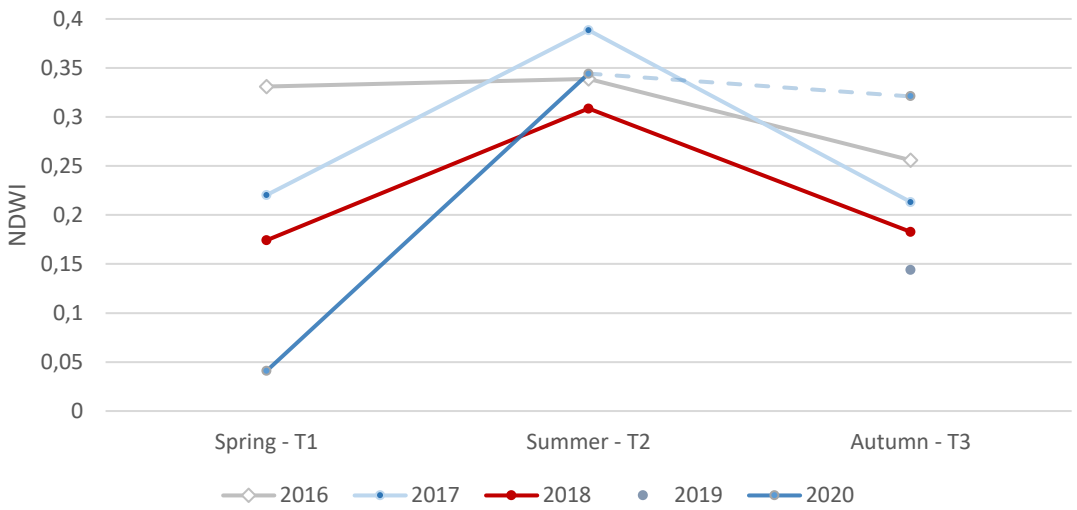

Figure 73. Mean intra-annual alterations in NDWI for the entire study area Isar Estuary. Dashed lines indicate the disregarded values, as outliers of investigation times may cause incomparability in obtained results.

Intra-annual alterations in NDWI values are depicted in Figure 73 for the entire study area Isar Estuary. As for the other study areas, the NDWI peaks during investigation point Summer-T2 of respective year. NDWI values for all investigated years subsequently decline to Autumn-T3, following the biomass built-up and therefore the plant water content, throughout the phenological cycle. Steepness of increase and decrease in NDWI values vary for each year. The NDWI regime in 2020 increases with the steepest gradient from Spring-T1 (0.04) to Summer-T3 (0.34), followed by 2017 (0.22 to 0.39) and 2018 (0.17 to 0.31). By reason of errors occurring during procession, no results could be calculated with the obtained satellite imagery for Spring-T1 and Summer-T2 2019. As for study area Lower Isar between Landau and Plattling, Spring-T1 for 2016 was obtained early May, the NDWI displays a fairly high value for this investigation point. Spring-T1 is significantly higher for 2016 (0.33), compared to 2018 (0.17), but converges at Summer-T2 (0.34 and 0.31). Both regimes subsequently decline with approx. the same gradient to Autumn-T3 (0.26 and 0.18). Overall, the NDWI regime of 2018 remains substantially lower than the 2016 regime. Disparate meteorological conditions within the investigation period (2016-2020), especially those of air temperature are closely tied to the obtained differences in NDWI regimes, resulting in impediments for plant growth and thus, reduced plant water content.

The following figures and maps exemplarily display this study areas intra-annual alterations in NDWI regimes for the reference year 2016 and the drought year 2018, respectively.

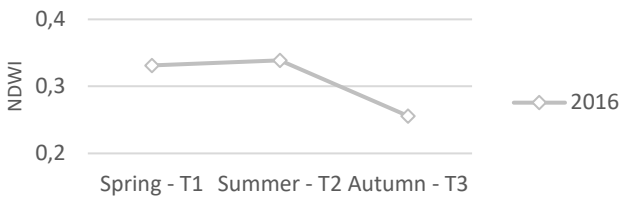

Figure 74. Mean intra-annual alterations of the NDWI 2016 for study area Isar Estuary, with Spring-T1(0.33), Summer-T2 (0.34) and Autumn-T3 (0.26). The following map visualizes the NDWI for T1, T2 and T3 in 2016.

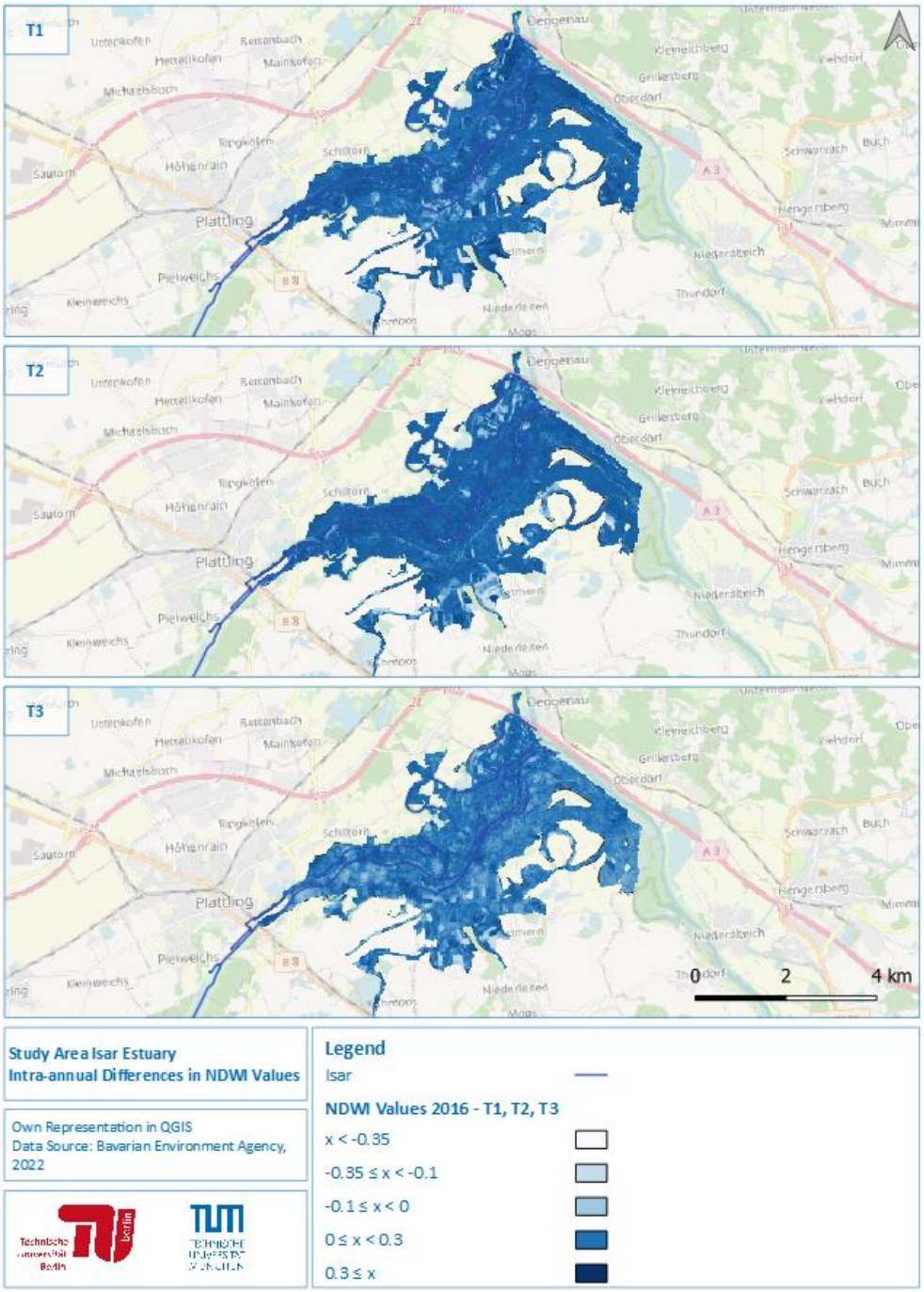

Map 43. A clear increase in NDWI is visible for the investigation point T2, adequately displayed by darker nuances in blue compared to investigation point T1, before decreasing NDWI causes lighter nuances in Autumn-T3.

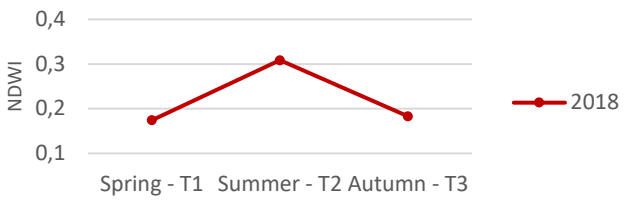

Figure 75. Mean intra-annual alterations of the NDWI 2018 for study area Isar Estuary with Spring (0.17), Summer-T2 (0.31) and Autumn-T3 (0.18). The following map visualizes the NDWI regime for 2018.

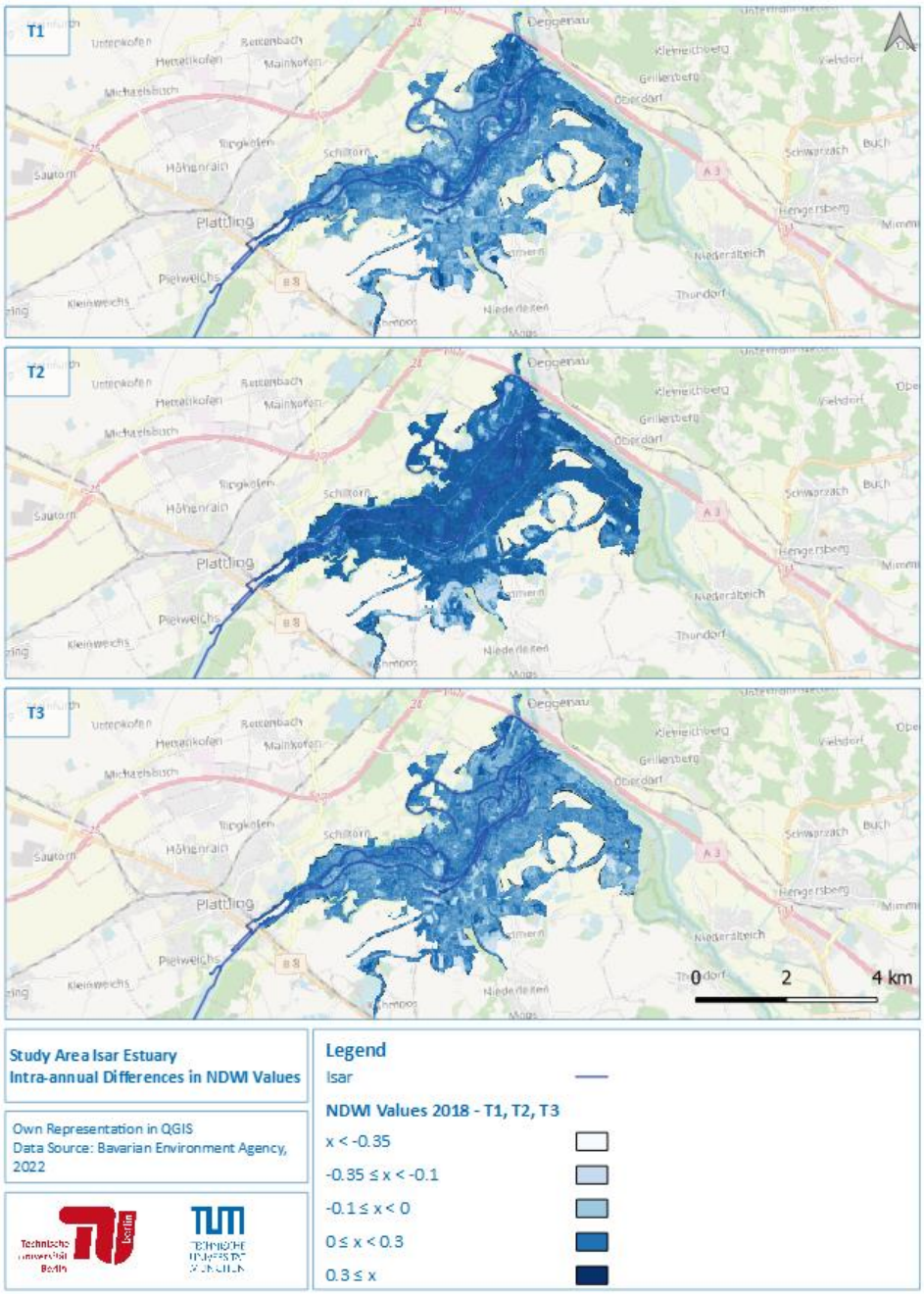

Map 44. A clear increase in NDWI is visible for the investigation point T2, adequately displayed by darker nuances in blue compared to investigation point T1. Autumn-T3 displays significant decreases in NDWI, compared to Summer-T2 for this study area in 2018.

Intra-annual alterations in NDWI values per biotope type and investigated year are depicted in Fig. 76. For all four biotope types the NDWI regime in 2018 is in average the lowest out of all investigated years.

Figure 76. Intra-annual alterations of the NDWI values per biotope type and investigated year. NDWI regimes display specific signatures for (a) Forested Areas (NDWI 0.01-0.43), (b) Shrubs, Hedges and Bushes (NDWI 0.01-0.37), (c) Dry Habitats of the Open Landscape (NDWI 0.04-0.31) and (d) Wet Habitats of the Open Landscape (NDWI 0.02-0.37). The 2016 and 2018 NDWI regimes for Dry Habitats of the Open Landscape (c) display an interesting course, starting with the highest value in Spring-T1 and then consistently decreasing throughout the vegetative period to Autumn-T3. The 2018 NDWI regimes are for all biotope types in comparison to the reference year 2016 significantly lower. These results can be connected to the meteorological and hydrological conditions, meaning that all biotope types experienced decreases in NDWI values throughout 2018. This indicates plant water stress following the drought event in 2018.

Inter-annual Differences in NDWI Values and per Biotope Type

Inter-annual courses of the mean NDWIs are visualized in Map 45 – 47 for each investigation point (Spring-T1, Summer-T2, Autumn-T3) and per year, respectively. Figures 77 – 79 display the mean NDWI course for each investigation point. These figures and maps are enclosed for one study area per river section and for comparison and comprehension reasons. They do not incorporate Change Detection as for the NDVI.

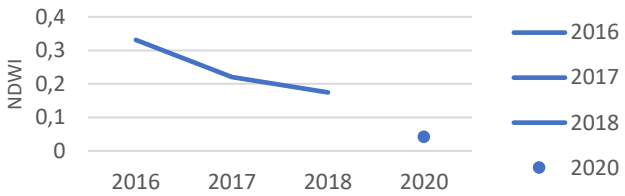

Figure 77. Inter-annual alterations of the NDWI throughout the investigation period (2016-2020) for study area Isar Estuary at Spring-T1. NDWI values are highest in 2016 (0.33), followed by 2017 (0.22) and 2018 (0.17). Lowest T1 NDWI value was recorded for 2020 (0.04). Map 45 visualizes the NDWI sequence of Spring-T1 for each investigated year.

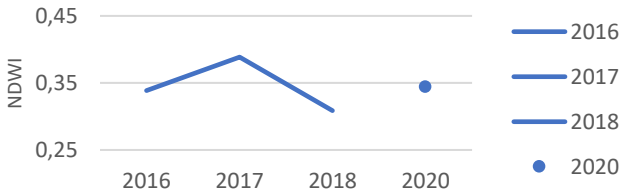

Figure 78. Inter-annual alterations of the NDWI throughout the investigation period (2016-2020) for study area Isar Estuary at Summer-T2. NDWI values are highest in 2017 (0.39), followed by 2020 (0.34) and 2016 (0.34) and 2018 (0.31) in decreasing order. Map 46 visualizes the NDWI of Summer-T2 for each investigated year.

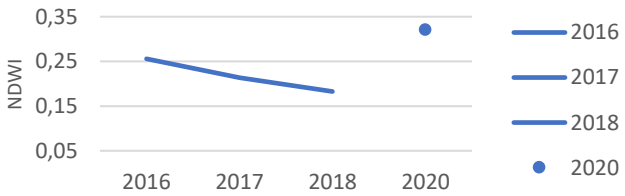

Figure 79. Inter-annual alterations of the NDWI throughout the investigation period (2016-2020) for study area Isar Estuary at Autumn-T3. NDWI values are highest in 2020 (0.32), followed by 2016 (0.26), 2017 (0.21) and 2018 (0.18) in decreasing order. 2020 is, however, disregarded in the analysis as high-quality satellite imagery was only obtainable for September 2020. Distortions in the NDWI results can therefore not be excluded. Map 47 visualizes the NDWIs of Autumn-T3 for each investigated year.

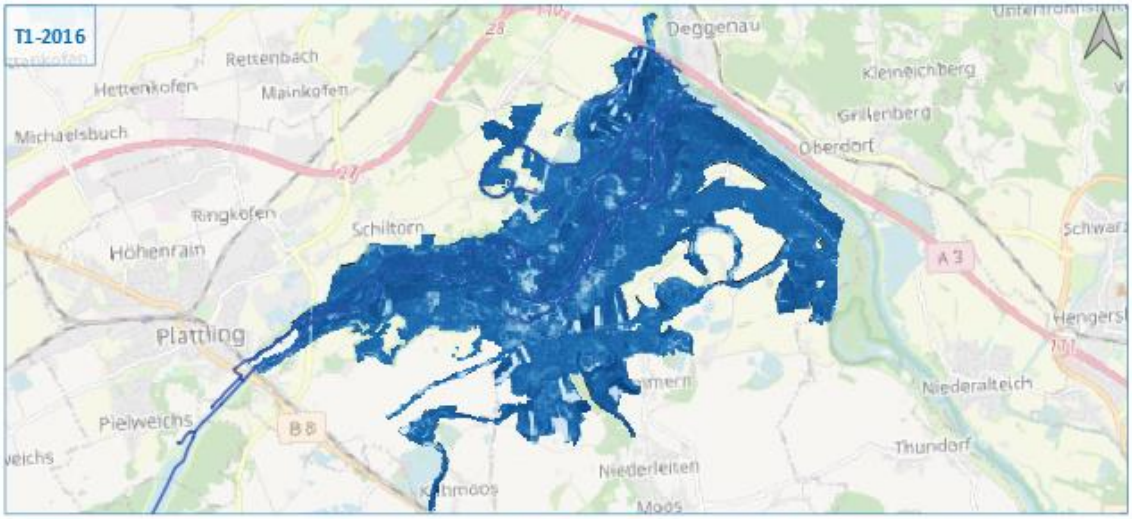
T1-2016
Deggenau
Rettenbach
Hettenkofen
Mainkofen
Michaelsbuch
Kleineichberg
Grillenberg
Oberdorf
Ringkofen
Schiltorn
Höhenrain
Plattling
A 3
Niederalteich
Pielweichs
B 8
Thundorf
Niederleiten

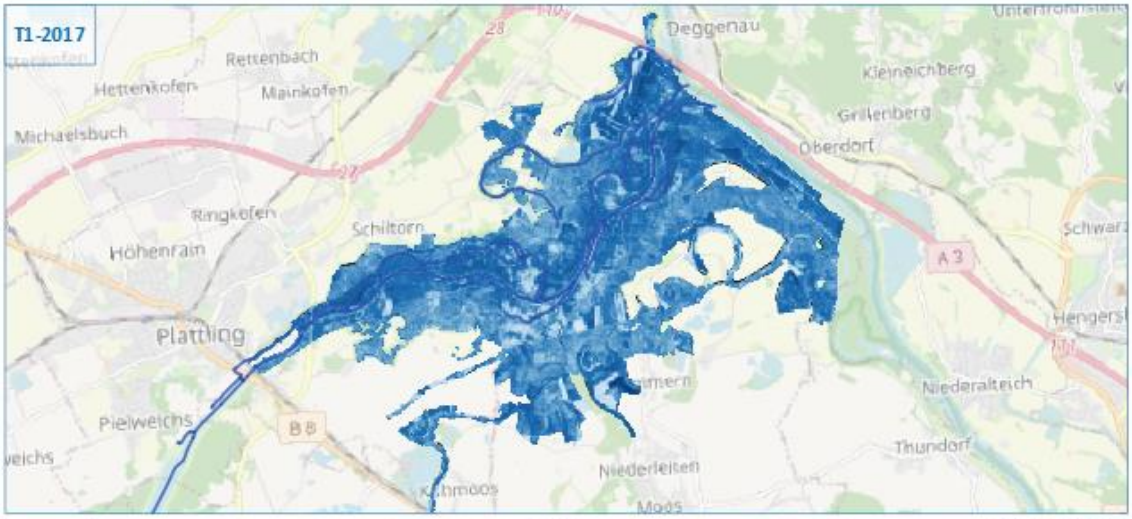
T1-2017
Deggenau
Rettenbach
Hettenkofen
Mainkofen
Michaelsbuch
Kleineichberg
Grillenberg
Oberdorf
Ringkofen
Schiltorn
Höhenrain
Plattling
A 3
Niederalteich
Pielweichs
B 8
Thundorf
Niederleiten

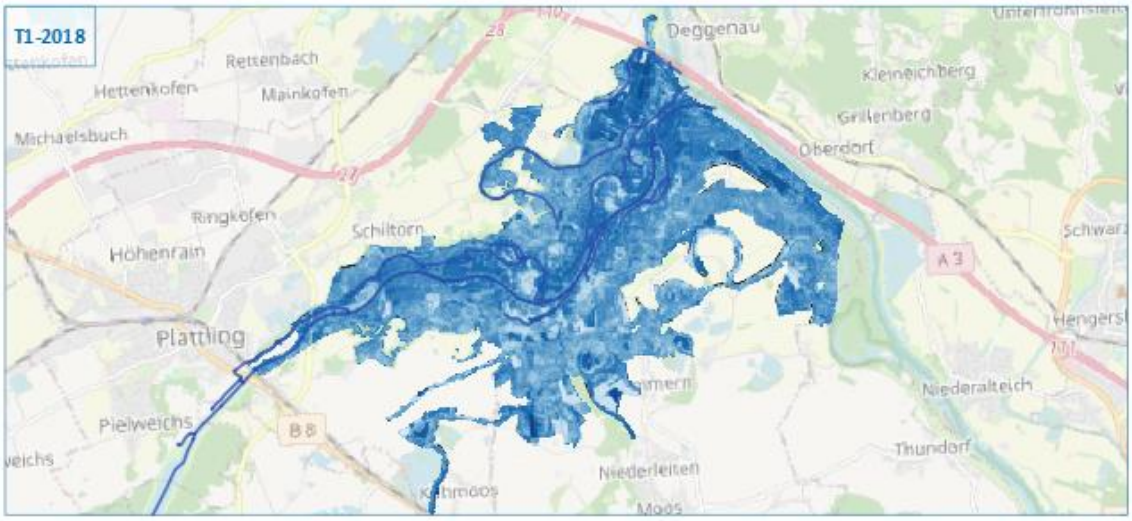
T1-2018
Deggenau
Rettenbach
Hettenkofen
Mainkofen
Michaelsbuch
Kleineichberg
Grillenberg
Oberdorf
Ringkofen
Schiltorn
Höhenrain
Plattling
A 3
Niederalteich
Pielweichs
B 8
Thundorf
Niederleiten

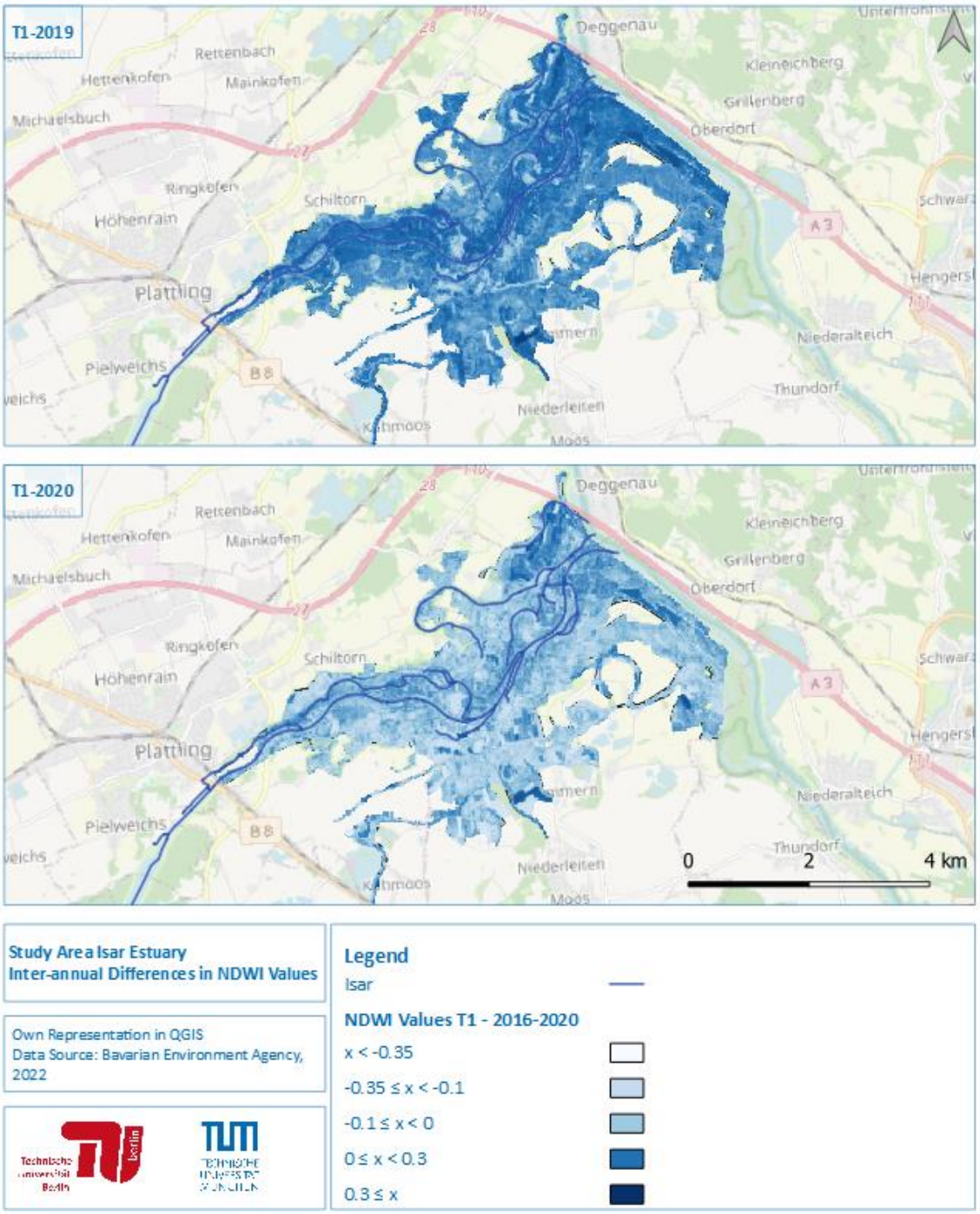

Map 45. Inter-annual alterations in NDWI values for study area Isar Estuary as depicted in Figure 77.

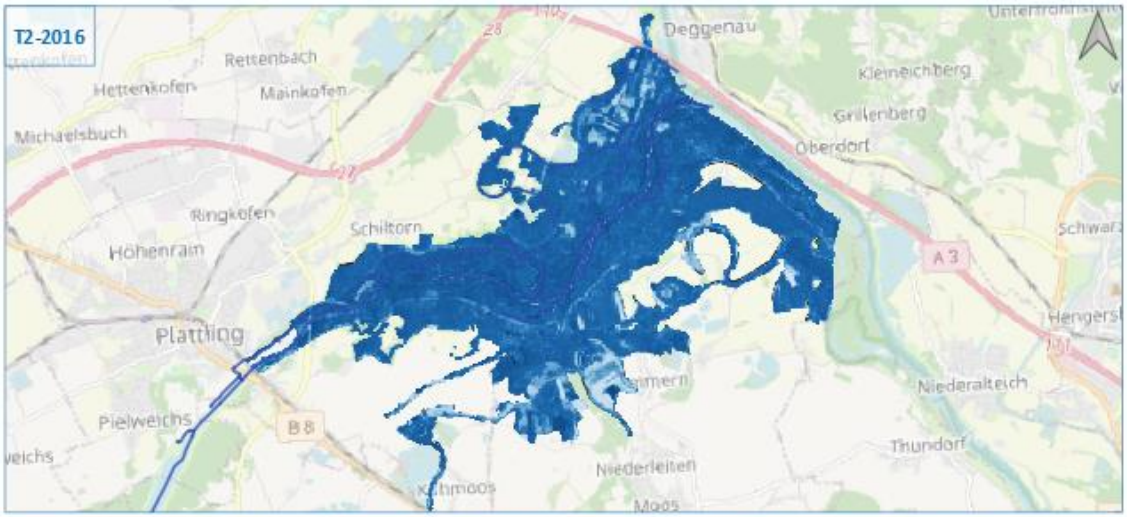
T2-2016
Deggenau
Rettenbach
Hettenkofen
Mainkofen
Michaelsbuch
Kleineichberg
Grillenberg
Oberdorf
Ringkofen
Schiltorn
Höhenrain
A 3
Plattling
Niederalteich
Pielweichs
B 8
Thundorf
Niederleiten
Kühmoos
Moos

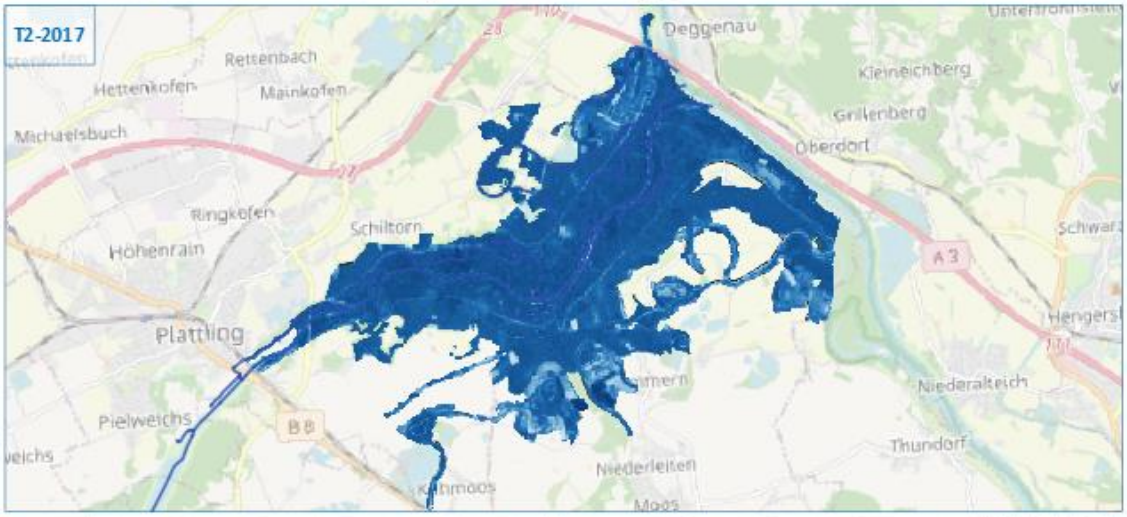
T2-2017
Deggenau
Rettenbach
Hettenkofen
Mainkofen
Michaelsbuch
Kleineichberg
Grillenberg
Oberdorf
Ringkofen
Schiltorn
Höhenrain
A 3
Plattling
Niederalteich
Pielweichs
B 8
Thundorf
Niederleiten
Kühmoos
Moos

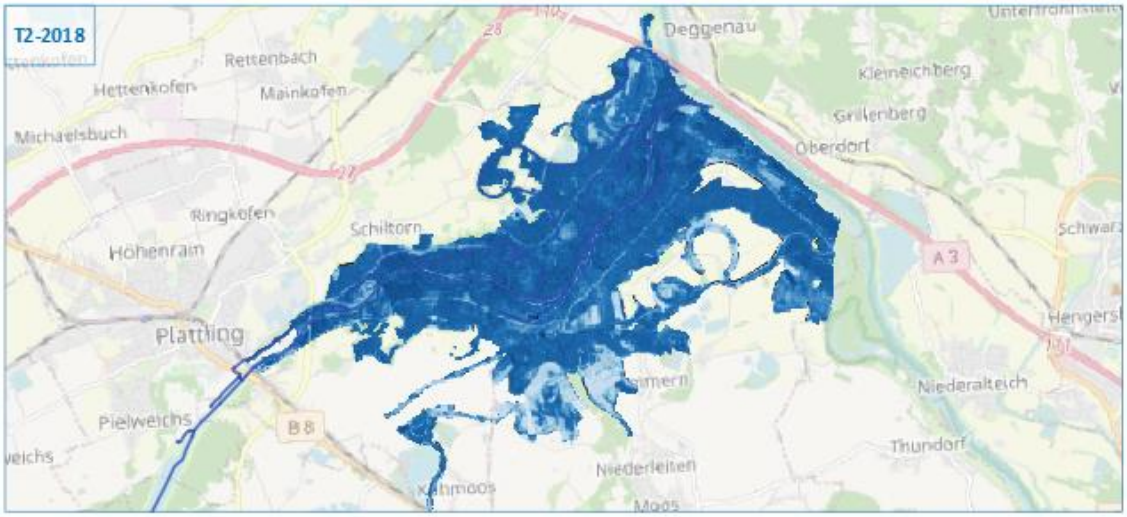
T2-2018
Deggenau
Rettenbach
Hettenkofen
Mainkofen
Michaelsbuch
Kleineichberg
Grillenberg
Oberdorf
Ringkofen
Schiltorn
Höhenrain
A 3
Plattling
Niederalteich
Pielweichs
B 8
Thundorf
Niederleiten
Kühmoos
Moos

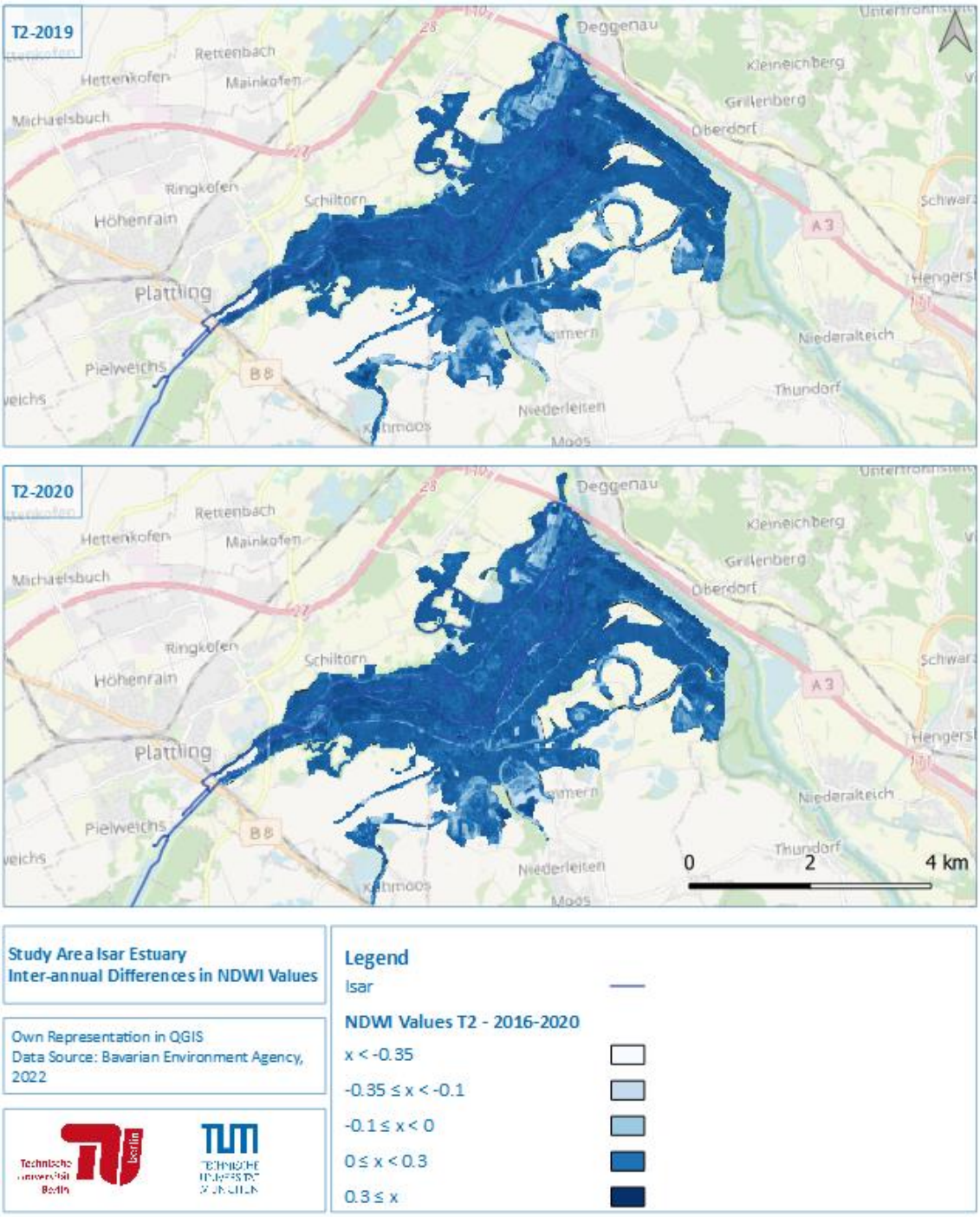

Map 46. Inter-annual alterations in NDWI values for study area Isar Estuary as depicted in Figure 78.

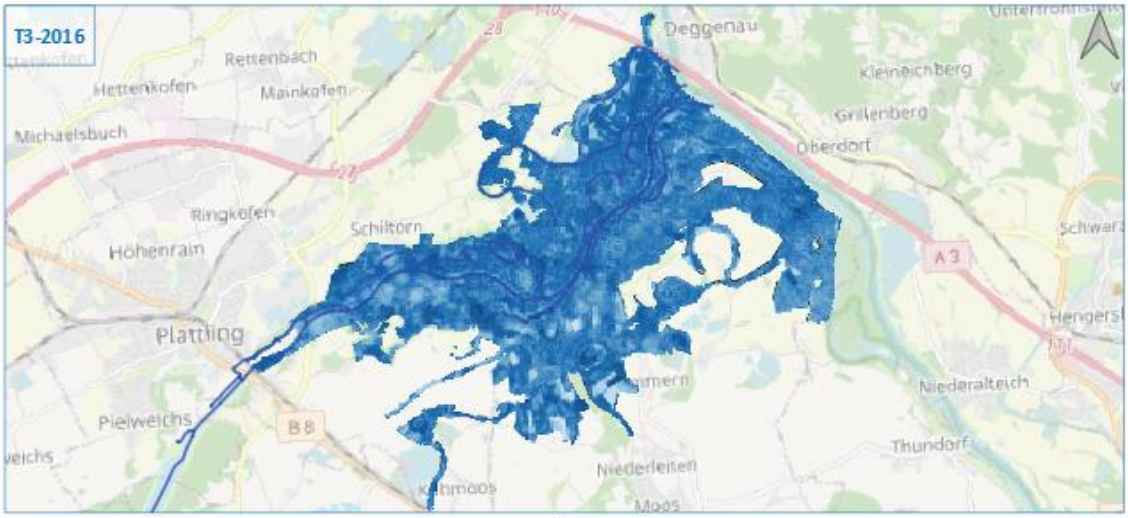
T3-2016
Deggenau
Rettenbach
Hettenkofen
Mainkofen
Michaelsbuch
Kleineichberg
Grillenberg
Oberdorf
Ringkofen
Schiltorn
Höhenrain
Plattling
A 3
B 8
Pielweichs
Niederalteich
Thundorf
Niederleiten
Moos

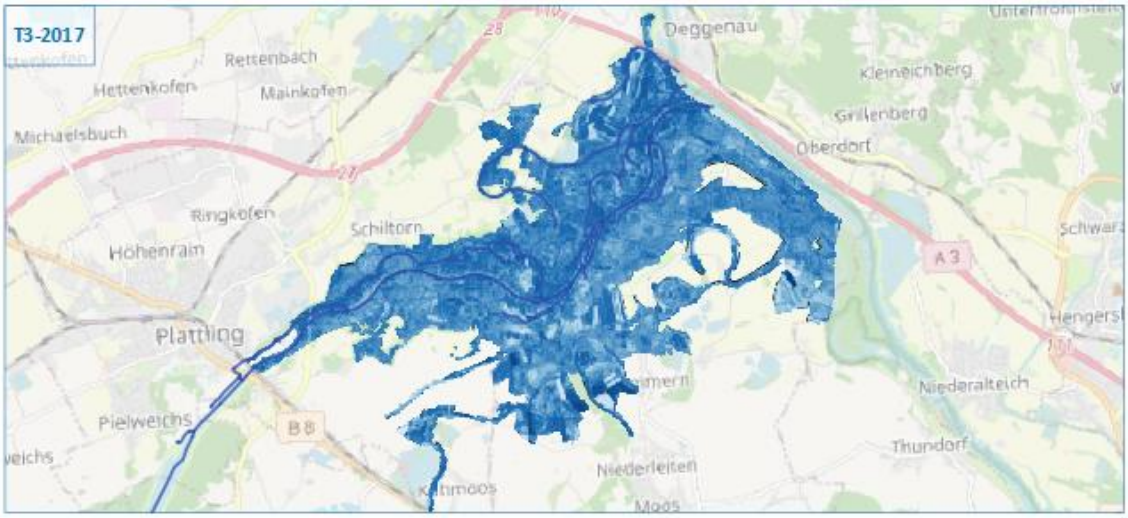
T3-2017
Deggenau
Rettenbach
Hettenkofen
Mainkofen
Michaelsbuch
Kleineichberg
Grillenberg
Oberdorf
Ringkofen
Schiltorn
Höhenrain
Plattling
A 3
B 8
Pielweichs
Niederalteich
Thundorf
Niederleiten
Moos

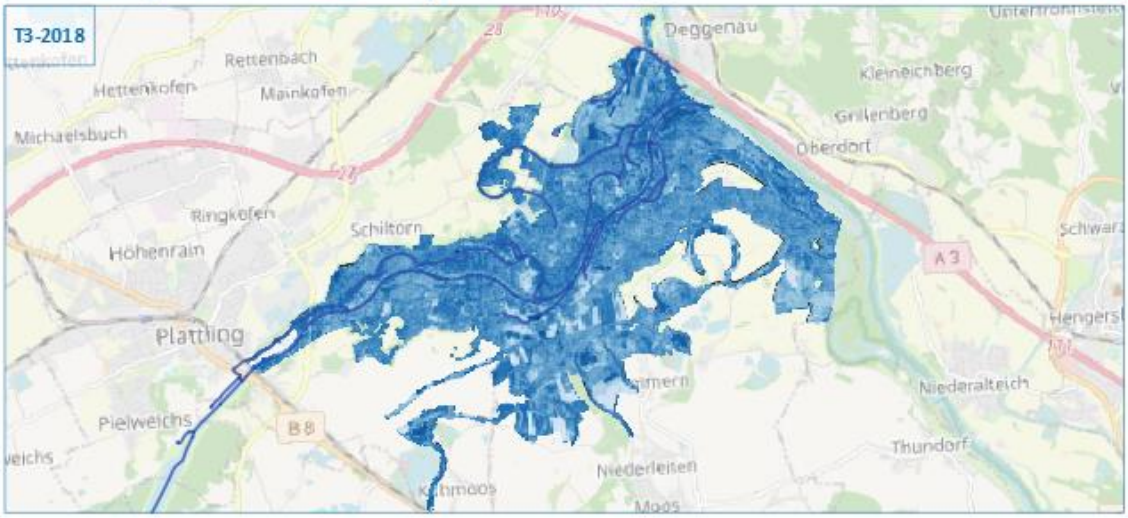
T3-2018
Deggenau
Rettenbach
Hettenkofen
Mainkofen
Michaelsbuch
Kleineichberg
Grillenberg
Oberdorf
Ringkofen
Schiltorn
Höhenrain
Plattling
A 3
B 8
Pielweichs
Niederalteich
Thundorf
Niederleiten
Moos

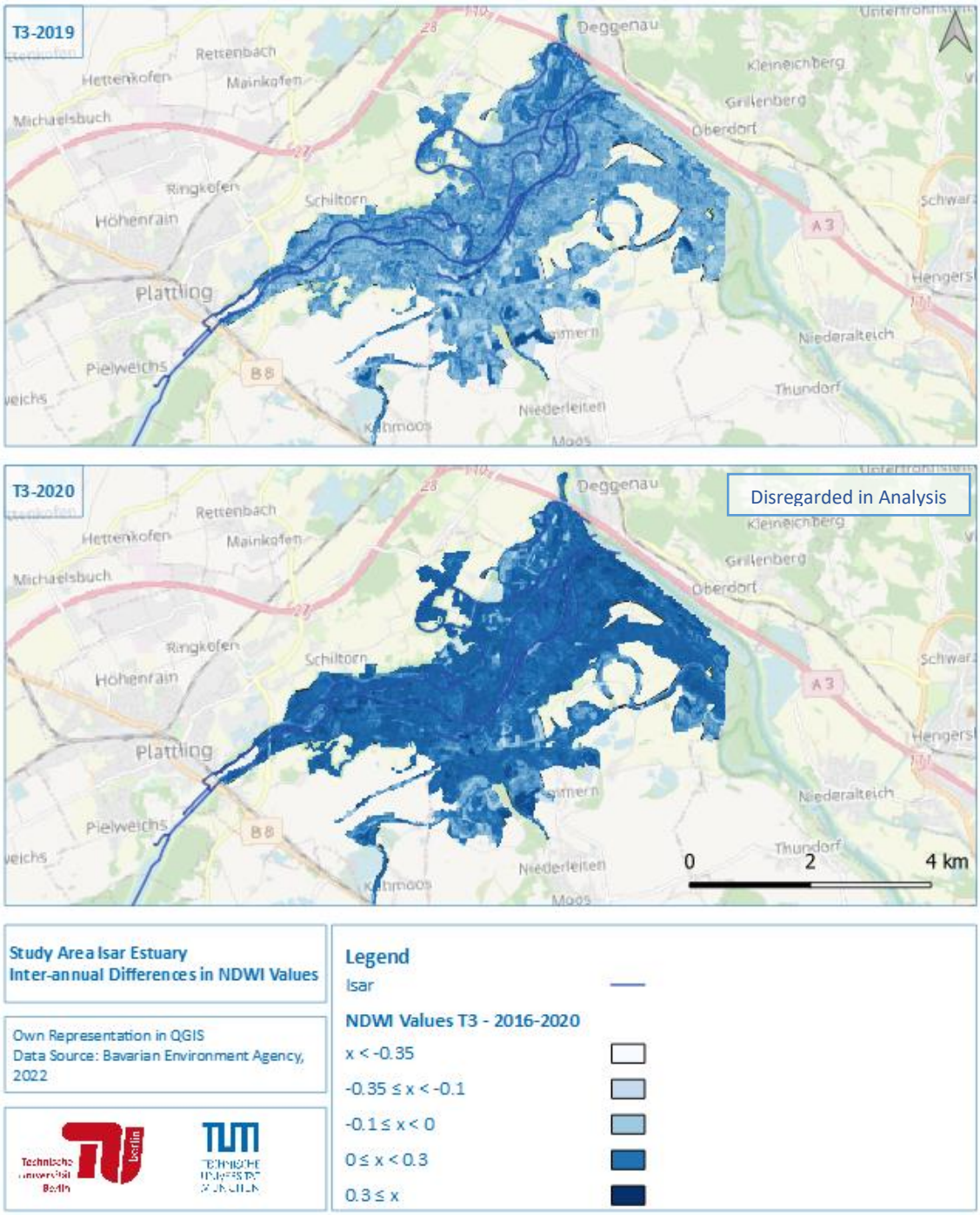

Map 47. Inter-annual alterations in NDWI values for study area Isar Estuary as depicted in Figure 79.

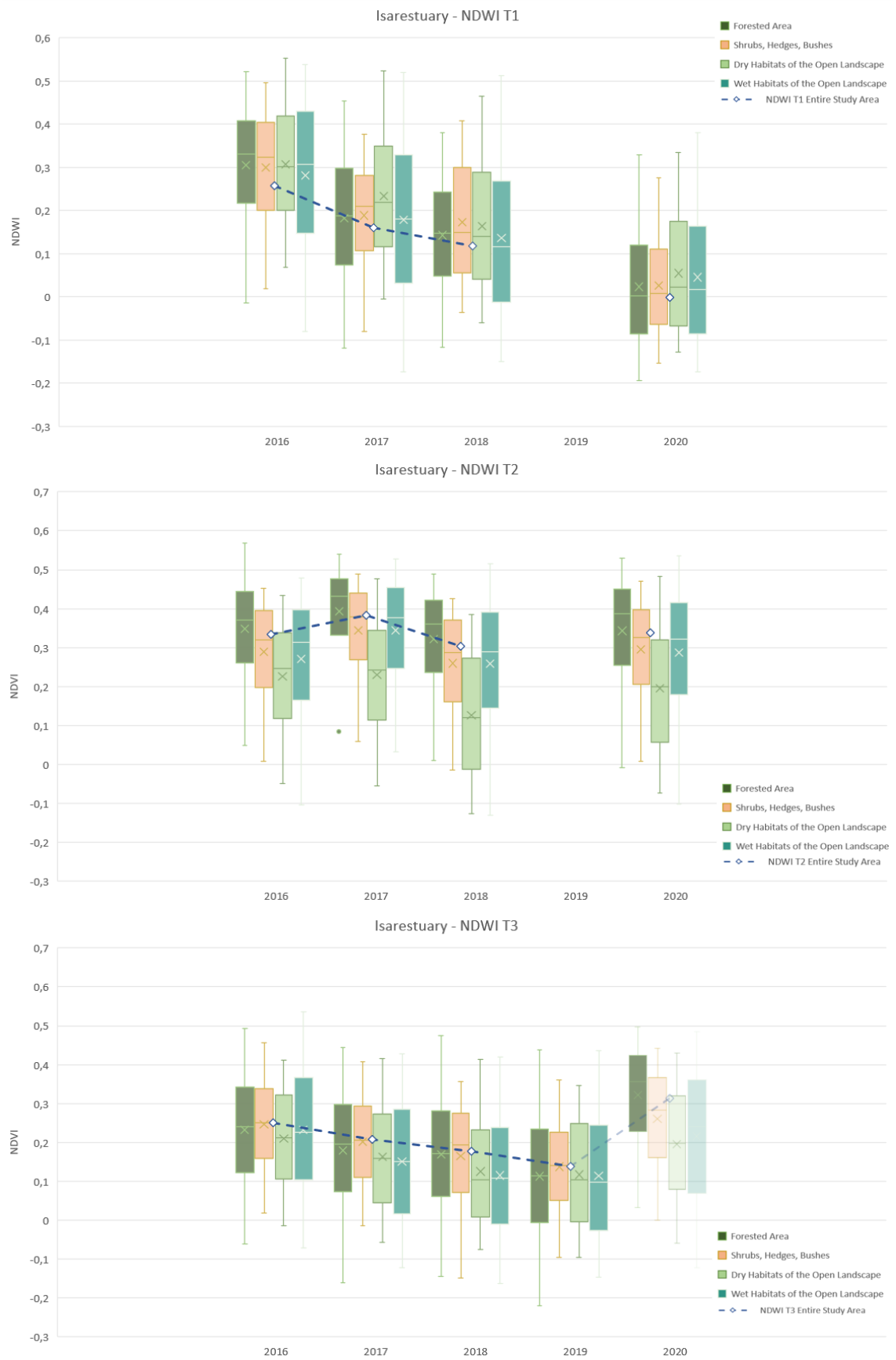

Figure 80. Inter-annual diffences in NDWI values per biotope type and year for study area Isar Estuary.

Box and whisker plots describe the variability of NDWI value distribution within each biotope type and depict the scatter range. Scattering is lowest for Dry Habitats of the Open Landscape, followed by Wet

Habitats of the Open Landscape, Shrubs, Hedges and Bushes and highest for Forested Areas. Dotted blue lines indicate mean NDWI values for the entire study area in relation to each biotope type. In comparison to reference year 2016, all biotope types depict lower values at each investigation point (Spring-T1, Summer-T2 and Autumn-T3) during drought year 2018.

In comparison with the other investigated years, however, mean NDWI values of each biotope type are not invariably lowest in 2018. All biotope types exhibit lowest values in 2020 at Spring-T1, whereas all biotope types display lowest values at Summer-T2 in 2018. At Autumn-T3 Forested Areas (0.11), Shrubs, Hedges and Bushes (0.13) and Wet Habitats of the Open Landscape are lowest in 2019 (0.10), while Dry Habitats of the Open Landscape (0.11) at Autumn-T3 are lowest in 2018.

3.6 Intra-annual NDVI and NDWI Regimes per Study Area

Intra-annual courses of both indices are displayed in the following graphs per study area and for all investigated years in order to obtain a more detailed comparison of the inter-annual difference in index values throughout the investigation period. In addition to this, potential differences between the intra-annual courses of the two indices per investigation point can be revealed and thereby their applicability and robustness compared.

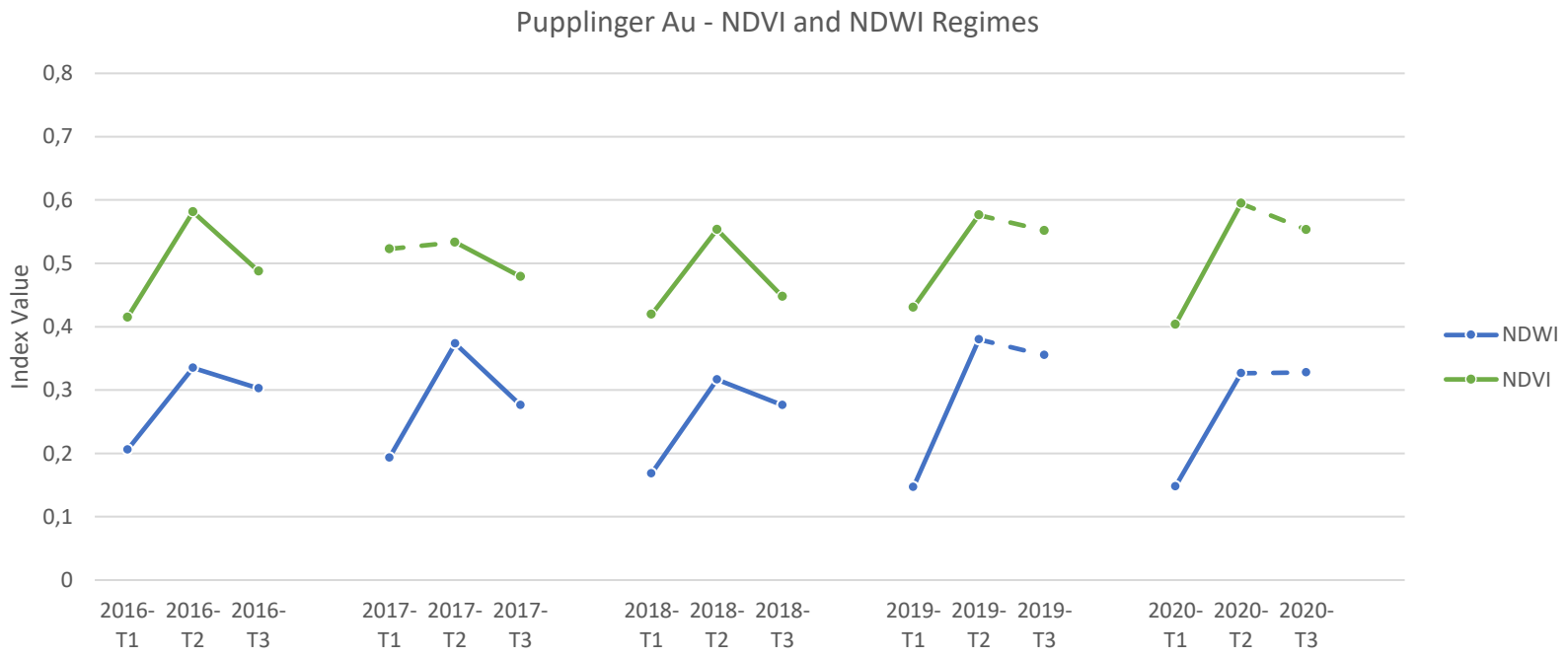

Figure 81. Intra-annual indices regimes of Pupplinger Au. This figure depicts the mean intra-annual development of the NDVI and NDWI for study area Pupplinger Au, based on a study area wide average per investigation point. It becomes clear, that both indices peak at Summer-T2 and decrease from there onwards to Autumn-T3 for all years, even though with different steepness gradients. This uniform course in index values reflects the phenological cycle with build-up and loss in plant biomass and therefore build-up and loss of chlorophyll-a content (measured by the NDVI), as well build-up and loss of intra-cellular water content (measured by the NDWI). The NDVI and NDWI show significant parallel courses in each year. The 2018 regimes of both indices depict lower values than the index regimes of 2016. This can be linked to the contrasting meteorological and hydrological conditions in 2018 with above-normal air temperatures and decreased precipitation rates compared to the reference year 2016. These conditions lead to decreases in plant vitality and water stress, as measurable by the NDVI and NDWI, respectively. In comparison to the other years, index regimes of 2018 remain in the low output range. In comparison to the other study areas, the index values of study area Pupplinger Au depict quite low ranges (low maximum values).

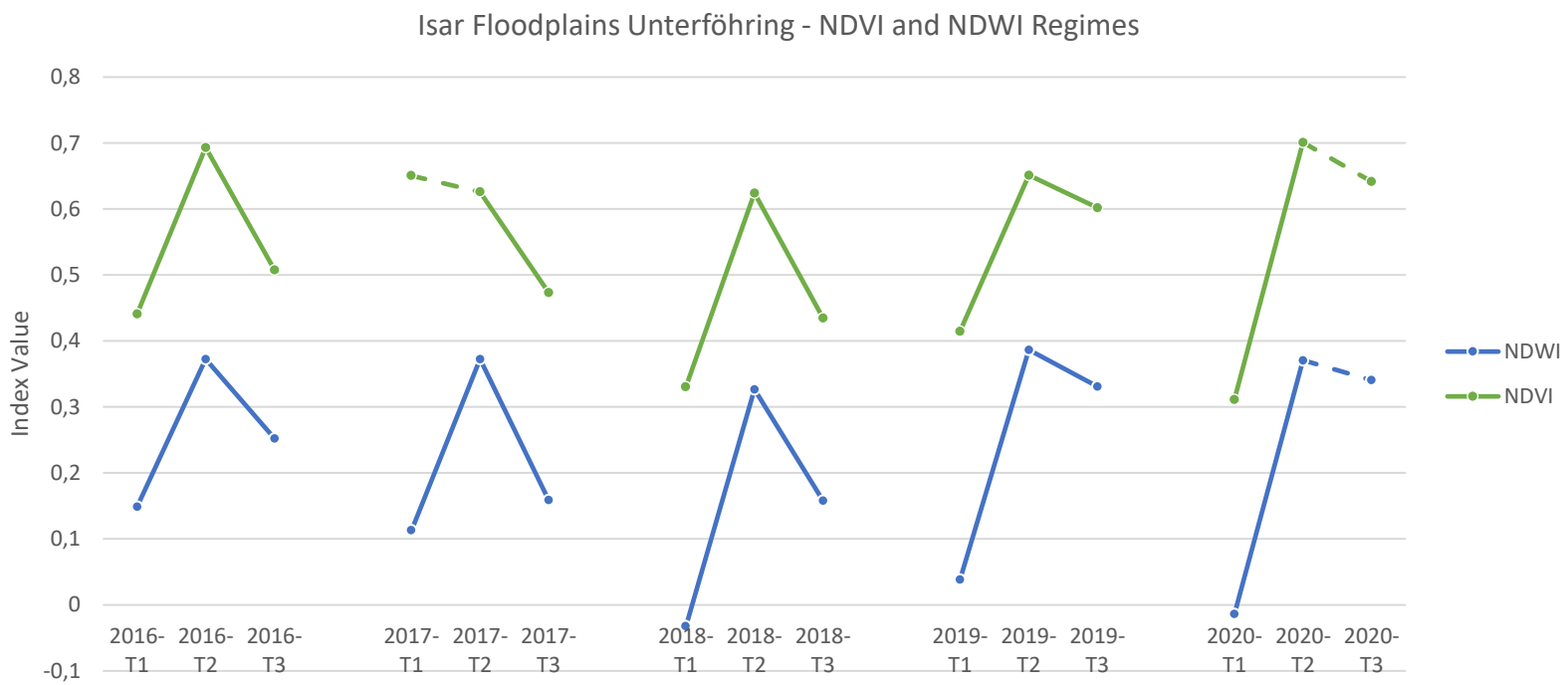

Figure 82. Intra-annual indices regimes of Isar Floodplains Unterföhring. This figure depicts the mean annual development of the NDVI and NDWI for study area Isar Floodplains Unterföhring, based on a study area wide average per investigation point. Similar to study area Pupplinger Au, both indices peak at Summer-T2 and decrease from there onwards to Autumn-T3 for every year, even though with different steepness gradients. Steepness gradients per year are, however, similar for both indices and cause significant parallelisms between NDVI and NDWI regimes in each year. Especially in comparison between the reference year 2016 and the drought year 2018, exhibits the latter significantly lower values for all investigation points (Spring-T1, Summer-T2 and Autumn-T3). In contrast to the other investigated years, both index regimes of 2018 remain in the lower output range. Index values at Spring- in 2020 are similarly low to index values in 2018, suggesting comparable meteorological and hydrological site conditions between those years. This however proved to be not entirely accurate, as mean monthly air temperature and mean precipitation rates in early 2020 deviate from those in early 2018. Flattening in groundwater fluctuations is akin early in both years. However, no direct link between the similar NDVI and NDWI values at Spring-T1 2018 and 2020 can be drawn (see Chapter Study Area – Isar Floodplains Unterföhring).

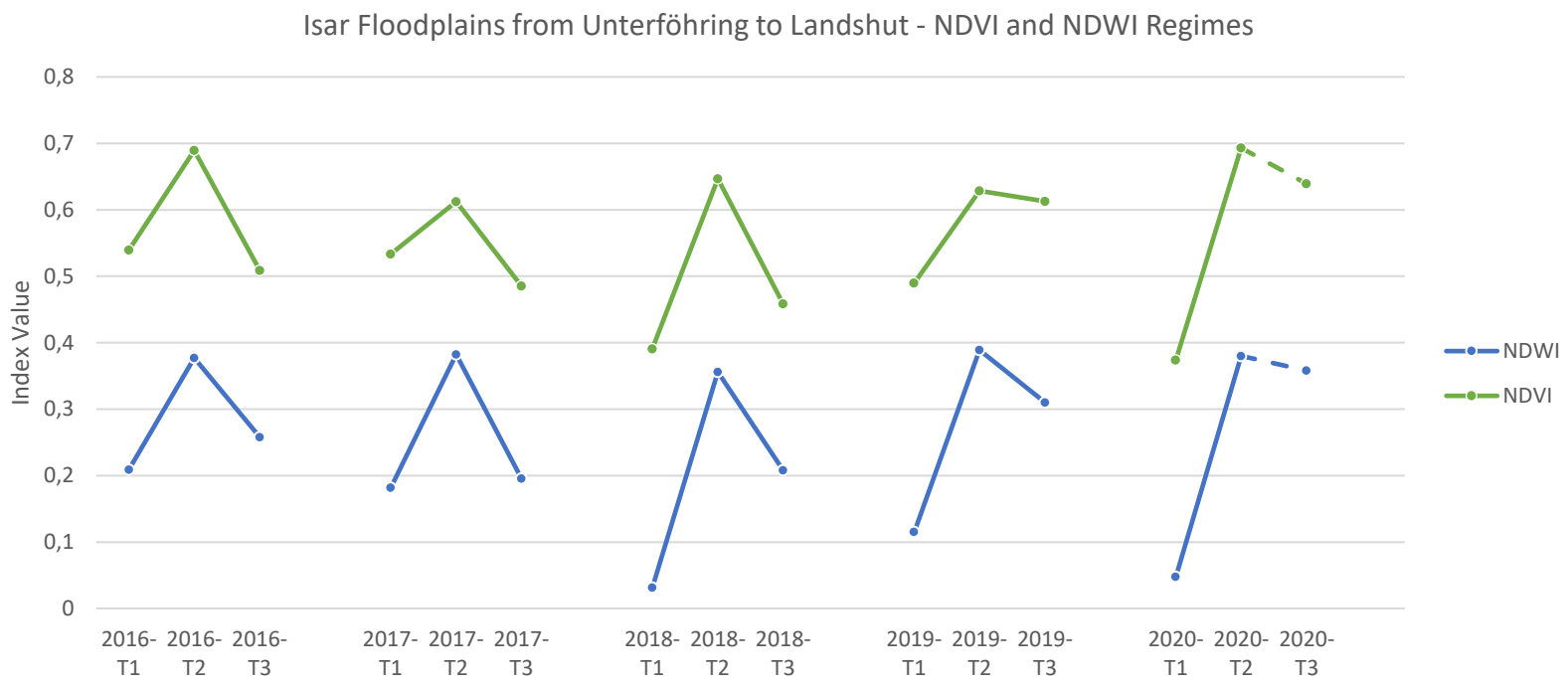

Figure 83. Intra-annual indices regimes of Isar Floodplains from Unterföhring to Landshut. This figure depicts the mean annual development of the NDVI and NDWI for study area Isar Floodplains from Unterföhring to Landshut, based on a study area wide average per investigation point. Similar to the previously described study areas, both indices peak at Summer-T2 and decrease from there onwards to Autumn-T3, even though with different steepness gradients in every year. Steepness gradients per year are, however, similar for both indices and cause significant parallelisms in NDVI and NDWI regimes of each year. Overall, the 2018 regimes of both indices depict in average the lowest values in comparison to the other investigated years. The differences are especially remarkable between the reference year 2016 and the drought year 2018, where the values for each investigation point (Spring-T1, Summer-T2 and Autumn-T3) of both indices were significantly lower for 2018. This can be linked to the contrasting meteorological and hydrological conditions in 2018, with abnormally higher temperatures and lower precipitation rates than in 2016. Overall, the regimes of both indices exhibit a low output range when placed in juxtaposition to the other investigation years.

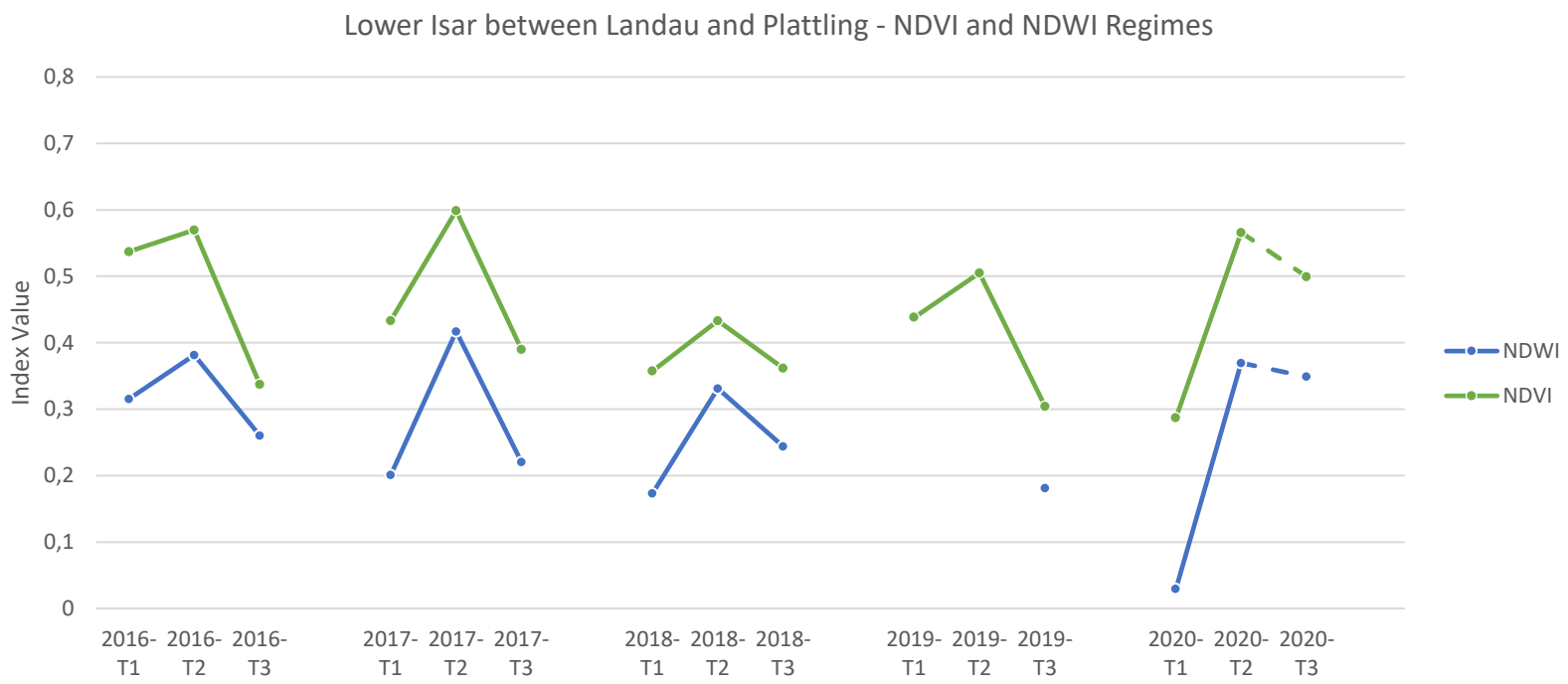

Figure 84. Intra-annual indices regimes of Lower Isar between Landau and Plattling. This figure depicts the mean annual development of the NDVI and NDWI for study area Lower Isar between Landau and Plattling, based on a study area wide average per investigation point. As for the other study areas, both indices peak at Summer-T2 and decrease from there onwards to Autumn-T3, even though with different steepness gradients in every year. Steepness gradients per year are, comparable for both indices, resulting significant parallelisms between NDVI and NDWI regimes in each year. Overall, the 2018 regimes of both indices depict quite low values in comparison to the other investigated years, but the differences for this study area are not as significant as for the other two study areas. Index values of each investigation point (Spring-T1, Summer-T2 and Autumn-T3) and of both indices were significantly lower for drought year 2018 in comparison to the reference year 2016. A slightly decreasing gradient for both indices throughout the entire investigation period (2016-2020) is notable. MGT has, as for the other study areas, been highest in 2018 with abnormally high mean monthly air temperatures in April, May, July, August and September, but the MGP was neither the lowest in 2018 (49 mm), nor exorbitantly lower than the MGP of 2016 (71 mm) for this particular study area. This indicates that both plant vitality and water stress are influenced by factors additionally to the ones investigated in this thesis (see Chapter Discussion).

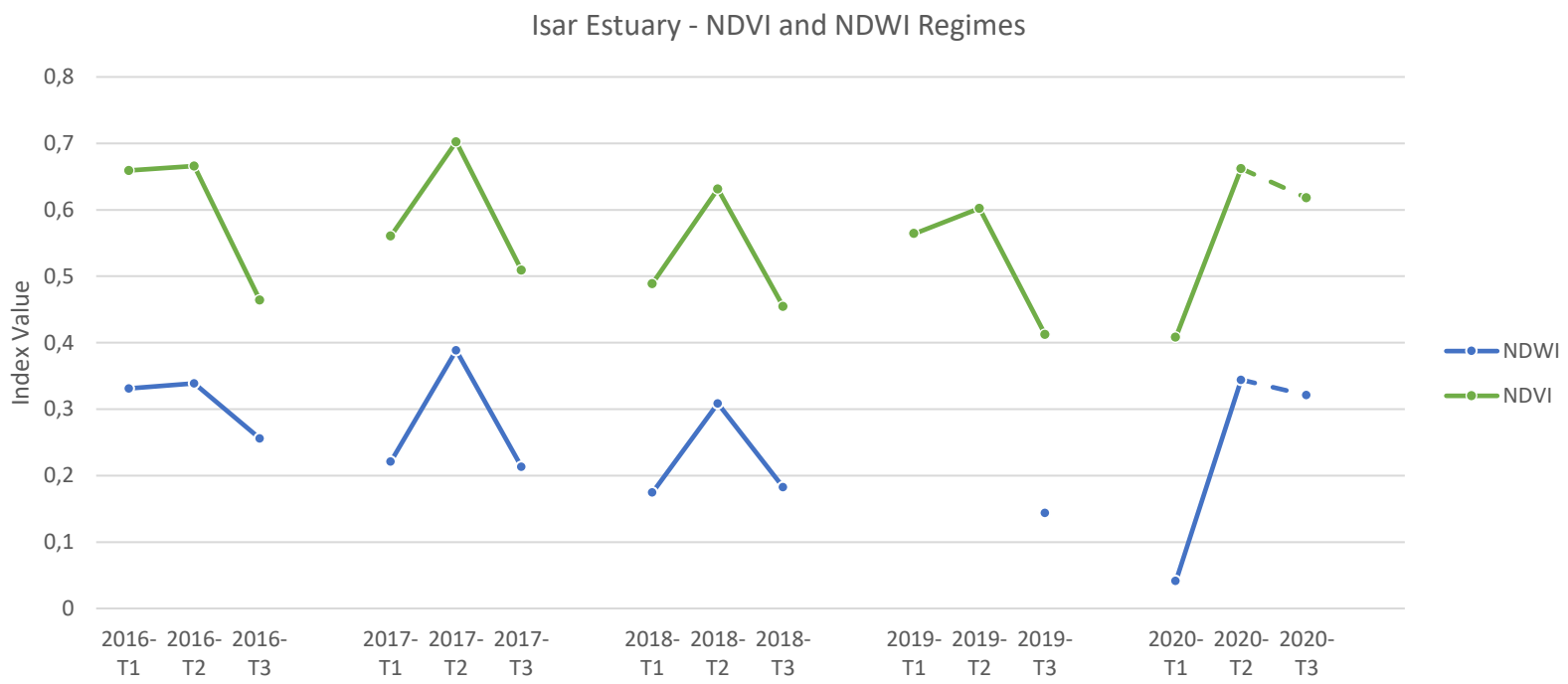

Figure 85. Intra-annual indices regimes of Isar Estuary. This figure depicts the mean annual development of the NDVI and NDWI for study area Isar Estuary, based on a study area wide average per investigation point. Similar to the previously described study areas, both indices peak at Summer-T2 and decrease from there onwards to Autumn-T3, even though with different steepness gradients in every year. Steepness gradients per year are akin for both indices, causing significant parallelisms in NDVI and NDWI regimes in each year. Overall, the 2018 regimes of both indices depict significantly lower values in comparison to reference year 2016, but the differences for this study area are not as significant as for the other study areas. A slight decreasing gradient for both indices throughout the entire investigation period (2016-2020) is notable. MGT has, as for the other study areas, been highest in 2018 with abnormally high mean monthly air temperatures in April, May, July, August and September. MGP was notably lower in 2018 (52 mm) than in 2016 (84 mm). Groundwater-surface distance for this study area is quite low, inducing good water availability even for fibrous root systems. The NDVI and NDWI regimes of this study area can be linked to the meteorological and hydrological site conditions, where plant vitality decreases and water stress increases following the exceptionally warm and dry spring in 2018.

4 Discussion

Spatial and Temporal Resolution of the underlying Data

Investigation points were chosen to be at the beginning (Spring-T1), the climax (Summer-T2) and towards the end (Autumn-T3) of the vegetation period in order to identify intra-annual alterations, as well as to establish comparability of inter-annual changes in index values per investigation point, study area and respective biotope types. Satellite imagery was obtained for each investigation point following the three-step process as described under Methodology. However, as the Sentinel-2 mission allows for a 5-day revisit time at best, and only high-quality imagery with a max. of 10% of cloud coverage was chosen, recording dates of investigation points throughout the years did not always coincide. Inter-annual temporal deferrals of max. 15 days per investigation point in source data resulted in incomparability for some of the acquired results. Therefore, some investigation times were excluded from the inter-annual assessment of index values (Figure 81 – 85).

In addition to this, the selection of solemnly three investigation points per year impeded a more sophisticated assessment of intra-annual index alterations. A higher temporal resolution with shorter intervals between the investigation points would facilitate the analysis of subtler index dynamics throughout the phenological cycle. This in turn would grant deeper knowledge on which momentary site-specific conditions dictate immediate increases and decreases in plant vitality or intensified water stress, as well as on the rapidity of index responses to drought conditions. Besides additional investigation points throughout the vegetative period, a more widely scattered assessment period, meaning to choose investigation points beyond the current vegetative period, will help to explore potential shifts throughout the entire phenological cycle of the respective study area. The chosen times of investigation in this work offer a good snapshot of respective time periods, but do not allow any conclusion on the preceding course. Nevertheless, as a total of at least 13 satisfactory scenes per study area could be obtained for the investigation period (2016-2020), reasonable conclusions could be drawn for both the intra-annual and the inter-annual comparison of index values. Noteworthy is the data basis for reference year 2016 and drought year 2018, to which this thesis pays special attention to. Data was obtained for both years and each investigation point without temporal deferrals, thus allowing for a reliable comparison of plant vitality and water stress between those two years.

Next to the temporal resolution, some uncertainties might have arisen due to the spatial resolution of obtained satellite imagery. Sentinel-2 data is provided with a resolution of minimum 10 m x 10 m, wherefor changes in index values of areas with a smaller extent might suffer from a lack in differentiation. Species level assessment for instance would be hampered using this kind of remote sensing data. As study areas in this thesis exceed this minimum unit by far, as well as biotope types assessed in this study generally exceed this minimum unit of 10 m x 10 m, this source of uncertainty can be ruled out. It is addressed for the sake of completeness. For more in-depth assessments of intra-annual and inter-annual index alterations or for study areas with small extents (e.g. singular biotopes), time series analyses targeting longer investigation periods with additional investigation points and source data with higher spatial resolution are recommended.

For the assessment of plant vitality and water stress experienced by riparian vegetation alongside the Isar River during drought year 2018 in comparison to reference year 2016, both the spatial and temporal resolution of obtained data proved to be sufficient. Results of each index are discussed in the following subchapters.

Chosen Indices – the NDVI and the NDWI

As introduced in chapters Introduction and Materials and Methods, remote sensing-based techniques applying both the NDVI and the NDWI have proven to function as fast, non-invasive and sustainable methods for the assessment of plant vitality and water stress in various contexts, respectively. Next to drought assessments the two indices have shown to work well for land cover change detection, flood detection, surface water monitoring or within agricultural focuses (Gu et al. 2007; El-Gammal, Ali, and Abou Samra 2014; Loránd Szabó et al. 2020; Nasser Mohamed Eid et al. 2020; Dennison et al. 2005; Sims and Thoms 2002; Chen, Huang, and Jackson 2005; Thapa et al. 2016; Buras, Rammig, and S. Zang 2020). Some authors emphasized the insensitivity of the NDWI to different land cover types, especially for water-related ecosystems such as floodplain areas. Here, the results exemplified classification distortions due to overlapping values for dense vegetation, surface waters and saturated soils (S. Szabó, Gácsi, and Balázs 2016b). The authors of this paper suggested another index, the Modified Normalized Difference Water Index (MNDWI) as a better proxy, as it performed best in the distinction of land cover types.

This source of uncertainty can, however, be particularly ruled out for the NDWI assessments per induvial biotope type in this thesis, as the outlines of all individual biotope types were derived from the Bavarian Biotope Mapping. Thereby interferences from surface waters can be excluded. For the NDVI and NDWI assessment per study area, distortions arising from overlapping values could, however, not be assuredly excluded. It is important to consider potential disturbance rates originating from reflectance of other adjacent land cover types. This accounts particularly for study cases within urban areas or with built-up land in the immediate surroundings.

In addition to this, the question arises as to what degree different stages of drought events (the stage in their course) actually affect the absorbance and reflectance rates of the electromagnetic radiation. The NIR (near infrared interval), used in the calculations of both indices for instance, was found to increase at the onset of measurable drought periods, but seems to decrease throughout their progression (Labovitz and Masuoka 1084; Riggs and Running 1991). This deceptive observation, indicating an initial increase in NDVI or NDWI for instance, may lead to falsified conclusions. Effects detached from specific wavelengths, including changes in in-leaf structures or in cellular shapes for example may have caused these alterations in scattering, absorbance and reflectance of electromagnetic radiation (Carter 1991) rather than altered meteorological or hydrological site conditions.

As both the NDVI and the NDWI have been applied in various contexts and have meanwhile proven to function as robust surrogates for plant vitality and water stress respectively, the above-described discussion points are listed by reason of completeness, but will not be further addressed.

For both indices applies, that uncertainties regarding their sensitivity towards cloud shadows or edge regions of cloud coverage exist. Although atmospheric correction and cloud masking was incorporated in this study, not all distortions resulting from this source of errors could be assuredly eliminated. Some satellite imagery used in the vitality assessment depicted minor cloud coverage, as cloud coverage is denoted per scene and may have occurred specifically within the study area scope. Values obtained for such regions do not accurately reflect the actual plant vitality or water stress and need to be more thoroughly removed from the analysis in further research. Even stricter selection criteria (cloud coverage = 0% for instance) or pre-enacted automatic classification tools could be a potential solution for large-scale analyses.

NDVI and NDWI Results

This thesis was designed to test different hypotheses, where (i) drought-induced changes in air temperature can be negatively linked to the vitality of riparian vegetation, (ii) drought-induced alterations in precipitation patterns can be negatively linked to the vitality of riparian vegetation, (iii) changes in ground-water levels can be negatively linked to the vitality of riparian vegetation and that (iv) those impacts resulted in drought-legacy effects in the following year(s).

The initial hypothesis that plant vitality is (i) negatively linked to drought-induced increases in air temperature and that those connections can be identified using remotely sensed data and two different vegetation indices was supported. Strong linkages between the positive anomalies in air temperature during the drought event 2018 and decreases in plant vitality are reflected by substantial decreases in NDVI regimes of 2018, when compared to NDVI regimes of reference year 2016. This applies for all study areas and all biotope types. Highest differences in NDVI regimes between 2016 and 2018 were measured for both scales (study area wide and per biotope type) at investigation point Spring-T1. The NDVI courses of those two years mostly converged towards Summer-T2 and/or Autumn-T3, but NDVI regimes of 2018 remained in almost all cases below the 2016 NDVI regimes. Strong linkages between the positive anomalies in air temperature during the drought event 2018 and intensified water stress for plants were identified by substantial decreases in NDWI regimes between 2018 in comparison to 2016. Highest differences in NDWIs between reference year 2016 and drought year 2018 were measured for both scales (study area wide and per biotope type) at investigation point Spring-T1. Similar to the NDVI regimes, differences in NDWI dwindled throughout the vegetative period, but 2018 regimes remained consistently below NDWI regimes of 2016. This applies for all study areas and all biotope types.

The initial hypothesis that (ii) drought-induced alterations in precipitation patterns can be negatively linked to the vitality of riparian vegetation was supported to a certain extent. Correlations between the negative anomalies in precipitation rates and the decrease in index values were found for all study areas and all biotope types, but were less distinct than the connection of plant vitality to air temperature. In example, although study area Pupplinger Au experienced substantial decreases in MGP between 2016 (149 mm) and 2018 (77 mm), MGP differences between 2018 (68 mm) and 2016 (73 mm) remained negligible for study area Isar Floodplains from Unterföhring to Landshut. However, significantly higher decreases in NDVI values between 2018 (Spring-T1 0.39, Summer-T2 0.65, Autumn-T3 0.46) and 2016 (Spring-T1 0.54, Summer-T2 0.69, Autumn-T3 0.51) were obtained for Isar Floodplains from Unterföhring to Landshut, compared to differences in NDVI values for Pupplinger Au. Here, the NDVI regime of 2018 (Spring-T1 0.42, Summer-T2 0.55, Autumn-T3 0.45) showed far lesser differences compared to the NDVI regime of 2016 (Spring-T1 0.41, Summer-T2 0.58, Autumn-T3 0.49). This leads to the conclusion, that negative anomalies in precipitation patterns affect plant vitality, as measured by the NDVI, only to a certain extent – at least when considered on a short-term temporal scale. The same conclusion accounts for the linkage between negative anomalies in precipitation patterns and water stress, as measured by the NDWI. The 2016 (Spring-T1 (0.21), Summer-T2 (0.33), Autumn-T3 (0.30)) and 2018 NDWI (Spring-T1 (0.17), Summer-T2 (0.32), Autumn-T3 (0.28)) regimes of study area Pupplinger Au depict slight reductions between those two years, whereas NDWI difference between 2016 (Spring-T1 (0.21), Summer-T2 (0.38), Autumn-T3 (0.26)) and 2018 (Spring-T1 (0.03), Summer-T2 (0.36), Autumn-T3 (0.21)) are substantial for Isar Floodplains from Unterföhring to Landshut, although this study areas experienced a lesser decrease in MGP. These results show that immediate responses in plant vitality, as measured by chlorophyll-a and intra-cellular water content

are somewhat detached from altered precipitation rates – at least on the temporal scale of this research. The results obtained in this study are in alignment with other studies, where higher temperatures during drought events have been observed to impact plant physiology in amplified ways, as well as increase the VPD and thus lower the NPP, when compared to cooler droughts events with similarly low precipitation rates (Adams et al. 2009; Park Williams et al. 2013; Yuan et al. 2019; Eamus et al. 2013). However, groundwater refilling and thus water availability is conditional upon precipitation rates throughout the previous year, respectively. Generally, reduced precipitation rates can be therefore connected to shortages in groundwater/ soil moisture availability, during the following vegetative period.

The hypothesis that (iii) changes in ground-water levels can be negatively linked to the vitality of riparian vegetation was not supported by the results of this work. Groundwater fluctuations throughout the investigation period (2016-2020) remained mostly mediocre. Spring peaks of groundwater recharge were oftentimes missing in 2018, but mean GW levels of 2018 showed unobtrusive ranges. Noteworthy are the differences of groundwater-surface distance, which partly differed significantly between the study areas. Groundwater-surface distance was lowest for study area Isar Estuary, followed by Pupplinger Au, Isar Floodplains from Unterföhring to Landshut, Isar Floodplains Unterföhring and Lower Isar between Landau and Plattling in increasing order. Those differences, however, may be led back to the location of the monitoring wells. No clear contextualization between the index results and the GW levels, and thus plant vitality and the GW levels, could be established. Soil moisture measurement is recommended for future analysis, by reason of depicting water availability for plants more adequately than groundwater levels. Several authors emphasized the importance of considering soil moisture depletion during or following drought events in the assessment of plant vitality (Hanel et al. 2018b; Van Lanen et al. 2016; Breshears et al. 2005). Some reports concluded that positive anomalies in air temperature early during drought episodes, but with sufficient soil moisture availability, led to increased rates in gross primary production, outweighing the negative impacts occurring over the course of tenacious drought events (Kowalska et al. 2020). Increases in gross primary production during early months can, however, subsequently lead to greater soil moisture depletion and thus contribute to or even amplify successive drought impacts. The immediacy to the quite regulated Isar River is identified as potential compensating factor in water availability. Through constant water flow even during the drought event 2018, the floodplain areas may have been able to rely on consistent water availability, therefore experiencing reduced hydrological drought impacts.

Although not all hypotheses (i – iii) could be supported so far, the discussed findings nevertheless resolutely indicate diminished plant vitality of, as well as intensified water stress experienced by, riparian vegetation following the abnormally dry and warm spring 2018. Whether (iv) the 2018 drought induced legacy effects in the vitality of riparian vegetation for the following years (2019 and 2020) could not entirely be clarified. Inter-annual alterations in meteorological and hydrological site conditions are generally adequately reflected by the results of both indices. 2016 was used as reference year for all study areas, as temperature regime and precipitation rates were most representative for the long-term average out of all investigated years. These conditions are mirrored by balanced NDVI and NDWI values. The 2016 regimes of both indices adequately reflect the phenological cycle with usual build-up in plant biomass, or rather chlorophyll-a and intra-cellular water content (Figures 81 – 85). Noteworthy for investigating the last hypothesis are the significant changes in index values especially for Spring-T1 of the later years (2018 – 2020). All of those three years depict

heavy decreases in index values at this investigation point in comparison to the index values obtained for 2016. This applies to all five study areas. However, both NDVI and NDWI usually recovered at Summer-T2 for the three later years (2018 – 2020), indicating no substantial legacy effects of the drought event in 2018. The temporal scale of drought-induced impacts on plant vitality needs to be considered more thoroughly in future work, incorporating continuous monitoring of upcoming years at best.

The NDVI change detection maps between the reference year 2016 and the other investigated years oftentimes depict a thoroughly fragmented spatial distribution in vitality differences. These results emphasize the importance of assessing individual biotope types and their particular responses to changes in meteorological and hydrological site conditions, in addition to the assessment of entire, heterogenous study areas. Differences between the responses in plant vitality of individual biotope types following the drought 2018 were observed for all study areas. Each biotope type exhibited specific intra-annual and inter-annual signatures in index values. In summary, the Dry Habitats of the Open Landscape and Shrubs, Hedges and Bushes were observed to have suffered to a greater degree from the drought conditions in 2016, than Forested Areas and Wet Habitats of the Open Landscape. This applies to all study areas. The results obtained in this thesis further emphasize the necessary differentiation between biotope types, as index values might be relatively low compared to the overall range of values (-1 to 1), but be already situated at the upper end of the respective biotope type-specific index range. Consequently, conclusions on plant vitality and water stress can only be drawn, when referring to the same biotope type and within the "normal range" of index value of such. Establishing such normal ranges for each biotope type prior to drought-induced plant vitality assessments will facilitate the evaluation of results.

Lastly, the NDVI and NDWI regimes of each study area exhibited strong parallelism throughout each investigated year (Figures 81 – 85). This implies that the photosynthetic activity of (riparian) vegetation is strongly dependent on site-specific water availability and limited by water stress. Similar results were found by other authors for woody vegetation (Aguilar et al. 2012). Differences in geographical location in this thesis were shown to have influenced the responses in plant vitality, as measured by the vegetation indices, only to a minor degree. Study area Pupplinger Au alongside the upper reaches of the Isar River is located at approx. 576 m above sea level for instance, while the study areas alongside the middle reaches of the Isar River are located at about 392 m – 500 m above sea level and the study areas of the lower reaches at 309 m – 337 m. The index regimes between the different river sections, however, exhibit only minor differences in value ranges. Low maximum values for both indices were obtained for Pupplinger Au (upper reaches) and Isar Floodplains between Landau and Plattling (lower reaches), for instance, while the other three study areas (middle and lower reaches) exhibited similarly high maximum index values. Nevertheless, all study areas display significantly reduced values of both indices during 2018 at all investigation points (Spring-T1, Summer-T2 and Autumn-T3) in comparison to index values recorded during the reference year 2016. Next to biotope type specific or even species-specific index ranges, it is thus recommended to characterize geographic and site-specific circumstances prior to vitality assessment. This will help to gain a deeper understanding of potential factors influencing plant vitality.

5 Conclusion

Floodplain areas and the invaluable services they offer to humankind have suffered not only from direct anthropogenic impacts, such as hydraulic modifications, but continue to be degraded and affected through indirect impacts. In the likelihood of increasingly frequent and intense extreme climate extremes, particularly droughts, the analysis of the concomitant impacts on plant vitality is essential for designing site-specific adaptation and mitigation measures. The drought event occurring in 2018 has clearly set a new tone for drought-induced alterations in temperature regimes and precipitation patterns. Concomitants, such as fluctuations in groundwater levels, soil moisture depletion or increases in water vapour deficits additionally aggravate the impacts on plant vitality. This thesis demonstrated that the drought of 2018, occurring over Central Europe, caused significant decreases in plant vitality of riparian vegetation alongside the Isar River. All biotope types assessed were significantly affected, although some differences in the extent were observed. Forested areas and Wet Habitats of the Open Landscape appeared to cope slightly better with drought-induced impacts than Shrubs, Hedges and Bushes and Dry Habitats of the Open Landscape. However, plant vitality of all biotope types was substantially degraded through the positive anomalies in MGT and negative anomalies in MGP during the drought event 2018. It is recommended so specifically address spatial and temporal scales in plant vitality assessment, as well as characterize regional and site-specific meteorological and hydrological conditions. This will help to reliably link changes in plant vitality to alterations in temperature regimes or precipitation patterns through the obtained results. In addition, soil moisture contents should be incorporated into the analysis, as legacy effects of drought episodes can be identified thereof. Biotope type – specific or species – specific index ranges can help to better contextualize the results.

Although some limitations in the application of remote sensing data and vegetation indices for the assessment of plant vitality in floodplain areas were identified, this methodology allows for fast and non-invasive investigations even on larger scales. Future remote sensing missions providing high resolution data to the open public will facilitate the timely observation of plant vitality and may be incorporated in early warning systems. Further research is needed to verify the results of this analysis for floodplain areas of other biogeographic regions, as well as to particularize the impacts of site-specific meteorological and hydrological conditions on the vitality of riparian vegetation.

References

ACADEMIC. n.d. “Pupplinger Au.” https://de-academic.com/dic.nsf/dewiki/1141588.

Adams, Henry D., M. Guardiola-Claramonte, G. A. Barron-Gafford, J. C. Villegas, D. D. Breshears, C. B. Zou, P. A. Troch, and T. E. Huxman. 2009. “Temperature Sensitivity of Drought-Induced Tree Mortality Portends Increased Regional Die-off under Global-Change-Type Drought.” *Proceedings of the National Academy of Sciences of the United States of America* 106 (17): 7063–66. https://doi.org/10.1073/pnas.0901438106.

Adams, Henry D., M. J.B. Zeppel, W. R.L. Anderegg, H. Hartmann, S. M. Landhäusser, D. T. Tissue, and T. E. Huxman. 2017. “A Multi-Species Synthesis of Physiological Mechanisms in Drought-Induced Tree Mortality.” *Nature Ecology and Evolution* 1 (9): 1285–91. https://doi.org/10.1038/s41559-017-0248-x.

Aguilar, Cristina; J. C. Zinnert, M.J. Polo, and D.R. Young. 2012. “NDVI as an indicator for changes in water availability to woody vegetation. ” *Ecological Indicators* 23: 290–300. DOI:10.1016/j.ecolind.2012.04.008.

Allen, Craig D., and D. D. Breshears. 2007. “Climate-Induced Forest Dieback as an Emergent Global Phenomenon.” *Eos* 88 (47): 504. https://doi.org/10.1029/2007EO470008.

Anyamba, Assaf, and C. J. Tucker. 2012. “Historical Perspectives on AVHRR NDVI and Vegetation Drought Monitoring.” *Remote Sensing of Drought: Innovative Monitoring Approaches*, 23–49. https://doi.org/10.1201/b11863.

Backlund, P., A. Janetos, D. Schimel, J. Hatfield, M. Ryan, S. Archer, and D. Lettenmaier. 2013. “The Effects of Climate Change on Agriculture, Land Resources, Water Resources, and Biodiversity.” *Intellectual History Review* 23 (1): 1–2. https://doi.org/10.1080/17496977.2012.737984.

Ballinger, Andrea, and P. S. Lake. 2006. “Energy and Nutrient Fluxes from Rivers and Streams into Terrestrial Food Webs.” *Marine and Freshwater Research* 57 (1): 15–28. https://doi.org/10.1071/MF05154.

Baptista, Marcelle Nardelli, R. Valcarcel, V. Maya, and F. Canto. 2014. “Selection of Preferred Floodplains for the Renaturalization of Hydrologic Functions: A Case Study of the Paraíba Do Sul River Basin, Brazil.” *Water Resources Management* 28 (13): 4781–93. https://doi.org/10.1007/s11269-014-0775-z.

Barriopedro, David, E. M. Fischer, J. Luterbacher, R. M. Trigo, and R. García-Herrera. 2011. “The Hot Summer of 2010: Redrawing the Temperature Record Map of Europe.” *Science* 332 (6026): 220–24. https://doi.org/10.1126/science.1201224.

Barros, Ceres, W. Thuiller, and T. Münkemüller. 2018. “Drought Effects on the Stability of Forest-Grassland Ecotones under Gradual Climate Change.” *PLoS ONE* 13 (10): 1–18. https://doi.org/10.1371/journal.pone.0206138.

Bastos, A., P. Ciais, P. Friedlingstein, S. Sitch, J. Pongratz, L. Fan, and J. P. Wigneron. 2020. “Direct and Seasonal Legacy Effects of the 2018 Heat Wave and Drought on European Ecosystem Productivity.” *Science Advances* 6 (24): 1–14. https://doi.org/10.1126/sciadv.aba2724.

Bastos, A., Z. Fu, P. Ciais, P. Friedlingstein, S. Sitch, J. Pongratz, and U. Weber. 2020. “Impacts of Extreme Summers on European Ecosystems: A Comparative Analysis of 2003, 2010 and 2018: European Extreme Summers and the C-Cycle.” *Philosophical Transactions of the Royal Society B: Biological Sciences* 375 (1810). https://doi.org/10.1098/rstb.2019.0507.

BayLfU. 2020a. “Auswirkungen auf den mittleren Abfluss und das Abflussregime.” 2020.

https://www.lfu.bayern.de/wasser/klimawandel_wasserhaushalt/auswirkung_auf_wasserhaushalt/abflussregime/index.htm

———. 2020b. “Lufttemperatur Bayern.” 2020. https://www.gkd.bayern.de/de/meteo/lufttemperatur.

———. 2020c. “Mittelwerte des Gebietsniederschlags.” 2020. https://www.lfu.bayern.de/wasser/klima_wandel/bayern/niederschlag/index.htm#:~:text=Zudem zeigt sich sehr ausgeprägt,Spessart%2C Rhön und Odenwald liegen.

———. 2020d. “Niederschlag Bayern.” 2020. https://www.gkd.bayern.de/de/meteo/niederschlag.

———. 2020e. “Oberes Grundwasserstockwerk Isar.” 2020. https://www.gkd.bayern.de/de/grundwasser/oberesstockwerk/isar.

———. 2021. “Biotopkartierung Bayern.” 2021. https://www.lfu.bayern.de/umweltdaten/geodatendienste/pretty_downloaddienst.htm?dld=biotopkartierung.

Beillouin, Damien, B. Schauberger, A. Bastos, P. Ciais, and David Makowski. 2020. “Impact of Extreme Weather Conditions on European Crop Production in 2018: Random Forest - Yield Anomalies.” *Philosophical Transactions of the Royal Society B: Biological Sciences* 375 (1810). https://doi.org/10.1098/rstb.2019.0510.

BfN. 2015a. “Den Flüssen mehr Raum geben. Renaturierung von Auen in Deutschland.” Berlin. https://www.bmuv.de/publikation/den-fluessen-mehr-raum-geben-renaturierung-von-auen-in-deutschland

———. 2015b. “Gewässer Und Auen - Nutzen Für Die Gesellschaft.” Berlin. https://www.bfn.de/oekosystemleistungen.

———. 2021. “Auenzustandsbericht 2021, Flussauen in Deutschland,” 72.

Bino, Gilad, S. Wassens, R. T. Kingsford, R. F. Thomas, and J. Spencer. 2018. “Floodplain Ecosystem Dynamics under Extreme Dry and Wet Phases in Semi-Arid Australia.” *Freshwater Biology* 63 (2): 224–41. https://doi.org/10.1111/fwb.13056.

BMU. 2021. “Auenzustandsbericht.” https://doi.org/10.19217/brs211.

Böck, Kerstin, R. Polt, and L. Schülting. 2018. “Ecosystem Services in River Landscapes.” In *Riverine Ecosystem Management*, 413–33. Cham: Springer International Publishing. https://doi.org/10.1007/978-3-319-73250-3_21.

Boelman, Natalie T., M. Stieglitz, H. M. Rueth, M. Sommerkorn, K. L. Griffin, G. R. Shaver, and J. A. Gamon. 2003. “Response of NDVI, Biomass, and Ecosystem Gas Exchange to Long-Term Warming and Fertilization in Wet Sedge Tundra.” *Oecologia* 135 (3): 414–21. https://doi.org/10.1007/s00442-003-1198-3.

BR. 2021. “Extremwetter durch Klimawandel. Mehr Hitzewellen, Dürren, Starkregen und Orkane.” 2021. https://www.br.de/wissen/wetter-extremwetter-klimawandel-100.html.

Brander, Luke, R. Brouwer, and A. Wagtendonk. 2013. “Economic Valuation of Regulating Services Provided by Wetlands in Agricultural Landscapes: A Meta-Analysis.” *Ecological Engineering* 56 (July): 89–96. https://doi.org/10.1016/j.ecoleng.2012.12.104.

Breshears, David D., N. S. Cobb, P. M. Rich, K. P. Price, C. D. Allen, R. G. Balice, and W. H. Romme. 2005. “Regional Vegetation Die-off in Response to Global-Change-Type Drought.” *Proceedings of the National Academy of Sciences of the United States of America* 102 (42): 15144–48. https://doi.org/10.1073/pnas.0505734102.

Buras, Allan, A. Rammig, and C. S. Zang. 2020. “Quantifying Impacts of the 2018 Drought on European Ecosystems in Comparison to 2003.” *Biogeosciences* 17 (6): 1655–72. https://doi.org/10.5194/bg-17-1655-2020.

Capon, Samantha J., L. E. Chambers, R. Mac Nally, R. J. Naiman, P. Davies, N. Marshall, and J. Pittock. 2013. “Riparian Ecosystems in the 21st Century: Hotspots for Climate Change Adaptation?” *Ecosystems* 16 (3): 359–81. https://doi.org/10.1007/s10021-013-9656-1.

Carter, Gregory. 1991. “Primary and Secondary Effects of Water Content on the Spectral Reflectance of Leaves.” *American Journal of Botany* 78 (7): 916–24. https://www.jstor.org/stable/2445170?seq=1#metadata_info_tab_contents.

Ceccato, Pietro, S. Flasse, S. Tarantola, S. Jacquemoud, and J. M. Grégoire. 2001. “Detecting Vegetation Leaf Water Content Using Reflectance in the Optical Domain.” *Remote Sensing of Environment* 77 (1): 22–33. https://doi.org/10.1016/S0034-4257(01)00191-2.

Chen, Daoyi, J. Huang, and T. J. Jackson. 2005. “Vegetation Water Content Estimation for Corn and Soybeans Using Spectral Indices Derived from MODIS Near- and Short-Wave Infrared Bands.” *Remote Sensing of Environment* 98 (2–3): 225–36. https://doi.org/10.1016/j.rse.2005.07.008.

Cherwin, Karie, and A. Knapp. 2012. “Unexpected Patterns of Sensitivity to Drought in Three Semi-Arid Grasslands.” *Oecologia* 169 (3): 845–52. https://doi.org/10.1007/s00442-011-2235-2.

Choat, Brendan, S. Jansen, T. J. Brodribb, H. Cochard, S. Delzon, R. Bhaskar, and S. J. Bucci. 2012. “Global Convergence in the Vulnerability of Forests to Drought.” *Nature* 491 (7426): 752–55. https://doi.org/10.1038/nature11688.

Ciais, Ph, M. Reichstein, N. Viovy, A. Granier, J. Ogée, V. Allard, and M. Aubinet. 2005. “Europe-Wide Reduction in Primary Productivity Caused by the Heat and Drought in 2003.” *Nature* 437 (7058): 529–33. https://doi.org/10.1038/nature03972.

ClimateData. 2021. “Klimaklassifikationen Bayern.” 2021. https://de.climate-data.org/europa/deutschland/bayern-396/.

Coumou, Dim, and S. Rahmstorf. 2012. “A Decade of Weather Extremes.” *Nature Climate Change* 2 (7): 491–96. https://doi.org/10.1038/nclimate1452.

Della-Marta, P. M., M. R. Haylock, J. Luterbacher, and H. Wanner. 2007. “Doubled Length of Western European Summer Heat Waves since 1880.” *Journal of Geophysical Research* 112 (D15): D15103. https://doi.org/10.1029/2007JD008510.

Dennison, P. E., D. A. Roberts, S. H. Peterson, and J. Rechel. 2005. “Use of Normalized Difference Water Index for Monitoring Live Fuel Moisture.” *International Journal of Remote Sensing* 26 (5): 1035–42. https://doi.org/10.1080/0143116042000273998.

DWD. 2008. “Extremwetterereignis.” 2008. https://www.dwd.de/DE/service/lexikon/Functions/glossar.html?lv2=100652&lv3=100780.

———. 2020. “Zeitreihen und Trends.” 2020. https://www.dwd.de/DE/leistungen/zeitreihen/zeitreihen.html?nn=495662#buehneTop.

———. 2021a. “Deutscher Klimaatlas.” 2021. https://www.dwd.de/DE/klimaumwelt/klimaatlas/klimaatlas_node.html.

———. 2021b. “Vegetationsperiode.” 2021. https://www.dwd.de/DE/service/lexikon/Functions/glossar.html?lv2=102868&lv3=102890.

Eamus, Derek, N. Boulain, J. Cleverly, and D. D. Breshears. 2013. “Global Change-Type Drought-Induced Tree Mortality: Vapor Pressure Deficit Is More Important than Temperature per Se in

Causing Decline in Tree Health." *Ecology and Evolution* 3 (8): 2711–29. https://doi.org/10.1002/ece3.664.

easac. 2018. "Extreme Weather Events in Europe." Halle (Saale). https://easac.eu/fileadmin/PDF_s/reports_statements/Extreme_Weather/EASAC_Statement_Extreme_Weather_Events_March_2018_FINAL.pdf

EEA. 2018. "Why Should We Care about Floodplains?" https://doi.org/10.2800/625828.

———. 2021. "Europe's Changing Climate Hazards — an Index-Based Interactive EEA Report." https://doi.org/10.2800/458052.

El-Gammal, M. I., R. R. Ali, and R. M. Abou Samra. 2014. "NDVI Threshold Classification for Detecting Vegetation Cover in Damietta Governorate, Egypt." *Journal of American Science* 10 (8): 108–13.

El-Madany, Tarek S., A. Carrara, M. Pilar Martín, G. Moreno, O. Kolle, J. Pacheco-Labrador, U. Weber, T. Wutzler, M. Reichstein, and M. Migliavacca. 2020. "Drought and Heatwave Impacts on Semi-Arid Ecosystems' Carbon Fluxes along a Precipitation Gradient." *Philosophical Transactions of the Royal Society B: Biological Sciences* 375 (1810): 20190519. https://doi.org/10.1098/rstb.2019.0519.

Emadodin, Iraj, D. E. Flores Corral, T. Reinsch, C. Kluß, and F. Taube. 2021a. "Climate Change Effects on Temperate Grassland and Its Implication for Forage Production: A Case Study from Northern Germany." *Agriculture (Switzerland)* 11 (3). https://doi.org/10.3390/agriculture11030232.

ESA. 2021. "Sentinel-2." 2021. https://sentinel.esa.int/web/sentinel/missions/sentinel-2.

Feld, Christian K., S. Birk, D. C. Bradley, D. Hering, J. Kail, A. Marzin, and A. Melcher. 2011. *From Natural to Degraded Rivers and Back Again. A Test of Restoration Ecology Theory and Practice*. *Advances in Ecological Research*. 1st ed. Vol. 44. Elsevier Ltd. https://doi.org/10.1016/B978-0-12-374794-5.00003-1.

Fu, Zheng, P. Ciais, A. Bastos, P. C. Stoy, H. Yang, J. K. Green, and B. Wang. 2020. "Sensitivity of Gross Primary Productivity to Climatic Drivers during the Summer Drought of 2018 in Europe." *Philosophical Transactions of the Royal Society B: Biological Sciences* 375 (1810): 20190747. https://doi.org/10.1098/rstb.2019.0747.

Gangashe, Andani Theophenia. 2018. "Assessing the Impacts of Flooding on Vegetation Cover in the Shashe-Limpopo Confluence Area Using Earth Observation Data." http://wiredspace.wits.ac.za/bitstream/handle/10539/25636/Research Final Andani .pdf?sequence=1&isAllowed=y.

Gao, Bo Cai. 1996. "NDWI - A Normalized Difference Water Index for Remote Sensing of Vegetation Liquid Water from Space." *Remote Sensing of Environment* 58 (3): 257–66. https://doi.org/10.1016/S0034-4257(96)00067-3.

Garcia-Herrera, R., J. Díaz, R. M. Trigo, J. Luterbacher, and E. M. Fischer. 2010. "A Review of the European Summer Heat Wave of 2003." *Critical Reviews in Environmental Science and Technology* 40 (4): 267–306. https://doi.org/10.1080/10643380802238137.

Gharun, Mana, L. Hörtnagl, E. Paul-Limoges, S. Ghiasi, I. Feigenwinter, S. Burri, and K. Marquardt. 2020. "Physiological Response of Swiss Ecosystems to 2018 Drought across Plant Types and Elevation." *Philosophical Transactions of the Royal Society B: Biological Sciences* 375 (1810): 20190521. https://doi.org/10.1098/rstb.2019.0521.

GISNOTE. 2019. "Lab11 - MicaSense RedEdge-M." 2019. https://www.gisnote.com/2019/04/15/l11-rededge/.

Griffith, Jerry A. 2002. “Geographic Techniques and Recent Applications of Remote Sensing to Landscape-Water Quality Studies.” *Water Air and Soil Pollution* 138: 181–197. https://www.proquest.com/docview/750369068?pq-origsite=gscholar&fromopenview=true.

Gu, Yingxin, J. F. Brown, J. P. Verdin, and B. Wardlow. 2007. “A Five-Year Analysis of MODIS NDVI and NDWI for Grassland Drought Assessment over the Central Great Plains of the United States.” *Geophysical Research Letters* 34 (6). https://doi.org/10.1029/2006GL029127.

Hanel, Martin, O. Rakovec, Y. Markonis, P. Máca, L. Samaniego, J. Kyselý, and R. Kumar. 2018. “Revisiting the Recent European Droughts from a Long-Term Perspective.” *Scientific Reports* 8 (1): 1–11. https://doi.org/10.1038/s41598-018-27464-4.

Horner, Gillis J., P. J. Baker, R. Macnally, S. C. Cnningham, J. R. Thomson, and F. Hamilton. 2009. “Mortality of Developing Floodplain Forests Subjected to a Drying Climate and Water Extraction.” *Global Change Biology* 15 (9): 2176–86.

IPCC. 2014. “Climate Change 2014: Synthesis Report. Contribution of Working Groups I, II and III to the Fifth Assessment Report of the Intergovernmental Panel on Climate Change.” https://archive.ipcc.ch/pdf/assessment-report/ar5/syr/AR5_SYR_FINAL_SPM.pdf.

Jones, Hamlyn G., and R. A. Vaughan. 2010. *Remote Sensing of Vegetation - Principles, Techniques, and Applications*. New York: Oxford University Press Inc.

Jongman, Rob H.G., M. Külvik, and I. Kristiansen. 2004. “European Ecological Networks and Greenways.” *Landscape and Urban Planning* 68 (2–3): 305–19. https://doi.org/10.1016/S0169-2046(03)00163-4.

JRC. 2011. “NDWI (Normalized Difference Water Index).” *Product Fact Sheet* 5 (July): 6–7.

Junk, W. J., P. B. Bayley, and R. E. Sparks. 1989. “The Flood Pulse Concept in River-Floodplain.” *Oil & Fat Industries* 7 (7): 249–50. http://ftp.cs.ru.nl/toinesmits/Recommended_readings_IWRM_2009/Water_Ecomorphological_principles/1989JunkThe flood pulse concept in.pdf.

Kowalska, Natalia, L. Šigut, M. Stojanović, M. Fischer, I. Kyselova, and M. Pavelka. 2020. “Analysis of Floodplain Forest Sensitivity to Drought: Floodplain Forest during Drought.” *Philosophical Transactions of the Royal Society B: Biological Sciences* 375 (1810): 0–6. https://doi.org/10.1098/rstb.2019.0518.

Labovitz, ML, and E.J. Masuoka. 1084. “Changes in Vegetation Spectra with Leaf Deterioration under Two Methods of Preservation.” *Photogrammetric Engineering and Remote Sensing* 50 (12): 1737–45. https://www.asprs.org/wp-content/uploads/pers/1984journal/dec/1984_dec_1737-1745.pdf.

Lanen, Henny A.J. Van, G. Laaha, D. G. Kingston, T. Gauster, M. Ionita, J. P. Vidal, and R. Vlnas. 2016. “Hydrology Needed to Manage Droughts: The 2015 European Case.” *Hydrological Processes* 30 (17): 3097–3104. https://doi.org/10.1002/hyp.10838.

Leach, Nicholas J., S. Li, S. Sparrow, G. J. van Oldenborgh, F. C. Lott, A. Weisheimer, and M. R. Allen. 2020. “Anthropogenic Influence on the 2018 Summer Warm Spell in Europe: The Impact of Different Spatio-Temporal Scales.” *Bulletin of the American Meteorological Society* 101 (1): S41–46. https://doi.org/10.1175/BAMS-D-19-0201.1.

Lindroth, Anders, J. Holst, M.-L. Linderson, M. Aurela, T. Biermann, M. Heliasz, and J. Chi. 2020. “Effects of Drought and Meteorological Forcing on Carbon and Water Fluxes in Nordic Forests during the Dry Summer of 2018.” *Philosophical Transactions of the Royal Society B: Biological Sciences* 375 (1810): 20190516. https://doi.org/10.1098/rstb.2019.0516.

Mancino, G, A Nolè, F Ripullone, and A Ferrara. 2014. “Landsat TM Imagery and NDVI Differencing to Detect Vegetation Change: Assessing Natural Forest Expansion in Basilicata, Southern Italy.” *IForest - Biogeosciences and Forestry* 7 (2): 75–84. https://doi.org/10.3832/ifor0909-007.

Manderbach, Randolf. 2020. “FFH-Gebiete in Deutschland.” 2020. http://www.ffh-gebiete.de/ffh-gebiete/.

McDowell, Nate, W. T. Pockman, C. D. Allen, D. D. Breshears, N. Cobb, T. Kolb, and J. Plaut. 2008. “Mechanisms of Plant Survival and Mortality during Drought: Why Do Some Plants Survive While Others Succumb to Drought?” *New Phytologist* 178 (4): 719–39. https://doi.org/10.1111/j.1469-8137.2008.02436.x.

Mikac, Stjepan, A. Žmegač, D. Trlin, V. Paulić, M. Oršanić, and I. Anić. 2018. “Drought-Induced Shift in Tree Response to Climate in Floodplain Forests of Southeastern Europe.” *Scientific Reports* 8 (1): 1–12. https://doi.org/10.1038/s41598-018-34875-w.

NASA. 2021. “What Is Remote Sensing?” 2021. https://earthdata.nasa.gov/learn/backgrounders/remote-sensing.

Nasser Mohamed Eid, Asmaa, C. O. Olatubara, T. A. Ewemoje, H. Farouk, and M. T. El-Hennawy. 2020. “Coastal Wetland Vegetation Features and Digital Change Detection Mapping Based on Remotely Sensed Imagery: El-Burullus Lake, Egypt.” *International Soil and Water Conservation Research*, no. February. https://doi.org/10.1016/j.iswcr.2020.01.004.

Nussbaumer, Anita, K. Meusburger, M. Schmitt, P. Waldner, R. Gehrig, M. Haeni, A. Rigling, I,. Brunner, and A. Thimonier. 2020. “Extreme Summer Heat and Drought Lead to Early Fruit Abortion in European Beech.” *Scientific Reports* 10 (1): 5334. https://doi.org/10.1038/s41598-020-62073-0.

Ogashawara, Igor, and V. Bastos. 2012. “A Quantitative Approach for Analyzing the Relationship between Urban Heat Islands and Land Cover.” *Remote Sensing* 4 (11): 3596–3618. https://doi.org/10.3390/rs4113596.

Park Williams, A., C. D. Allen, A. K. Macalady, D. Griffin, C. A. Woodhouse, D. M. Meko, and T. W. Swetnam. 2013. “Temperature as a Potent Driver of Regional Forest Drought Stress and Tree Mortality.” *Nature Climate Change* 3 (3): 292–97. https://doi.org/10.1038/nclimate1693.

Peters, Wouter, A. Bastos, P. Ciais, and A. Vermeulen. 2020. “A Historical, Geographical and Ecological Perspective on the 2018 European Summer Drought: Perspective on the 2018 European Drought.” *Philosophical Transactions of the Royal Society B: Biological Sciences* 375 (1810). https://doi.org/10.1098/rstb.2019.0505.

Rebetez, Martine, H. Mayer, O. Dupont, D. Schindler, K. Gartner, J. P. Kropp, and A. Menzel. 2006. “Heat and Drought 2003 in Europe: A Climate Synthesis.” *Annals of Forest Science* 63 (6): 569–77. https://doi.org/10.1051/forest:2006043.

Rembold, Felix, M. Meroni, F. Urbano, G. Csak, H. Kerdiles, A. Perez-Hoyos, G. Lemoine, O. Leo, and T. Negre. 2019. “ASAP: A New Global Early Warning System to Detect Anomaly Hot Spots of Agricultural Production for Food Security Analysis.” *Agricultural Systems* 168 (July 2018): 247–57. https://doi.org/10.1016/j.agsy.2018.07.002.

Riggs, George A., and S. W. Running. 1991. “Detection of Canopy Water Stress in Conifers Using the Airborne Imaging Spectrometer.” *Remote Sensing of Environment* 35 (1): 51–68. https://doi.org/10.1016/0034-4257(91)90065-E.

Rinne, J., J.-P. Tuovinen, L. Klemedtsson, M. Aurela, J. Holst, A. Lohila, and P. Weslien. 2020. “Effect of the 2018 European Drought on Methane and Carbon Dioxide Exchange of Northern Mire Ecosystems.” *Philosophical Transactions of the Royal Society B: Biological Sciences* 375 (1810):

20190517. https://doi.org/10.1098/rstb.2019.0517.

Rivero, R.G., S. Grunwald, M.W. Binford, and T.Z. Osborne. 2009. “Integrating Spectral Indices into Prediction Models of Soil Phosphorus in a Subtropical Wetland.” *Remote Sensing of Environment* 113 (11): 2389–2402. https://doi.org/10.1016/j.rse.2009.07.015.

Rödenbeck, C., S. Zaehle, R. Keeling, and M. Heimann. 2020. “The European Carbon Cycle Response to Heat and Drought as Seen from Atmospheric CO 2 Data for 1999–2018.” *Philosophical Transactions of the Royal Society B: Biological Sciences* 375 (1810): 20190506. https://doi.org/10.1098/rstb.2019.0506.

Rohner, Brigitte, S. Kumar, K. Liechti, A. Gessler, and M. Ferretti. 2021. “Tree Vitality Indicators Revealed a Rapid Response of Beech Forests to the 2018 Drought.” *Ecological Indicators* 120 (September 2020): 106903. https://doi.org/10.1016/j.ecolind.2020.106903.

Russi, D., P. ten Brink, A. Farmer, T. Badura, D. Coates, J. Förster, R. Kumar, and N. Davidson. 2013. “The Economics of Ecosystems and Biodiversity for Water and Wetlands.” London and Burssels.

Russi, Daniela, P. ten Brink, A. Farmer, T. Bandura, D. Coates, J. Dorster, R. Kumar, and N. Davidson. 2013. “The Economics of Ecosystems and Biodiversity for Water and Wetlands: A Final Consultation Draft.” *IEEP, London and Brussels; Ramsar Secretaria*, 119.

Schindler, Stefan, F. H. O’Neill, M. Biró, C. Damm, V. Gasso, R. Kanka, and T. van der Sluis,. 2016. “Multifunctional Floodplain Management and Biodiversity Effects: A Knowledge Synthesis for Six European Countries.” *Biodiversity and Conservation* 25 (7): 1349–82. https://doi.org/10.1007/s10531-016-1129-3.

Schober, Bernhard, C. Hauer, and H. Habersack. 2015. “A Novel Assessment of the Role of Danube Floodplains in Flood Hazard Reduction (FEM Method).” *Natural Hazards* 75 (S1): 33–50. https://doi.org/10.1007/s11069-013-0880-y.

Schönwiese, Christian D., T. Staeger, and S. Trömel. 2004. “The Hot Summer 2003 in Germany. Some Preliminary Results of a Statistical Time Series Analysis.” *Meteorologische Zeitschrift* 13 (4): 323–27. https://doi.org/10.1127/0941-2948/2004/0013-0323.

Schuldt, Bernhard, A. Buras, M. Arend, Y. Vitasse, C. Beierkuhnlein, A. Damm, and M Gharun. 2020. “A First Assessment of the Impact of the Extreme 2018 Summer Drought on Central European Forests.” *Basic and Applied Ecology* 45: 86–103. https://doi.org/10.1016/j.baae.2020.04.003.

Seneviratne, Sonia I., N. Nicholls, D. Easterling, C. M. Goodess, S. Kanae, J. Kossin, and Y. Luo. 2012. “Changes in Climate Extremes and Their Impacts on the Natural Physical Environment.” *Managing the Risks of Extreme Events and Disasters to Advance Climate Change Adaptation: Special Report of the Intergovernmental Panel on Climate Change* 9781107025: 109–230. https://doi.org/10.1017/CBO9781139177245.006.

Sevanto, Sanna, N. G. McDowell, L. T. Dickman, R. Pangle, and W. T. Pockman. 2014. “How Do Trees Die? A Test of the Hydraulic Failure and Carbon Starvation Hypotheses.” *Plant, Cell & Environment* 37 (1): 153–61. https://doi.org/10.1111/pce.12141.

Sims, Neil C., and M. C. Thoms. 2002. “What Happens When Flood Plains Wet Themselves: Vegetation Response to Inundation on the Lower Balonne Flood Plain.” *IAHS-AISH Publication*, no. 276: 195–202.

Smith, Naomi E., L. M. J. Kooijmans, G. Koren, E. van Schaik, A. M. van der Woude, N. Wanders, and M. Ramonet. 2020. “Spring Enhancement and Summer Reduction in Carbon Uptake during the 2018 Drought in Northwestern Europe.” *Philosophical Transactions of the Royal Society B: Biological Sciences* 375 (1810): 20190509. https://doi.org/10.1098/rstb.2019.0509.

Sousa-Silva, Rita, K. Verheyen, Q. Ponette, E. Bay, G. Sioen, H. Titeux, T. van de Peer, K. Van Meerbeek, and B. Muys. 2018. "Tree Diversity Mitigates Defoliation after a Drought-Induced Tipping Point." *Global Change Biology* 24 (9): 4304–15. https://doi.org/10.1111/gcb.14326.

Spinoni, Jonathan, G. Naumann, J. V. Vogt, and P. Barbosa. 2015. "The Biggest Drought Events in Europe from 1950 to 2012." *Journal of Hydrology: Regional Studies* 3 (March): 509–24. https://doi.org/10.1016/j.ejrh.2015.01.001.

Stephenson, David B. 2008. "Definition, Diagnosis, and Origin of Extreme Weather and Climate Events." In *Climate Extremes and Society*, edited by Henry F. Diaz and Richard J. Murnane, 11–23. Cambridge: Cambridge University Press. https://doi.org/10.1017/CBO9780511535840.004.

Szabó, Loránd, B. Deák, T. Bíró, G. J. Dyke, and S. Szabó. 2020. "NDVI as a Proxy for Estimating Sedimentation and Vegetation Spread in Artificial Lakes-Monitoring of Spatial and Temporal Changes by Using Satellite Images Overarching Three Decades." *Remote Sensing* 12 (9). https://doi.org/10.3390/RS12091468.

Szabó, Szilárd, Z. Gácsi, and B. Balázs. 2016. "Specific Features of NDVI, NDWI and MNDWI as Reflected in Land Cover Categories." *Landscape & Environment* 10 (3–4): 194–202. https://doi.org/10.21120/LE/10/3-4/13.

Thapa, R., M. C. Thoms, M. Parsons, and M. Reid. 2016. "Adaptive Cycles of Floodplain Vegetation Response to Flooding and Drying." *Earth Surface Dynamics* 4 (1): 175–91. https://doi.org/10.5194/esurf-4-175-2016.

Thompson, R. L., G. Broquet, C. Gerbig, T. Koch, M. Lang, G. Monteil, and S. Munassar. 2020. "Changes in Net Ecosystem Exchange over Europe during the 2018 Drought Based on Atmospheric Observations." *Philosophical Transactions of the Royal Society B: Biological Sciences* 375 (1810): 20190512. https://doi.org/10.1098/rstb.2019.0512.

Tockner, Klement, and J. A. Stanford. 2002. "Riverine Flood Plains: Present State and Future Trends." *Environmental Conservation* 29 (3): 308–30. https://doi.org/10.1017/S037689290200022X.

Trenberth, K.E., P.D. Jones, P. Ambenje, R. Bojariu, D. Easterling, A. Klein Tank, and D. Parker. 2007. "Observations: Surface and Atmospheric Climate (Supplementary Materials)." *Climate Change 2007: The Physical Science Basis. Contribution of Working Group I to the Fourth Assessment Report of the Intergovernmental Panel on Climate Change*, 11.

UNEP. 2004. "Impacts of Summer 2003 Heat Wave in Europe."

Velde, Marijn van der, F. N. Tubiello, A. Vrieling, and F. Bouraoui. 2012. "Impacts of Extreme Weather on Wheat and Maize in France: Evaluating Regional Crop Simulations against Observed Data." *Climatic Change* 113 (3–4): 751–65. https://doi.org/10.1007/s10584-011-0368-2.

Vogel, M. M., J. Zscheischler, R. Wartenburger, D. Dee, and S. I. Seneviratne. 2019. "Concurrent 2018 Hot Extremes Across Northern Hemisphere Due to Human-Induced Climate Change." *Earth's Future* 7 (7): 692–703. https://doi.org/10.1029/2019EF001189.

Wilhite, Donald A., and M. H. Glantz. 1985. "Understanding: The Drought Phenomenon: The Role of Definitions." *Water International* 10 (3): 111–20. https://doi.org/10.1080/02508068508686328.

WWA Landshut. 2020. "Isar." 2020. https://www.wwa-la.bayern.de/fluesse_seen/gewaesserportraits/isar/index.htm.

Yiou, Pascal, J. Cattiaux, D. Faranda, N. Kadygrov, A. Jézéquel, P. Naveau, and A. Ribes. 2020. "Analyses of the Northern European Summer Heatwave of 2018." *Bulletin of the American Meteorological Society* 101 (1): S35–40. https://doi.org/10.1175/BAMS-D-19-0170.1.

Yuan, Wenping, Y. Zheng, S. Piao, P. Ciais, D. Lombardozzi, Y. Wang, and Y. Ryu. 2019. “Increased Atmospheric Vapor Pressure Deficit Reduces Global Vegetation Growth.” *Science Advances* 5 (8): 1–13. https://doi.org/10.1126/sciadv.aax1396.

Zellweger, Florian, P. De Frenne, J. Lenoir, P. Vangansbeke, K. Verheyen, M. Bernhardt-Römermann, and L. Baeten. 2020. “Forest Microclimate Dynamics Drive Plant Responses to Warming.” *Science* 368 (6492): 772–75. https://doi.org/10.1126/science.aba6880.

Zhao, Maosheng, and S. W. Running. 2010. “Drought-Induced Reduction in Global Terrestrial Net Primary Production from 2000 Through 2009.” *Science* 329 (5994): 940–43. https://doi.org/10.1126/science.1192666.

Appendices

Meteorological and Hydrological Data, as well as study area specific NDVI and NDWI statistics are enclosed as electronic supplementary material.

I) Meteorological and Hydrological Data.

II) Study Area Pupplinger Au NDVI Statistics

III) Study Area Pupplinger Au NDWI Statistics

IV) Study Area Isar Floodplains Unterföhring NDVI Statistics

V) Study Area Isar Floodplains Unterföhring NDWI Statistics

VI) Study Area Isar Floodplains from Unterföhring to Landshut NDVI Statistics

VII) Study Area Isar Floodplains from Unterföhring to Landshut NDWI Statistics

VIII) Study Area Lower Isar between Landau and Plattling NDVI Statistics

IX) Study Area Lower Isar between Landau and Plattling NDWI Statistics

X) Study Area Isar Estuary NDVI Statistics

XI) Study Area Isar Estuary NDWI Statistics